

**Evolutionary relationships and morphological
variation between *Antirrhinum* species**



**Yvette Wilson
PhD Thesis**

**The University of Edinburgh
2010**

Abstract

The Old World *Antirrhinum* genus consists of ~20 species that are endemic to the Mediterranean region and grow in a range of habitats from desert to alpine and have a corresponding diversity of morphologies and growth habits. The genus also contains the plant developmental genetics model species *A. majus*. There is therefore a well-developed genetic infrastructure for identifying the molecular basis of variation within the genus. However, attempts at reconstructing a phylogeny of *Antirrhinum* have been inconclusive, which makes it difficult to infer the processes underlying this variation. This is due to the *Antirrhinum* species having diverged recently and there is likely to have been hybridisation between species.

In this study, populations are sampled from throughout the distribution of each species and genotyped for Amplified Fragment Length Polymorphisms (AFLPs) and chloroplast haplotypes. Population assignment, phylogenetic and ordination analyses were carried out on this data to test species delimitation and identify hybridisation between species. Based on the results of these analyses it is inferred that two main *Antirrhinum* lineages diverged with there being frequent episodes of hybridisation between species of these lineages in regions where they come into contact.

Accessions from these populations were also grown in standard conditions and their morphologies characterised. This was to quantify morphological variation within *Antirrhinum* to provide a framework for evolutionary research. A further aim was to compare the distribution of morphological variation to that of genetic variation. This analysis showed that despite extensive hybridisation between the main *Antirrhinum* lineages, the morphologies of species are constrained within the boundaries of two main morphological types. These results indicate which selective pressures may act on *Antirrhinum* morphology. Furthermore, as the *Antirrhinum* genus is endemic to the Mediterranean region and characteristic of Mediterranean flora in terms of its patterns of diversity and distribution, this study provides an insight into the processes leading to plant diversification within the region.

Acknowledgments

There are many people without whose help and support much of this work would not have been possible. I would especially like to thank my supervisor, Andrew Hudson, for his support and making my PhD such an enjoyable experience. I am also grateful to my second advisor, Toby Pennington, for his helpful comments and suggestions.

Enrico Coen and Christophe Thébaud kindly gave me seed and DNA for many accessions that were vital to this project. Christophe Thebaude and Monique Burrus also rescued me during a tough spell of fieldwork, helping me find populations of endemic species.

I am grateful to many people who have helped me with various aspects of my project. Alan Forest and Pablo Vargas shared unpublished data, gave me useful advice and gave me samples of DNA. Richard Milne has also given me encouragement and guidance and John Decker assisted me with GIS. Julia, Sebastian, Alexandre Beck and Mael Le Guevel helped me with plant measurements.

I would like to thank my colleagues in the Rutherford ‘big lab’ for their help in the lab and friendship.

I would also like to thank Fenton (Woody) Cotterill for his inspiration as a scientist, encouragement and support since I left Zimbabwe and for helping me with the GIS figures and thesis formatting.

Special thank-you to all my field assistants, Andrew and Catrina Hudson, Kim and Mary Coulson, Manuela Costa, Maureen Erasmus and Niall Wilson for their enthusiasm, navigational skills, sense of humour and hard work. They each shared an unforgettable part of a 6000 mile journey with me.

I am also indebted to Phil Smith for his excellent proof reading of my thesis.

This project was funded by the BBSRC, with additional funds for fieldwork from the Genetics Society and the University of Edinburgh Moray Endowment Award.

I am grateful to my family for their love, support and for always encouraging me to study. Thank-you Niall for broadening my horizons and looking after me during my PhD.

Table of Contents

Declaration	i
Acknowledgments	ii
Contents	iii
List of figures	vii
List of tables	xii
Abbreviations	xiv
Chapter 1: Introduction	1
1.1 The <i>Antirrhinum</i> genus	3
1.1.1 Distribution and habitat of <i>Antirrhinum</i> species	12
1.1.2 Life history and breeding systems	17
1.2 Taxonomy of the <i>Antirrhinum</i> genus	18
1.2.1 <i>Antirrhinum</i> species delimitation	18
1.2.2 Previous phylogenetic studies of the <i>Antirrhinum</i> genus	18
1.3 Thesis aims	21
Chapter 2: Materials and methods	22
2.1 Plant Material	22
2.1.1 Locations of populations sampled	22
2.1.2 Fieldwork methods	22
2.1.3 Plant growth	28
2.2. Morphological analysis	28
2.2.1 Growing conditions	28
2.2.2 Plant measurements	
2.2.3 Principal Components Analysis (PCA) of leaf and flower shapes	32
2.2.4 Data analysis	33
2.3 Molecular methods	34
2.3.1 DNA extraction	34
2.3.2 Amplified Fragment Length Polymorphisms (AFLPs)	35
2.3.3 Chloroplast loci amplification and sequencing	38
2.3.4 Restriction enzyme digests of PCR products	38
2.3.5 Agarose gel electrophoresis of DNA	38
2.4 Population genetic and phylogenetic methods	41
2.4.1 AFLP scoring	41
2.4.2 Neighbour-joining phylogenies using Jaccard distances	41
2.4.3 Principal Coordinates Analysis (PCoA) of AFLPs	41
2.4.4 AFLP band frequency estimation within species	42
2.4.5 Neighbour-joining phylogenies using Nei's Genetic distance	42
2.4.6 Chloroplast sequence analysis	42

2.4.7	Structure analysis	43
Chapter 3: Genetic delimitation of <i>Antirrhinum</i> species and analysis of their evolutionary relationships		44
3.1	Introduction	44
3.1.1	Chapter aims	44
3.1.2	Molecular approaches and taxon sampling	44
3.2	Phylogeographic analysis of chloroplast markers	46
3.2.1	Rooting the haplotype network	51
3.3	Testing species relationships using AFLP markers	51
3.3.1	Estimating the phylogenetic signal within the AFLP dataset	58
i)	Error due to variation in the amplification of loci	58
ii)	Error due to band size homoplasy	58
iii)	Descriptions of band frequencies within species	62
3.3.2	Clustering analyses of all genotyped individuals	62
i)	Neighbour-joining analysis of all individuals	62
ii)	Principal coordinates analysis of all individuals	64
iii)	Neighbour-joining analysis of species	68
3.3.3	Comparison of the AFLP results with those from the chloroplast analysis	71
i)	Neighbour-joining analysis based on AFLPs of all individuals	71
ii)	Excluding putative hybrid individuals from neighbour-joining analyses	71
3.3.4	Exploring the genetic structure within <i>Antirrhinum</i> using Bayesian assignment	73
3.4	Discussion	85
3.4.1	A model for the evolutionary relationships between <i>Antirrhinum</i> species	85
3.4.2	Distinguishing hybridisation from lineage sorting in causing incongruence	88
3.4.3	The effect of hybrids on the AFLP neighbour-joining phylogenies	91
3.4.4	Reliability of rooting the phylogeny using <i>Misopates</i>	93
3.4.5	Summary of the genetic delimitation of <i>Antirrhinum</i> species	93
3.5	Conclusions	95
Chapter 4: Morphological characterisation of the <i>Antirrhinum</i> species		96
4.1	Introduction	96
4.1.1	Background and aims	96
4.1.2	Choice of morphological characters	97
4.1.3	Approaches in developing metrics that describe morphology	97
i)	Describing complex morphological characters	97
ii)	Strategy in developing descriptive variables	98
4.1.4	Structure of the morphological descriptions	98
4.2	Experimental approach and sampling	99

4.3	Leaf characters	105
4.3.1	Leaf size and shape	105
4.3.2	Leaf cell size	110
4.3.3	Summary of leaf characters	110
4.4	Flower characters	113
4.4.1	Corolla size and shape	113
i)	<i>Dorsal petal tube and lobe</i>	113
ii)	<i>Flower side</i>	120
4.4.2	Dorsal petal cell size	124
4.4.3	Sepal size and shape	126
4.4.4	Androecium and gynoecium measurements	131
i)	<i>Style length</i>	131
ii)	<i>Dorsal and ventral stamen filament length</i>	136
4.4.5	Pedicel length	136
4.4.6	Corolla colour patterning	136
i)	<i>Corolla colour</i>	137
ii)	<i>Purple patch in the centre of the dorsal flower face</i>	140
iii)	<i>Purple region proximal to the hinge of dorsal petal lobes</i>	144
iv)	<i>Yellow patch on the ventral face of the flower</i>	147
v)	<i>Extent of yellow colouration of hairs on the adaxial surface of ventral petal</i>	147
vi)	<i>Yellow patch at the base of the tube</i>	150
4.4.7	Summary of flower characters	150
4.5	Plant architecture	154
4.5.1	Flowering time	154
4.5.2	Plant height	154
4.5.3	Inflorescence density	157
4.5.4	Width of the main stem at the base of the plant	157
4.5.5	Outgrowth of branches	157
4.5.6	Summary of characters describing plant architecture	160
4.6	Trichome morphology and density	160
4.7	Discussion	163
4.7.1	A quantitative description of <i>Antirrhinum</i> morphology	163
4.7.2	Morphological delimitation of <i>Antirrhinum</i> species	170
4.7.3	Identifying patterns of variation within the genus	171
Chapter 5: The phenotypic space of <i>Antirrhinum</i> species		172
5.1	Introduction	172
5.2	Definition of phenotypic space	172
5.3	Numerical approaches	173

5.4	Clustering individuals using flower characters	174
5.4.1	PCA of all flower characters	174
5.4.2	PCA of continuous flower characters	182
5.5	Clustering of populations using flower characters	186
5.6	PCA of populations using all morphological characters	186
5.6.1	PCA of populations using all characters	195
5.6.2	PCA of populations using continuous characters	203
5.7	Neighbour-joining analysis of populations based on morphological distances	209
5.7.1	Neighbour-joining populations based on all characters	209
5.7.2	Neighbour-joining populations based on continuous characters	212
5.7.3	Summary of morphological relationships inferred by neighbour-joining	212
5.8	Discussion	214
5.8.1	The multivariate compared to the univariate analysis	214
5.8.2	Evaluation of the principal component analyses	215
5.8.3	Species delimitation	215
5.8.4	Morphological characteristics of the main <i>Antirrhinum</i> lineages	217
5.8.5	Morphologies of species that have undergone hybridisation	218
5.9.	Conclusions	219
	Chapter 6: Discussion	220
6.1	Association of <i>Antirrhinum</i> and <i>Kickxiella</i> morphologies with their ecology	221
6.2	The evolution of the <i>Antirrhinum</i> genus in the context of the geological history of the Mediterranean region	222
6.2.1	The Mediterranean climate since the late Tertiary	222
6.2.2	The diversification of the main <i>Antirrhinum</i> lineages	223
6.2.3	Phylogeographic comparisons of <i>Antirrhinum</i> to other organisms	224
6.3	The role of hybridisation in the evolution of <i>Antirrhinum</i>	225
6.3.1	Evidence for <i>Antirrhinum</i> morphology being constrained	226
6.3.2	Possible Adaptive constraints	227
6.3.3	Testing models of hybridisation in <i>Antirrhinum</i>	229
6.3.4	The potential for hybridisation to generate diversity	229
6.3.5	Summary	230
6.4	Conclusions and general significance of results	230
	References	231

List of Figures	Page
Figure 1.1. Images of Kickxiella species <i>A. microphyllum</i> , <i>A. molle</i> , <i>A. pulverulentum</i> , <i>A. sempervirens</i> , <i>A. subbaeticum</i> and <i>A. pertegasii</i> .	4
Figure 1.2. Images of Kickxiella species <i>A. hispanicum</i> , <i>A. mollisimum</i> , <i>A. charidemi</i> and <i>A. rupestre</i> .	5
Figure 1.3 Images of the Streptosepalum species, <i>A. braun-blanquetii</i> and <i>A. meonanthum</i> .	6
Figure 1.4. Subsection Antirrhinum species <i>A. australe</i> and <i>A. barrelieri</i>	7
Figure 1.5. Images of subsection Antirrhinum species <i>A. graniticum</i> and <i>A. boissieri</i> .	8
Figure 1.6. Images of subsection Antirrhinum species <i>A. majus cirrhigerum</i> and <i>A. majus linkianum</i> .	9
Figure 1.7. Images of subsection Antirrhinum species <i>A. majus pseudomajus</i> , <i>A. majus striatum</i> , and <i>A. majus litigiosum</i> .	10
Figure 1.8. Images of subsection Antirrhinum species <i>A. majus tortuosum</i> and <i>A. majus siculum</i> .	11
Figure 1.9. Map of the western Mediterranean region showing the distributions of all <i>Antirrhinum</i> species.	13
Figure 1.10. Images showing examples of the habitats in which Kickxiella species grow.	14
Figure 1.11. Images showing some examples of the habitats in which Antirrhinum subsection species grow.	15
Figure 1.12. Pollination of flowers by a bumblebee.	16
Figure 2.1. Schematic diagram illustrating the labeling of plant parts and the measurements that were taken on the plant.	29
Figure 2.2. Figure showing how the style length, pedicel length and stamen filament length were measured.	31
Figure 3.1. Graph showing the number of polymorphisms per 100 bp for each of the chloroplast loci sequenced from one individual of different species.	48
Figure 3.2. Diagram showing the relationships of the haplotypes that were identified through sequencing the chloroplast loci <i>trnD-trnT</i> , <i>trnS-trnFM</i> , and <i>trnS-trnR</i> loci in 90 accessions representing all Antirrhinum species.	50
Figure 3.3. Map showing the geographic distribution of chloroplast haplotypes.	56
Figure 3.4. Diagram showing the position of the out-group, <i>Misopates orontium</i> ,	57

haplotype within the *Antirrhinum* chloroplast haplotype network shown in Figure 3.2.

Figure 3.5. Graphs showing the consistency of amplification of AFLP loci in multiple replications of the same individual (A) and two replications of numerous individuals (B).	61
Figure 3.6. Neighbour-joining phylogeny of all individuals based on genetic distances estimated from AFLPs.	63
Figure 3.7. The positions of individuals in the main axes of the principal coordinates analysis (PCoA) analysis carried out on the distances estimated from AFLP scores.	65-66
Figure 3.8. Neighbour-joining tree showing the relationships of <i>Antirrhinum</i> species based on genetic distances estimated by allele frequencies.	69
Figure 3.9. Neighbour-joining phylogeny of the individuals included in the chloroplast haplotype network, based on AFLPs	72
Figure 3.10. Un-rooted neighbour-joining phylogeny with inferred hybrid individuals removed from the analysis.	74
Figure 3.11. Rooted neighbour-joining phylogeny with inferred hybrid individuals removed from the analysis.	75
Figure 3.12. Graph showing the log likelihood values for all of the runs of each K, for each of the models of Table 3.4.	77
Figure 3.13. Graphs showing the genetic make-up of each individual, based on <i>Structure</i> simulations.	79-80
Figure 3.14. Map showing the geographic patterns of the average genetic make-up of sampled populations when K=47.	82-83
Figure 3.15. Map showing the geographic patterns of the average genetic make-up of sampled populations when K=7.	84
Figure 3.16. The model proposed to describe the evolutionary relationships of the <i>Antirrhinum</i> species.	86
Figure 4.1. The point model template used to capture leaf shape (A) and the variation represented by the resulting axes from PCA metamer 6 leaves (B).	106
Figure 4.2. Mean values of LePC1 for each taxon (A) and results of tests for significant differences in LePC1 values between all pairs of taxa (B).	107
Figure 4.3. Mean values of LePC2 for each taxon (A) and results of tests for significant differences in LePC2 values between all pairs of taxa (B).	108
Figure 4.4. Mean values of LePC3 for each taxon (A) and results of tests for significant differences in LePC3 values between all pairs of taxa (B).	109
Figure 4.5. Mean values of the number of cells in an 50 x 50 μm area of the	111

adaxial m4 leaf surface for each taxon (A) and results of tests for significant differences between all pairs of taxa (B).

Figure 4.6. Diagram showing the structure of the <i>Antirrhinum</i> flower	112
Figure 4.7. The point model template used to capture the dorsal petal size and shape (A) and the variation represented by the resulting PCA axes (B).	114
Figure 4.8. Mean values of FpPC1 for each taxon (A) and results of tests for significant differences in FpPC1 values between all pairs of taxa (B).	115
Figure 4.9. Mean values of FpPC2 for each taxon (A) and results of tests for significant differences in FpPC2 values between all pairs of taxa (B).	116
Figure 4.10. Mean values of FpPC3 for each taxon (A) and results of tests for significant differences in FpPC3 values between all pairs of taxa (B).	117
Figure 4.11. Mean values of FpPC4 for each taxon (A) and results of tests for significant differences in FpPC4 values between all pairs of taxa (B).	118
Figure 4.12. The point model template used to describe the flower side outline (A) and the variation described by the resulting PCA axes (B).	121
Figure 4.13. Mean values of FsPC1 for each taxon (A) and results of tests for significant differences in FsPC1 values between all pairs of taxa (B).	122
Figure 4.14. Mean values of FsPC3 for each taxon (A) and results of tests for significant differences in FsPC3 values between all pairs of taxa (B).	123
Figure 4.15. Mean values of the number of cells in an 25 x 25 μm area on the adaxial surface of the dorsal petal lobe for each taxon (A) and results of tests for significant differences between all pairs of taxa (B).	125
Figure 4.16. The point model template used to capture the dorsal sepal size and shape (A) and variation represented by the resulting PCA axes (B).	127
Figure 4.17. Mean values of SePC1 for each taxon (A) and results of tests for significant differences in SePC1 values between all pairs of taxa (B).	128
Figure 4.18. Mean values of SePC2 for each taxon (A) and results of tests for significant differences in SePC2 values between all pairs of taxa (B).	129
Figure 4.19. Mean values of SePC3 for each taxon (A) and results of tests for significant differences in SePC3 values between all pairs of taxa (B).	130
Figure 4.20. Mean values of the style length for each taxon (A) and results of tests for significant differences the mean style length values between all pairs of taxa (B).	132
Figure 4.21. Mean values of the dorsal filament length for each taxon (A) and results of tests for significant differences the mean dorsal filament length values between all pairs of taxa (B).	133

Figure 4.22. Mean values of the ventral filament length for each taxon (A) and results of tests for significant differences the mean ventral filament length values between all pairs of taxa (B).	134
Figure 4.23. Mean values of the pedicel length for each taxon (A) and results of tests for significant differences the mean pedicel length values between all pairs of taxa (B).	135
Figure 4.24. Figure showing examples of flower images and their corresponding colour scores	138
Figure 4.25. Graph showing the number of individuals with flowers of each colour score for the species in subsection <i>Antirrhinum</i> (A) and subsection <i>Kickxiella</i> (B).	139
Figure 4.26. An image showing the distinctive purple patch of an <i>A. sempervirens</i> flower.	141
Figure 4.27. Figure showing examples of images of dorsal petals and their corresponding scores for the purple patch in the centre of the dorsal flower face.	142
Figure 4.28. Graphs showing the number of individuals of scoring category of the dorsal petal purple patch for the species in subsection <i>Antirrhinum</i> (A) and subsections <i>Kickxiella</i> and <i>Streptosepalum</i> (B).	143
Figure 4.29. Figure showing examples of images of dorsal petals and their corresponding scores for the purple zone on the adaxial dorsal petal lobe, proximal to the hinge of the flower.	145
Figure 4.30. Graphs showing the number of individuals of each scoring category for the dorsal lobe purple region proximal to the hinge of the petal. The species in subsection <i>Antirrhinum</i> are plotted in (A) and those in subsections <i>Kickxiella</i> and <i>Streptosepalum</i> in (B).	146
Figure 4.31. Example scoring of the yellow patch on the ventral face of the flower.	148
Figure 4.32. Graphs showing the number of individuals of each species for each scoring category for the yellow patch on the face of the flower in subsection <i>Antirrhinum</i> species (A) and subsections <i>Kickxiella</i> and <i>Streptosepalum</i> species (B).	149
Figure 4.33. Examples of the scoring for yellow colouration of the strips of hair (A) and the yellow patch (B) on the adaxial surface of the ventral petal	151
Figure 4.34. Graphs showing the number of individuals of each species of each score for the extent of yellow colouration of the strips of hairs on the adaxial surface of the ventral petal in subsection <i>Antirrhinum</i> (A) and subsections <i>Streptosepalum</i> and <i>Kickxiella</i> (B).	152
Figure 4.35. Graphs showing the number of individuals of each species of each score for the size of the yellow patch on the adaxial surface of the ventral tube base in subsection <i>Antirrhinum</i> species (A) and subsections <i>Kickxiella</i> and <i>Streptosepalum</i> (B).	153

Figure 4.36. Mean values of the flowering time for each taxon (A) and results of tests for significant differences of flowering time between all pairs of taxa (B).	155
Figure 4.37. Mean values of the height for each taxon (A) and results of tests for significant differences in the mean height between all pairs of taxa (B).	156
Figure 4.38. Mean values of the inflorescence density for each taxon (A) and results of tests for significant differences in the inflorescence density between all pairs of taxa (B).	158
Figure 4.39. Mean values of the stem diameter for each taxon (A) and results of tests for significant differences in stem diameter between all pairs of taxa (B).	159
Figure 4.40. Examples of the architecture of plants with differing branch index estimates.	161
Figure 4.41. Mean values of the branching index for each taxon (A) and results of tests for significant differences in the branching index between all pairs of taxa (B).	162
Figure 4.42. Graphs showing the number of trichomes in a 50 x 50 μm area on the adaxial surface of the m4 leaf (A), the stem at the base of the plant (B) and the stem of the inflorescence (C).	167
Figure 5.1. The positions of <i>Antirrhinum</i> individuals plotted within the axes identified by PCA analysis using all flower characters (Section 5.4.1).	177-179
Figure 5.2. The positions of <i>Antirrhinum</i> individuals plotted within the axes identified by PCA analysis using continuous flower characters (Section 5.4.2).	183-185
Figure 5.3. The positions of <i>Antirrhinum</i> populations plotted within the axes identified by PCA analysis using all flower characters (Section 5.5).	192-194
Figure 5.4. The positions of <i>Antirrhinum</i> populations plotted within the axes identified by PCA analysis using all characters (Section 5.6.1).	200-202
Figure 5.5. The positions of <i>Antirrhinum</i> populations plotted within the axes identified by PCA analysis using all continuous characters (Section 5.6.2).	205-207
Figure 5.6. Neighbour-joining phenogram based on Euclidean distances between populations in the space defined by axes 1-4 of the PCA of all characters.	210
Figure 5.7. Neighbour-joining phenogram based on Euclidean distances between populations in the space defined by axes 1-4 of the PCA of continuous characters.	213

List of tables	Page
Table 2.1. Details of the localities of populations that were sampled.	23-27
Table 2.2. AFLP primer sequences.	36
Table 2.3. Primer combinations used for the AFLP selective PCRs.	36
Table 2.4. The sequences of the primers and the PCR programs used to amplify chloroplast loci	39
Table 2.5. PCR programs	40
Table 3.1. Details of chloroplast loci tested in <i>Antirrhinum</i>	47
Table 3.2. Table showing the details and chloroplast haplotype clades of all populations.	52-55
Table 3.3. Details of the sampling of populations of each species for AFLP genotyping and descriptions of the resulting band frequencies.	59
Table 4.1. Details of the number of plants from each population included in the morphological analysis	101-104
Table 4.2. Table summarising the types of trichomes observed on the leaves of each species.	164
Table 4.3. Table summarising the types of trichomes observed on the stem of each species.	165
Table 4.4. Table summarising the types of trichomes observed on the inflorescence stem of each species.	166
Table 4.5. Table listing all (A) continuous and (B) discrete morphological characters that were described.	169
Table 5.1. Continuous and discrete flower characters included in PCA of <i>Antirrhinum</i> individuals (Section 5.4.1) and their correlation value with each of the main axes.	175
Table 5.2. The percentage of variance accounted for by each of the principal components (PCs), or axes, of the PCA carried out on all flower characters, and on continuous flower characters only.	176
Table 5.3. Continuous flower characters included in PCA of <i>Antirrhinum</i> individuals (Section 5.4.2) and their correlation value with each of the main axes.	181
Table 5.4. Populations included in PCA analyses and the missing characters for each population.	187-190

Table 5.5. Continuous and discrete flower characters included in the PCA of populations (Section 5.5) and their correlation value with each of the main axes.	191
Table 5.6. Continuous and discrete characters included in PCA of all populations (Section 5.6.1) and the correlation value of each character with the main axes.	197
Table 5.7. The percentage of variance accounted for by the first 24 principle components (PCs) of the PCA carried out on all populations using all characters, and continuous characters only.	198
Table 5.8. Continuous characters included in PCA of all populations (Section 5.6.3) and the correlation value of each character with each of the main axes.	204

Abbreviations

Ac	Acetate
AFLP	Amplified Fragment Length Polymorphism
bp	base pairs
BSA	bovine serum albumin
CTAB	cetyltrimethyl ammonium bromide
DTT	dithiothreitol
EDTA	ethylenediaminetetraacetic acid
HCl	hydrochloric acid
indel	insertion deletion polymorphism
kb	kilobases
Ma	millions of years ago
MCE	mercaptoethanol
Ka	thousands of years ago
PC	principal component
PCA	principal components analysis
PCoA	principle coordinates analysis
PCR	polymerase chain reaction
pers. comm.	personal communication
pers. observ.	personal observation
QTL	quantitative trait locus
SD	standard deviations
SNP	single nucleotide polymorphism
TBE	Tris-borate/EDTA buffer
TE	Tris/EDTA buffer
Tris	tris(hydroxymethyl)aminomethane

Chapter 1: Introduction

The fact that evolution occurs is undisputed amongst biologists; however, determining the mechanisms underlying the evolution of biological diversity is challenging (Gould 1981). The process of evolution is difficult to dissect in two broad areas. The first is summarised by Stern (2000) as identifying “evolutionarily relevant mutations”. Developmental genetic studies of laboratory mutants in numerous model organisms have been successful in correlating the expression and function of genes to phenotype. However, the methodology of isolating genes and determining their function usually relies on mutations that disrupt development. This approach therefore does not sample the whole genome. Furthermore, it does not reveal the molecular basis of natural variation. The second broad area in which the process of evolution is poorly understood is in determining the roles of selection, mutation, recombination and genetic drift in determining the genetic composition of populations and therefore the phenotypes and fitness of individuals (Lynch 2007).

Plants are ideal for addressing these questions because they are amenable to genetic study as species crosses can be generated within many genera, and the sessile nature of plants makes it easier to relate their fitness to the environment. For example, Bradshaw and Schemske (2003) were able to test the role of the *YELLOW UPPER (YUP)* locus, which controls carotenoid pigment synthesis in the petals of flowers, in reproductive isolation between the monkeyflower species *Mimulus lewisii* and *M. cardinalis*. They introgressed the *YUP* locus of each species into the other and compared hummingbird versus bee visitation frequency to plants grown next to sympatric populations of these species.

Numerous approaches are used to address the first problem of identifying evolutionarily relevant loci, depending on the availability of genetic markers and the amenability of the study system to crossing experiments. One approach is to use Quantitative Trait Loci (QTL) analysis to identify loci that underlie traits that differ between divergent populations or species. QTL analysis identifies associations between markers and phenotype within a segregating population, usually an F₂ population of a cross between two individuals, each from one of the populations of interest. Other techniques are admixture mapping (Lexer *et al* 2007) and association mapping, but both require numerous markers from throughout the genome. The other main approach is to carry out a genome scan to compare the variation of allele frequencies between divergent populations and detect loci that have outlying F_{ST} values consistent with selection (Beaumont and Balding 2004, Savolainen *et al* 2006, Minder and Widmer 2008). Loci underlying phenotypic divergence have also been

identified using micro-arrays. For example, Abzhanov *et al* (2006) identified the molecular basis of divergent beak sizes in Darwin's finches (genus *Geospiza*) by comparing levels of cDNA transcripts between five *Geospiza* species. Recent extensions to these techniques are eQTL methods, which associate expression levels of genes with polymorphisms that are linked to causal loci (Gilad *et al* 2008) and can therefore be used to identify how the architecture of genetic pathways varies (Hodges and Derieg 2009).

Although all these approaches have been successful in identifying loci that underlie natural variation, it is often only possible to move from locus to meaningful sequence variation in model systems where there is a good infrastructure for genetic research. The majority of studies in plants have therefore focussed on identifying the molecular basis of natural variation in model species, in particular *Arabidopsis thaliana*, reviewed in Mitchell-Olds and Schmitt (2006). However, studies within *A. thaliana* characterise variation between populations and are not representative of most plant species as *A. thaliana* may have undergone similar selective pressures to domesticated species due to its spread with agriculture and it is highly selfing. Furthermore, to test current hypotheses on the predictability of genetic evolution such as whether the basis of intra-specific variation is different to that of inter-specific variation (Stern and Orgogozo 2008, 2009) it is necessary to sample across taxonomic levels. It is also essential to sample genera of independent evolutionary history and ecology to develop rigorous evolutionary theory (Karrenberg and Widmer 2008).

The Old World *Antirrhinum* genus (Plantaginaceae, Albach *et al* 2005; tribe Antirrhineae) is a good model system for complementing studies of other model plant genera. It consists of approximately 20 species that are endemic to the Mediterranean region that vary in morphology, habitat, and breeding system. There is evidence that the *Antirrhinum* genus diversified recently, at least within the last 5 million years (Gübitz *et al* 2003, Vargas *et al* 2009). Studies of variation within and between *Antirrhinum* species therefore address a time frame appropriate for identifying the population genetic processes that underlie the evolution of inter-specific variation. *Antirrhinum* species have the same chromosome number ($n = 8$) and are all inter-fertile and are therefore amenable to crossing experiments and QTL analysis. Furthermore, a well-developed genetic infrastructure for identifying the molecular basis of variation has come from the use of *A. majus* in plant genetic research (Schwarz-Sommer *et al* 2003a, Hudson *et al* 2009). In particular, detailed linkage maps of markers throughout the genome have been developed (Schwarz-Sommer *et al* 2003a and b) and recent studies have identified QTL that underlie morphological variation between *Antirrhinum* species (Langlade *et al* 2005, Yang 2006, Feng *et al* 2009).

However, to address the second broad area where the process of evolution is poorly understood, a historical framework is essential to infer the population genetic forces that act on molecular variation. A phylogeny provides information on the shared history of lineages and under what circumstances they may have diverged (O'Hara 1997). It is also difficult to distinguish ancestral from causal molecular variation that is responsible for the phenotypic differences without a strong phylogenetic hypothesis. It is currently difficult to test evolutionary hypotheses in *Antirrhinum* because resolving a phylogeny of the genus is challenging. In addition, morphological variation within and between *Antirrhinum* species is largely unknown, partly due to the unclear taxonomy of the genus.

The objective of this study is to unravel the evolutionary history of *Antirrhinum* and to describe morphological variation within the genus. This is to provide a framework for both identifying the molecular basis of variation in *Antirrhinum* and to test evolutionary hypotheses.

1.1 The *Antirrhinum* genus

The Old World *Antirrhinum* genus consists of 17 to 26 species, depending on taxonomic account, which are endemic to the western Mediterranean region (Rothmaler 1956, Webb 1971, Sutton 1988). For clarity of reference and consistency, the nomenclature of Sutton (1988) is used in this thesis. Previous authors also include the North American species of the genera *Sairocarpus*, *Howeliella* and *Neogaerrhinum* and the old word *Misopates* species within the genus *Antirrhinum* (Thompson 1986). However, there is both morphological and genetic evidence for the monophyly of the Old World *Antirrhinum* species as described within Sutton (Rothmaler 1956, Vargas *et al* 2004).

The first extensive taxonomic treatment of *Antirrhinum* by Rothmaler (1956) recognised 26 species and organised them into three morphological subsections – Kickxiella, *Antirrhinum* and Streptosepalum. Although this subdivision of the genus has been criticised (see below), the subsections give a broad framework for structuring the main morphological and ecological characteristics of *Antirrhinum* species and are used in this thesis to describe variation within the genus. The following description summarises the general characteristics of these three subsections, as described in Rothmaler (1956).



Figure 1.1. Images of *Kickxiella* species *A. microphyllum*, *A. molle*, *A. pulverulentum*, *A. sempervirens*, *A. subbaeticum* and *A. pertegasii*. (A) *A. microphyllum* (L72), (B) *A. microphyllum* inflorescence, (C) *A. pulverulentum* (L68) inflorescence, (D) *A. molle* (E51), (E) *A. molle* inflorescence, (F) *A. sempervirens* (L50), (G) *A. subbaeticum* (E72), (H) *A. subbaeticum* inflorescence, (I) *A. sempervirens* inflorescence, (J) *A. sempervirens* inflorescence, (K) *A. pertegasii* (E65) inflorescence, (L) *A. pertegasii*. For images A, D, F, G, H and L the scale bar is 10 cm and for images B, C, E, I, J and K the scale bar is 5 cm. All accessions were grown from seed in standard conditions. The brackets after the species names indicate the locations from which the seed for each species was collected (Table 2.1).



Figure 1.2. Images of *Kickxiella* species *A. hispanicum*, *A. mollisimum*, *A. charidemi* and *A. rupestre*. (A) *A. hispanicum* (E31), (B) *A. hispanicum* inflorescence, (C) *A. mollisimum* (L19), (D) *A. charidemi*, (E) *A. charidemi* (inflorescence), (F) *A. mollisimum* inflorescence, (G) *A. rupestre* (L139) inflorescence, (H) *A. rupestre*. For images A, C, D, and H the scale bar is 10 cm and for images B, E, G and F the scale bar is 5 cm. All accessions were grown from seed in the same conditions. The brackets after the species names indicate the locations from which the seed for each species was collected (Table 2.1).



Figure 1.3 Images of the *Streptosepalum* species, *A. braun-blauquetii* and *A. meonanthum*. (A) *A. braun-blauquetii* (E20), (B) *A. braun-blauquetii* inflorescence, (C) *A. meonanthum* (L118), (D), *A. meonanthum* inflorescence. For images A and C the scale bar is 10 cm and for images B and D the scale bar is 5 cm. All accessions were grown from seed in the same conditions. The brackets after the species names indicate the locations from which the seed for each species was collected (Table 2.1).



Figure 1.4. Subsection *Antirrhinum* species *A. australe* and *A. barrelieri* (A) *A. australe* (L83), (B) *A. australe* inflorescence, (C) *A. barrelieri* (L131), (D) *A. barrelieri* inflorescence. For images A and C the scale bar is 10 cm and for images B and D the scale bar is 5 cm. The accessions were grown from seed in the same conditions. The brackets after the species names indicate the locations from which the seed for each species was collected (Table 2.1)



Figure 1.5. Images of subsection *Antirrhinum* species *A. graniticum* and *A. boissieri*.
 (A) *A. graniticum* (L75), (B) *A. graniticum* inflorescence, (C) *A. boissieri* (L104), (D) *A. boissieri* inflorescence. For images A and C the scale bar is 10 cm and for images B and D the scale bar is 5 cm. The accessions were grown from seed in the same conditions. The brackets after the species names indicate the locations from which the seed for each species was collected (Table 2.1)



Figure 1.6. Images of subsection *Antirrhinum* species *A. majus cirrhigerum* and *A. majus linkianum*. (A) *A. majus cirrhigerum* (L113), (B), *A. majus cirrhigerum* inflorescence, (C) *A. majus linkianum* (L107), (D) *A. majus linkianum* inflorescence. For images A and C the scale bar is 10 cm and for images B and D the scale bar is 5 cm. The accessions were grown from seed in the same conditions. The brackets after the species names indicate the locations from which the seed for each species was collected (Table 2.1).

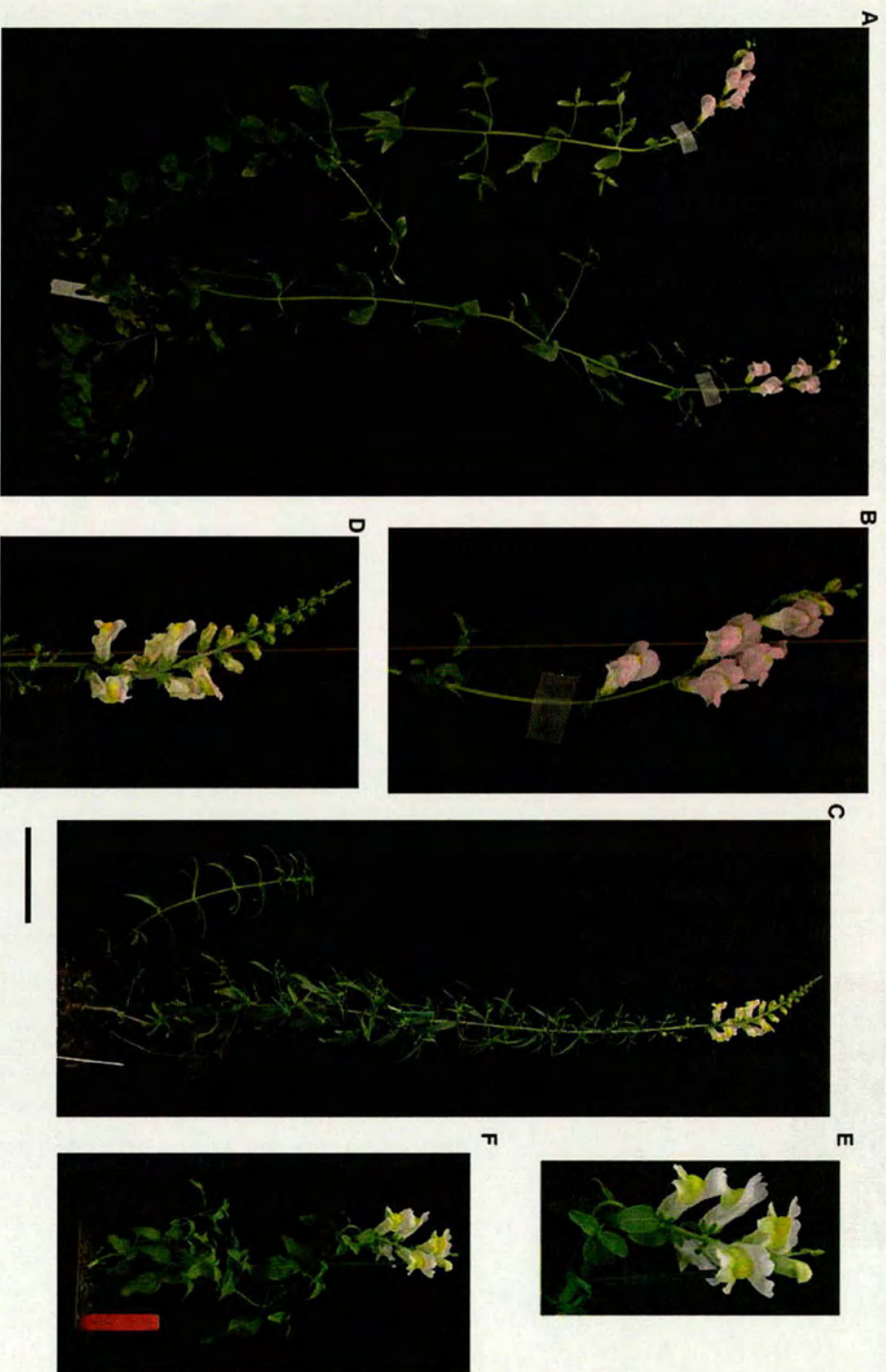


Figure 1.8. Images of subsection Antirrhinum species *A. majus tortuosum*, *A. majus siculum* and *A. latifolium*
 (A) *A. majus tortuosum* (L106), (B) *A. majus tortuosum* inflorescence, (C) *A. siculum* (E68), (D) *A. siculum* inflorescence, (E) *A. latifolium* (N1047)
 inflorescence and (F) *A. latifolium*.. For images A, C and F the scale bar is 10 cm and for images B, D and E the scale bar is 5 cm. The accessions were
 grown from seed in the same conditions. The brackets after the species names indicate the locations from which the seed for each species was collected
 (Table 2.1).

There are approximately 14 species in subsection Kickxiella (Figures 1.1 and 1.2, images of *A. grosii*, *A. lopesianum* and *A. martenii* are unavailable), which are mostly small suffrutescent herbs with decumbent, branching stems of < 40 cm. They have small round leaves with dense trichomes. Their inflorescences are not well-defined racemes like those of species within the other subsections; rather their flowers are subtended by bracts that are similar to vegetative leaves. Most of the species within the Kickxiella have small white/ivory flowers, except for *A. charidemi*, *A. subbaeticum*, *A. mollisimum* and *A. hispanicum*, which all have white to pale pink flowers. The flowers are borne on long and often arcuate pedicels and the sepals are lanceolate and bend backwards from the corolla.

There are two species within subsection Streptosepalum, *A. meonanthum* and *A. braun-blanquetii* (Figure 1.3). Both are tall, erect, herbs that grow up to ~120 cm. Their stems are simple or sparingly branched and develop well-defined inflorescences consisting of yellow flowers with a large gibba. The flowers have short, straight pedicels and are subtended by long, lanceolate bracts that are similar to leaves at the base of the inflorescence. The leaves are generally glabrous, although some *A. meonanthum* populations have hairy leaves that vary in shape from lanceolate to ovate.

The Antirrhinum subsection consists of approximately 12 species (and subspecies of *A. majus*), of tall, erect herbs with stems growing to ~120 cm (Figures 1.4-1.8). They vary in the extent to which the stems branch, but all develop well-defined raceme inflorescences. Both stems and inflorescences may be glabrous or hairy. The leaves of subsection Antirrhinum species may also be glabrous or hairy and vary from linear to lanceolate or ovate. Species of subsection Antirrhinum have either pink or yellow flowers. For example, the flowers of *A. majus pseudomajus* are deep pink, those of *A. majus striatum* are yellow and *A. siculum* has ivory to yellow coloured flowers. The flowers are subtended by distinct bracts and the pedicels are generally short and straight, the sepals also vary in shape from lanceolate to ovate.

1.1.1 Distribution and habitat of *Antirrhinum* species

The majority of the *Antirrhinum* species are endemic to the Iberian peninsular (Figure 1.9). The exceptions are *A. siculum*, which occurs in Italy, *A. martenii*, which occurs in Morocco, and *A. majus tortuosum*, which is distributed throughout the Mediterranean, including the Balkans, the

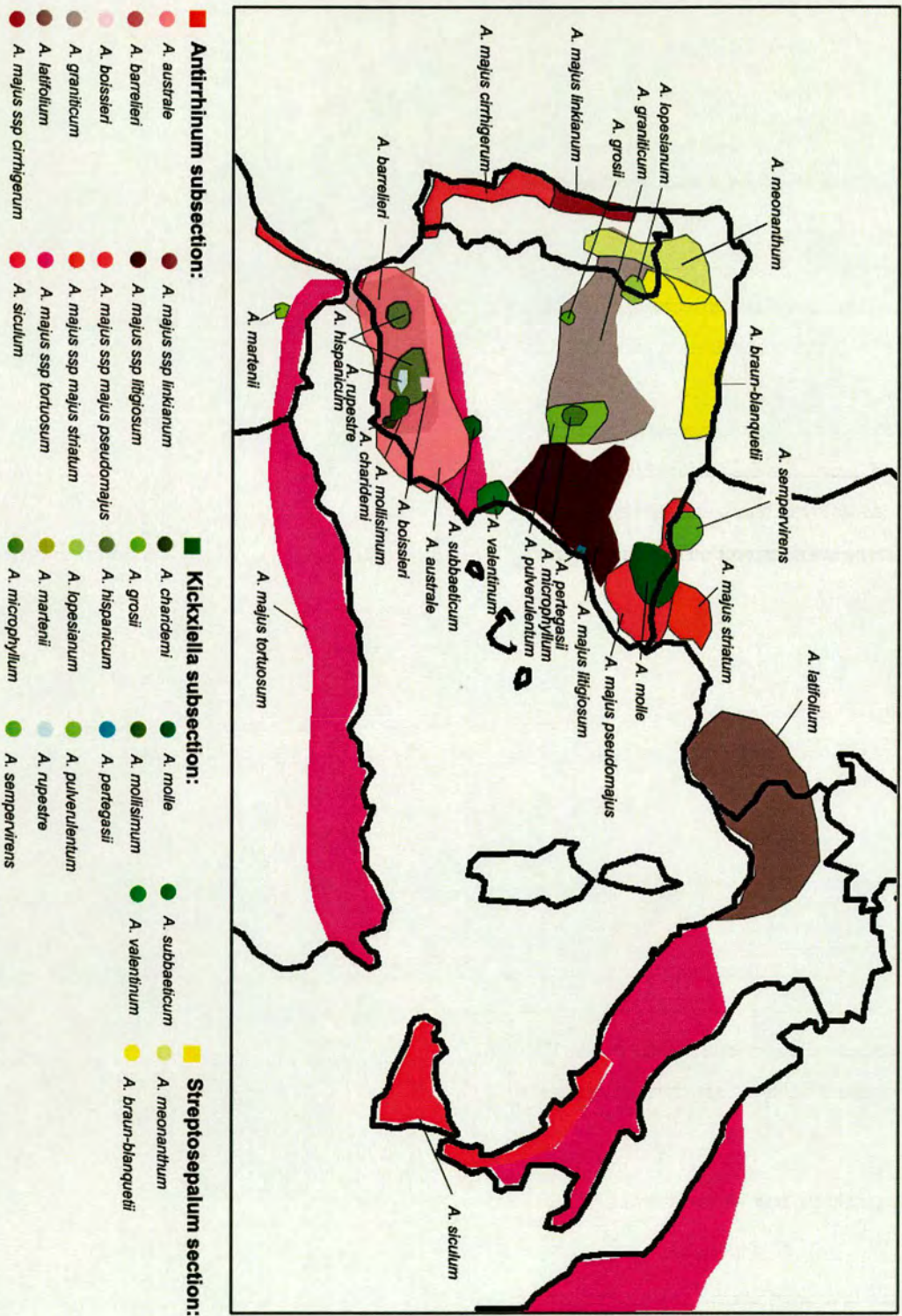


Figure 1.9. Map of the western Mediterranean region showing the distributions of all *Antirrhinum* species. The species distributions are adapted from Rothmaler (1956) and from the locations of populations that were collected from in this study.



Figure 1.10. Images showing examples of the habitats in which *Kickxiella* species grow.
 (A) *A. grosii*, Sierra de Gredos, Toledo Province, Spain, (B) *A. molissimum*, Canjazar, Almeria Province, Spain, (C) *A. pulverulentum*, Pelegrina, Guadalajara Province, Spain, (D) *A. microphyllum*, Pantano de Buendia, Guadalajara Province, Spain. Images not to scale.



Figure 1.11 Images showing some examples of the habitats in which *Antirrhinum* subsection species grow.
 (A) *A. australe*, Grazalema, Cadiz province, Spain (B) *A. graniticum*, Berninches, Guadalupe province
 (C) *A. barrelieri*, Laroles, Granda province, Spain (D) *A. majus pseudomajus*, Prades, Pyrenees-Orientales province, France (E) *A. majus cirrhigerum*, Gala, Coimbra province, Portugal



Figure 1.12. Pollination of flowers by a bumblebee.
The images show the bumblebee landing on the lower palate of the flower to force it open and then enter the flower.

Middle East and North Africa. Populations classified as *A. hispanicum* and *A. barrelieri* from Morocco are also described by Rothmaler (1956).

The *Kickxiella* species are all extremely endemic, with each species being confined to a single mountain range, apart from *A. hispanicum*, which occurs in several mountain ranges within southern Spain, mainly in Granada province. Many *Kickxiella* species consist of just a few known populations, for example, *A. grosii*, *A. charidemi*, *A. lopesianum*, *A. pertegasii*, *A. valentinum*, *A. subbaeticum* and *A. microphyllum*. All *Kickxiella* species grow on rock faces (Figure 1.10), although there have been no detailed studies of the specific rock type, i.e. igneous or limestone, on which each species grows.

In comparison to the *Kickxiella* species, the majority of species within subsections *Antirrhinum* and *Streptosepalum* are widespread and abundant. Plants within most of these species are observed growing in a variety of different habitats, for example, along roadsides, in hedges, on rock faces and on rock walls (Figure 1.11). The majority of these species, apart from *A. graniticum*, are reported to be calcicoles. However, field observations are inconsistent with these generalisations (pers. observ.); for example, some *A. australe* and *A. majus tortuosum* populations were observed growing on igneous rock faces.

1.1.2 Life history and breeding systems

Antirrhinum species are all perennial; however, the lifespan of individual plants is unknown. Most *Antirrhinum* species are self-incompatible, apart from *A. majus* and *A. siculum*. There are also reports of partial self-compatibility in *A. majus cirrhigerum*, *A. majus linkianum* (Vieira and Charlesworth 2002), *A. subbaeticum* (Jiminez *et al* 2002) and *A. valentinum* (Mateu-Andres and Segarra-Moragues 2003c). *Antirrhinum* species rely almost exclusively on bumblebees and carpenter bees for cross-pollination (Whibley 2004). Bees land on the lower palate of the flower, with their weight forcing the flower open so they can enter the corolla and gain access to nectar at the base of the corolla tube (Figure 1.12). The anthers and style are positioned within the corolla tube to make contact with the dorsal surface of the bee's thorax when it enters the flower. There is currently little evidence for any *Antirrhinum* species having specific pollinator species, but there is ongoing research in this area.

1.2 Taxonomy of the *Antirrhinum* genus

1.2.1 *Antirrhinum* species delimitation

Despite the broad differences between *Antirrhinum* species, there is much debate over the delimitation and morphological relationships of most species; furthermore, the species nomenclature used by *Antirrhinum* researchers has been inconsistent. The history of classification of the *Antirrhinum* genus was summarised by Webb (1971) and Sutton (1988), with Fernandez-Casas (1997) restructuring the genus, mainly following Rothmaler's (1956) classification. In subsequent population genetic studies, which were based on Rothmaler's classification, further taxa were recognised as species and populations of some widespread species were defined as subspecies (Mateu-Andres and Segarra-Moragues 2003a and b, Mateu-Andres and de Paco 2005). Most *A. majus* subspecies were elevated to specific rank and *A. australe* was included into *A. majus tortuosum* by Mateu-Andres and de Paco (2005).

However, Webb (1971) was critical of Rothmaler's (1956) classification on two main grounds. The first is that the subsections defined by Rothmaler are typological and some taxa do not fit within a single category or are intermediate between subsections. The second is that some characters that Rothmaler placed a large emphasis on in defining species are variable, for example, trichome morphology. Furthermore, Webb claimed "...it would be possible to pick out a graded series of plants linking the two extremes" of *A. majus tortuosum* and *A. mollissimum*. This claim is consistent with observations of variation among populations of southern Spanish species and *A. majus* subspecies. The hypothesis put forward to explain the patterns of morphological variation and taxonomic complications within the genus was that endemic species within Spain have arisen because of geographical isolation and subsequently more widespread subsection *Antirrhinum* species have dispersed and hybridised with these localised species (Webb 1971).

1.2.2 Previous phylogenetic studies of the *Antirrhinum* genus

There have been several attempts to reconstruct a phylogeny of the *Antirrhinum* species, using morphological characters as well as nuclear and chloroplast loci sequence data. Most of these studies sampled one to two individuals from each species (Adeyanju 2003, Chaffe 2003, Gübitz *et al* 2003 and *unpublished*, Vargas *et al* 2004). Parsimony analysis of leaf epidermal characters (Adeyanju 2003) and characters considered to be taxonomically important such as trichome morphology and distribution, branch twining, bract and sepal shape, the orientation of the dorsal

petal lobes and seed ornamentation (Vargas *et al* 2004) failed to resolve any species relationships. These results suggest that there are few synapomorphic morphological characters.

Phylogenetic reconstructions based on *ITS-1* and *ITS-2* sequences using neighbour-joining, parsimony and Bayesian analyses also failed to resolve species relationships (Chaffe 2003, Vargas *et al* 2004 and 2009). In these studies, few species were grouped with reliable support and there was also evidence of nucleotide additivity, which is when two or more bases are detected at the same locus in the sequence. The *ITS* region consists of numerous repeats throughout the genome (there are at least two different regions in *A. majus*; A. Hudson, pers. comm.), but copies are rapidly homogenised by concerted evolution (Baldwin *et al* 1995). The presence of nucleotide additivity could be because *Antirrhinum* species have diverged recently, so there has been insufficient time for *ITS* homogenisation within species and polymorphic *ITS* copies remain within individuals. However, as concerted evolution of the *ITS* region is rapid, nucleotide additivity is more likely the result of hybridisation or of some *ITS* regions having become isolated from concerted evolution (Sang *et al* 1995, Chaffe 2003, Vargas *et al* 2004 and 2009). Phylogenetic analyses of other nuclear loci sequences - the *FIM-ERG* intergenic region (Adeyanju 2003), *CYCLOIDEA* (*CYC*) (Gübitz *et al* 2003), the 5' region of *INCOLORATA* (*INC*) (Chaffe 2003) and Amplified Fragment Length Polymorphisms (AFLPs; Gübitz *et al* unpublished) all showed similar lack of resolution. In each of these phylogenies very few clades (each usually consisting of up to three species) are resolved with significant support and comparison across phylogenies shows that the species clustered within resolved clades differ, depending on the locus used.

The lack of resolution and conflicting topologies obtained using morphological and nuclear sequence characters could be the result of hybridisation or rapid diversification of *Antirrhinum* species. Rapid diversification of species can result in multiple ancestral alleles being retained within divergent species (incomplete lineage sorting) or the same allele becoming fixed within non-sibling species (lineage sorting). Hybridisation can result in alleles of one species being transferred to another, possibly unrelated, species. Therefore, the phylogenetic signals of hybridisation and lineage sorting are similar and it is difficult to distinguish them (Wendel and Doyle 1998, Linder and Rieseberg 2004, Muir and Schlotterer 2005).

As the chloroplast is maternally inherited in most angiosperm families, including *Antirrhinum*, relationships inferred by chloroplast markers reflect evolutionary lineages of the chloroplast without recombination. Therefore incongruence between relationships inferred by chloroplast markers and those inferred by nuclear markers or morphology may indicate hybridisation. However, phylogenies using individual chloroplast loci, the *trnL-F* locus (Gübitz *unpublished*) and the *trnT-L* locus (Jimenez *et al* 2005) are also poorly resolved. In these studies, one or two individuals were sampled from each species and phylogenies reconstructed using either minimum evolution or parsimony methods. In both cases, a few clades were resolved with high support, but they clustered species with divergent morphologies.

Recently, Vargas *et al* (2009) sampled more individuals from each species (83 individuals covering all species apart from *A. martenii*) and used the combined sequences of the chloroplast loci *trnS-G* and *trnK-matK* to infer evolutionary relationships. They resolved a star-like network connecting chloroplast haplotypes, with limited support for monophyletic groups. In addition, some evidence was found for species within the same broad geographic region sharing haplotypes, consistent with hybridisation between species.

Based on the combined evidence from these studies, it is difficult to develop a rigorous phylogenetic hypothesis for the *Antirrhinum* genus because it may have diversified recently, with subsequent hybridisation having occurred between species. Evidence for the recent diversification of the genus is there is little sequence divergence between chloroplast loci and many nuclear loci (Gübitz *et al* 2003, Jimenez *et al* 2005, A. Hudson pers. comm.). Evidence for hybridisation between species is the difficulty of morphological delimitation of species in regions of sympatry and nucleotide additivity of *ITS* sequence copies within individuals.

This hypothesis is supported by reconstructions of the recent climatic history of the Mediterranean region (Rothmaler 1956, Webb 1971, Vargas *et al* 2009). The first change in climate that may have prompted diversification of the *Antirrhinum* genus is the onset of the cooler and drier Mediterranean climate approximately 3 million years ago (Suc 1984). Subsequent glacial cycles will have forced populations to track suitable climatic conditions by either latitudinal or altitudinal range shifts (Hewitt 1996). Con-specific populations may therefore have diverged through becoming isolated in different regions of suitable habitat and microclimatic conditions, leading to allopatric speciation

and therefore diversification of the genus (Willis and Niklas 2004). These distribution shifts may also have resulted in previously isolated and divergent lineages coming into contact and hybridising (Hewitt 1996 and 2000, Willis and Niklas 2004). *Antirrhinum* species all form fertile hybrids with each other, which both provides evidence for their recent origin and increases the likelihood of hybridisation having occurred between species.

1.3 Thesis aims

Antirrhinum diversity provides an interesting system to study evolution at the interface between population genetic and phylogenetic processes, particularly as there is good genetic infrastructure for dissecting the underlying molecular variation. The aim of this thesis is to describe the morphological variation within *Antirrhinum* and relate it to the evolutionary history of the genus. This is to provide a framework for identifying the genetic pathways that underlie morphological diversity and for testing evolutionary hypotheses.

The specific aims are to:

- i) Sample populations from throughout the distribution of each *Antirrhinum* species and use genetic fingerprinting techniques to test *Antirrhinum* species delimitation and identify hybrid populations.
- ii) Characterise morphological variation within the genus.
- iii) Develop a rigorous hypothesis of the evolutionary relationships of the *Antirrhinum* species by distinguishing hybridisation from lineage sorting as a cause of phylogenetic incongruence. This is to infer the tempo of diversification of *Antirrhinum* species and the processes such as selection, genetic drift or recombination which may have driven their diversification. Furthermore, an evolutionary framework will indicate whether a group of species share a phenotypic trait because of shared ancestry, or whether it evolved independently numerous times. It will also enable molecular variation to be associated with morphological variation.
- iv) Compare the structure of morphological variation to that of genetic variation. This is to develop hypotheses on the developmental and ecological constraints that may have shaped *Antirrhinum* evolution.

Chapter 2: Materials and Methods

2.1 Plant Material

2.1.1 Locations of populations sampled

Populations from throughout the distribution of each species were sampled. Many of the endemic species were donated by Professor I. Mateu-Andres (Universidad de Valencia, Spain) for previous studies and have been maintained at the University of Edinburgh. T. Gübitz collected accessions of *A. molle*, *A. subbaeticum* and *A. braun-blanquetii*, which are also maintained at Edinburgh.

Professors E. Coen (JIC, Norwich) and C. Thébaud (CNRS, Université Paul Sabatier, Toulouse, France) kindly donated seed and tissue of *A. majus pseudomajus*, *A. majus striatum*, *A. siculum* and *A. latifolium*. Fieldwork was carried out during May-July in 2006 and 2007 to collect accessions from populations of the remaining species. To relate the results of this study to previous taxonomic accounts, many of the locations detailed in Rothmaler (1956), Mateu-Andres and Segarra-Moragues (2003), Mateu-Andres and de Paco (2003 and 2006), Mateu-Andres (2004) and Jimenez (2005) were visited and the populations detailed in these studies were located with varying degrees of success.

Table 2.1 describes the locations of all populations that were sampled. The exact localities and coordinates of many of the accessions that have been maintained at Edinburgh were not catalogued. Where possible, the locations from which these accessions were validated and the coordinates of the nearest town were taken to facilitate plotting their geographic positions. However, the original locations of some accessions remain unknown, but as many of them are of the extremely endemic *Kickxiella* species, there are only a few localities within a very small geographic area where they could have originated from.

2.1.2 Fieldwork methods

The coordinates describing the location of each population were taken using a Garmin GPS handset. For each population two plants that were spaced more than 3 m apart were selected to avoid sampling siblings. Each of these plants were photographed and tissue, cuttings and where possible seed were collected from them. To preserve the tissue for DNA extraction approximately 10 fresh, young and as far as possible disease-free leaves were placed in a vacuum-sealable polythene bag containing approximately 15 ml of silica beads (Type II silica gel, Sigma Aldrich). A small branch, approximately 15 cm long was cut from the plant at its base and placed in water in a 50 ml falcon tube. These cuttings were transported back to Edinburgh, the cut end was dipped in an auxin-based

DB	Location, Province, country	Lat.	Long.	Collector
Subsection Antirrhinum				
<i>A. australe</i> Rothm.				
83	Benamahoma, Cadiz, S	36.76	-5.40	YW
84	El Boyar, Cadiz, S	36.76	-5.38	YW
85	Grazelema, Cadiz, S	36.76	-5.37	YW
86	Villaluenga del Rosario, Cadiz, S	36.70	-5.37	YW
87	Benaocaz, Cadiz, S	36.69	-5.42	YW
88	Cortes de la Frontera, Malaga, S	36.63	-5.46	YW
89	Cortes de la Frontera, Malaga, S	36.61	-5.36	YW
90	Benaolan, Malaga, S	36.68	-5.28	YW
91	Gaucin, Malaga, S	36.62	-5.27	YW
95	El Burgo, Malaga, S	36.78	-4.94	YW
97	Torcal de Antequera, Malaga, S	36.96	-4.54	YW
<i>A. barrelieri</i> Boreau				
24	Paternal del Rio, Almeria, S	37.03	-2.95	YW
27	Laroles, Granada, S	37.01	-3.01	YW
28	Berja to Laujar, Almeria, S	36.95	-2.96	YW
29	Ugija to Murtas, Granada, S	36.95	-3.06	YW
33	Trevez, Granada, S	37.00	-3.27	YW
34	Busquistar, Granada, S	36.94	-3.30	YW
96	Alora, Malaga, S	36.80	-4.71	YW
101	Algarinejo, Granada, S	37.31	-4.14	YW
131	Padul, Granada, S	36.86	-3.49	YW
150	Cadiar, Granada, S	36.94	-3.18	YW
161	Tetuan to Chefchauen, Morocco	35.51	-5.44	YW
162	N of Chefchauen, Morocco	35.31	-5.52	YW
163	Chefchauen, Morocco	35.17	-5.26	YW
167	Taineste, Morocco	34.63	-4.19	YW
168	Taineste, Morocco	34.60	-4.09	YW
<i>A. boissieri</i> Rothm.				
18	Guadahortuna, Granada, S	37.59	-3.41	YW
E15*	Albanchez de Bela - Pegalajar, Jaen, S	37.45	-3.39	TG
104	Ermita Virgen de la Sierra, Cordoba, S	37.45	-4.38	YW
<i>A. graniticum</i> Rothm.				
40	Braganca, Braganca, P	41.80	-6.75	YW
67	Pelegina, Guadalajara, S	41.01	-2.61	YW
69	Ledanca, Guadalajara, S	40.87	-2.84	YW
71	Berninches, Guadalajara, S	40.55	-2.80	YW
75	Fuentiduena de Tajo, Madrid, S	40.14	-3.18	YW
76	Chinchon, Madrid, S	40.16	-3.43	YW
79	Priego, Cuenca, S	40.45	-2.29	YW
115	Lamego, Viseu, P	41.08	-7.97	YW
116	Celorica da beira, Guarda, P	40.64	-7.39	YW
117	Celorica da Beira, Guarda, P	40.64	-7.39	YW
119	Tornavacos, Caceres, S	40.25	-5.69	YW
121	Navacepeda de Tormes, Toledo, S	40.53	-5.25	YW
120	Navall de Tormes, Toledo, S	40.18	-5.29	YW

A. graniticum continued...

174	Collado-Villalba, Madrid, S	40.63	-3.99	YW
176	Miranda do Duoro, Braganca, P	41.50	-6.27	YW

A. latifolium Miller

AC1045	Marseille, Bouches-du-Rhone, F	-		Gatersleben
AC1046	Pyrenees	-		Gatersleben
AC1047	Entrevaux, Alpes-de-Ht.-Provence, F	43.95	6.80	Gatersleben
AC1053	Mt. Boron, Nice, Alpes-Maritimes, F	43.68	7.30	EC
AC1054	col d'Eze, Nice, Alpes-Maritimes, F	43.73	7.34	EC
AC1055	St Jean-Cap-Ferrat, Alpes-Maritimes, F	43.71	7.33	EC
AC1056	Menton, Alpes-Maritimes, F	43.77	7.50	EC
AC1057	Sospel, Alpes-Maritimes, F	43.88	7.44	EC
AC1058	col de Turini, Alpes-Maritimes, F	43.98	7.36	EC
AC1061	Entrevaux, Alpes-de-Ht.-Provence, F	43.95	6.80	EC
AC1066	St Martin d'Entraunes, Alpes-Maritimes, F	44.15	6.75	EC
AC1069	Entrevaux, Alpes-de-Ht.-Provence, F	43.97	6.76	EC
AC1070	Entrevaux, Alpes-de-Ht.-Provence, F	43.97	6.76	EC
AC1071	Rigaud, Alpes-Maritimes, F	44.00	6.98	EC
AC1072	Roubion, Alpes-Maritimes, F	44.09	7.05	EC
AC1079	Embrun, Hautes-Alpes, F	44.58	6.51	EC
AC1081	Mirabeau, Alpes-de-Ht.-Provence, F	43.70	5.72	EC

A. majus cirrhigerum Filcaho

113	Gala, Coimbra, P	40.12	-8.86	YW
114	Praia de Mira, Coimbra, P	40.42	-8.78	YW
122	Lisbon, Lisboa, P	-		MC
125	Algave, P	-		AH

A. majus linkianum Boiss & Reuter

107	Sierra de Arrabida, Setubal, P	38.49	-8.97	YW
108	Almada, Setubal, P	38.67	-9.17	YW
109	Sintra, Lisboa, P	38.67	-9.16	YW
110	Pernes, Santarem, P	39.40	-8.68	YW
111	Porto de Mos, Leiria, P	39.59	-8.81	YW
112	Coimbra, Coimbra, P	40.13	-8.48	YW

A. majus litigiosum Pau

1	BenioValencia, S	39.00	-0.27	YW
2	La Drova, Valencia, S	39.01	-0.27	YW
3	Chesta, Valencia, S	39.50	-0.69	YW
4	Lliria, Valencia, S	39.64	-0.58	YW
5	Olocau, Valencia, S	39.70	-0.53	YW
6	Segorbe, Castello, S	39.81	-0.52	YW
7	Vall d'Alba, Castello, S	40.19	-0.04	YW
8	Morella, Castello, S	40.55	0.00	YW
9	Traiguera, Castello, S	40.62	-0.32	YW
11	Casas de El Canizar, Cuenca, S	39.94	-1.71	YW
12	Elche, Albacete, S	39.45	-2.03	YW
13	Bogarra, Albacete, S	38.58	-2.20	YW
61	Santes Creus, Tarragona, S	41.36	1.36	YW
62	Santes Creus, Tarragona, S	41.32	1.35	YW
63	Borja, Zaragoza, S	41.84	1.33	YW

A. majus litigiosum continued...

64	Borja, Zaragoza, S	41.84	1.33	YW
65	Tarazona, Zaragoza, S	41.88	1.71	YW
66	Gallur, Zaragoza, S	41.84	-1.33	YW
80	Daroca, Zaragoza, S	41.05	-1.46	YW

A. majus pseudomajus

45	Jaca, Huesca, S	42.56	-0.66	YW
46	Biescas, Huesca, S	42.65	-0.32	YW
48	Panticosa, Huesca, S	42.73	-0.30	YW
49	Gave de Ossau, Hautes-Pyrenees, F	42.94	-0.44	YW
53	Minerve, Herault, F	42.35	-2.75	YW
59	Prades, Pyrenees-Orientales, F	42.77	1.86	YW
60	Berga, Barcelona, S	42.11	1.84	YW

A. majus striatum

55	N of Limoux, Aude, F	43.12	2.28	YW
56	S of Limoux, Aude, F	43.01	2.25	YW
58	Belcaire, Aude, F	42.80	1.93	YW
E039*	Avellanet, Lleida, S	-		TG
AC1100	Prats-de-Mollo-la-Preste, Pyrenees-Orientales, F	42.38	2.49	EC
AC1125	Alet les Bains, Aude, F	42.99	2.25	EC

A. majus tortuosum Vent.

81	El Tem Cadiz, S	36.63	-5.66	YW
82	El Bosque, Cadiz, S	36.76	-5.51	YW
92	Casares, Malaga, S	36.45	-5.26	YW
93	Marbella, Malaga, S	36.53	-4.89	YW
98	Almargen, Malaga, S	37.01	-4.56	YW
100	Loja, Granada, S	37.14	-4.26	YW
102	Priego de Cordoba, Cordoba, S	37.35	-4.19	YW
103	Alcaudete, Jaen, S	37.60	-4.07	YW
105	Cabra, Cordoba, S	37.46	-4.45	YW
106	Cerro Muriano, Cordoba, S	37.98	-4.76	YW
160	Gibraltar	36.12	-5.35	YW
165	Targha, Morocco	35.40	-5.04	YW
169	Taza, Morocco	34.15	-4.01	YW
AC1143	Mazzaro, Sicily, near Taormina	37.86	15.30	EC
AC1144	Near Cefalu, Sicily	38.04	14.03	EC

A. siculum Millar

AC1176	Palermo, Sicily	38.11	13.36	Gatersleben
AC1177	Taormina, Sicily	37.86	15.29	EC
E68	Syracuse	37.04	15.18	unknown
u	unknown	-		unknown
183		-		RM

Subsection Kickxiella

A. charidemi Lange

E23*	Cabo de Gata, Almeria, S	36.48	-2.14	TG
------	--------------------------	-------	-------	----

A. grosii Font Quer

175	Sierra de Gredos, Toledo, S	40.26	-5.27	YW
-----	-----------------------------	-------	-------	----

<i>A. hispanicum</i> Chav. (S)				
E30	Alhama de Granada, Granada, S	-		TG
E31*	Lanjaron, Granada, S	36.92	-3.47	TG
36	Balcon de Canales, Granada, S	37.15	-3.48	YW
99	Almargan, Malaga, S	37.01	-5.02	YW
132	Lanjaron, Granada, S	36.92	-3.47	YW
171	Source de Oum-er-Rubia, Morocco	33.05	-5.42	YW
172	El kebab, Morocco	32.74	-5.51	YW
173	El Ksiba, Morocco	32.58	-6.04	YW
<i>A. lopesianum</i>				
*	Vimioso, Braganca, P	41.58	-6.52	unknown
<i>A. microphyllum</i> Rothm				
72	Sacedon, Guadalajara, S	40.49	-2.75	YW
73	Pantano de Buendia, Guadalajara, S	40.40	-2.79	YW
74	Buendia, Guadalajara, S	40.36	-2.76	YW
<i>A. molle</i> Lange				
E51*	Gerri de la Sal, Lleida, S	42.20	1.04	TG
E52*	la Seu de Urgel, Lleida, S	42.37	1.78	TG
E53*	Saldes, Barcelona, S	42.23	1.74	TG
E54*	Montsec, S near Seu de Urgel	42.03	0.45	TG
E55*	Baga, Barcelona, S	42.15	1.52	TG
E56*	El Segre	-		TG
E57*	Las Lagunes, S near Gerri de la sal.	-		TG
E60*	Bellver de Cerdanya	-		TG
<i>A. mollisimum</i> Rothm.				
19	Abrucena, Almeria, S	37.13	-2.80	YW
20	Felix, Almeria, S	36.87	-2.65	YW
21, 157	Enix, Almeria, S	36.88	-2.61	YW
<i>A. pertegasii</i> Rothm.				
E65*	unknown, Castellon, Spain	40.66	0.40	IM
<i>A. pulverulentum</i> Lazaro				
68	Pelegrina, Guadalajara, S	41.01	-2.64	YW
70	Alcorlo, Guadalajara, S	41.01	-3.03	YW
77	Poveda de la Sierra, Guadalajara, S	40.66	-2.02	YW
78	Hoz de Beteta, Cuenca, S	40.55	-2.13	YW
<i>A. rupestre</i> Rothm.				
22	Canjayar, Almeria, S	36.96	-2.59	YW
139	Capiliera, Granada, S	36.96	-3.34	YW
<i>A. sempervirens</i> Lapeyr.				
47	Panticosa, Huesca, S	42.74	-0.26	YW
50	Col d'Aubisque, Hautes-Pyrenees, F	42.96	-0.29	YW
52	Luz, Hautes-Pyrenees, F	42.93	-0.05	YW
<i>A. subbaeticum</i> Guemes				
E72*	unknown, Albacete, S	38.58	-2.21	TG

<i>A. valentinum</i> Font Quer				
AC1173	La Drova, Valencia, S	39.01	-0.28	IM
Subsection Streptosepalum				
<i>A. braun-blanquetii</i> Rothm.				
44	Sobron, Alava, S	42.76	-3.09	YW
E18*	La Pinda, Corvera de Asturias, Asturias, S	43.23	-4.36	TG
E19*	RiGorge Ceneya	43.24	-5.09	TG
E20*	St Pietro de Villanueva, Asturias, S	43.35	-5.13	TG
E21*	Braganca, Braganca, P	41.47	-6.46	TG
<i>A. meonanthum</i> Hoffmans. & Link.				
118	Poco do Inferno, Manteigas, Guarda, P	40.37	-7.52	YW
180	Sobredelo, Ourense, S	42.40	-6.91	YW
181	Robledo de Fenar, Leon, S	42.83	-5.54	YW
E48	unknown	-		unknown
E49	unknown	-		IM
Other				
Sierra Nevada hybrid populations (<i>A. barrelieri</i> × <i>A. rupestre</i>)				
23	Luajar to Paterna del Rio, Almeria, S	37.03	-2.95	YW
24	Paterna del Rio, Almeria, S	37.03	-2.95	YW
25	Bayarcal, Almeria, S	37.06	-3.00	YW
26	Bayarcal to Laroles, Granada, S	37.05	-3.02	YW
30	Cadiar to Mecina Bombarron, Granada, S	36.96	-3.17	YW
31	Juviles to Trevelez, Granada, S	36.96	-3.22	YW
32	Nr Juviles, Granada, S	36.95	-3.24	YW
33	Trevelez, Granada, S	37.00	-3.27	YW
35	Nr, Pampaneira, Granada, S	36.93	-3.36	YW

Table 2.1. Details of the localities of populations that were sampled.

'DB' is the database number allocated to every *Antirrhinum* population for which there is material at the University of Edinburgh. An '*' next to the database number indicates populations for which the coordinates were not recorded; therefore the coordinates of the nearest town are entered to facilitate plotting these populations in the maps shown in the following chapters. Database numbers beginning with E are those that have been maintained at Edinburgh prior to this study, those beginning with 'AC' are accessions from the JIC, Norwich (these accession number have been carried over from the Norwich accession database). 'Location' is the nearest town to the population, followed by the province and country. 'S' is Spain, 'P' is Portugal and 'F' is France. The latitude and longitude follows, in decimals. The final column indicates the collector of the material: AH = Andrew Hudson, EC = Enrico Coen, IM = Isabel Mateu-Andres, MC = Manuela Costa, RM = Richard Milne, TG = Thomas Gübitz, YW = Yvette Wilson.

rooting powder and they were planted in soil. Seed from three further plants were collected from each population, when possible. For the locations where seed had not yet matured, flowers from the plants propagated from cuttings were cross-pollinated back in Edinburgh to obtain seed.

2.1.3 Plant growth

All plants were grown in the glass-houses at the Institute of Molecular Plant Sciences, University of Edinburgh. The growth conditions and compost are as detailed in Hudson *et al* (2009).

2.2. Morphological analysis

2.2.1 Growing conditions

Seed collected from wild populations (Table 2.1) were grown in standard conditions to characterise morphological variation within *Antirrhinum*. This was carried out during the summer, from March to September 2007, to utilise natural light and temperature. The seed from each accession were soaked in 100 µl of 10 µM gibberellic acid at 4 °C for 5 days before being sown on soil in the glasshouse. Once germinated, individual seedlings were transplanted into 11cm x 11cm x 11 cm pots approximately when the 3rd pair of leaves were visible (when the plants are ~ 15 cm high), with accessions being transplanted throughout the month of May. Plants were potted on into larger pots when necessary. At the commencement of flowering, the plants were given extra nutrients in the form of plant food to boost their growth. This would not have affected the characteristics of the vegetative parts of the plant that were measured as they were already developed.

Unfortunately, more than half of these plants were accidentally pruned so it was necessary to re-sow these accessions, with the second batch of seedlings being transplanted into the glasshouse at the end of July. To check whether plants grown at this later stage of the season were affected by the different conditions, a few accessions from the first sowing that grew successfully were also re-sown and measured with the second sowing. Due to the shorter day-length before the second batch of plants were expected to flower it was necessary to turn the glasshouse lights on in mid October. This did not seem to affect any of the measurements as it was only for the very end stages of the growth of the plants.

2.2.2 Plant measurements

To characterise the morphology of plants at approximately the same stage of development, each plant was examined and photographed when five flowers on the main inflorescence were open. For those plants that did not develop more than four flowers, it was ensured that the first few flowers

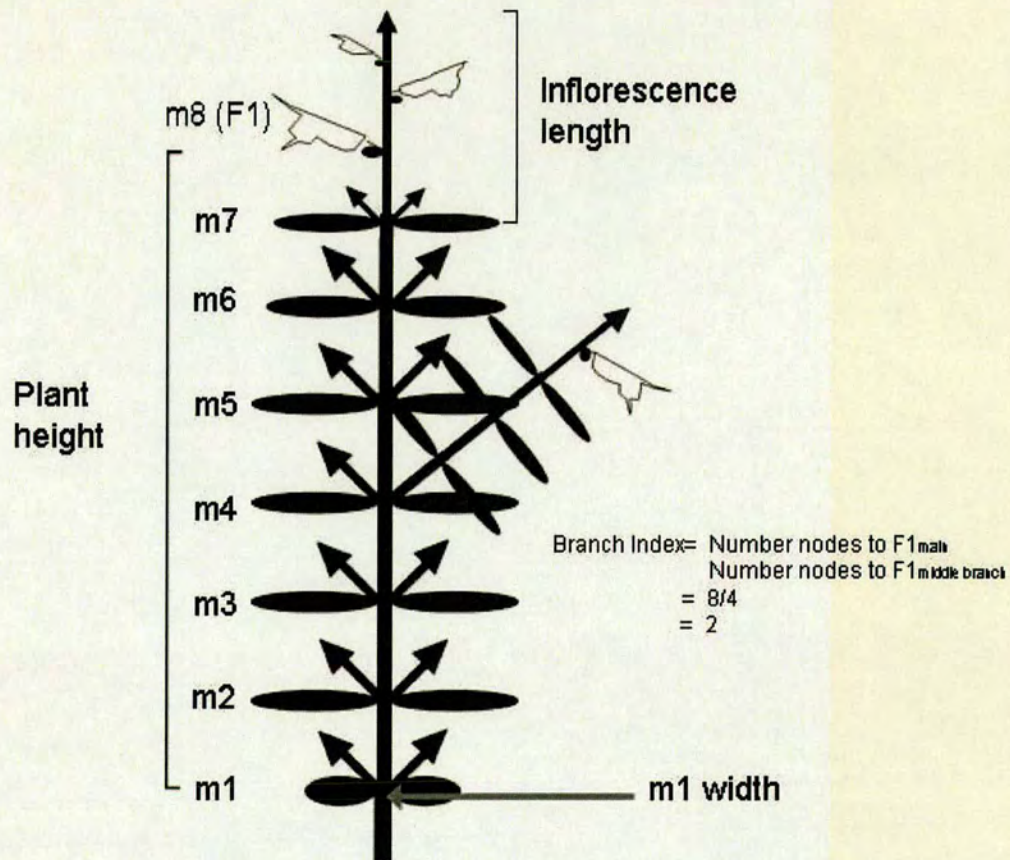


Figure 2.1. Schematic diagram illustrating the labeling of plant parts and the measurements that were taken on the plant.

A metamer consists of an internode and its subtended leaf/bract and branch/flower. Each metamer on the main stem is labelled as 'm1', 'm2', etc. starting from the base of the stem with the cotyledons being m1. Arrows represent branches which grow from the axillary meristem of the leaf. The full branch is shown for metamer 4 only. 'F1' is the first flowering metamer on the main stem, 'stem width' is the diameter of the stem below the cotyledons, plant height is measured from the cotyledons to the first flower and inflorescence length is measured from the base of the first metamer of the inflorescence to its tip. The branch index is calculated as the first flowering metamer on the main stem (m8) divided by the first flowering metamer of the middle branch (in this example the branch subtended by metamer 4, $F1 = m4$).

were fully mature before collecting data from the plant. Occasionally, to avoid losing leaf shape information due to leaves senescing, the metamer 4 leaf of some plants was harvested before this stage. Each plant was photographed in detail in the glasshouse before harvesting its flowers and leaves.

The nomenclature used for the parts of the plant is shown in Figure 2.1. The methods used to collect data for each morphological character described in Chapter 4 are as follows:

Leaf size and shape

One leaf from each main stem metamer of the plant was cut at the base of its petiole. The leaves were arranged on a grid on an A4 piece of white paper, flattened and adhered to the page using transparent tape. Each page was imaged using a Nikon Coolpix 4500 digital camera. Leaf shape and size was then analysed digitally, as described in Section 2.2.3.

Flower characters

Flowers were dissected from each plant at the base of the petiole. Detailed digital images of a single harvested flower from each plant were then taken. To standardise the photographic conditions, the same camera settings were used for all images (the zoom was calibrated to the same value, white balance = AUTO, aperture = 9.5, shutter speed 1/1000 s). The images were taken in a blackened room, using the camera flash. The camera was positioned 55 cm from the flowers. The flowers were then dissected. The dorsal and ventral petals were flattened and adhered to a card covered by black velvet (for optimum photographic conditions) using two-sided cellotape. Each was imaged in standard conditions, as described above. The petals, sepals and stamens were then dissected from the flower and imaged. The style, pedicel, and stamen filament lengths were measured from the digital images, as shown in Figure 2.2. The Matlab program 'Lenwid', written by Anne-Gaelle Rolland-Lagan in Enrico Coen's lab (JIC, Norwich), was used to take linear measurements from the digital images.

Flower colour characters were scored manually from the digital images taken in standard conditions. The corolla, flattened dorsal petal and sepal size and shape were analysed digitally, as described in Section 2.2.3.

Plant architecture

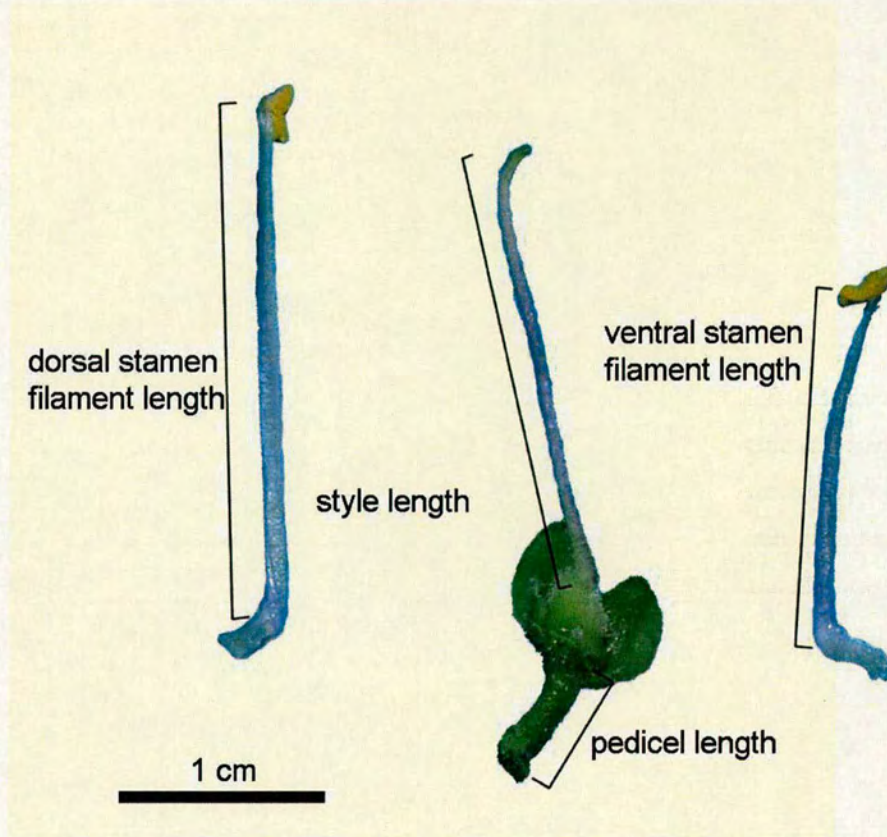


Figure 2.2. Figure showing how the style length, pedicel length and stamen filament length were measured.

The plant architecture measurements - plant height, flowering time, stem width and branching index are described in Figure 2.1.

Epidermal characters

Epidermal imprints were taken from (1) the stem between metamers 1 and 2, (2) the inflorescence stem, (3) the adaxial surface of the metamer 4 leaf (in the middle of the lamina at the widest point of the leaf) and (4) the adaxial surface of the middle of the dorsal petal lobe. Imprints were obtained by placing a small (~2 mm diameter) blob of Loctite superglue on a 76 mm x 26 mm glass microscope slide and then pressing the glue against the surface of the plant for approximately 3 minutes.

The slides were then examined under a Nikon Eclipse E600 microscope and imaged with a Nikon Coolpix 4500 camera. The images were calibrated by first taking an image of a graticule. This scale was then transferred to the images in Adobe Photoshop and used to define an area in which to count the number of cells and the number of trichomes. Trichome morphology was also characterised from these images.

2.2.3 Principal Components Analysis (PCA) of leaf and flower shapes

Shape analysis was carried out using AAMToolbox developed by Andrew Hanna, Andrew Bangham and Enrico Coen (University of East Anglia and JIC, Norwich). Further details can be found on the website <http://fizz.cmp.uea.ac.uk/wiki/AAMToolbox/index.php/AAMToolbox>. It is also described in the publications by Langlade *et al* (2005) and Bensmihen *et al* (2008).

Images were scaled to the same resolution using the 'ImagePrep' module within AAMToolbox. Four projects were created in AAMToolbox, one each to describe the variation of (1) the metamer 4 leaf, (2) the dorsal petal, (3) the flower side and (4) the sepal. Within each project, a point model template was designed to describe the shape under investigation. Each template consists of primary points, which are anchored to key landmarks and secondary points, which are smoothed to capture features between landmarks. The shape within each image was then captured by placing the points defined in the template on the corresponding positions in the image. Each shape is therefore defined by a series of x- and y-coordinates representing the points within the point model. Therefore the dataset consists of a set of point models, with each point model describing the shape of one sample. PCA was carried out on the dataset to summarise the covariances of the coordinates in a few axes that account for most of the variation.

The PCA defines the mean shape and a series of vectors (one for each axis) that describe how the points vary from this shape along each axis. Shapes are therefore quantified by their values along these axes, usually in Standard Deviations (SD) from the mean shape.

2.2.4 Data analysis

Characterisation of morphological variation within and between species

The morphological characterisation described in Section 2.2.2 and 2.2.3 resulted in a set of both continuous and discrete variables for each species. For each species, histograms of each continuous variable were plotted in Origin (OriginLab Corporation, Version 7) and the Shapiro-Wilk normality test was carried out on each of these distributions. In the majority of cases in which normality was rejected it was because there were one or two outlying data points. These were assumed to be caused by experimental error and were removed from the dataset; subsequently nearly all of the distributions were normal. To determine the amount of within- compared to between-species variation one-way ANOVA was then carried out in Minitab v.15 on each continuous variable, after testing that the variances were similar within all species. The variances of each character within each species were generally similar to each other, apart for in species in which one or two individuals were measured. For these species, despite the poor sampling, it was assumed that the variances were the same as for the rest of the species. Fisher's Least Significant Difference test was carried out to test for significant differences between the means all for pair-wise comparisons of species at the 0.05 level.

Phenotypic analysis

To define the phenotypic space using PCA, the values of both the continuous and discrete variables of each individual were combined in a matrix, with the individuals as rows and the variables as columns. The data were then standardised to have similar means and variation: each case had the mean column value subtracted and was then divided by the standard deviation of the column. Two sets of PCA were carried out. The first set was on the 'individuals \times variables' matrix. For the second set, the mean values for each population were calculated and PCA was carried out on the resulting 'population \times variables' matrix. These analyses were carried out using PAST (Hammer *et al* 2001). Each sample was then plotted in the space defined by axes 1 and 2, axes 1 and 3, axes 1 and 4, and axes 2 and 4. The vectors showing the effects of each character in the plots of axes 1 and 2, and 1 and 3 were obtained from the bi-plot option within PAST.

To determine the extent to which populations of each species cluster together in the phenotypic space, neighbour-joining was carried out on the distances between populations in the space defined by the first four axes of PCA analysis. The Euclidian distance, D_E , between two populations, '1' and '2', was calculated by the formula:

$$D_E = \sqrt{((x_1 - x_2)^2 + (y_1 - y_2)^2 + (z_1 - z_2)^2 + (v_1 - v_2)^2)}$$

where x, y, z and v are the axis values of the populations.

The Euclidian distance was calculated between all pair-wise combinations of populations using Excel. Neighbour-joining analysis was carried out using NEIGHBOUR in PHYLIP.

2.3 Molecular methods

2.3.1 DNA extraction

DNA was extracted from either fresh or dried leaf tissue. Fresh tissue was frozen at -80 °C before commencing the extraction protocol. Approximately 0.1 g tissue was placed in a 1.5 ml Eppendorf tube with two carbide beads. The tissue was ground using a Retsch MM300 tissue lyser for 2 minutes at 30 s⁻¹ frequency. Immediately after grinding the tissue, 600 µl extraction buffer [100 mM Tris-HCl (pH 8.0), 1.4 M NaCl, 20mM EDTA, 2% CTAB and 0.2% MCE (mercaptoethanol)] was added to the Eppendorf and the mix was ground for a further 1 minute. The tube was then placed in a heating block at 65°C. After 20-30 minutes 600 µl chloroform (CH₃Cl₃) was added and the tube was briefly vortexed and then centrifuged at 18 000 g in an Eppendorf 5417 centrifuge for 5 minutes. The supernatant (containing the DNA) was then transferred to a new Eppendorf tube and 400 µl isopropanol was added and the tube contents were mixed briefly. The DNA pellet was then precipitated by centrifuging the tube at 18 000 g for 10 minutes. The supernatant was pipetted off the pellet and the tube was left open under a fume hood for approximately 1 hour for all the isopropanol to evaporate from the tube. To remove the RNA, 50 µl TE buffer [10mM Tris-HCl (pH 8.0), 1 mM EDTA] with 1/1000th RNAase was added to the pellet and the Eppendorf left 4°C overnight.

The DNA was then washed by adding 1/10th the starting value of 3M NaOAc (pH 5.2) and 2½ times the starting volume of ethanol. The contents of the tube were mixed and then centrifuged for 10 minutes at 20 800 g. The solution was pipetted from the DNA pellet and the tube was left open

under a fume hood for approximately one hour for the alcohol to evaporate from it. The DNA was then dissolved in 50 µl TE buffer.

The DNA concentration was measured using an ND-1000 NanoDrop spectrophotometer and diluted to the correct concentration for subsequent techniques in water. To check the quality and quantity of the DNA before AFLPs, 2 µl of each sample were run out on an 0.8% agarose gel.

2.3.2 Amplified Fragment Length Polymorphisms (AFLPs)

The AFLP method consists of several steps. Genomic DNA is first digested by (usually) two restriction enzymes, which leave overhangs at each end of the fragment. This enables adapters (one specific to each enzyme) that have one longer strand, the end of which is complementary to the overhang of the DNA fragment, to be ligated to the fragments. The fragments can then be amplified using primers specific to the adapter sequences. Two rounds of PCR are then carried out: the first (pre-selective PCR) is to amplify all fragments and the second (selective PCR) is to amplify a subset of fragments by adding selective bases to the primers. This is to reduce the number of homoplasious fragments obtained.

Preparation of adapters

The adapters were prepared by heating equimolar volumes of the adapter strands (Table 2.2) with 1/10th volume 1x OnePhorAll buffer [10 x buffer contains 100mM Tris-Ac (Tris-acetate; pH 7.5), 100 mM MgAc and 500 mM KAc] to 94°C and leaving them on the bench to gradually cool to room temperature.

Preparation of DNA template

Approximately 250 ng genomic DNA was digested with 5 units each of *MseI* and *PstI* restriction enzymes (New England Biolab (NEB)). Digestions were carried out in a total volume of 20 µl, consisting of the template, restriction enzymes and 1x Restriction-Ligation (RL) buffer [5x RL buffer consists of 50mM Tris-Ac (pH 7.5), 50mM MgAc, 250 mM KAc, 25 mM DTT (dithiothreitol), 250 ng/µl BSA (bovine serum albumin)]. The digestion reactions were incubated for 2 hours at 37°C.

The adapters were then ligated to the DNA fragments. This was carried out by adding 5 µl of ligation mix [1 µl of 5x RL buffer, 0.5 µl of the *Pst* adapter (5µM), 0.5 µl of the *Mse* adapter (50 µM), 0.5 µl rATP (10 mM) and 0.4 units T4 DNA ligase (New England Biolabs), made up to 5 µl

Primer function	Primer name: sequence (5' → 3')
Mse adapter strands	MseI AdF: GAC GAT GAG TCC TGA G MseI AdR: TAC TCA GGA CTC AT
Pst adapter strands	PstI AdF: CTC GTA GAC TGC GTA CAT GCA PstI AdR: TGT ACG CAG TCT AC
pre-selective primer combination	M00: GAT GAG TCC TGA GTA A (complementary to Mse adapter) P00: GAC TGC GTA CAT GCA G (complementary to Pst adapter)
Pst selective primers	P11: GAC TGC GTA CAT GCA GAA P12: GAC TGC GTA CAT GCA GAC P14: GAC TGC GTA CAT GCA GAT
Mse selective primers	Mse-CAC: GAT GAG TCC TGA GTA A CAC Mse-AGG: GAT GAG TCC TGA GTA A AGG Mse-ACG: GAT GAG TCC TGA GTA A ACG Mse-ACA: GAT GAG TCC TGA GTA A ACA

Table 2.2. AFLP primer sequences.

Primer combination	ABI3730 channel	Pst primer- fluorescent label	Mse primer
1	blue	P11-6FAM	Mse-CAC
2	red	P11-PET	Mse-AGG
3	green	P12-VIC	Mse-ACG
4	yellow	P14-NED	Mse-ACA

Table 2.3. Primer combinations used for the AFLP selective PCRs.

with water] to the digestion reaction. Ligation reactions were carried out overnight at room temperature.

Pre-selective PCR

Pre-selective amplification reactions were carried out in a total volume of 20 μ l. The reaction mix contained 5 μ l of the template from the digestion-ligation reactions, 1x PCR buffer (Roche, supplied with the enzyme [100mM Tris-HCl, 15 mM MgCl₂, 500 mM KCl (pH 8.3)]), 0.4 μ l dNTPs (10 mM), 0.6 μ l (10 μ M) each of the primers P00 and M00 (Table 2.2) and 0.5 units of *Taq* DNA polymerase (Roche). The PCR reactions were carried out using the AFLP-PCR1 program (Table 2.5). The success of digestion, ligation and pre-selective PCR was checked by running 4 μ l of the PCR product on a 1% agarose gel. A smear of bands from 100 bp to 800 bp indicated that the reactions were successful.

Selective PCR

In addition to selecting a subset of fragments for amplification, the selective PCR uses one primer that is fluorescently labelled to enable fragments to be detected. Therefore, the primer complementary to the Pst adapter (P00) has two extra selective bases added and is labelled with one of the ABI (Applied Biosystems, ABI) dyes compatible with the ABI filter set G5. The primer complementary to the Mse adapter (M00) has three selective bases added (Table 2.3). The reactions consisted of 1 μ l of the template DNA from the pre-selective PCR, 1x PCR buffer (Roche, supplied with the enzyme), 0.2 μ l dNTPs (10 mM), 0.25 μ l (10 μ M) each of the Pst and Mse selective primers (Table 2.2) and 0.25 units of *Taq* DNA polymerase (Roche). The reaction mix was made up to 10 μ l volume with water. The PCR reactions were carried out using the AFLP-PCR2 program (Table 2.5).

Selective PCR II

The method of O'Hanlon and Peakall (2000) was used to test for band size homoplasy within a subset of samples. An additional base, one of each of the nucleotides, was added to the Mse selective primer and selective PCR was carried out as described in the previous section. The PCR reactions were carried out using the AFLP-PCR3 program (Table 2.5).

Preparation of samples for running on the ABI3730

The AFLP samples were scanned using an ABI3070 sequencer at the University of Edinburgh sequencing service (the Gene Pool). Typically, four selective PCRs were carried out, each using a

different set of selective primers (Table 2.3). Each Pst selective primer was labelled with a different fluorescent dye of the ABI dye set DS-33. Samples were therefore prepared by mixing 1 µl of each reaction in a new tube. The tubes were vortexed and briefly centrifuged, then 1 µl of this mix was added to 9 µl Hi-Di Formamide (ABI) containing the LIZ size standard (ABI). This was prepared by diluting 1 µl of the size standard in 1 ml of the formamide.

2.3.3 Chloroplast loci amplification and sequencing

PCR reactions

The chloroplast loci from Shaw *et al* (2005) and (2007) were tested within *Antirrhinum* to determine if they amplified and which were the most informative for phylogenetic analysis. Table 2.4 summarises the primer sequences and PCR programs (Table 2.5) used to carry out the reactions.

A standard PCR reaction mix was used, consisting of 2 µl template DNA (2.5 – 5 ng/µl), 1 µl PCR buffer (NEB, supplied with the enzyme [10mM KCl, 10mM (NH)₄ SO₄, 20mM Tris-HCl, 2 mM MgSO₄, 0.1% Triton x100, pH 8.8]), 0.1 µl dNTPs (10 mM), 0.1 µl (10 µM) each of the forward and reverse primer and 0.1 µl *Taq* DNA polymerase (NEB). The reaction mix was made up to 10 µl volume by adding water.

Sequencing reactions

Sequencing reactions were carried out by the University of Edinburgh sequencing service (the Gene Pool). Samples were prepared by adding 0.6 µl of the PCR product and 1 µl primer (10 mM) to 4.4 µl water.

2.3.4 Restriction enzyme digests of PCR products

Sequence information of the chloroplast loci was used to develop cleaved amplified polymorphism (CAP) markers to enable easier genotyping of chloroplast haplotype. Digestion reactions were carried out by adding 4 µl of the PCR product to a reaction mix containing 2 units of the restriction enzyme (supplied by NEB), 1 µl of the corresponding enzyme buffer (supplied with enzyme), 0.1 µl BSA and 4.8 µl water. Digestions were incubated as instructed by the enzyme supplier (NEB). The products were then separated by agarose gel electrophoresis to determine the samples that were digested; 10 µl were run out on 2.5 % agarose gels, as described below.

2.3.5 Agarose gel electrophoresis of DNA

Locus	Forward Primer [name: sequence (5'→3')]	Reverse Primer [name: sequence (5'→3')]	PCR Program
<i>atpB-rbcL</i>	atpB: ACATCKARTACKGGACCAATAA	rbcL: AACACCAGCTTTRAATCCAA	atpB
<i>atpI-atpH</i>	atpI: TATTACACACYGGTATTCAGCT	atpH: CCAAYCCAGCAGCAATAAC	THIII
<i>ndhL-TabE</i>	ndhL: ATGCCYGAAGTTGGATAGG	tabE: GGTTCAGTCCCTCTATCCC	THIII
<i>petL-psbE</i>	petL: AGTAGAAACCGAAATTAAGTTA	psbE: TATCGAATACTGGTAATAATATCAGC	THIII
<i>psbD-trnT</i>	psbD: CTCCGTARCCAGTCATCCATA	trnT-R: CCTTTTAACTCAGTGGTAG	THIII
<i>psbI-petA</i>	psbI: ATAGGTACTGTARCYGGTATT	petA: AACARTTYGARAAGGTTCAATT	THIII
<i>rpl14-rpl36</i>	rpl14: AAGGAAATCCAAAGAAGAACTCG	rpl36: GGRITGGAAACAATTACTATAATTGG	THIII
<i>rps16-trnK</i>	rps16F2: AAAAGTGGGTTTATATGATCC	trnKb: TTAAGGCGGAGTACTTACC	THIII
<i>trnC-ycf6R</i>	trnCD: CCAGTTCAATCTGGGTGTC	Ycf6R: TACCATTAAAGCAGCCCAAG	trnCDY
<i>trnH-PsbA</i>	psbA: CGCGCATGGTGGATTCAACAATC	trnH: GTTATGCATGAA CGTAATGCTC	trnH-PsbA
<i>trnH-trnK</i>	trnHb: ACGGGAATTGAACCCGCGCA	trnK: CCGACTAGTTCGGGTTCTGA	trnHK
<i>trnK-trnK</i>	trnK(F): AACCCGGAAC TAGTCGGATG	trnK(R): TCAATGGTAGAGTACTCGGC	trnKK
<i>trnL-ndhF</i>	trnL: CTGCTTCCTAAGAGCAGCGT	ndhF: GAAAGGTATKATCCAYGMATATT	THIII
<i>trnD-trnT</i>	trnD: ACCAATTGAAC TACAATCCC	trnT: CTACCACTGAGTTAAGG	trnDT
<i>trnS-trnFM</i>	trnSb: GAGAGAGAGGGAATTCGAACC	trnFM: CATTAACCTTGAGGTC ACGGG	trnSFM
<i>trnS-trnG</i>	trnSa: GCCGCTTTAGTCCACTCAGC	trnG: GAACGAATCACA CTTTACCCAC	trnSG
<i>trnS-trnR</i>	trnSRF: CGCCGCTTTAGTCCACTCA	trnSRK: ATTGCGTCCCAATAGGATTTGAA	trnSR
<i>trnQ-rps16</i>	trnQ: GCGTGCGCCAAGYGGTAAAGGC	rps16: GTTGCTTTTACACATCGTTT	THIII
<i>trnT-ndhC</i>	trnV: GTCTACGGTTCGARTCCGTA	ndhC: ATTATTAGAAATGYCCARAAATATCATATTC	THIII

Table 2.4. The sequences of the primers and the PCR programs used to amplify chloroplast loci

Program name	Program
AFLP-PCR1	1x (72 °C, 120s), 20x (94 °C, 20s; 56 °C, 30s; 72 °C, 120s), 1x (60 °C, 30 minutes), 4 °C
AFLP-PCR2	1x (94 °C, 120s), 10x (94 °C, 20s; 66 °C decreasing 1 °C each cycle until 56 °C, 30s; 72 °C, 120s), 20x (94 °C, 20s; 56 °C, 30s; 72 °C, 120s), 1x (60 °C, 30 minutes), 4 °C
AFLP-PCR3	1x (94 °C, 120s), 10x (94 °C, 20s; 70 °C decreasing 1 °C each cycle until 61 °C, 30s; 72 °C, 120s), 20x (94 °C, 20s; 61 °C, 30s; 72 °C, 120s), 1x (60 °C, 30 minutes), 4 °C
atpB	1x (94 °C, 4 minutes), 40x (94 °C, 45s; *49 °C, 75 s; 72 °C, 75s), 1x (72 °C, 10 minutes), 4 °C * tried lowering annealing temperature to 47 °C to be able to amplify across all samples.
THIII	1x (80 °C, 5 minutes), 30x (95 °C, 60s; 50 °C, 60s; 0.3 °C/s ramp to 65 °C; 65 °C, 4 minutes), 1x (65 °C, 5 minutes), 4 °C
trnDT	1x (94 °C, 4 minutes), 40x (94 °C, 45s; 54.5 °C, 30 s; 72 °C, 2 minutes), 1x (72 °C, 10 minutes), 4 °C
trnHK	1x (94 °C, 4 minutes), 40x (94 °C, 45s; 62 °C, 45 s; 72 °C, 2 minutes), 1x (72 °C, 10 minutes), 4 °C
trnH-psbA	1x (94 °C, 4 minutes), 40x (94 °C, 30s; 53 °C, 30 s; 72 °C, 60s), 1x (72 °C, 10 minutes), 4 °C
trnKK	1x (94 °C, 4 minutes), 40x (94 °C, 45s; *53.5 °C, 45 s; 72 °C, 3 minutes), 1x (72 °C, 10 minutes), 4 °C * lowered annealing temperature to 47 °C to be able to amplify across all samples.
trnSG	1x (96 °C, 5 minutes), 40x (96 °C, 45s; 52 °C, 45 s; 72 °C, 1 minute), 1x (72 °C, 10 minutes), 4 °C
trnSFM	1x (94 °C, 4 minutes), 40x (94 °C, 45s; 62 °C, 30 s; 72 °C, 2 minutes), 1x (72 °C, 10 minutes), 4 °C
trnSR	1x (94 °C, 4 minutes), 40x (94 °C, 45s; 53 °C, 45 s; 72 °C, 3 minutes), 1x (72 °C, 10 minutes), 4 °C

Table 2.5. PCR programs

Nuclear DNA, PCR products and restriction enzyme digests were visualised by gel electrophoresis. The gels were prepared by heating of 0.8-2.5% (w/v) agarose in $\frac{1}{2} \times$ TBE buffer [0.089 M Tris-borate, 0.089 M boric acid and 0.022 M EDTA] in a microwave oven, until the agarose was fully dissolved. The gel was then allowed to cool to approximately 65 °C before adding ethidium bromide. The concentration of ethidium bromide in the gel was 0.5 µg/ml. The solution was then poured into a horizontal tray until approximately 3-5 mm thick and left to set, before being submerged horizontally in a tank containing $\frac{1}{2} \times$ TBE buffer. Approximately 1/10th volume loading buffer [0.25% bromophenol blue, 0.25% xylene cyanol and 30 % glycerol in water] was added to each sample before loading it to the gel. Samples were then loaded into the gel lanes and the gels were run at 100-150 volts, for the appropriate amount of time, depending on the size of the fragments being analysed and the resolution required. To calibrate the sizes of the fragments obtained, DNA ladder with loading buffer (approximately 250 ng DNA) added was loaded into one lane of the gel.

The DNA fragments within the gel were visualised and photographed using a GeneFlash (Syngene) UV illuminator.

2.4 Population genetic and phylogenetic methods

2.4.1 AFLP scoring

The FSA files containing the AFLP profiles were converted from MAC to PC format. The fragment sizes were then calibrated using Genescan (ABI). The files were uploaded into Genographer (v1.6.0; Benham 2001) and scored manually within Genographer. The same six samples were included on each 96 well plate to ensure that the fragment sizes were correctly aligned between all plates.

2.4.2 Neighbour-joining phylogenies using Jaccard distances

The matrix consisting of the AFLP scores for all individuals was loaded into PAST (Hammer *et al* 2001). The Jaccard distance was calculated between all pair-wise combinations of individuals within PAST and neighbour-joining analysis carried out. Bootstrap sampling of loci was carried out to estimate the support of nodes.

2.4.3 Principal Coordinates Analysis (PCoA) of AFLPs

PCoA was carried out on the matrix of AFLP scores for all individuals, using the Jaccard similarity index in PAST. The transformation exponent, 'c', was set to 2.

2.4.4 AFLP band frequency estimation within species

AFLP allele frequencies were calculated using the method of Zhivotovsky (1999) with uniform prior distribution of allele frequencies, in the program AFLPSurv (Vekemans *et al* 2002). This method estimates the frequency of the null allele at each locus based on the sample size and the number of individuals in the sample that lack the AFLP fragment using a Bayesian method that assumes a uniform distribution of allele frequencies (Vekemans *et al* 2002).

2.4.5 Neighbour-joining phylogenies using Nei's Genetic distance

Genetic distances between populations were estimated using AFLPSurv. Nei's D genetic distance (Nei 1972) was estimated using the method of Lynch and Milligan (1994), which adjusts for the bias introduced by using dominant markers. To estimate the support of each node, bootstrapping of AFLP loci was also carried out in AFLPSurv. Neighbour-joining analysis of the resulting distance matrices was carried out in 'NEIGHBOUR' (PHYLIP, Felsenstein 1985). The 'M₁' majority rule method within 'consense' (PHYLIP) was then used to resolve the consensus tree. The frequency at which a set of species must occur among the input trees to be represented was set to 0.6. The support of each node was obtained from the outfile of the analysis. The program 'drawtree' (PHYLIP) was then used to render the tree, with the support for nodes being put in by hand in Adobe Photoshop.

2.4.6 Chloroplast sequence analysis

The chloroplast sequence files (AB1 format) were converted to 'phred' format by the Gene Pool (University of Edinburgh sequencing service). This was because the sequence files were not truncated prematurely using this method. Within each sequence loci for which the nucleotide assignments were ambiguous were determined by inspecting the trace file using Chromas Lite (v2.01, Technelysium Pty Ltd).

To identify chloroplast haplotypes from the chloroplast sequences and resolve a chloroplast haplotype network, all sequences were aligned using T-coffee (Notredame *et al* 2000).

Polymorphic loci were then identified by comparing all aligned sequences and the characters at these loci were scored. The chloroplast haplotype network was resolved by hand, by first grouping species that shared the least frequent polymorphisms. Using this approach it was possible to identify polymorphisms that contradicted multiple other characters and were therefore assumed to be homoplasious. A matrix of the scoring of all polymorphic loci was also analysed using

parsimony in PAUP* (Version 4.0b10, Swofford 2001). The most resolved phylogeny was obtained after removing the loci that were assumed to be homoplasious. The topology of this phylogeny was identical to that resolved by hand.

2.4.7 Structure analysis

To identify the patterns of genetic structure within *Antirrhinum*, *Structure* (Pritchard *et al* 2000, Falush *et al* 2003 and 2007) simulations were carried out on a dataset of 293 individuals that were genotyped at 506 AFLP loci. Default parameter settings were used (Table 2.6) with some key parameters being varied for different simulations to determine whether further populations could be detected by the model.

INFERALPHA=1	INFERLAMBD= 0 or 1
POPSPECIFICALAMBD=0	POPALPHAS=0
ADMBURNIN=2500	MIGRPRIOR=0.001
FPRIORMEAN= varied	FPRIORS= varied
ONEFST=0	LAMBD=1
UNIFPRIORALPHA=1	ALPHAMAX=20
ALPHAPRIORA=0.05	ALPHAPRIORB=0.001
ALPHAPROPSD=0.0250	

Table 2.6 **Parameter settings for *Structure* models.**

The parameters that were varied were the settings of the prior ‘F’ values (FPRIOR mean, and FPRIORS), which influence the ability of the model to detect population sub-division, and whether uniform allele frequencies are assumed for each population (INFERLAMBD). The parameters were varied within the limits tested by Falush *et al* (2003). Admixture was allowed for all simulations of the model and both models that assumed correlated allele frequencies between populations and models that assumed independent allele frequencies were used. This was to determine the robustness of the results obtained. For all simulations, the burn-in was set to 20 000 and the 120 000 replications were carried out. For each number of inferred populations (‘K’), the model was run 5 to 8 times. For each value of K the extent to which the inferred ancestral populations were congruent between different runs of the model was assessed using CLUMPP (Jakobsson and Rosenberg 2007). The results of the simulations were then visualised using DISTRUCT (Rosenberg 2004).

Chapter 3: Genetic delimitation of *Antirrhinum* species and analysis of their evolutionary relationships

3.1 Introduction

3.1.1 Chapter aims

The *Antirrhinum* species are difficult to delimit using morphological characters and previous studies using both morphological and molecular characters have failed to resolve species relationships, as discussed in Chapter 1. There are two main aims of this chapter. The first is to delimit *Antirrhinum* species using genetic fingerprinting techniques. The second aim is to resolve the genetic relationships of *Antirrhinum* species and develop an explicit hypothesis on their evolutionary history.

3.1.2 Molecular approaches and taxon sampling

It is difficult to resolve a phylogeny of the *Antirrhinum* species because of their recent diversification, which may have led to lineage sorting of nuclear and chloroplast polymorphisms, and because they may have undergone subsequent hybridisation with each other. The phylogenetic signal of lineage sorting and hybridisation is identical, as discussed in Section 1.2.2. Therefore, it is often necessary to use a combination of approaches to distinguish these two processes.

One approach is to sequence multiple nuclear loci in order to identify phylogenetic signal against noise generated by stochastic processes, such as lineage sorting and gene duplication and subsequent loss (e.g. Rokas *et al* 2003, Alvarez *et al* 2005). Hybridisation would be inferred when sets of topologies, which are incongruent, occur more frequently than by chance (Linder and Rieseberg 2004). However, I did not think this a suitable approach for the *Antirrhinum* genus for several reasons. The first is that previous studies have shown a low level of sequence variation for most nuclear genes (Gübitz *et al* 2003). Secondly, because of this low sequence variation in combination with either lineage sorting or hybridisation, little phylogenetic resolution has been obtained for any nuclear locus (Chaffe 2003, Gübitz *et al* 2003, Vargas 2004 and 2009). It is therefore likely that sequencing of numerous nuclear loci would be necessary to make strong phylogenetic inference. Furthermore, given the poor species delimitation and evidence of hybridisation, adequate sampling within each species was considered essential to test for geographic structuring of genetic variation and to delimit species. Sequencing multiple nuclear loci of numerous individuals of each species was unfeasible for this study.

Amplified Fragment Length Polymorphisms (AFLPs, Vos *et al* 1995) are potentially more suitable markers for resolving the phylogeny of the *Antirrhinum* species as they provide information from numerous loci distributed throughout the genome (Mueller and Wolfenbarger 1999). The use of AFLPs in phylogenetic reconstruction has successfully resolved relationships in many groups of closely related species (Koopman 2005, Mendelson and Simons 2006). Furthermore, numerous individuals can be genotyped for a reasonable cost, making AFLP analysis feasible for identifying clusters of related individuals and therefore delimiting species.

A second approach that can be used to detect hybridization is to test for discordance between nuclear genotypes and chloroplast haplotypes, which are maternally inherited in most flowering plant families (Wendel and Doyle 1998). As lineage sorting may also influence the distribution of cytoplasmic markers, such cytonuclear incongruence should be interpreted in a phylogeographic context (Wendel and Doyle 1998, Comes and Abbott 2001, Funk and Omland 2003). Hybridisation is inferred when species from the same geographic region have divergent nuclear genotypes or morphology, but related chloroplast haplotypes. The maternal inheritance and haploid nature of the chloroplast confers two further advantages in using chloroplast sequence information to infer evolutionary relationships. The first is that relationships of chloroplast haplotypes reflect evolutionary lineages that have not been influenced by recombination. The second is that the effective population size is half that of nuclear loci, leading to its more rapid fixation in populations, so there is less likelihood of lineage sorting causing inaccurate phylogenetic inference (Avice 1994).

A third approach to explicitly test hypotheses of recent population divergence compared to population divergence over a long time period with gene flow is to use Isolation with Migration (IM) modelling (Hey and Nielsen 2004). These models are most suitable for testing recently diverged sister populations and assume that there are no unsampled populations exchanging genes with the studied populations and their ancestors (Hey and Nielsen 2004, Strasburg and Rieseberg 2010). They were therefore considered inappropriate for the *Antirrhinum* genus at the commencement of this project given our poor understanding of *Antirrhinum* species delimitation and relationships. The results described in the following chapters provide a framework for designing robust models for testing recent divergence versus hybridisation within the *Antirrhinum* genus.

The aim of this chapter is to delimit *Antirrhinum* species and infer their relationships with AFLPs, the same samples also are genotyped at chloroplast loci to further resolve evolutionary lineages and

identify episodes of hybridisation. To identify geographic structure using this approach, populations from throughout the distribution of each species were sampled, as detailed in Chapter 2.1.

3.2 Phylogeographic analysis of chloroplast markers

Previous phylogenetic studies using chloroplast sequence information of individual loci revealed little sequence variation, as discussed in Chapter 1.2.2. Therefore, to identify the most informative markers, the chloroplast loci detailed in Shaw *et al* (2005 and 2007) were screened in a few individuals from the different morphological subsections of *Antirrhinum*. Amplification of 19 loci was attempted for one individual from each of the species *A. siculum*, *A. latifolium*, *A. majus tortuosum*, *A. majus*, *A. valentinum*, *A. pulverulentum*, *A. braun-blanquetii*, *A. mollissimum*, *A. hispanicum* and *A. majus linkianum*. The loci that were tested and the success with which they were amplified and sequenced are indicated in Table 3.1. Little sequence variation was found in the loci, with an average of one polymorphism per 100 bases (Figure 3.1). Despite having the highest occurrence of polymorphisms, the *psbA-trnH* and *atbI-atbH* were considered unsuitable for further use because the *psbA-trnH* locus was too short to contain many informative polymorphisms and both loci contained repeats that made their sequences difficult to align.

Regions of three loci, *trnD-trnT*, *trnS-trnR*, and *trnS-trnFM* were determined to be the most informative and were sequenced for 90 accessions that represent the geographic range of each *Antirrhinum* species. Within the combined sequence of 2580 bp, 81 single nucleotide polymorphisms (SNPs) and three indels were found. Of these polymorphisms, 30 SNPs were detected in only one accession and were therefore phylogenetically uninformative. Based on the remaining 54 informative sites, 34 haplotypes were identified and the evolutionary relationships between the haplotypes were reconstructed by parsimony. To allow full resolution of the haplotype network, 12 SNPs were assumed to be homoplasious because they were not fixed in any species and contradicted multiple polymorphisms supporting deeper divergences and so were removed from the analysis. In the resulting haplotype network shown in Figure 3.2, these polymorphisms have been returned to terminal branches.

The chloroplast haplotype network consists of four main clades, labelled I-IV in Figure 3.2. Clade I consists of *A. siculum*, with all sampled *A. siculum* accessions being placed in this clade. Clade II, which consists predominantly of species in subsections *Antirrhinum* and *Streptosepalum*, then diverges from clades III and IV, which comprise mainly species in subsection *Kickxiella*.

Locus	Approximate fragment size (Kb)	Sequencing comments (primer: comment)
<i>atpB-rbcL</i>	did not amplify	
<i>atpI-atpH</i>	1.2	atpI: only ~260 bp sequenced successfully atpH: ~ 500 bp sequenced successfully
<i>ndhJ-trnF</i>	1.2	ndhJ: ~ 400 bp sequenced successfully tabE: ~ 540 bp sequenced successfully
<i>petL-psbE</i>	did not amplify	
<i>psbD-trnT</i>	1.6	psbD: poor sequence obtained trnT: poor sequence obtained
<i>psbJ-petA</i>	did not amplify	
<i>rpL14-rpL36</i>	1.1	Poor amplification
<i>rps16-trnK</i>	did not amplify	
<i>trnC-ycf6R</i>	0.3	TrnCD
<i>trnD-trnT</i>	1.0	*trnT
<i>trnH-trnK</i>	1.7	trnH: ~ 700 bp sequenced successfully trnK: ~ 550 bp sequenced successfully
<i>trnH-PsbA</i>	0.4	psbA
<i>trnK-trnK</i>	1.8, 2.8	Two fragments obtained. Not sequenced
<i>trnL-ndhF</i>	did not amplify	
<i>trnS-trnG</i>	0.7	trnSa
<i>trnS-trnFM</i>	1.4	trnSb *trnFM: sequence from this end of fragment more polymorphic
<i>trnS-trnR</i>	1.7	*trnSRF: sequence from this end of fragment more polymorphic trnSRR
<i>trnQ-rps16</i>	0.8	trnQ: ~ 450 bp sequenced successfully
<i>trnV-ndhC</i>	1.2	TrnV: ~ 540 bp sequenced successfully ndhC: ~ 500 bp sequenced successfully

Table 3.1. Details of chloroplast loci tested in *Antirrhinum*

Chloroplast loci were tested in one individual from each species *A. siculum*, *A. latifolium*, *A. majus tortuosum*, *A. majus*, *A. valentinum*, *A. pulverulentum*, *A. braun-blauetii*, *A. mollissimum*, *A. hispanicum* and *A. majus linkianum*. The fragment size was estimated from agarose gel electrophoresis. The sequencing comments indicate which primer was used to sequence the fragment. The comments indicate when the sequencing reactions were not fully successful i.e. only part of the fragment could be sequenced. This usually occurred when there were a high number of repeats in the locus. ‘*’ indicates the sequences that were used to reconstruct the chloroplast haplotype network

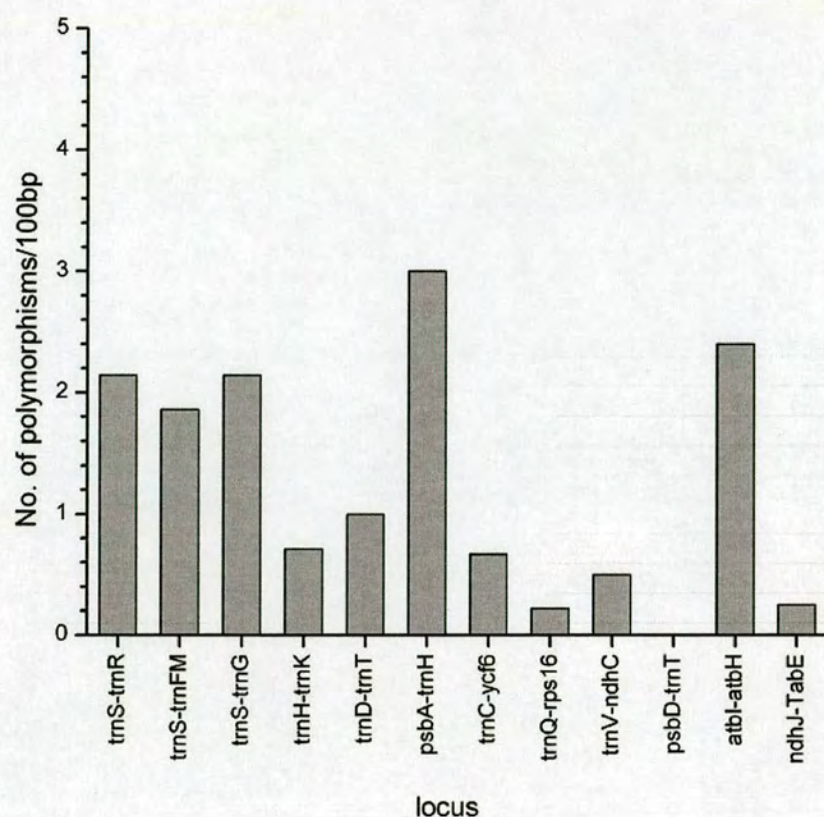


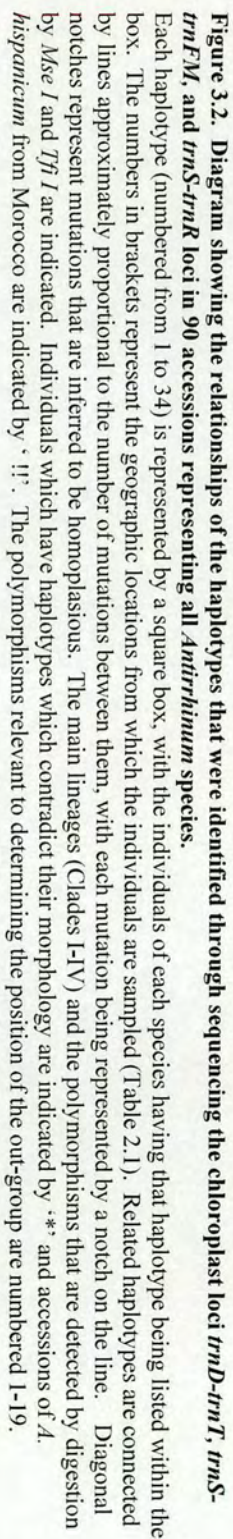
Figure 3.1. Graph showing the number of polymorphisms per 100 bp for each of the chloroplast loci sequenced from one individual of different species.

One individual each of *A. siculum*, *A. latifolium*, *A. majus tortuosum*, *A. majus*, *A. valentinum*, *A. pulverulentum*, *A. braun-blauquetii*, *A. mollissimum*, *A. hispanicum* and *A. majus linkianum* was sequenced at each of the loci shown. The number of polymorphisms per 100 bp was then estimated by comparing the sequences of the above individuals. Details of the sequence length and primers used to sequence the fragments are described in Table 3.1.

Chloroplast haplotypes therefore provide general support for the classical morphological subsections Antirrhinum and Kickxiella. However, several taxa have chloroplast haplotypes that are incongruent with their morphology in one of two respects. Firstly, all accessions of *A. latifolium* (subsection Antirrhinum) carry Clade IV haplotypes normally associated with subsection Kickxiella and *A. sempervirens*, *A. lopesianum*, *A. pertegasii* and *A. molle* (subsection Kickxiella) are fixed for Clade II haplotypes more commonly found in subsections Antirrhinum and Streptosepalum. The second type of incongruence involves *A. majus tortuosum*, *A. barrelieri* and *A. australe* from subsection Antirrhinum and *A. pulverulentum* from subsection Kickxiella. Each of these species contains haplotypes from the Antirrhinum clade as well as from the Kickxiella clade.

To determine the geographic pattern of the haplotype clade distribution and the extent to which the haplotype clades are fixed within species and subsections, a further 273 accessions were genotyped, bringing the total number of locations sampled to 156. Haplotypes belonging to Clade IV are distinguished by an *MseI* restriction site in the *trnD-trnT* locus, while a *TfiI* restriction site in the *trnS-trnR* locus identifies Clade II haplotypes. The mutations associated with these restriction site polymorphisms are indicated on Figure 3.2. Digestion of PCR products was therefore used to identify additional accessions with Clade II or Clade IV haplotypes, while haplotypes that lacked both restriction sites were assumed to belong to Clade III, unless they were from *A. siculum*, in which case they were assumed to belong to Clade I. The resulting clade designations of the 273 additional accessions are shown in Table 3.2. The patterns of occurrence of the different haplotypes within species is consistent with those observed in the haplotype network obtained by sequencing and the deeper taxon sampling confirmed the previous patterns of incongruence between morphology and haplotype. All accessions sampled of *A. sempervirens* and *A. molle* from subsection Kickxiella were fixed for Clade II haplotypes and *A. australe*, *A. barrelieri* and *A. majus tortuosum* accessions from southern Spain have both Clade IV and Clade II haplotypes. Inclusion of additional samples also identified an additional source of incongruence in that the previous *A. majus litigiosum* accessions from central Spain had only Clade II haplotypes, whereas additional populations from the Valencia region were found to carry Clade IV haplotypes.

These analyses revealed a geographic component to chloroplast haplotype distribution and incongruence (Figure 3.3). The Clade I haplotype is restricted to southern Italy, where *A. siculum* is the only species present. Incongruence between morphology and haplotype occurs in regions where members of subsection Antirrhinum and Streptosepalum overlap in range with subsection Kickxiella. One notable exception is that *A. latifolium*, which carries Kickxiella haplotype IV and



is restricted to southeast France, does not currently occur in sympatry with *Kickxiella* species. Elsewhere, where *Antirrhinum* and *Streptosepalum* species grow in the absence of *Kickxiella* (e.g. in Morocco, Western Portugal and Northern Spain), haplotypes were always found to be congruent with morphology.

3.2.1 Rooting the haplotype network

Previous molecular studies have shown that the most closely related genera to *Antirrhinum* are *Mohavea* and *Sairocarpus* (also known as the new world *Antirrhinum* genera), and the old world *Misopates* genus (Ghebrehiwet *et al* 1988, Chaffe 2003, Oyama *et al* 2004, Vargas *et al* 2004). However, the relationships between these genera have been difficult to resolve (Alan Forrest, pers. comm.). Previous studies have either placed *Antirrhinum* as sister to the new world *Antirrhinum* genera (Chaffe 2003, Gübitz *et al* 2003 and Vargas *et al* 2004), or as sister to *Misopates* (Ghebrehiwet *et al* 1988, Oyama *et al* 2004). However, these studies suggest that *Misopates* is one of the closest extant genera to *Antirrhinum* and suitable for use as an out-group. Therefore the three chloroplast loci were sequenced in *Misopates orontium* in order to root the haplotype network for *Antirrhinum*.

Although some regions of the *trnS-trnFM* locus of *M. orontium* were difficult to align with the *Antirrhinum* sequences, all but one of the polymorphic sites determining the haplotype network in Figure 3.2 could be identified in the *M. orontium* sequences. Comparison of the polymorphisms that separate clades I-IV, which are numbered in Figure 3.2, revealed the position of *M. orontium* within the haplotype network (Figure 3.4), joining the branch separating Clade III from the common ancestor of the other clades. Rooting the network at this point placed the Clade III *Kickxiella* lineage as ancestral to the other *Antirrhinum* lineages. This position is congruent with all polymorphisms of the haplotype network apart from one, labelled as number 19, which distinguishes the subsection *Antirrhinum* Clade II haplotypes. Excluding the regions that do not align, *M. orontium* had 39 further polymorphisms compared to the in-group sequences, consistent with its earlier divergence from the *Antirrhinum* genus.

3.3 Testing species relationships using AFLP markers

AFLP genotyping was carried out on a subset of 293 of the individuals that had been used for chloroplast haplotype analysis (Table 3.3). Populations were sampled throughout the distribution of each species, with up to two individuals of each population being included. The AFLP bands

Map No.	Location, province, country	Location	Clade, Haplotype No
Subsection Antirrhinum			
<i>A. australe</i>			
1	Benamahoma, Cadiz, S	83	II, II
2	El Boyar, Cadiz, S	84	II, II
3	Grazelema, Cadiz, S	85	(II,14), II
4	Villaluenga del Rosario, Cadiz, S	86	II, II
5	Cortes de la Frontera, Malaga, S	89	II
6	Benaolan, Malaga, S	90	(II,14)
7	Gaucin, Malaga, S	91	(II,14), II
8	El Burgo, Malaga, S	95	IV, IV
9	Torcal de Antequera, Malaga, S	97	(IV,33), IV
<i>A. barrelieri</i>			
10	Paternal del Rio, Almeria, S	24	IV
11	Laroles, Granada, S	27	IV, IV
12	Berja to Laujar, Almeria, S	28	IV, IV
13	Ugija to Murtas, Granada, S	29	IV, IV
14	Trevez, Granada, S	33	IV
15	Busquistar, Granada, S	34	IV, IV
16	Alora, Malaga, S	96	IV, IV
17	Algarinejo, Granada, S	101	IV, II
18	Cadiar, Granada, S	150	IV,26
<i>A. graniticum</i>			
19	Braganca, Braganca, P	40	II, II, II
20	Pelegriña, Guadalajara, S	67	(II,3) II
21	Ledanca, Guadalajara, S	69	II, II
22	Berninches, Guadalajara, S	71	II, II
23	Fuentiduena de Tajo, Madrid, S	75	II, II
24	Chinchon, Madrid, S	76	II, II
25	Priego, Cuenca, S	79	II, II
26	Lamego, Viseu, P	115	(II,10), II
27	Celorica da beira, Guarda, P	116	(II,10), II, II
28	Navalperal de Tormes, Toledo, S	120	II
29	Collado-Villalba, Madrid, S	174	(II,3)
30	Miranda do Duoro, Braganca, P	176	(II,10)
<i>A. latifolium</i>			
31	Pyrenees	AC1046	II
32	Mt Bastide nr col d'Eze, Nice, Alpes Cote-d'Azur, F	AC1054	(IV,25)
33	nr St Jean-Cap-Ferrat, Alpes Cote-d'Azur, F	AC1055	IV
34	west of col. Turini, Alpes Cote-d'Azur, F	AC1058	(IV,25)
35	St Martin d'Entraunes, Alpes-Maritimes, F	AC1066	IV
36	Gorges de Daluis, Entrevaux, Alpes-de-The.-Povence, F	AC1069	IV
37	Pont de Gueydan, Entrevaux, Alpes-de-Ht.-Povence, F	AC1070	IV
38	Rigaud, Alpes-Maritimes, F	AC1071	IV
39	Embrun, Hautes-Alpes, F	AC1079	(IV,24)
40	Mirabeau, Alpes-de-Ht. Provence, F	AC1081	(IV,25)
<i>A. majus cirrhigerum</i>			
41	Gala, Coimbra, P	113	(II,7)
42	Praia de Mira, Coimbra, P	114	(II,7)
<i>A. majus linkianum</i>			
43	Sierra de Arrabida, Setubal, P	107	(II,3), II
44	Almada, Setubal, P	108	(II,3)
45	Sintra, Lisboa, P	109	II, II
46	Pernes, Santarem, P	110	(II,3),II
47	Porto de Mos, Leiria, P	111	II, II
<i>A. majus litigiosum</i>			
48	Beniopa, Valencia, S	1	III&IV, III&IV
49	La Drova, Valencia, S	2	III&IV
50	Chesta, Valencia, S	3	III&IV, III&IV, III&IV
51	nr Llíria, Valencia, S	4	(II,3), III&IV
52	Olocau, Valencia, S	5	III&IV

53	Segorbe, Castello	6	IV
54	Vall d'Alba, Castello, S	7	IV
55	Morella, Castello, S	8	IV, III
56	Traiguera, Castello, S	9	III, III
57	Casas de El Canizar, Cuenca, S	11	IV, IV
58	Elche, Albacete, S	12	IV, IV
59	Bogarra, Albacete, S	13	II, II
60	Santes Creus, Tarragona, S	61	(II,11), II
61	Santes Creus, Tarragona, S	62	II
62	Borja, Zaragoza, S	63	II
63	Borja, Zaragoza, S	64	II, II
64	Tarazona, Zaragoza, S	65	II
65	Gallur, Zaragoza, S	66	II, II
66	Daroca, Zaragoza, S	80	II, II
<i>A. majus majus</i>			
67	Vinhais, Branganca, P	41	II
68	Nogarejas, Leon, S	42	II
<i>A. majus pseudomajus</i>			
69	Jaca, Huesca, S	45	II, II
70	Biescas, Huesca, S	46	II, II
71	Panticosa, Huesca, S	48	II, II
72	Gave de Ossau, Hautes-Pyrenees, F	49	II, II
73	Minerve, Herault, F	53	II, II
74	Prades, Pyrenees-Orientales, F	59	II II
75	Berga, Barcelona, S	60	(II,12), II
<i>A. majus striatum</i>			
76	N of Limoux, Aude, F	55	II, (II,12)
77	S of Limoux, Aude, F	56	II, II, (II,14)
78	Belcaire, Aude, F	58	II, II
<i>A. majus tortuosum</i>			
79	El Tempul, Cadiz, S	81	II
80	El Bosque, Cadiz, S	82	II, II
81	Casares, Malaga, S	92	IV, IV
82	Marbella, Malaga, S	93	(IV,26) IV
83	Almargen, Malaga, S	98	II
84	Loja, Granada, S	100	IV, IV
85	Priego de Cordoba, Cordoba, S	102	IV, IV
86	Alcaudete, Jaen, S	103	(II,14)
87	Cabra, Cordoba, S	105	IV, IV
88	Cerro Muriano, Cordoba, S	106	(III,22), III
89	Gibraltar	160	(II,14)
<i>A. majus tortuosum (M & It)</i>			
90	Mazzaro, Sicily, near Taormina	AC1143	(II,14)
91	Near Cefalu, Sicily	AC1144	(II,14)
92	Tetuan to Chefchauen, Morocco	161	(II,15)
93	N of Chefchauen, Morocco	162	(II,14)
94	Chefchauen, Morocco	163	(II,14)
95	Targha, Morocco	165	(II,14)
96	Taineste, Morocco	167	(II,14)
97	Taineste, Morocco	168	(II,3)
98	Taza, Morocco	169	(II,14)
<i>A. siculum</i>			
99	Palermo, Sicily	AC1176	I,1
100	Taormina, Sicily	AC1177	I,1
101	Syracuse	E68	I, 2
Subsection Kickxiella			
<i>A. boissieri</i>			
102	Guadahortuna, Granada, S	18	II, II
103	Albanchez de Bela - Pegalajar, Jaen, S	E15	IV
104	Ermita Virgen de la Sierra, Cordoba, S	104	IV, (IV,32)

<i>A. charidemi</i>			
105	Cabo de Gata, Almeria, S	E23	(IV,31), (IV,31)
<i>A. grosii</i>			
106	Sierra de Gredos, Toledo, S	175	(III,19), (III,20)
<i>A. hispanicum</i>			
107	Balcon de Canales, Granada, S	36	(IV,26), (IV,26)
108	Lanjaron, Granada, S	132	(IV,26), (IV,26)
109	Almargan, Malaga, S	99	(II,17)
<i>A. hispanicum</i> (M)			
110	Source de Oum-er-Rubia, Morocco	171	(II,14)
111	El kebab, Morocco	172	(II,14)
112	El Ksiba, Morocco	173	(II,16)
<i>A. lopesianum</i>			
113	unknown		(II,3)
<i>A. microphyllum</i>			
114	Sacedon, Guadalajara, S	72	(III,18), III
115	Pantano de Buendia, Guadalajara, S	73	(IV,26), III
116	Buendia, Guadalajara, S	74	(IV,34), (IV,23)
<i>A. molle</i>			
117	Gerri de la Sal, Lleida, S	E51	(II,11)
118	la Seu de Urgel, Lleida, S	E52	(II,5)
119	Saldes, Barcelona, S	E53	(II,12)
120	Montsec, S near Seu de Urgel	E54	(II,11)
121	Baga, Barcelona, S	E55	II
122	Las Lagunes, S near Gerri de la sal. Isolated.	E57	II
123	Bellver de Cerdanya	E60	II
<i>A. mollisimum</i>			
124	Canjayar, Almeria, S	22	IV, IV
125	Enix, Almeria, S	21	(IV,26), IV (IV,26)
<i>A. pertegasii</i>			
126	unknown	E65	(II,3), (II,3)
<i>A. pulverulentum</i>			
127	Pelegriana, Guadalajara, S	68	(II,3), II
128	Alcorlo, Guadalajara, S	70	IV, (IV,26)
129	Poveda de la Sierra, Guadalajara, S	77	(IV,27), IV
130	Hoz de Beteta, Cuenca, S	78	III, III
<i>A. rupestre</i>			
131	Bayarcal, Almeria, S	25	IV, IV
132	Bayarcal to Laroles, Granada, S	26	IV, IV
133	Juviles to Trevelez, Granada, S	31	IV
134	Trevelez, Granada, S	32	IV
135	Bubion, Granada, S	35	IV
136	Trevelez, Granada, S	136	(IV,26)
137	Capiliera, Granada, S	139	(IV,11)
<i>A. sempervirens</i>			
138	Panticosa, Huesca, S	47	(II,8), (II,7)
139	Col d'Aubisque, Hautes-Pyrenees, F	50	(II,9), II
140	Luz, Hautes-Pyrenees, F	52	(II,6), (II,5)
<i>A. subbaeticum</i>			
141	unknown	E72	(III,21), (III,22), (III,22)
<i>A. valentinum</i>			
142	La Drova	AC1173	(IV,29)
143	unknown		(IV,28)

Subsection Streptosepalum

A. braun-blanquetii

144	Sobron, Alava, S	44	(II,3), II
145	La Pinda, Corvera de Asturias, Asturias, S	E18	II
146	Ripol Gorge Ceneya	E19	II
147	St Pietro de Villanueva, Cangas de Onis, Asturias, S	E20	II
148	Braganca, Braganca, P	E21	II

A. meonanthum

149	Poco do Inferno, Manteigas, Guarda, P	118	II, II, (II,3)
150	Sobredelo, Ourense, S	180	(II,3)
151	Robledo de Fenar, Leon, S	181	(II,3)
152	unknown	E48	(II,13)
153	unknown	E49	(II,13)

Hybrid populations

A. barrelieri x *A. rupestre*

154	Luajar to Paterna del Rio, Almeria, S	23	IV, IV
155	Cadiar to Mecina Bombarron, Granada, S	30	IV, IV

A. majus tortuosum x *A. boissieri* Putative hybrid

156	Reolid, Albacete, S	15	IV, IV
-----	---------------------	----	--------

Table 3.2. Table showing the details and chloroplast haplotype clades of all populations.

'Map No' corresponds to the numbering of the populations on Figure 3.3. 'Location' corresponds to the data-base number of each population (Table 2.1). Clade = the haplotype clade as indicated on Figure 3.2. The numbers following the clade, in brackets, indicate the haplotype number of plants that were sequenced.

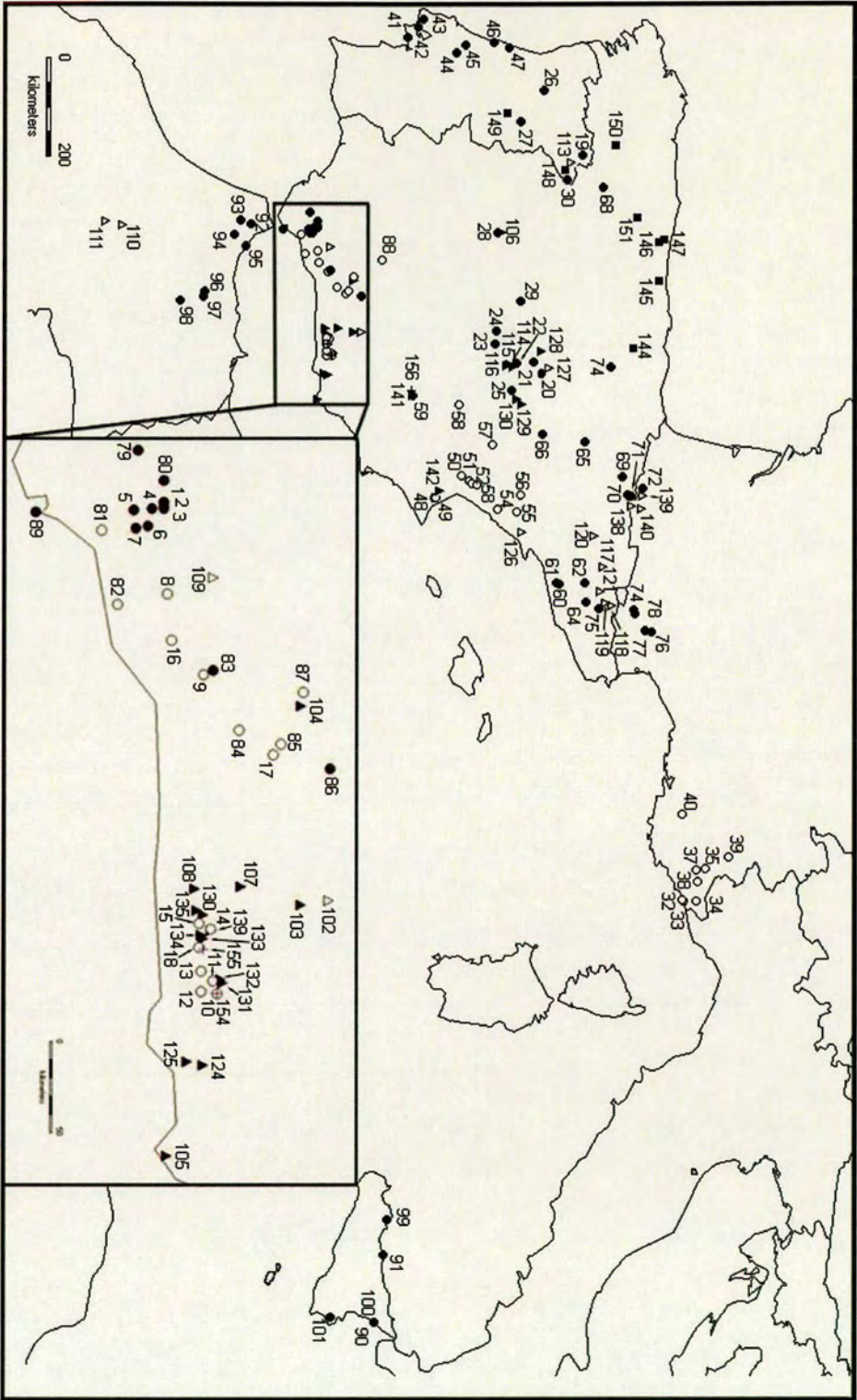


Figure 3.3. Map showing the geographic distribution of chloroplast haplotypes.
 Each population is represented by a symbol, with circles indicating subsection Antirrhinum species, squares Streptosepalum species and triangles Kickxiella species. Filled symbols indicate populations that have haplotypes congruent with morphological subsection (Clade II haplotypes for Antirrhinum and Streptosepalum species and Clades III and IV haplotypes for Kickxiella species). Open symbols indicate incongruent populations. The numbers correspond to the 'map number' in Table 3.2, which gives further details on the populations that were sampled. The bounded region is referred to in the text as the southern Spanish region.

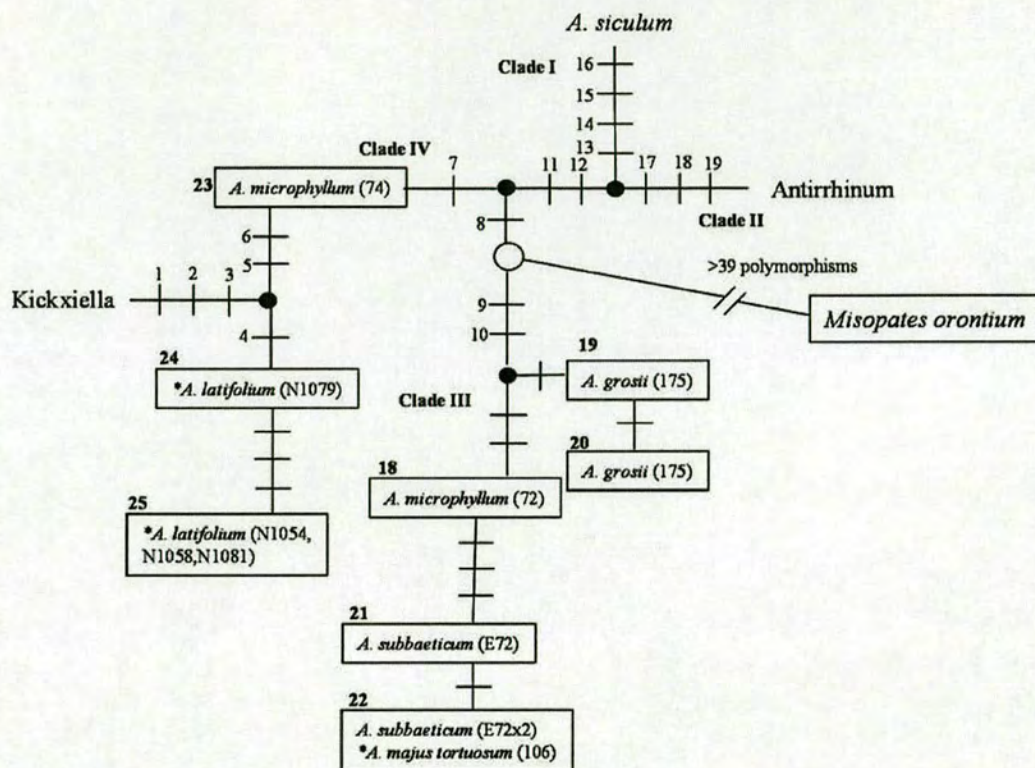


Figure 3.4. Diagram showing the position of the out-group, *Misopates orontium*, haplotype within the *Antirrhinum* chloroplast haplotype network shown in Figure 3.2.

The resolved position of the out-group to the main clades of the haplotype in Figure 3.2 is shown. Key polymorphisms that determine the relationships of the main clades to the out-group are numbered 1-19.

obtained from four different primer combinations were analysed to give 506 loci, with band sizes ranging from 70 to 390 bases.

3.3.1 Estimating the phylogenetic signal within the AFLP dataset

Several sources of noise associated with AFLP data may lead to inaccurate phylogenetic inference. The levels of these artefacts in the AFLP results were therefore estimated to determine their impact on the analyses that were undertaken. The first is the reliability of band amplification. The AFLP technique is sensitive to experimental conditions, DNA quality and changes in reagents. Given that the DNA quality in particular varies across samples, there may be variation in the amplification of some loci, resulting in false negative errors. This would lead to inaccurate estimates of genetic distances between individuals. The second main source of error is band size homoplasy, in which AFLP bands of the same size originate from different loci. This can have similar effects on phylogenetic reconstruction as lineage sorting and hybridisation. Estimates of the possible influence of these two sources of error and the steps taken to minimise them are described below.

i) Error due to variation in the amplification of loci

Two approaches were taken to estimate and minimise the effects of variation in amplification of loci. The first was to repeat the AFLP analysis up to three times on four different DNA extractions of the same individual, giving 10 replications in total. An average of 136 bands were detected. The majority of bands (80%) are amplified in all ten replicates and 89% of the bands were present in eight out of the ten samples (Figure 3.5A). However, there was appreciable variation in the amplification of homologous bands; for example, 5% of the loci are amplified in only one or two replications.

A second estimate of the reliability of the dataset was obtained by repeating AFLP analysis on 31 samples, consisting of individuals of different species, using different reagents for the two replicates. The number of loci for which a band was present in one replicate but not the other of the same individual was counted as a disagreement. This gives an estimate of the number of disagreements for each locus (Figure 3.5B). Similar to the previous estimate of reliability, 90% of the loci were repeated in 80% of the samples. This left ~10% of the 506 loci having contradictory scores in more than 7 of the 31 samples that were repeated. These loci were considered unreliable and were not used in subsequent analyses.

ii) Error due to band size homoplasy

Species	Locations	N	#L _r	%L _{pm}	B _{<25%}	B _{<50%}
<i>A. australe</i>	83, 84, 85, 86, 88, 89, 90, 91, 95, 97	17	158	31	17 (11%)	61 (39%)
<i>A. barrelieri</i>	27, 28, 29, 33, 34, 96, 101, 131, 150, 156	17	207	47	36 (17%)	108 (52%)
<i>A. boissieri</i>	104	2	88	6	1 (1%)	10 (11%)
<i>A. braun-blanchetii</i>	43, 44, E20	6	144	28	20 (14%)	63 (44%)
<i>A. charidemi</i>	E23	2	103	2	6 (6%)	28 (27%)
<i>A. graniticum</i>	40, 67, 69, 75, 76, 79, 115, 116, 117, 119, 120, 174, 176	24	201	43	38 (19%)	102 (51%)
<i>A. grossii</i>	175	1	94	-	10 (11%)	28 (30%)
<i>A. hispanicum</i>	35, 36, 99, 132, 138, 140	16	206	45	39 (19%)	100 (49%)
<i>A. hispanicum M</i>	171, 172, 173	4	116	11	7 (6%)	31 (27%)
<i>A. latifolium</i>	AC: 1045, 1046, 1047, 1054, 1055, 1056, 1057, 1058, 1061, 1063, 1064, 1066, 1069, 1070, 1071, 1072, 1079, 1081	19	220	54	74 (34%)	132 (60%)
<i>A. lopesianum</i>	Edinburgh accession	1	106	-	9 (8%)	34 (32%)
<i>A. majus cirrhigerum</i>	113, 114	3	89	5	2 (2%)	13 (15%)
<i>A. majus linkianum</i>	107, 108, 109, 110, 11	10	155	33	21 (14%)	59 (38%)
<i>A. majus litigiosum</i>	1, 2, 3, 4, 6, 7, 12, 13, 61, 62, 63, 64, 65, 66, 80	27	250	64	63 (25%)	146 (58%)
<i>A. majus majus</i>	39, 41, 42, 51, 54	10	152	30	20 (13%)	65 (43%)
<i>A. majus pseudomajus</i>	45, 46, 47, 48, 49, 59, 60	17	200	46	40 (20%)	98 (49%)
<i>A. majus strictum</i>	55, 57, 58	4	126	19	12 (10%)	39 (31%)
<i>A. majus tortuosum</i>	81, 82, 92, 93, 94, 98, 100, 102, 103, 105, 106, 159, AC1143, AC1144	25	185	39	28 (15%)	86 (46%)
<i>A. m. tortuosum M</i>	161, 162, 163, 165, 167, 168, 169	7	150	27	17 (11%)	56 (37%)
<i>A. microphyllum</i>	72, 73, 74	7	164	32	32 (20%)	86 (52%)
<i>A. molle</i>	E51, E52, E53, E54	4	106	12	13 (12%)	33 (31%)
<i>A. mollissimum</i>	20, 21, 157, 158	9	180	36	29 (16%)	82 (46%)
<i>A. peregasi</i>	E65	2	84	4	6 (7%)	23 (27%)
<i>A. pulverulentum</i>	68, 70, 77, 78	8	193	41	39 (20%)	103 (53%)
<i>A. rupestre</i>	32, 136, 139, 152	13	165	33	24 (15%)	71 (43%)
<i>A. sempervirens</i>	47, 50, 52	6	142	21	29 (20%)	68 (48%)
<i>A. siculum</i>	AC1176, AC1177, E68, Eunkown, E70	5	137	24	25 (18%)	52 (38%)
<i>A. subbaeticum</i>	E72	2	95	4	15 (16%)	34 (36%)
<i>A. valentinum</i>	AC1173, E74	2	91	7	14 (15%)	34 (37%)
<i>A. meonanthurum</i>	118, 180, 181	6	158	29	22 (14%)	71 (45%)

Table 3.3. Details of the sampling of populations of each species for AFLP genotyping and descriptions of the resulting band frequencies.
The location corresponds to the population data-base number (Table 2.1). 'N' is the number of individuals, '#L_r' is the average number of bands, '%L_{pm}' is the percentage of polymorphic loci, 'B_{<25%}' is the percentage of loci that have an overall frequency less than 25% in the entire dataset, and 'B_{<50%}' is the percentage of loci that have an overall frequency less than 50%. 'M' denotes populations from Morocco that were grouped together.

Two approaches, one experimental and one model based, were taken to identify size homoplasy within the AFLP dataset. The experimental approach of O'Hanlon and Peakall (2000) was attempted. This involves adding a further selective base to an AFLP primer and carrying out four additional amplifications, each with a different selective base. Homoplasy is inferred at a locus if a band of the same size is produced in amplifications with primers that have different selective bases. This approach was applied to two individuals for each of the species *A. microphyllum*, *A. siculum*, *A. braun-blanquetii* and *A. majus linkianum*. These species were selected to represent different morphological subsections and so are likely to be the most divergent. Their use should therefore give a maximum estimate of band size homoplasy. As more stringent PCR conditions were used the PCRs were successful for only one individual of each of the four species and out of these individuals, only 44 out of the possible 64 amplifications were successful. These 44 amplifications suggested that the total proportion of homoplasy, due to both within-individual and between-species comparisons, was 13%. This leads to a loose estimate of 19% ($64/44 \times 13\%$) of loci being homoplasious. However, this is probably an over-estimate of the level of homoplasy within the dataset as it was difficult to identify bands of the same size unambiguously in different experiments, leading to a potential over-estimate of the number of loci that amplified with more than one selective primer. In addition, despite the stringency of the PCR conditions being increased, bands that were not present in the AFLP profiles produced without additional selective bases were amplified. For these reasons, the loci that were identified as potentially homoplasious were not excluded from further analyses.

As the experimental approach to identify homoplasious bands was largely unsuccessful, homoplasy within the dataset was also estimated using the method of Vekemans *et al* (2002). This assumes that smaller bands are more common within an AFLP profile and are therefore more likely to be homoplasious and that homoplasy can be detected as a higher than expected frequency of smaller bands within a group of individuals (Innan *et al* 1999, Vekemans *et al* 2002, Koopman and Gort 2004). This is indicated by a negative correlation between band size and frequency. Correlations between band size and frequency were tested for each primer combination separately using AFLPSurv (Vekemans *et al* 2002). Significant negative correlations ($r = -0.3$, $p < 0.001$) were found for two of the primer combinations, suggesting size homoplasy. This is consistent with the identification of homoplasious bands using the experimental approach, in which a high proportion of the potentially homoplasious bands were smaller than 100 bases. Therefore, to reduce the possible error resulting from size homoplasy, loci smaller than 100 bases were not used in subsequent analyses. This reduced the magnitude of the correlations between band size and

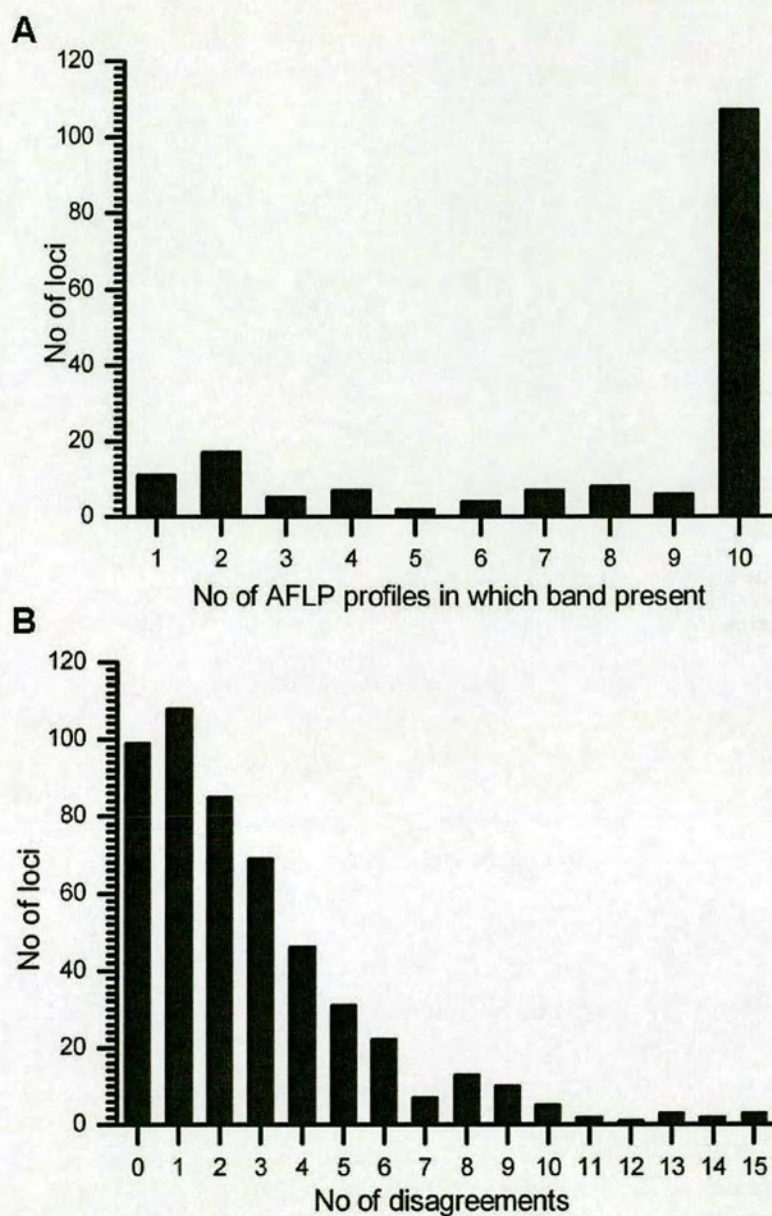


Figure 3.5. Graphs showing the consistency of amplification of AFLP loci in multiple replications of the same individual (A) and two replications of numerous individuals (B).

- (A) The frequencies of loci that are amplified in just one through to all ten replications of the same individual.
- (B) Frequencies of loci that ‘disagree’ in 0 out of 31 through to 15 out of 31 individuals. A locus is considered to ‘disagree’ if it is amplified in one replication of the same individual and not the other. The maximum number of ‘disagreements’ observed is 15.

frequency to $r = -0.2$ ($p=0.01$) and $r = -0.16$ ($p=0.06$) for the two primer combinations for which high negative correlations had been detected.

After removing these loci and the loci for which amplification had been found to be unreliable, 381 loci remained for use in the subsequent analyses.

iii) Descriptions of band frequencies within species

Very few of the AFLP bands were found to be unique to one species. The maximum number of private bands in a species was three, occurring in *A. latifolium*, *A. majus pseudomajus* and *A. hispanicum*. Variation in amplification and band-size homoplasy might contribute to this unexpectedly low proportion of private bands. However, it might also reflect hybridisation, lineage sorting or lack of species delimitation. Table 3.3 shows the distributions of AFLP bands within and between species. Each species has an average of 14% of less common bands (band with an overall frequency <25%) and an average of 40% of bands of overall frequency <50%. A high proportion of loci were fixed within in each species (an average of 70%). This distribution of variation suggested that there was phylogenetic signal within the dataset. However, 54% of the loci in *A. latifolium* and 64% of the loci in *A. majus litigiosum* were not fixed. The high levels of polymorphism within these species may be a result of unreliable amplification of AFLP bands or reflect their genetic structure.

3.3.2 Clustering analyses of all genotyped individuals

i) Neighbour-joining analysis of all individuals

To determine whether the AFLP markers delimit species and resolve species relationships neighbour-joining was carried out on the estimated genetic distances (Jaccard distances) between all pair-wise combinations of individuals, including *Misopates orontium*, the out-group. In the resulting phylogeny the majority of species are delimited, but many with little or no bootstrap support (Figure 3.6). Mostly *Kicxiella* species receive support and *A. majus cirrhigerum*, *A. siculum* and *A. latifolium* (apart from two individuals) are also supported. The individuals of species that are not delimited generally cluster with other species that occur in the same geographic region. Individuals of the southern Spanish species *A. majus tortuosum*, *A. australe* and *A. boissieri* cluster together as do *A. rupestre*, *A. hispanicum* and *A. barrelieri* from the Sierra Nevada mountain range in southern Spain. Similarly, accessions of *A. meonanthum* and *A. braun-blauquetii*, which are both distributed in northern Spain, cluster together. The accessions of *A. majus tortuosum* and

A. hispanicum from Morocco cluster with each other rather than with con-specific accessions from other localities.

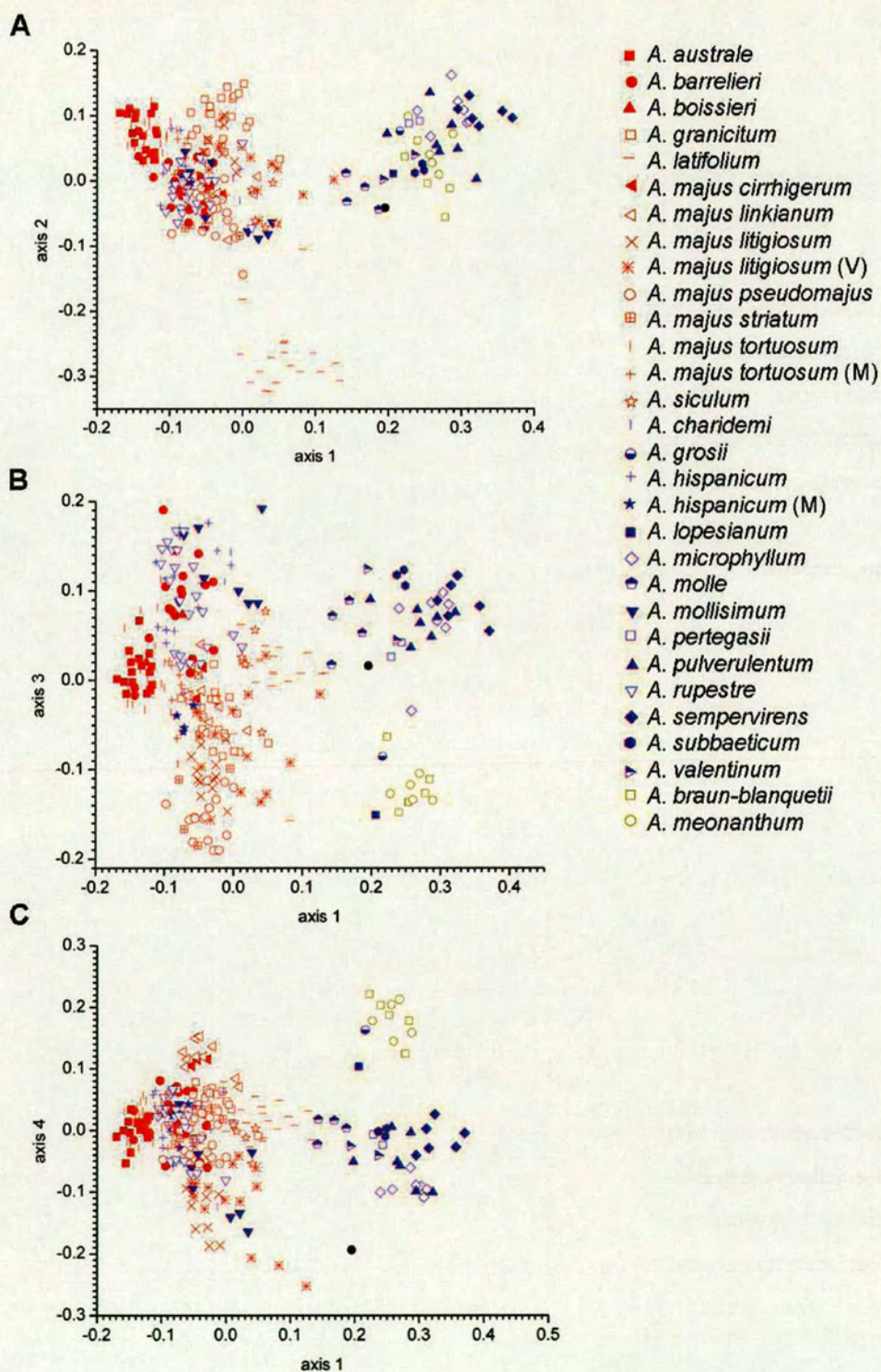
Few of the relationships between species are resolved and shallow branches that have low bootstrap support hold most groups of species. The main exception is that the Kickxiella species *A. pulverulentum*, *A. microphyllum*, *A. sempervirens*, *A. subbaeticum*, *A. pertegasii* and *A. valentinum* form a clade with 50% support. In future discussion these species are referred to as the core Kickxiella species, to distinguish them from other Kickxiella species distributed in southern and northwest Spain with which they do not cluster in AFLP analysis. Accessions of the species distributed in northern Spain and Portugal also cluster together with strong support. This group consists of the Streptosepalum species *A. braun-blanquetii* and *A. meonanthum* and the Kickxiella species *A. lopesianum* and *A. grosii*. It is subsequently referred to as the northern Iberian group.

ii) *Principal coordinates analysis of all individuals*

As in the chloroplast genotyping, the neighbour-joining analysis of the AFLP markers revealed that there is a geographic component to the genetic relationships among species, suggestive of hybridisation between lineages. Hierarchical clustering methods such as neighbour-joining are not suitable for describing phylogenetic relationships when there has been hybridisation between taxa as they assume descent from a common ancestor (Funk 1985, Vriesendorp and Bakker 2005). Therefore it is difficult to know whether the low bootstrap support for the clustering of accessions into species is the result of hybridisation, or lack of species delineation. A complementary technique that clusters individuals without assuming descent from a common ancestor is principal coordinates analysis (PCoA). PCoA identifies the axes that describe the most variation in a dataset and describes the positions of all individuals in terms of these axes, therefore summarizing the distances between individuals in a few key dimensions.

PCoA was carried out on the AFLP dataset, using the Jaccard distance to estimate the pair-wise distances between all individuals. The first few axes resulting from the analysis describe a small percentage of the overall variation; the first four axes account for 8%, 5%, 4% and 3% of the variation respectively. This is consistent with the high level of independent genetic variation detected in Section 3.3.1.

The first axis from PCoA separates subsection Antirrhinum from Streptosepalum and Kickxiella (Figure 3.7A). The Kickxiella species *A. mollissimum*, *A. rupestre*, *A. hispanicum* and *A. charidemi*



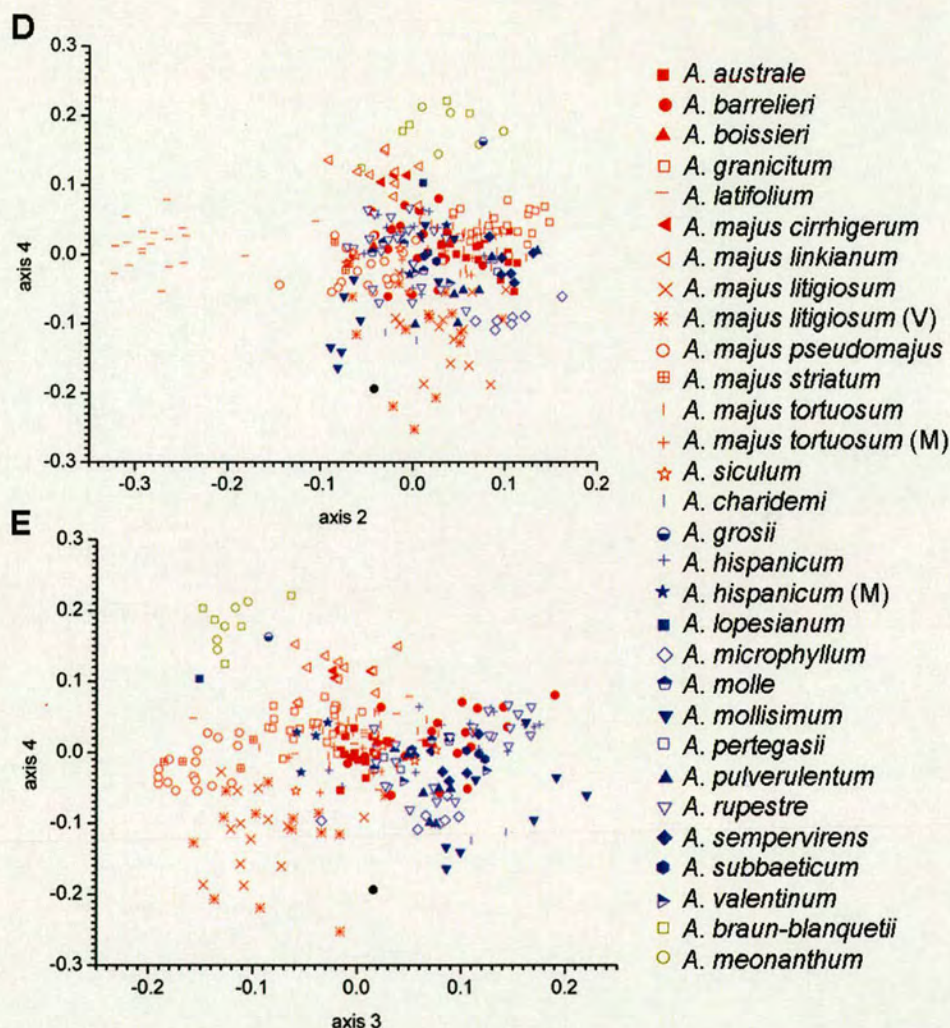


Figure 3.7. The positions of individuals in the main axes of the principal coordinates analysis (PCoA) analysis carried out on the distances estimated from AFLP scores.

The Jaccard distances between all pair-wise combinations of individuals were estimated from the AFLP scores of all accessions detailed in Table 3.3 and PCoA was then carried out on these distances. The positions of each individual are plotted in axes 1 and 2 (A), 1 and 3 (B), 1 and 4 (C), 2 and 4 (D), and 3 and 4 (E). Red symbols represent subsection *Antirrhinum* species, blue symbols subsection *Kickxiella* and dark yellow symbols subsection *Streptosepalum* species.

from southern Spain, however, remain grouped with subsection Antirrhinum. *A. latifolium* individuals are placed midway between the two groups, but are differentiated from all other species by their low axis 2 values. While axis 2 mainly differentiates *A. latifolium*, other species are spread along this axis with *A. graniticum* individuals having the highest values, followed by *A. majus litigiosum*, then *A. majus pseudomajus* and *A. majus striatum*.

There is little clear delimitation of species in the space defined by axes 1 and 2. Accessions of *A. majus tortuosum* cluster with *A. australe* with low axis 1 values and accessions of *A. majus linkianum*, *A. majus pseudomajus*, *A. majus striatum*, *A. majus litigiosum*, *A. siculum*, the Moroccan taxa and the Kickxiella species from southern Spain all overlap. Within the Kickxiella, only *A. molle* and *A. subbaeticum* are partially delimited.

Axis 3 differentiates the group of species from the Sierra Nevada and neighbouring mountain ranges of southern Spain; *A. barrelieri*, *A. hispanicum*, *A. rupestre*, *A. mollisimum* and *A. charidemi*, which have higher values than the Antirrhinum subsection species (Figure 3.7B). The core Kickxiella species have high axis 3 values compared to the rest of the genus and the northern Iberian group is distinguished by low axis 3 values.

The species of the northern Iberian group are further delimited from the other species by their high axis 4 values (Figure 3.7C). The two species in subsection Antirrhinum from Portugal, *A. majus cirrhigerum* and *A. majus linkianum*, also have high axis 4 values, distinguishing them from the rest of subsection Antirrhinum. *A. majus litigiosum* individuals have low axis 4 values compared to the other Antirrhinum species. Comparison of axes 2, 3 and 4 (Figure 3.7C, D, and E) shows that *A. graniticum* is differentiated from *A. majus litigiosum*, and *A. majus pseudomajus* and *A. majus striatum* are differentiated from the other Antirrhinum subsection species.

Overall, there is little clear species delimitation within the Antirrhinum and Kickxiella subsections. However, the Kickxiella species are generally delimited within the space defined by the first four axes of PCoA. Individuals of *A. pulverulentum*, *A. microphyllum* and *A. mollisimum* individuals cluster into their respective species along axes 2 and 4 (Figure 3.7D), and *A. sempervirens* is clustered along axes 1 and 4 (Figure 3.7C). Likewise, the main species of the Antirrhinum subsection can be identified, including *A. graniticum*, *A. majus litigiosum* and the two species pairs *A. majus cirrhigerum* and *A. majus linkianum* from Portugal and *A. majus pseudomajus* and *A. majus striatum* from the Pyrenees.

Notably, there are several cases where sympatric species are not separated from each other. The first group consists of *A. majus tortuosum* and *A. australe*, which are both of subsection Antirrhinum and are distributed in southern Spain. The second group comprises the subsection Antirrhinum species, *A. barrelieri*, and the Kickxiella species *A. hispanicum* and *A. rupestre*, which occur together in the Sierra Nevada. *A. hispanicum* and *A. rupestre* overlap in the PCoA with the two Kickxiella species *A. mollisimum*, distributed in the Sierra Nevada and neighbouring mountain ranges, and *A. charidemi*, which is found in close proximity near Almeria. Due to their close geographic and genetic relationships, the group consisting of *A. hispanicum*, *A. rupestre*, *A. charidemi* and *A. mollisimum* is referred to as the southern Spanish Kickxiella species. The final group of sympatric species that are similar genetically are the two members of subsection Streptosepalum, *A. meonanthum* and *A. braun-blanquetii*.

Despite *A. siculum* being of a divergent chloroplast haplotype, there is no indication of its differentiation from the rest of the genus in the PCoA. *A. siculum* individuals lie near the origin of all axes and generally overlap with subsection Antirrhinum species, being most similar to *A. majus litigiosum* and the Sierra Nevada species *A. barrelieri*, *A. hispanicum*, *A. rupestre* and *A. mollisimum*.

iii) Neighbour-joining analysis of species

Despite many species being poorly delimited by the PCoA analysis, accessions of each species do cluster together. The poor differentiation of species may be a consequence of the high levels of noise in the AFLP dataset. Therefore Nei's D genetic distance (Nei 1972) was estimated between species. This measure decreases the potential influence of the errors in the AFLP dataset by calculating an average distance between species and, in addition, it incorporates information about allele frequencies into the distance measure. The details of the locations included in the analysis for each species are as listed in Table 3.3. Due to the evidence in the neighbour-joining phylogeny that the accessions of *A. majus tortuosum* and *A. hispanicum* from Morocco are distinct from their conspecific accessions in Spain, they were treated as separate species in this analysis.

The general patterns of relationships between species observed in PCoA were also detected by neighbour-joining analysis using Nei's genetic distances. Two main lineages are identified in the resulting phylogeny with 94% support (Figure 3.8). The first consists of the species in subsection Antirrhinum and the southern Spanish Kickxiella species and the second of the species of the

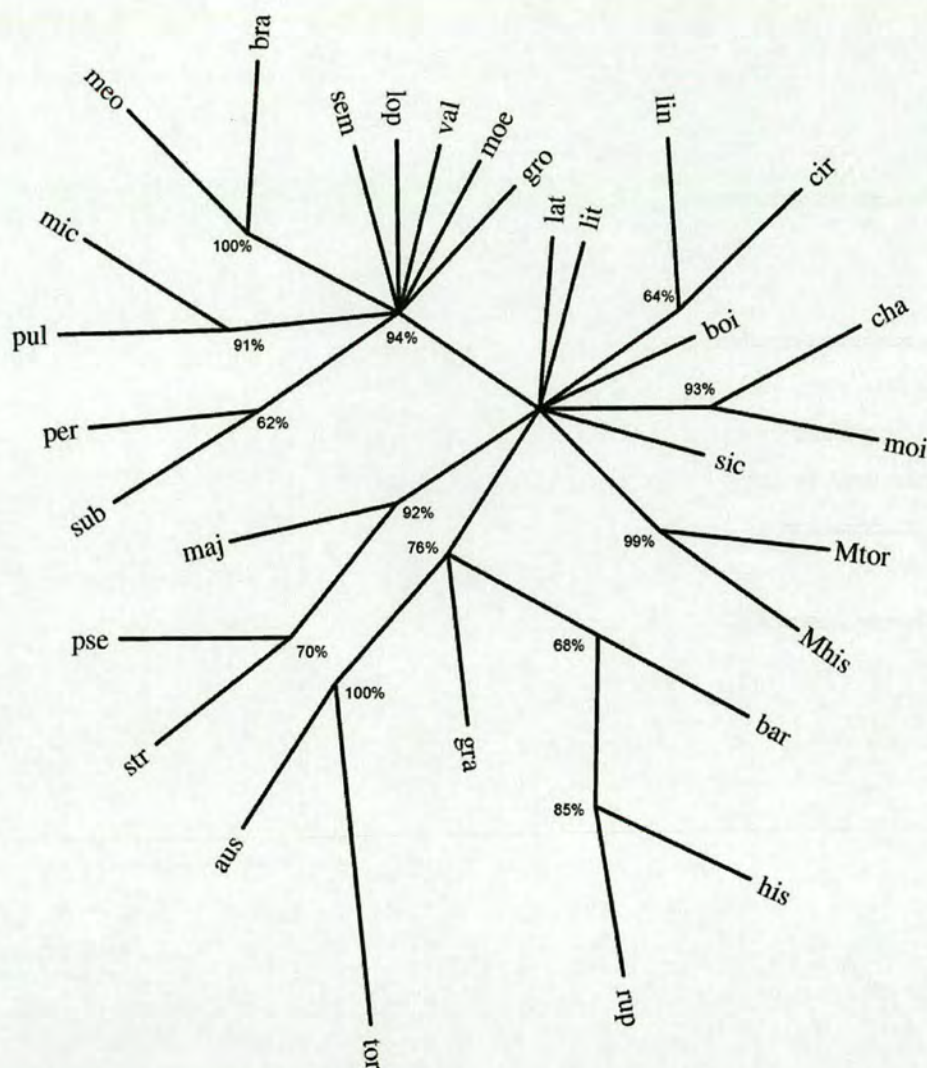


Figure 3.8. Neighbour-joining tree showing the relationships of *Antirrhinum* species based on genetic distances estimated by allele frequencies.

Neighbour-joining tree constructed from a matrix of Nei's D genetic distances between species. AFLPSurv (Vekemans *et al* 2002) was used to calculate genetic distances and to generate bootstrap matrices and PHYLIP (Felsenstein 1985) was used for neighbour-joining analysis and to estimate support for nodes. The branch lengths are not to scale and nodes with less than 60% support are collapsed.

'aus' = *A. australe*, 'bar' = *A. barrelieri*, 'boi' = *A. boissieri*, 'bra' = *A. braun-blauquetii*, 'cha' = *A. charidemi*, 'cir' = *A. majus cirrhigerum*, 'gra' = *A. graniticum*, 'gro' = *A. grosii*, 'his' = *A. hispanicum*, 'hisM' = *A. hispanicum* (Morocco), 'lat' = *A. latifolium*, 'lit' = *A. majus litigiosum*, 'lop' = *A. lopesianum*, 'lin' = *A. majus linkianum*, 'maj' = *A. majus majus*, 'meo' = *A. meonanthum*, 'mic' = *A. microphyllum*, 'moe' = *A. molle*, 'moi' = *A. mollisimum*, 'per' = *A. pertegasii*, 'pse' = *A. majus pseudomajus*, 'pul' = *A. pulverulentum*, 'rup' = *A. rupestre*, 'sem' = *A. sempervirens*, 'sic' = *A. siculum*, 'str' = *A. majus striatum*, 'sub' = *A. subbaeticum*, 'tor' = *A. majus tortuosum*, 'torM' = *A. majus tortuosum* (Morocco), 'val' = *A. valentinum*, 'mis' = *Misopates orontium*. The location number (Table 2.1) is added to the end of each species abbreviation, with letters 'a', 'b' etc denoting different plants of the same location

northern Iberian group and the core Kickxiella. The species groups detected in PCoA were also recognized as clusters with high support: (1) the Streptosepalum species *A. meonanthum* and *A. braun-blanquetii*, (2) the *A. majus majus* subspecies *striatum* and *pseudomajus*, (3) *A. majus cirrhigerum* and *A. majus linkianum*, (4) the Sierra Nevada species *A. barrelieri*, *A. rupestre* and *A. hispanicum* and (5) *A. majus tortuosum* and *A. australe*.

Additional relationships within the genus are also uncovered. *A. barrelieri*, *A. hispanicum*, and *A. rupestre*, which all occur mainly in the Sierra Nevada mountains of southern Spain, are clustered with strong support with the other southern Spanish taxa, *A. majus tortuosum* and *A. australe*, and with *A. graniticum*. However, *A. charidemi* and *A. mollisimum*, which occur in close proximity, are not included. The distinctiveness of *A. majus tortuosum* (Morocco) and *A. majus hispanicum* (Morocco) from their respective con-specific populations in Spain are also supported.

The patterns of incongruence between chloroplast haplotype and morphological relationships are corroborated by the neighbour-joining analysis. The Kickxiella species that are all fixed for chloroplast haplotypes associated with subsection Antirrhinum; *A. molle*, *A. sempervirens*, *A. pertegasii* and *A. lopesianum*, all cluster with the other Kickxiella species (apart from the southern Spanish Kickxiella) based on AFLP markers. Likewise, *A. latifolium*, which has a Kickxiella chloroplast haplotype, clusters with the other members of subsection Antirrhinum. These species therefore have chloroplast haplotypes that are discordant with both morphology and nuclear genotypes. The neighbour-joining analysis identifies additional incongruence as the Streptosepalum species cluster with Kickxiella in the neighbour-joining analysis but have chloroplast haplotypes and morphology similar to members of subsection Antirrhinum. They may cluster with the Kickxiella because of their genetic similarity to the two Kickxiella species *A. grosii* and *A. lopesianum*, which are from the same geographic region.

The southern Spanish species *A. majus tortuosum*, *A. australe* and *A. barrelieri* and *A. hispanicum*, which contain both Antirrhinum and Kickxiella chloroplast haplotypes, cluster with the southern Spanish Kickxiella. This association, which is supported by the PCoA, suggests the geographic relationship of these species has contributed to their genetic similarities, even though they are morphologically diverse. *A. australe*, *A. barrelieri* and *A. majus tortuosum* have characteristic subsection Antirrhinum morphologies and *A. hispanicum* Kickxiella morphology. The other species that has haplotypes of both clades, *A. pulverulentum*, clusters with strong support with the Kickxiella species in the AFLP analyses.

3.3.3 Comparison of the AFLP results with those from the chloroplast analysis

The involvement of hybridisation between *Antirrhinum* lineages is suggested by the geographic distribution of cytonuclear discordance. However, the distribution of chloroplast haplotypes within species suggests that lineage sorting of chloroplast haplotypes might also have occurred. Therefore further tests were carried out to determine whether species that show cytonuclear discordance might have undergone hybridisation and to further resolve species relationships. In these analyses, the plants that had contributed to the chloroplast haplotype network shown in Figure 3.2 were re-genotyped for AFLPs in the same experiment to remove noise due to variation between AFLP experiments. Individuals of species inferred to have undergone hybridisation were then removed from phylogenetic reconstructions to determine their effect on the support and topology of the resulting phylogenies.

i) Neighbour-joining analysis based on AFLPs of all individuals

Neighbour-joining analysis was carried out on Jaccard genetic distances between all individuals. The resulting phylogeny is similar to that obtained from the similar analysis of the large AFLP dataset in Section 3.3.2.i. Most species are resolved, but with higher support than in the previous analysis (Figure 3.9), suggesting that variation between AFLP experiments had contributed to inaccurate distance estimates. A few individuals were not clustered into species; these are mainly individuals of *A. majus tortuosum* from both southern Spain and northern Morocco, and individuals of *A. australe* and *A. hispanicum*, also from southern Spain.

Species relationships were observed that were concordant with the previous analysis but better resolved. The core *Kickxiella* species clustered with 60% support, and the northern Iberian group with 99% support. The accessions of *A. hispanicum* and *A. majus tortuosum* collected from central Morocco and the Middle Atlas Mountains clustered together with 80% support. Few further relationships between species were identified, except that *A. pulverulentum* was placed with *A. microphyllum*, *A. pertegasii* with *A. subbaeticum*, *A. rupestre* with *A. charidemi*, and *A. majus pseudomajus* with *A. majus striatum*. The species relationships within subsection *Antirrhinum* in particular were not resolved.

ii) Excluding putative hybrid individuals from neighbour-joining analyses

Hybrids are likely to carry characters from more than one lineage; therefore their inclusion in phylogenetic analysis can reduce support for their parental lineages. To test whether the lack of resolution of species relationships may be a consequence of the presence of hybrids within the

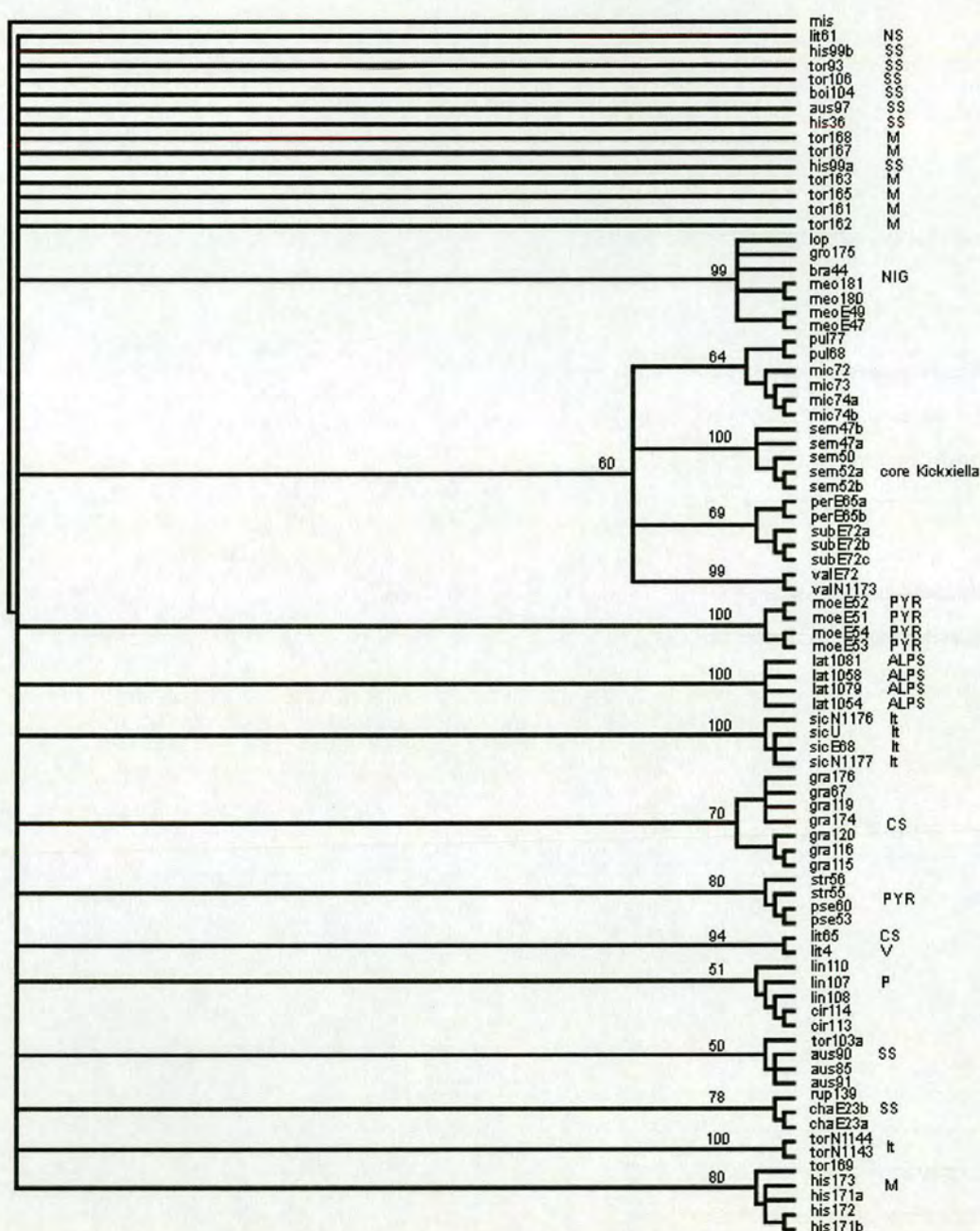


Figure 3.9. Neighbour-joining phylogeny of the individuals included in the chloroplast haplotype network, based on AFLPs

The Jaccard distance was estimated between all pair-wise combinations of individuals and neighbour-joining analysis carried out on the resulting distance matrix in PAST. The percentage support out of 5000 bootstrap replications is shown for species and higher level clusters only. The phylogeny is visualized in Treeview (Page 2001), with branches with less than 50% support collapsed. Population abbreviations are the same as in Figure 3.6. The geographic locations of populations are indicated by the following abbreviations NS=Northern Spain, SS=Southern Spain, M = Morocco, PYR = Pyrenees, ALP = Alps, It = Italy, CS = Central Spain. The core Kickxiella and northern Iberian group (NIG) are also indicated.

analysis, putative hybrid species were removed and the topologies and support of the resulting phylogenies compared. Removal of individuals of *A. molle*, the southern Spanish Kickxiella species, *A. barrelieri*, *A. latifolium*, and the individuals of *A. australe* and *A. majus tortuosum* that are not clustered in Figure 3.9 resulted in phylogenies with the most resolution and strongest bootstrap support. Removal of *A. sempervirens*, *A. lopesianum* or *A. pertegasii*, in contrast, did not affect topology or support, so these species were reintroduced into the subsequent phylogenetic analysis.

In the resulting phylogeny the core Kickxiella-northern Iberian cluster diverges from *A. siculum* with *A. graniticum* diverging from this clade followed by the remaining subsection Antirrhinum species (Figure 3.10). Further relationships between subsection Antirrhinum species are not resolved, apart from *A. majus litigiosum*, from northern Spain, being clustered with *A. majus pseudomajus* and *A. majus striatum*.

On rooting this phylogeny with *Misopates orontium*, the species relationships remained the same except that the branch supporting the core Kickxiella and the northern Iberian species collapses and support for the core Kickxiella decreased (Figure 3.11). *A. siculum* was placed at the base of a clade comprising the members of subsection Antirrhinum. The distinction of *A. graniticum* from the rest of subsection Antirrhinum also received higher support in the rooted phylogeny.

3.3.4 Exploring the genetic structure within *Antirrhinum* using Bayesian assignment

The chloroplast and AFLP analyses described in Sections 3.2 and 3.3 suggest that there are two signals, phylogenetic and geographical, within the genetic structure of the *Antirrhinum* genus. The phylogenetic signal identifies two main lineages that broadly correspond with subsections Antirrhinum and Kickxiella. The geographical signal is consistent with recurrent episodes of hybridisation between the two major lineages in the regions where their species come into contact.

However, the analyses above do not fully describe this genetic structure within the genus. The neighbour-joining and PCoA of genetic distances between individuals do not incorporate information about allele frequencies within and between species. To address this, neighbour-joining analysis had been carried out using Nei's genetic distances between species. However, this is a potentially unsound approach given the unclear taxonomy of the genus, because individuals had been assigned to predefined groups based on morphological criteria. A further shortcoming of these

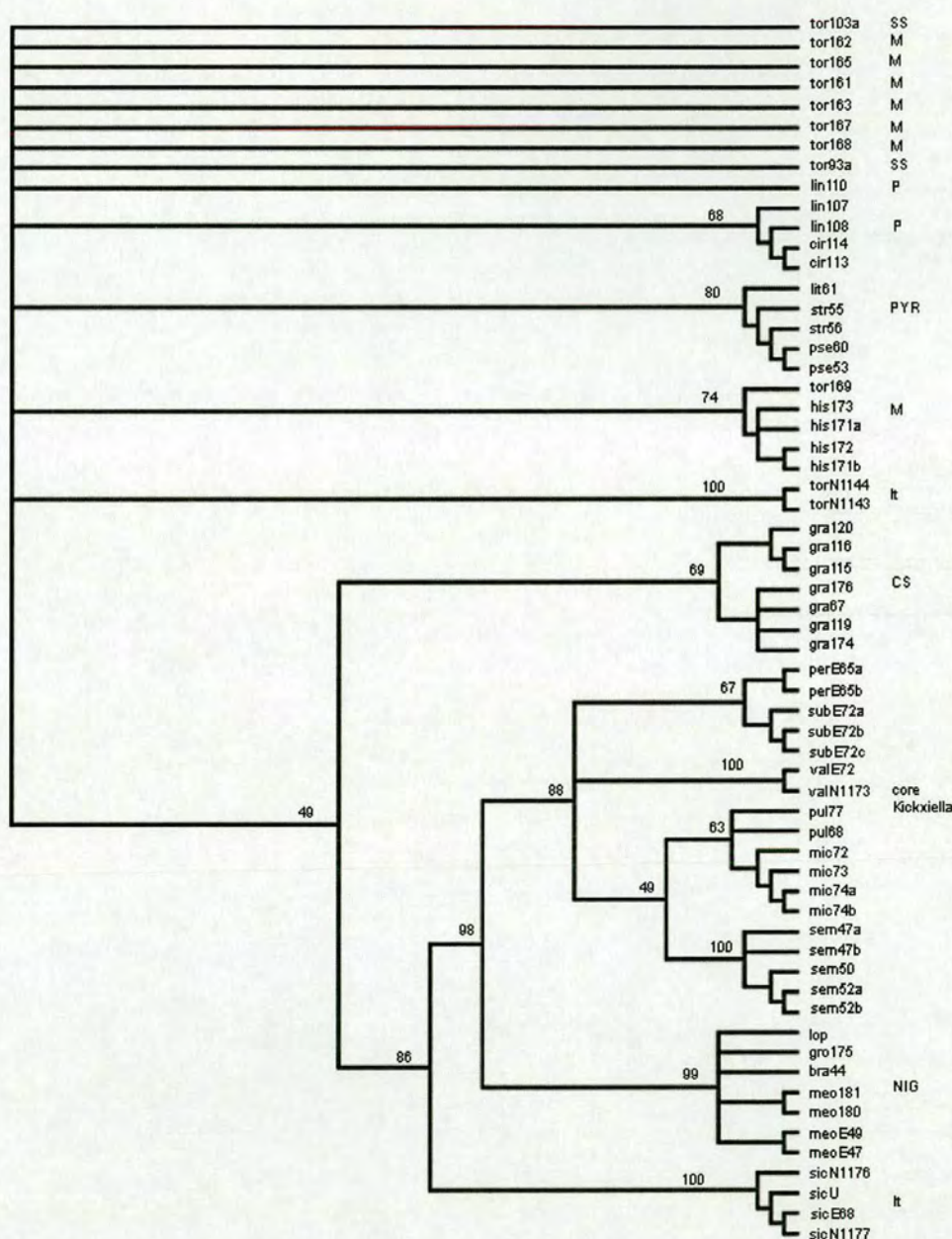


Figure 3.10. Un-rooted neighbour-joining phylogeny with inferred hybrid individuals removed from the analysis.

The Jaccard distance was estimated between all pair-wise combinations of individuals using AFLP scores and neighbour-joining analysis carried out on the resulting distance matrix in PAST. The percentage support out of 5000 bootstrap replications is shown for species and higher level clusters only. The phylogeny is visualized in Treeview, with branches with less than 50% support collapsed, apart from the *A. graniticum* lineage which is left for comparison with Figure 3.11. Population abbreviations are the same as in Figure 3.6. The geographic locations of populations are indicated by the following abbreviations NS=Northern Spain, SS=Southern Spain, M = Morocco, PYR = Pyrenees, ALP = Alps, It = Italy, CS = Central Spain. The core Kickxiella and northern Iberian group (NIG) are also indicated.

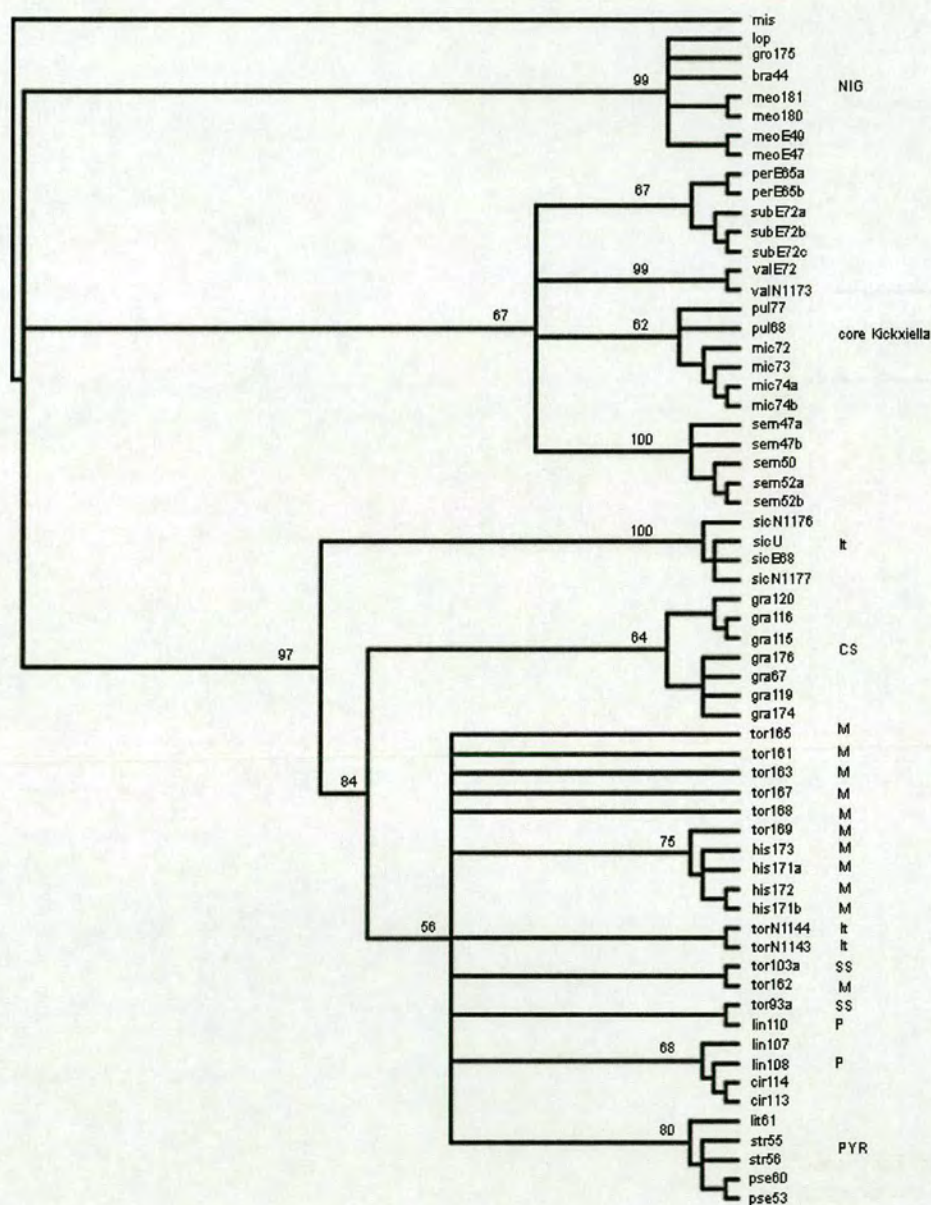


Figure 3.11. Rooted neighbour-joining phylogeny with inferred hybrid individuals removed from the analysis.

The Jaccard distance was estimated between all pair-wise combinations of individuals using AFLP scores and neighbour-joining analysis carried out on the resulting distance matrix in PAST. The percentage support out of 5000 bootstrap replications is shown for species and higher level clusters only. The phylogeny is visualized in Treeview, with branches with less than 50% support collapsed. Population abbreviations are the same as in Figure 3.6. The geographic locations of populations are indicated by the following abbreviations NS=Northern Spain, SS=Southern Spain, M = Morocco, PYR = Pyrenees, ALP = Alps, It = Italy, CS = Central Spain. The core Kickxiella and northern Iberian group (NIG) are also indicated.

analyses is that hierarchical clustering techniques such as neighbour-joining cannot accurately represent evolutionary relationships when there has been hybridisation between lineages.

Therefore a Bayesian population assignment model, *Structure* (Pritchard *et al* 2000, Falush *et al* 2003), was used to explore the distribution of genetic variation within the genus as it takes into account allele frequency distributions and can represent hybrid individuals. In this model individuals are not pre-assigned to populations based on possibly arbitrary criteria. Instead, the model simultaneously identifies populations and their allele frequency distributions, and assigns individuals to these populations (Pritchard *et al* 2000). In addition, individuals can be admixed (i.e. have proportions of loci from different ancestral populations), allowing representation of hybrids.

The version of *Structure* adjusted to account for dominant markers described by Falush *et al* (2007) was used, incorporating the individuals that had been used to produce Figure 3.6 (Table 3.2 gives further population details). Five different models were run with these data, differing in parameter settings and initial parameters (priors), as shown in Table 3.4. These included a model that allows correlations between allele frequencies to account for shared ancestry of alleles and models in which the prior distribution of population subdivision are higher ('FPRIORES' in Falush *et al* 2003). These parameters were varied to determine the maximum resolution of population structure and to test the robustness of the results. For all models the number of populations to be identified, K, was varied from 2-20, with each value of K being repeated 5-8 times.

All models converged to similar results for the same value of K, regardless of the other parameters used, and the log likelihood estimates of the data fitting the models were also similar for all simulations using the same K (Figure 3.12). Slightly different genetic structures were occasionally recovered for the same value of K, mainly for low values of K. In general, the rarer structures had much lower log likelihood values (Figure 3.12). However, these rarer structures were always recognised at higher values of K, suggesting that the strength of the signal for the different outcomes is similar, but the model is constrained by the number of populations allowed. The log likelihood values increase with K, starting to plateau around 14 populations (Figure 3.12). Although K was set to values as high as 21, in most cases the maximum number of populations recovered remains 17.

The output of *Structure* simulations shows the proportions of each individual's loci that descend from the inferred ancestral populations (Figure 3.13). In the following description these proportions

Model No.	No. of runs for each K	Alleles correlated	Infer λ	FPRIORMEAN, FPRIORS
1	8	1	0	0.01, 0.05
2	8	1	0	0.1, 0.1
3	8	1	0	0.1, 0.1
4	8	0	0	-
5	5	0	1	-

Table 3.4. Parameters (as defined by Falush *et al* 2003) for each of five Structure simulations carried out on AFLPs of all individuals. Model number 3 had the same parameter settings as 2 but twice the burn-in and twice the number of replications.

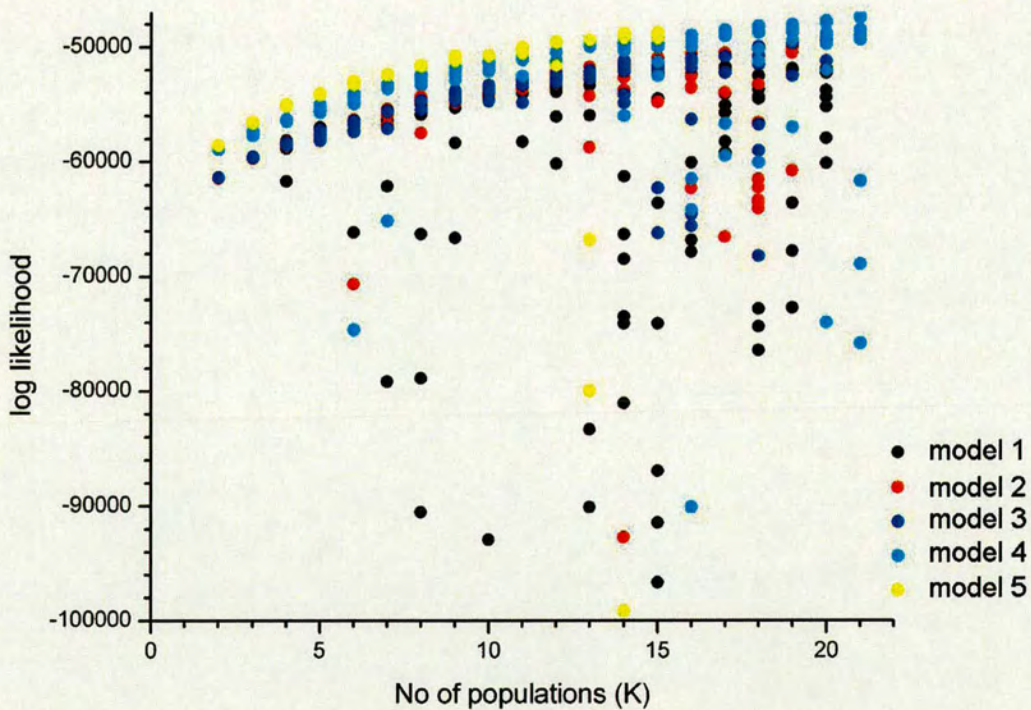


Figure 3.12. Graph showing the log likelihood values for all of the runs of each K, for each of the models of Table 3.4.

are referred to as each individual's genetic make-up. When $K=2$, i.e. there are 2 ancestral populations, the genetic make-up of the core Kickxiella species consists entirely of one ancestral population while the genetic make-up of individuals in subsection Antirrhinum consists predominantly of the other (Figure 3.13). These inferred populations therefore show that the dominant signal in the data is that of the two main lineages corresponding to subsections Antirrhinum and Kickxiella. However, the geographic patterns are also identified. The Streptosepalum species have the genetic make-up of the core Kickxiella and the southern Spanish Kickxiella have a genetic make-up comprising mainly that of subsection Antirrhinum with a small proportion of Kickxiella in the majority of individuals. Individuals of *A. siculum*, *A. molle*, *A. latifolium* and the accessions of *A. majus litigiosum* from Valencia province have a genetic make-up of approximately half of each ancestral population.

When three ancestral populations are inferred the genetic make-up of the core Kickxiella, northern Iberian group, *A. siculum* and *A. molle* remains the same, but the species distributed in southern and central Spain are recognised as a single population and a new population corresponding to *A. latifolium* emerges. The new population is predominantly defined by geography as individuals of subsection Antirrhinum from the Pyrenees and Alps have a large proportion of loci belonging to this population. This becomes more evident when K is increased to 4 as the model is now able to recognise the southern Spanish species as being a single population distinct from the other subsection Antirrhinum species *A. majus pseudomajus*, *A. majus striatum*, *A. majus cirrhigerum*, *A. majus linkianum* and *A. majus litigiosum*. This results in *A. molle* and *A. siculum* having a genetic make-up consisting of a large proportion of the *A. latifolium* population loci (represented by blue shading on Figure 3.13). The representation of the average genetic make-up of each sampled location shows these geographic patterns (Figure 3.14). However, a phylogenetic signal is also present, as the core Kickxiella species, which are widely distributed, remain within the same genetic population. In addition, *A. majus cirrhigerum* and *A. majus linkianum* retain a similar genetic make-up to the other accessions of *A. majus*.

Additional species and species groups that were identified in previous analyses are defined as K is increased, with the geographic structure of variation within the genus becoming increasingly evident (Figures 3.13 and 3.15). When $K=7$ the central and southern Spanish population fragments into several populations that correspond to geographical sub-regions (Figure 3.15). The Sierra Nevada species, *A. barrelieri*, *A. hispanicum* and *A. rupestre*, and the two species that grow in close proximity, *A. mollissimum* and *A. charidemi*, become distinct from the other southern Spanish taxa,

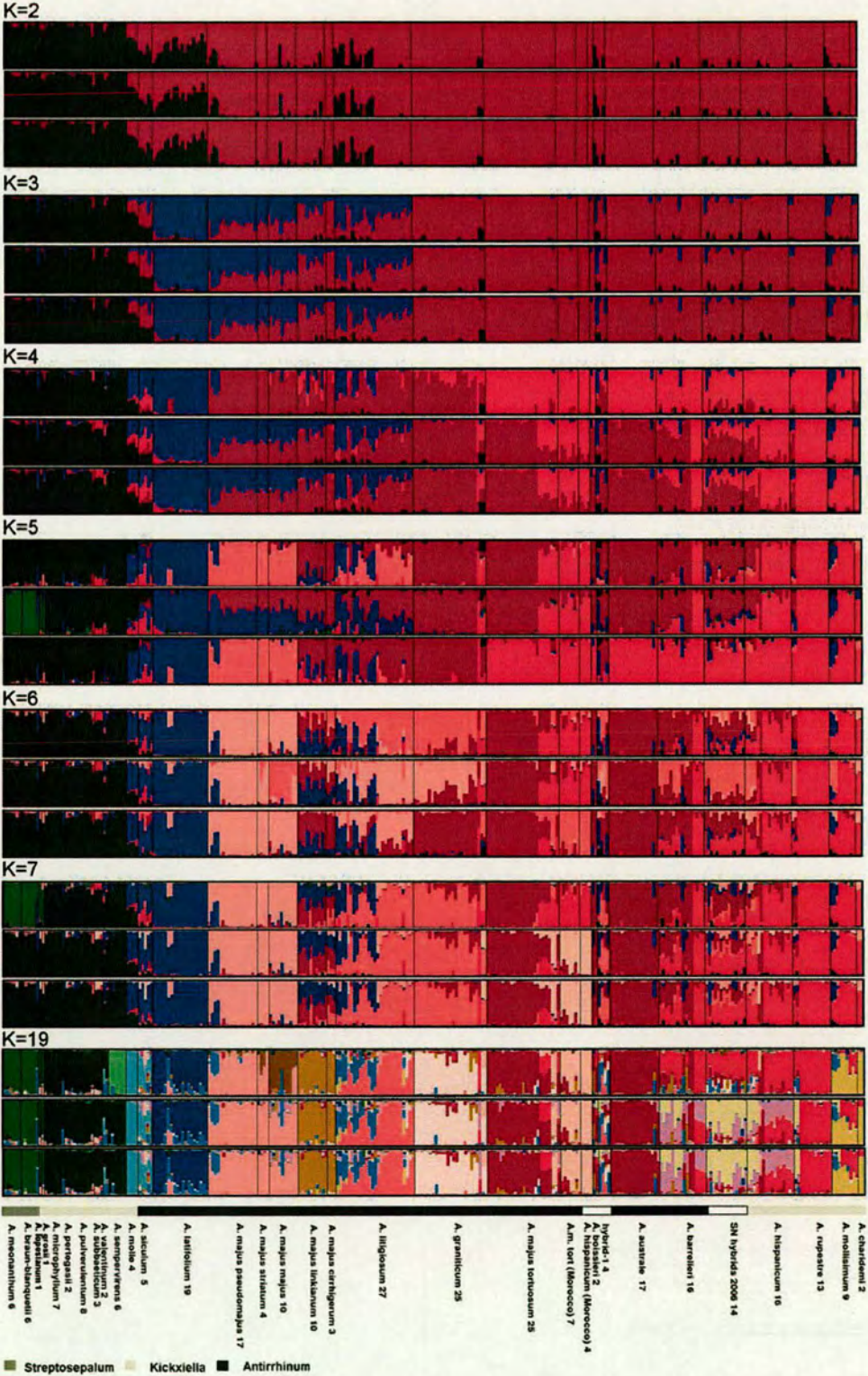


Figure 3.13. Graphs showing the genetic make-up of each individual, based on *Structure* simulations. The results of the *Structure* simulations using the parameters of model 2 (Table 3.4) are shown for when the number of populations (K) is set to 2, 3, 4, 5, 6, 7 and 19. For each of these values of K, the results of three simulations are shown. Each population that is inferred is represented by a different colour. Individuals are grouped by species along the x-axis, with each column representing an individual. The y-axis shows the proportions of each individual's genome that consists of each inferred population. The category 'SN hybrids' consists of *A. barrelieri* x *A. rupestre* individuals from the Sierra Nevada mountain range (Table 2.1). Otherwise the individuals of each species that were included are as detailed in Table 3.2. The ordering of individuals along the x-axis is shown in Appendix A.

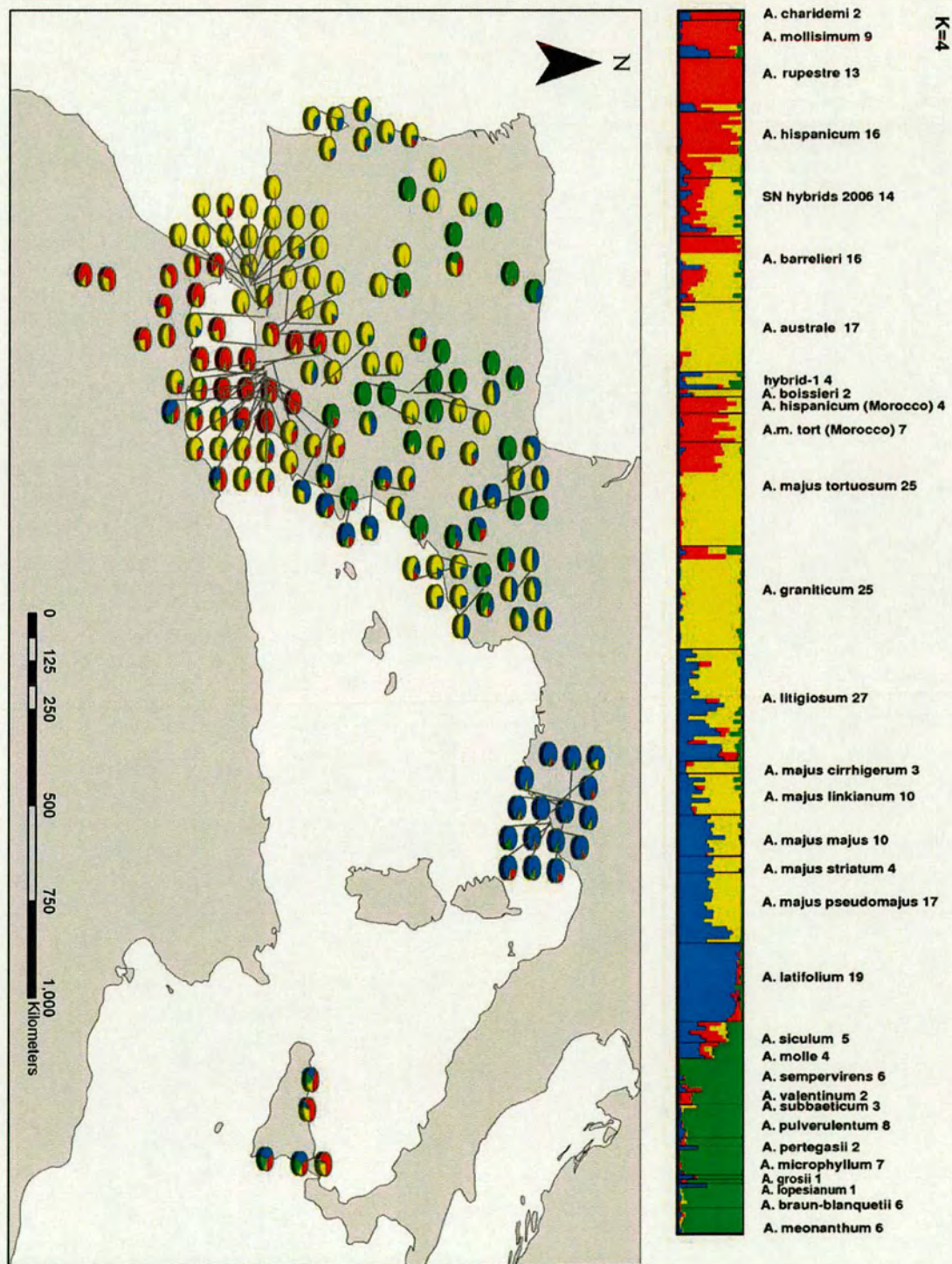
A. majus tortuosum and *A. majus australe*. The accessions of *A. majus tortuosum* and *A. hispanicum* distributed in Morocco and Italy are recognised as a separate population and the central and north-east Spanish species, *A. graniticum* and *A. majus litigiosum* form another population. However, *A. majus cirrhigerum* and *A. majus linkianum* are shown to be admixed, both having equal proportions of the *A. latifolium* population loci and *A. majus tortuosum* loci. This may be because they are genetically distinct from the other inferred populations, but K is too low to enable them to be delimited, so the model approximates their genetic make-up. This view is supported by the finding that they are recognised as distinct at higher values of K .

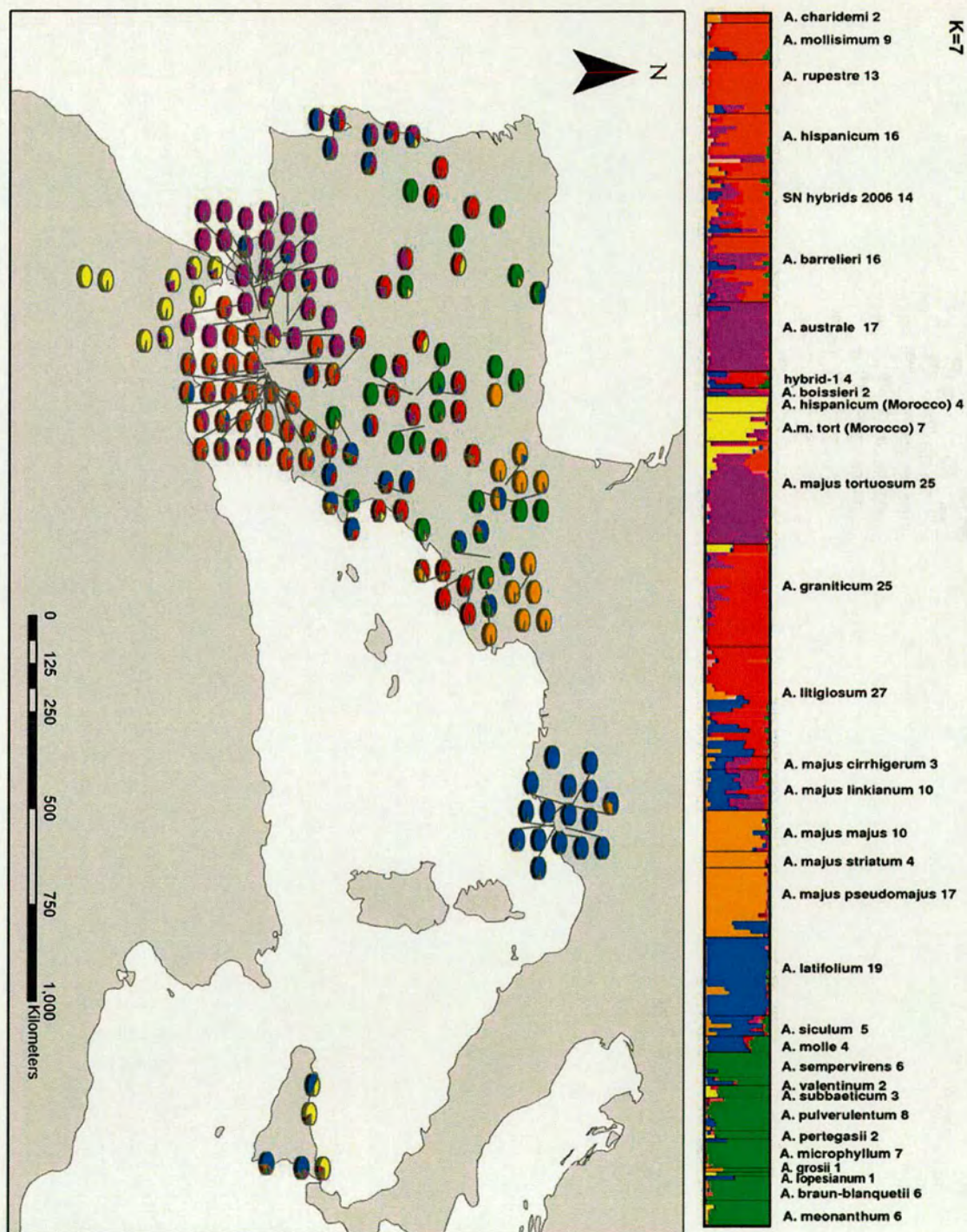
The maximum number of populations recognised by the model is shown for $K=19$ in Figure 3.13. The northern Iberia group is now distinct from the core Kickxiella with *A. sempervirens* being recognised as a separate population in some simulations. Similarly, *A. majus striatum* and *A. majus pseudomajus* are occasionally identified from *A. majus majus*. The genetic structure of the species distributed in the Sierra Nevada region, *A. barrelieri*, *A. hispanicum*, *A. rupestre* and the hybrids between these species, remains poorly defined, except that *A. rupestre* is recognised as distinct in some cases. The neighbouring and closely related species, *A. mollissimum* and *A. charidemi* are distinguished from the Sierra Nevada populations. *A. graniticum* is also recognised as a separate population from all other species. The individuals of *A. majus litigiosum* distributed in the Valencia region are admixed with their genetic make-up consisting of loci from both *A. majus litigiosum* and from a different population, which does not correspond to any of the taxa analysed here. Small proportions of this other population also occur in the genetic make-up in individuals of *A. latifolium*, the *A. majus* species of the Pyrenees and the southern Spanish Kickxiella. This population could represent an ancestral lineage of the Kickxiella as its signal emerged from the *A. latifolium* population recognised at lower values of K . Its emergence from *A. latifolium* is significant as *A. latifolium* has an incongruent Kickxiella chloroplast haplotype and there is evidence of hybridisation between Kickxiella and Antirrhinum species in the Pyrenees. This is further supported by the presence of incongruent Kickxiella chloroplast haplotypes in these individuals of *A. majus litigiosum*.

The sequence in which populations are identified with increasing values of K (Figure 3.13) is not taken to reflect the sequence of divergence of lineages. Instead, it is likely to reflect the relative distribution of genetic variation within and between each of the species. Given that there is a strong geographic component to the distribution of genetic variation, this is likely to be affected by the geographic density of species sampling. Therefore *A. latifolium* may be recognised as a distinct

Figures 3.14 and 3.15. Map showing the geographic patterns of the average genetic make-up of sampled populations when $K=4$ and when $K=7$.

The top panel shows the results of one simulation for $K=4$ (Figure 3.14) and $K=7$ (Figure 3.15). Each ancestral population inferred by *Structure* is represented by a different colour. Individuals are grouped by species along the x-axis, with each column representing an individual. The y-axis shows the proportions of each individual's genome that consists of each inferred ancestral population. In the map below, the average proportions of each inferred ancestral population are within each sampled population are represented by a pie-chart at each location.





population because all individuals were sampled from a relatively small geographic area (Figure 3.14). Likewise, the southern and central Spanish population may be clearly delimited at low values of K because of the high density of sampling of the species in these regions.

The clustering of individuals into populations by *Structure* is, however, largely consistent with the results of the previous analyses. The only major difference is that *A. siculum* and *A. molle* share the same genetic make-up for even high values of K (Figure 3.13). Both phylogenetic and geographic signals are recognised, as shown in Figures 3.14 and 3.15. While there is a spatial patterning in the populations identified by *Structure*, the core Kickxiella species remain distinct from subsection Antirrhinum and the southern Spanish Kickxiella carry a small proportion of core Kickxiella loci in their genetic make-up. The northern Iberian group consisting of both Streptosepalum and Kickxiella species is also identified as a single population by the *Structure* analyses.

3.4 Discussion

3.4.1 A model for the evolutionary relationships between *Antirrhinum* species

By integrating the results of the analyses carried out in this chapter, I propose a simplistic model to describe the evolutionary relationships of the Antirrhinum species (Figure 3.16). In this model the lineages leading to *A. siculum* and to subsection Antirrhinum diverged from the Kickxiella lineage. Numerous episodes of hybridisation then occurred in geographic regions where species of the Antirrhinum and Kickxiella lineages come into contact, shown in Figure 3.16B.

The relative times of the hybridisations are suggested by various sources of evidence. The populations of *A. majus litigiosum* from Valencia are inferred to be the result of ancient hybridisation between an *A. majus* subspecies with an ancestral Kickxiella species. The Kickxiella parent, or close relatives, possibly also hybridised with *A. latifolium* and the Pyrenean *A. molle* and *A. sempervirens*. This proposal is based on the genetic make-up of these taxa estimated by *Structure* and the fact that all these species are fixed for incongruent chloroplast haplotypes. The genetic delimitation of *A. latifolium*, *A. molle* and *A. majus striatum* and *pseudomajus* in both the neighbour-joining and PCoA analyses also supports an ancient hybrid origin.

The northern Iberian group is also proposed to be the result of ancient hybridisation that allowed subsequent fixation of chloroplast haplotypes in each of the species, their definitive clustering with the core Kickxiella by *Structure* and the divergent morphologies of the Streptosepalum compared to the Kickxiella species. As only one individual of *A. lopesianum*, two individuals of *A. grosii* and

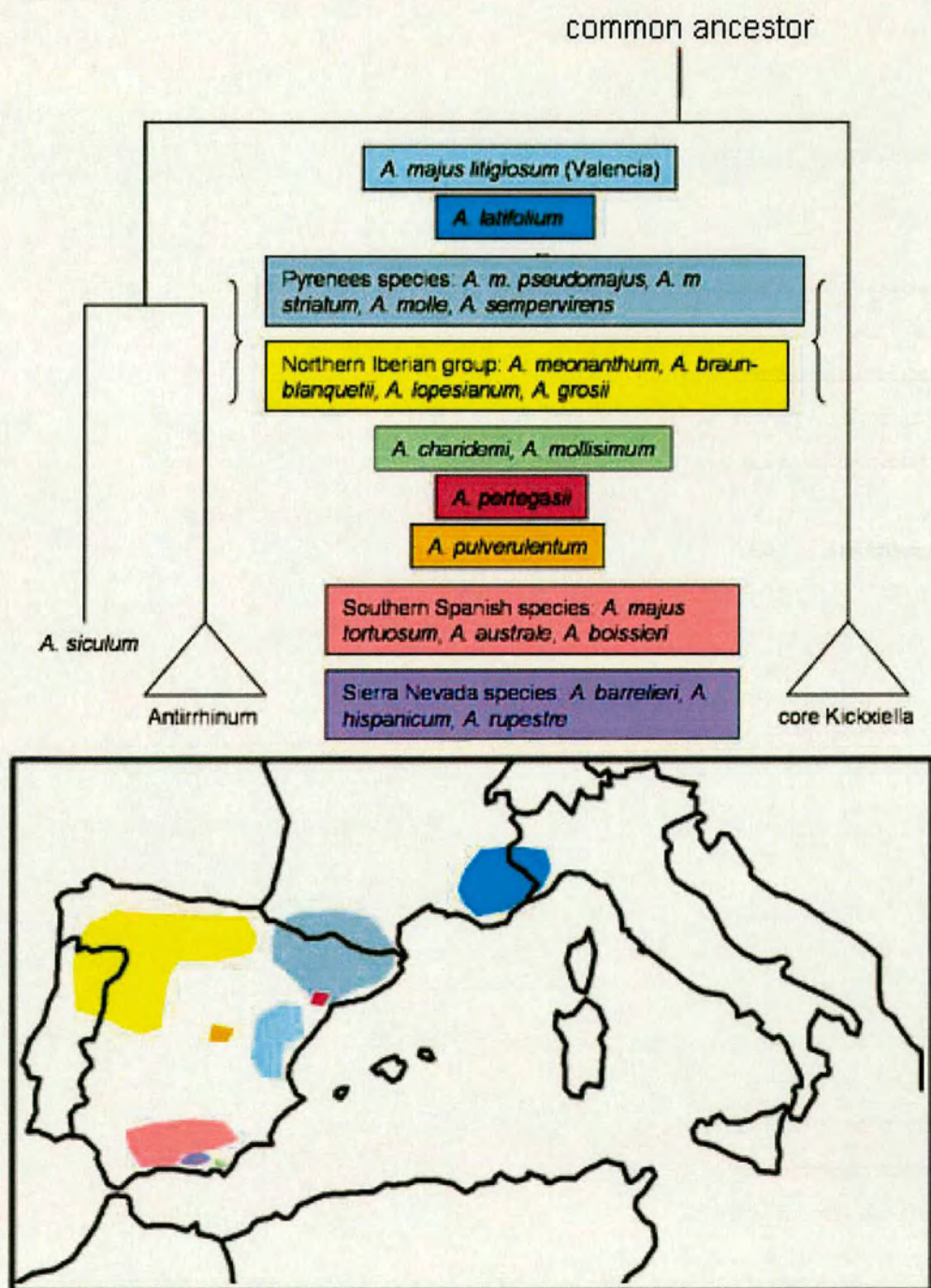


Figure 3.16. The model proposed to describe the evolutionary relationships of the *Antirrhinum* species.

The relationships of the main lineages identified by the chloroplast haplotype and AFLP analyses are shown. The species groups that are inferred to be the result of hybridisation between the two main lineages are shown. The estimated time of hybridisation is also indicated by the position of the box in relation to the time since divergence of the main lineages. The colours in the boxes correspond with the shading on the map below to indicate the geographic regions where these species occur.

relatively few accessions of *A. meonanthum* and *A. braun-blanquetii* were sampled, it is possible that the chloroplast haplotypes observed are not fixed in these species, however, similar results were also obtained by Vargas *et al* (2009).

The southern Spanish species *A. charidemi* and *A. mollisimum* are also inferred to result from hybridisation that was relatively ancient, because they are genetically distinct enough to be delimited by the neighbour-joining and *Structure* analyses. Again, sampling further accessions of these species would test whether the Kickxiella clade haplotype is fixed in these species, providing further evidence for ancient hybridisation.

The southern Spanish species *A. majus tortuosum* and *A. australe* are inferred to be the result of more recent hybridisations. *A. australe* is possibly the result of hybridisation with sympatric Kickxiella species as its distinguishing characteristic is the presence of trichomes on the stem and sometimes the leaves, whereas the majority of subsection Antirrhinum species, including *A. majus tortuosum*, are glabrous. This inference of recent hybridisation is supported by the morphological variation observed within and between *A. majus tortuosum* and *A. australe*, the occurrence of both Antirrhinum and Kickxiella haplotypes within these species, as well as their lack of delimitation in the neighbour-joining and PCo analyses.

The lack of delimitation of the species occurring in the Sierra Nevada region of southern Spain, *A. hispanicum*, *A. rupestre* and *A. barrelieri*, by any of the analyses described in this Chapter is inferred to be the result of ongoing gene-flow between them. This was further supported by population genetic analysis of AFLP and microsatellite markers and morphological characterisation of ~200 individuals from 20 populations and by the existence of current hybrid zones where *A. rupestre* and *A. barrelieri* are in contact in the Sierra Nevada (results not shown).

Extensive morphological variation was observed between populations of *A. majus tortuosum* collected in Morocco, with some of these populations resembling *A. barrelieri*. However, the AFLP analyses did not identify corresponding genetic structure and placed these accessions with the accessions of *A. hispanicum* also collected in Morocco. All Moroccan accessions were delimited from the rest of the genus by the neighbour-joining and *Structure* analyses; however, their delimitation was not clear in the PCoA. This might reflect noise within the AFLP dataset (Section 3.3.1) and sparse sampling. The Moroccan accessions, including those of *A. hispanicum*, share a derived chloroplast haplotype lineage within the subsection Antirrhinum clade, which indicates

their divergence from the rest of the genus. However, accessions of *A. majus tortuosum*, *A. majus australe* and *A. majus striatum* also shared this haplotype, possibly due to incomplete lineage sorting.

Unfortunately I was unable to locate populations of *A. martenii*, which is the only *Kickxiella* species occurring in Morocco. It would have been interesting to determine the relationships of *A. martenii* to the other *Kickxiella* species. Further sampling of populations in this region would also be necessary to gain a better understanding and classification of the Moroccan *Antirrhinum* populations.

3.4.2 Distinguishing hybridisation from lineage sorting

The hypothesis for the evolutionary relationships of the *Antirrhinum* species developed in this chapter is based partly on the identification of divergent lineages in the chloroplast haplotype network and the inference that incongruence between chloroplast haplotypes and morphological and nuclear characters reflects hybridisation. However, lineage sorting may also have contributed to incongruence, despite the smaller effective population size of chloroplast markers. Such lineage sorting has been detected with intensive intra-specific sampling in other genera (Comes and Abbott 2001, Jakob and Blattner 2006). Particularly relevant to this study is that incomplete lineage sorting of chloroplast haplotypes was found to be common in a study of the Mediterranean *Senecio* sect. *Senecio* (Comes and Abbott 2001), which also probably diversified recently and shares a common geological history with *Antirrhinum*. However, *Antirrhinum* differs from *Senecio* in life history traits that are likely to influence the occurrence of incomplete lineage sorting in *Senecio*. The fruit of *Senecio* are adapted to long-range dispersal by wind, whereas those of *Antirrhinum* show no obvious adaptation for dispersal. Therefore chloroplast haplotypes, which are dispersed only in seed, should migrate less in *Antirrhinum* than *Senecio* so the effective population size is likely to be smaller for *Antirrhinum* and chloroplast haplotypes are more likely to become fixed in the smaller more isolated *Antirrhinum* lineages. Geographic relationships between chloroplast haplotypes are also more likely in *Antirrhinum*.

Some aspects of the *Antirrhinum* chloroplast haplotype network shown in Figure 3.2 are consistent with incomplete lineage sorting, but only within the main clades. Within each clade many species share the same haplotype, which because it is the most abundant is likely to be ancestral (Posada and Crandall 2001), with some species such as *A. graniticum*, *A. sempervirens* and *A. valentinum* having haplotypes derived from these ancestral haplotypes. For example, *A. graniticum* carries both

a derived haplotype (haplotype 10 in Figure 3.2) and more ancestral haplotypes (haplotype 3) that it shares with a number of other species. In contrast, the ancestral haplotypes of the major clades are distinct from each other. For example, haplotype 3 in the *Antirrhinum* clade and haplotype 26 in the *Kickxiella* clade are separated by 11 polymorphisms, which supports the inference of separate lineages.

The instances of nuclear and morphological incongruence with chloroplast haplotype have a geographic pattern. Furthermore, incongruent individuals mostly have derived chloroplast haplotypes that are placed at the tips of the branches in the chloroplast haplotype network. Both these factors are consistent with hybridisation rather than lineage sorting. For example, in the Pyrenees all sampled of *A. sempervirens* and *A. molle* are fixed for haplotypes that are incongruent with their morphologies. *A. molle* and *A. sempervirens* grow in sympatry with *A. majus* subspecies *striatum* and *pseudomajus* in this region. An *A. sempervirens* individual shares a derived haplotype with an *A. molle* individual, whilst other *A. molle* individuals share derived haplotypes with *A. m. striatum* and *A. m. pseudomajus* individuals, indicating hybridization between all three species in this region. *A. latifolium* provides another example where all individuals of the species are fixed for chloroplast haplotypes incongruent with morphology. The morphology of *A. latifolium*, which is similar to that of subsection *Antirrhinum*, is very different from the *Kickxiella* species, yet all individuals (one from each of 10 populations) carry derived haplotypes in the *Kickxiella* lineage. This was confirmed by restriction enzyme genotyping for the mutation leading to haplotype 24 of *A. latifolium* (Figure 3.2), which adds an extra *MseI* digestion site to the *trnD-trnT* locus (data not shown). This incongruence is more easily explained by hybridisation than lineage sorting.

Further evidence that supports the inference of hybridisation leading to incongruencies between morphology and chloroplast haplotype is provided by the species that are not fixed for chloroplast polymorphisms. In these cases, the chloroplast haplotypes occurring in each species represent extremes of sequence divergence. For example, the haplotypes in *A. australe* differ by up to 17 sites, while those within either *A. tortuosum* or *A. hispanicum* differ by up to 14 sites.

The chloroplast has been shown to be predominantly maternally inherited in most angiosperms. However, low levels of paternal transmission have been suggested to occur in *Antirrhinum majus*, based on the detection of extra-nuclear DNA in pollen grains, although genetic tests have detected only maternal transmission (Corriveau and Coleman 1988, Harris and Ingram 1991). Low levels of

paternal chloroplast transmission are assumed insignificant in affecting the hypotheses being tested here. No evidence of bi-paternal chloroplast transmission was suggested by potential recombination between chloroplast haplotypes and, if it has influenced the topology of the chloroplast haplotype network, it does not affect the evidence for extensive hybridisation.

In addition to genetic evidence of historical hybridisation between *Antirrhinum* species, there was also morphological evidence of current hybridisation in several locations:

- 1) Reolid, Albacete province, Spain, and Arroyo, Jaen province, Spain.
Plants of *A. majus ssp. majus* habit with a dense, sticky indumentum were observed in several populations along the N322 road. These plants were difficult to identify and are possibly hybrids between the garden *A. majus* and *A. boissieri* or *A. australe*.
- 2) Gallur, Zaragoza province, Spain.
Plants of *A. majus ssp. litigiosum* habit and flower colour with a dense, sticky indumentum were sampled from a population on a stop along the A68 motorway. They are likely to be hybrids between *A. majus ssp. litigiosum* and *A. graniticum*, which are sympatric in this area.
- 3) Panticosa, Huesca province, Spain.
A population of plants of *A. majus ssp. majus pseudomajus* habit and flower colour with a dense, sticky indumentum were discovered. These are possibly hybrids between *A. majus ssp. majus pseudomajus* and *A. sempervirens*, which grow sympatrically in this area.
- 4) The Sierra Nevada mountain range, Granada province, Spain.
Populations segregating for morphological characteristics of *A. barrelieri*, *A. majus tortuosum* and *A. hispanicum* were sampled. Genetic analyses provided strong evidence for hybridisation.

Further hybrid populations of *A. majus tortuosum* × *A. mollisimum* (*A. x kretschmeri*) in the Sierra de los Filabres and *A. barrelieri* × *A. mollisimum* (*A. x chavannesii*) in Sierra de Gador, both in Almeria province, were documented by Rothmaler (1956). Mateu-Andres (2003) also documents hybridisation between *A. australe* and *A. boissieri*.

Although in most cases hybridisation is inferred based on morphological characteristics that could have evolved independently, hybridisation is the most likely explanation as in all cases the populations have mixed characteristics of species that grow in sympatry. These examples of ongoing hybridisation show that there are few barriers to gene flow between *Antirrhinum* species

and give further support to the inference of extensive hybridisation having occurred within the genus.

The geographically defined populations inferred by the *Structure* analyses corroborate this interpretation. Although *Structure* is usually used to analyse intraspecific variation (Manel *et al* 2005), it has been successfully used to address similar questions to this study in *Conradina* (Lamiaceae) by Edwards *et al* (2008) and *Argyroderma* (Aizoaceae) by Ellis *et al* (2006). This is possible because the allele frequency distributions of multiple loci in each population ('P' in Pritchard *et al* 2001) are inferred from coalescent models, which are probably appropriate for the short time-scale involved in the diversification of the *Antirrhinum* species and the other taxa. The genetic similarities inferred by *Structure* are therefore taken to reflect the main evolutionary patterns in *Antirrhinum*.

3.4.3 The effect of hybrids on the AFLP neighbour-joining phylogenies

The effect of hybrid individuals on phylogenetic tree reconstruction is largely unpredictable and depends on the divergence of the parental taxa, the extent of subsequent back-crossing of the hybrid population with one of its parents and the time since the hybridisation event (McDade 1992, Posada and Crandall 2002, Vriesendorp and Bakker 2005, Reeves and Richards 2007). However, several characteristics of the phylogenies resulting from the neighbour-joining analyses of the pair-wise distances between individuals suggest hybridisation within *Antirrhinum*. One such indication is the shallow, or non-existent, internal branches compared to the long terminal branches in the phylogenies shown in Figures 3.6 and 3.9. Simulations have shown that the inclusion of recombinant sequences in distance based phylogenetic analyses can cause this effect (Schierup and Hein 2000).

The hybridisation of *Antirrhinum* species inferred in this study involves divergent lineages. This has been shown to be the most disruptive to phylogenetic reconstruction by decreasing both the accuracy of the resulting topology and the support for the tree (McDade 1992, Posada and Crandall 2002). Evidence for this effect is provided by the analysis carried out without putative hybrid individuals in Section 3.3.3.ii. In the resulting phylogeny internal branches are longer, supporting deep divergence events of the main lineages, and have increased bootstrap support. As the main lineages correspond largely with those of the chloroplast haplotype network, they are taken to represent early species diversification within the genus. An indication of the conflicting signal that is introduced to the dataset by a proportion of the loci within the hybrids is the decreased bootstrap

value for the nodes supporting these main lineages when hybrids are included. Such comparison of bootstrap support for detection of homoplasy and hybridisation is advocated in techniques such as reduced consensus methods (Wilkinson 1996).

The accessions that were removed in order to resolve the main lineages in the neighbour-joining phylogenies of Figures 3.10 and 3.11 all showed at least one type of prior evidence of having undergone hybridisation. *A. molle*, *A. boissieri*, *A. latifolium*, *A. majus litigiosum*, *A. mollissimum*, *A. charidemi*, *A. hispanicum* and *A. rupestre* all show incongruence of chloroplast haplotypes with nuclear marker and/or morphology (compare Figure 3.2 to Figure 3.8). *A. barrelieri*, *A. majus tortuosum* and *A. australe* each carry divergent chloroplast haplotypes and grow in sympatry with species listed above. Putative hybrids have been removed prior to phylogenetic analysis in numerous studies of both plants and other taxonomic groups, to allow resolution of phylogenetic relationships (examples in Vriesendorp and Bakker 2005, van der Niet and Linder 2008). This approach was also taken here, but mainly to test the hypothesis of hybridisation. Given the extent of hybridisation inferred, and the possibility that other hybridisation events have remained undetected because they have not resulted in incongruence, it is difficult to determine the extent to which the resulting phylogenies reflect the relationships of the remaining species. However, the main clades that correspond with the clades of the chloroplast haplotype network are taken to be accurate.

Other inferred hybrid species and individuals do not seem to affect the topology or support of the main lineages in the phylogenies studied. These include *A. meonanthum* and *A. braun-blauquetii*, *A. lopesianum*, *A. grosii* and *A. pertegasii*. A likely explanation is that these hybridisation events were ancient and there has been extensive back-crossing between the hybrid population and one of the parental populations, so that the nuclear genotypes of the species are essentially those of the recurrent parent.

The alternative interpretation of the lack of resolution in AFLP phylogenies of all accessions is that the genus diversified rapidly and lineage sorting occurred. This interpretation cannot be ruled out because of the similarity of the phylogenetic signals of lineage sorting and hybridisation. However, lineage sorting is unlikely to explain all cases of incongruence, because this would imply that speciation had been followed by divergent evolution - to the morphology typical of subsection *Antirrhinum* or subsection *Kickxiella* in all cases. Hybridisation therefore provides the simpler explanation, particularly given the geographic pattern to cytonuclear discordance.

3.4.4 Reliability of rooting the phylogeny using *Misopates*

Ideally, accessions from the new world *Antirrhinum* genera *Mohavea* and *Sairocarpus* should have been used with *Misopates orontium* to give more reliable rooting. I was unable to obtain DNA from accessions of these genera at the time of carrying out the AFLP analysis and have yet to sequence the chloroplast loci from the samples that I have subsequently obtained.

Despite the extensive divergence of the *M. orontium* chloroplast loci from those of the *Antirrhinum* species, it was still possible to root the chloroplast haplotype network by sequence comparison. All but one of the polymorphisms that underlie the haplotype network support the position of *M. orontium*; this polymorphism is therefore assumed homoplasious. Given the divergence of the *M. orontium* chloroplast sequence from the *Antirrhinum* sequences, using *M. orontium* to root the AFLP phylogenies may lead to incorrect phylogenetic inference as the proportion of homologous AFLP bands shared by *M. orontium* with the *Antirrhinum* species may be low, possibly leading to long branch attraction (Koopman 2005). However, the sequence of divergence of the main lineages inferred by the rooting of the AFLP phylogeny and from the chloroplast haplotype network is similar, supporting the proposed model of the evolutionary history of the *Antirrhinum* species outlined above.

Regardless of the rooting, the relationships between *A. siculum*, subsection *Antirrhinum* and subsection *Kickxiella* are all congruent in both the rooted and the un-rooted nuclear phylogenies and in the chloroplast haplotype network.

3.4.5 Summary of the genetic delimitation of *Antirrhinum* species.

In addition to resolving the evolutionary relationships within *Antirrhinum*, the work in this chapter also addressed the extent to which the *Antirrhinum* species are genetically delimited from each other. The majority of species were found to cluster genetically, as shown in the neighbour-joining analysis and PCoA of all individuals (Figure 3.6 and Figure 3.7). However, there was no clear delimitation as species closely neighboured and sometimes overlapped with others in the ordination (Figure 3.7). This may be the result of extensive hybridisation. Noise in the AFLP dataset was found to be relatively high (Section 3.3.1) and this might also have contributed to the lack of delimitation. However, the effect of noise is less likely given the phylogenetic signal that is evident when putative hybrids are removed from neighbour-joining analysis.

There are several different outcomes resulting from the hybridisation on the delimitation and relationships of the *Antirrhinum* species that are inferred by AFLP markers. In the species in the north east of the Iberian peninsular, in the Pyrenees and Alps, relationships inferred by nuclear markers are congruent with morphological subsection; *A. latifolium*, *A. majus pseudomajus* and *A. majus striatum* are clustered with the Antirrhinum subsection species and *A. molle* and *A. sempervirens* cluster with the Kickxiella species. Accessions of these species cluster with strong support into their respective species.

In the northwest of the Iberian peninsular the *Streptosepalum* species, *A. meonanthum* and *A. braun-blanquetii*, which are of similar morphology to Antirrhinum subsection species, are shown to be more closely related to the Kickxiella species *A. lopesianum* and *A. grosii* and they cluster with the Kickxiella species in neighbour-joining phylogenies. There is weak species delimitation of the accessions of these species.

In central Spain, the distribution of *A. majus litigiosum* borders that of *A. graniticum* and these two species are clustered in the same population by analyses carried out in *Structure*. These species are delimited from each other in all analyses, but are close to each other in the space defined by the axes of the PCoA and a population of putative hybrids between these species was discovered (Section 3.4.2). The model proposed for the evolutionary history of the genus therefore is likely to be simplistic as there is no other genetic evidence to suggest that *A. graniticum* and the northern populations of *A. majus litigiosum* have undergone hybridisation, yet there is a spatial component to their relationships with other species. Furthermore, in the neighbour-joining phylogenetic analyses *A. majus litigiosum* is clustered with *A. majus pseudomajus*, which borders its distribution to the north and *A. graniticum* is clustered with *A. australe* and *A. majus tortuosum*, which border it to the south. The patterns of relationship within the Antirrhinum subsection species are therefore defined mainly by geography.

The species distributed in southern Spain all cluster with the Antirrhinum subsection species. Therefore *A. charidemi*, *A. mollisimum*, *A. hispanicum*, and *A. rupestre* have incongruent morphologies compared to nuclear markers. The two Antirrhinum subsection species, *A. australe* and *A. majus tortuosum* are not delimited from each other. This is supported by population genetic analyses using allozyme markers carried out by Mateu-Andres and de Paco (2005). The other southern Spanish subsection Antirrhinum species, *A. barrelieri*, is delimited from the rest of the subsection including *A. majus litigiosum*, which it is morphologically similar to, although a few

individuals overlap with *A. majus tortuosum* in the ordination. However, it is not differentiated from the southern Spanish Kickxiella species.

The subsection Antirrhinum species from Portugal, *A. majus cirrhigerum* and *A. majus linkianum* are distinguished from all other species. There is some evidence of delimitation from each other in the neighbour-joining analysis (Figure 3.6), although they do overlap slightly in the PCoA (Figure 3.7).

The lack of resolution of many species by the *Structure* analysis, in particular within subsection Kickxiella, is not unexpected given the poor intra-specific sampling.

3.5 Conclusions

The molecular marker analyses of this chapter identify two lineages within *Antirrhinum* that correspond to the classical morphological subsections Antirrhinum and Kickxiella. The species of the third morphological subsection, Streptosepalum, are suggested to be the result of ancient hybridisation between Antirrhinum and Kickxiella species. The Kickxiella species are endemic to particular mountain ranges within the Iberian peninsula and mostly grow on rock faces, whereas the Antirrhinum species are widespread and abundant and grow in a variety of different habitats. The geographic structure of genetic variation within the genus is consistent with species of the Antirrhinum subsection hybridizing with the Kickxiella that are endemic to the same region. The majority of populations resulting from this hybridisation, particularly the currently recognized species of subsection Antirrhinum, have cohesive genetic similarities but overall are not clearly delimited. Too few populations of each Kickxiella species were sampled to estimate their delimitation and relationships accurately; however, they show similar patterns of delimitation to the species in subsection Antirrhinum.

Chapter 4: Morphological characterisation of the *Antirrhinum* species

4.1 Introduction

4.1.1 Background and aims

The current taxonomy of the *Antirrhinum* genus is based predominantly on morphological characters and can be best described by the criteria summarised by Cronquist (1978): “species are the smallest groups that are consistently and persistently distinct and distinguishable by ordinary means” (cited in Sites 2004). However, by this operational criterion, there does not seem to be a well-defined classification *Antirrhinum* (Jimenez *et al* 2005). This is for several reasons: most morphological characters overlap between species, not all characteristics are measured consistently across all species and mostly herbarium specimens collected from the field have been characterised and their growth could therefore be influenced by environmental conditions. Furthermore, on many of these specimens it is not possible to characterise all parts of the plant (Webb 1971, Sutton 1988). This situation is exacerbated by the inconsistent species nomenclature used by different authors, making it difficult to define some species and to integrate information on the morphology of species. Therefore, there is a broad, qualitative, understanding of the morphological characteristics of *Antirrhinum* species, but there are no explicit accounts of intra- and inter-specific morphological variation and correlations between morphological traits. This lack of a quantitative morphological framework makes it difficult to design experiments to test for associations between morphological and molecular variation.

The results of the molecular analyses in Chapter 3 provide support for the hypothesis put forward by Webb (1971) that the more widespread subsection *Antirrhinum* species hybridise with *Kickxiella* species where they come into contact. This makes the morphological delimitation of species and their organisation into higher categories difficult. A pertinent question is to what extent do *Antirrhinum* species differ morphologically given this reticulate evolution? There are vast perceived morphological differences between ‘good’ examples of each of the two main lineages that may be related to their different habitats and ecologies. A further question is therefore what forms do hybrid species take – are they similar to one of the parental species, intermediate between them, or are they of novel morphology? Insights on constraints to *Antirrhinum* morphology can be gained from addressing these questions.

The aim of this chapter is to provide a quantitative description of morphological variation based on the accessions used to determine the structure of genetic variation within the genus. This

description is for three purposes. The first is to test species delimitation using morphological characters. The second is to relate morphological variation within *Antirrhinum* to the distribution of genetic variation, thus further clarifying the taxonomy of the genus. The third purpose is to provide a morphological framework for identifying the molecular basis of variation and inferring the evolutionary processes underlying this variation.

4.1.2 Choice of morphological characters

As the following morphological description is to both delimit species and to further develop *Antirrhinum* as a model system for evolutionary genetics, both characters considered appropriate for the taxonomy of the genus and those that might be more related to species ecology were analysed. Trichome morphology, stem width and sepal size and shape are examples of classical taxonomic characters, whilst characters such as plant height, flowering time, inflorescence architecture, growth form, and leaf and flower size are of interest in studies of morphological evolution. These latter characters were chosen for analysis because their genetic basis has been characterised in *Antirrhinum* and other model species and ongoing research is to understand how their respective developmental pathways have evolved to give rise to morphological diversity. Although this group of characters might be inappropriate for taxonomy because of the increased likelihood of convergent evolution, many of them are used implicitly in taxonomic descriptions of *Antirrhinum* species and they may therefore delimit species.

4.1.3 Approaches in developing metrics that describe morphology

i) Describing complex morphological characters

Many features of *Antirrhinum* morphology can be captured either as discrete characters, for example, the presence or absence of certain types of trichomes, or as continuous characters, for example, plant height, flowering time, and flower stigma and anther filament length. However, the effective description of complex morphological characters such as leaf and flower shape is challenging because one-dimensional measurements are often inadequate in conveying key attributes of biological form. This is particularly relevant in attempting accurate morphological delimitation of *Antirrhinum* species as at low taxonomic levels phylogenetic signal is potentially lost through using univariate or discrete coding for morphological structures (Gonzalez-Jose *et al* 2008).

A suitable technique that summarises variation in complex morphological characters is Principal Components Analysis (PCA) of cartesian coordinates that are positioned to capture key attributes of

the character under investigation. This technique describes the shape of the character using a set of cartesian coordinates, called here a point-model. Each sample is described by a point-model. PCA on the point-models representing the sample population identifies the principal components (axes) that describe the covariances between the x- and y-values of the coordinates describing the shape. As a result, the variation in shape is summarised by a set of axes, with the main axis accounting for the highest proportion of variation and subsequent axes accounting for residual variation and being orthogonal to the previous axes. As all axes are orthogonal, unique correlations between characters are identified by each axis.

PCA has been used effectively to describe and test hypotheses on the development and evolution of a variety of different morphological structures, for example, human cranium morphology (Gonzalez-Jose *et al* 2008), butterfly genitalia (Nice *et al* 2002) and cichlid jaw and skull morphology (Albertson and Kocher 2005). It has also been used to describe leaf shape in mutant lines of *A. majus* (Bensmihen *et al* 2008) and leaf and flower shape variation in populations derived from crosses of *A. majus* to *A. charidemi* (Langlade *et al* 2005, Feng *et al* 2009) and *A. majus* to *A. molle* (Yang 2006). These latter studies in *Antirrhinum* identified QTL that are associated with the derived PCA parameters. Therefore, parameters derived from similar PCA analysis of leaf and flower variation within *Antirrhinum* can be related to genetic variation.

ii) *Strategy in developing descriptive variables*

Different metrics such as discrete scoring, univariate measures and parameters obtained from multivariate analyses are developed to describe nearly all aspects of *Antirrhinum* morphology. However, it proved difficult to identify patterns of variation and correlations between characters to address the more complex questions formulated at the beginning of the chapter through comparing these measures individually. PCA is also a suitable technique for summarising the patterns of variation in this situation. Therefore, the metrics used to describe morphology were developed to be compatible with subsequent multivariate analyses, which are carried out in Chapter 5.

4.1.4 **Structure of the morphological descriptions**

In the subsequent descriptions, several general features of the variation of each character are explored. For continuous characters, one-way ANOVA is carried out to describe the distribution of variation within compared to between species, with the R^2 value being used to estimate the proportion of variation that is attributable to between species comparisons. Tables indicating

whether the mean values of each character differ significantly between pair-wise comparisons of all species are also shown.

In addition to providing a quantitative description of morphology, the interpretation of the variation of each character is focussed on addressing the two main questions outlined at the beginning of the chapter. The first is to compare the structure of morphological variation with that of genetic variation identified in Chapter 3. Therefore, the extent to which the character is divergent in the *Kickxiella* and *Antirrhinum* lineages is assessed. For some comparisons, the groups identified in the previous chapter such as the southern Spanish *Kickxiella* and the core *Kickxiella* are also referred to.

The second focus is to determine the morphological delimitation of similar species. These comparisons fall into several overlapping categories. The first category is those species that are not clearly delimited by the genetic analyses. Examples are: *A. australe* compared to *A. majus tortuosum*, *A. majus cirrhigerum* to *A. majus linkianum*, *A. braun-blanquetii* to *A. meonanthum*, and the differences between the southern Spanish *Kickxiella* species. The second category comprises species that are difficult to delimit based on taxonomic accounts, the main such comparison being between *A. barrelieri*, *A. majus tortuosum* and *A. majus litigiosum*. The final category is the comparison of diverged populations of species that were identified by the genetic analysis of Chapter 3. Therefore, accessions of *A. majus litigiosum* from the area surrounding Valencia are compared to those distributed further north and accessions of *A. hispanicum*, *A. majus tortuosum* and *A. barrelieri* from Morocco (and Italy for *A. m. tortuosum*) are compared to their respective con-specific accessions from Spain.

4.2 Experimental approach and sampling

An extensive morphological analysis of accessions from throughout the distribution of each species was carried out using plants that have been grown in standard conditions. Where possible seed from up to five plants from each location was sown and up to three siblings from each of these families were measured. This experimental design was to estimate how much of the variation is determined by genetic differences, rather than by environmental variation or experimental errors and artefacts, by comparing the variance between genetically identical families (which is genetically determined) with the variance within families, which will have other causes. This would provide a minimum estimate of heritability as the majority of species are out-breeding and therefore siblings are unlikely to be genetically identical. However, such an analysis of variation could not be carried out

rigorously due to circumstances occurring during the growth experiment that reduced the number of plants of each family that it was possible to measure. Although the effect of differing environmental conditions on the growth of the plants was not statistically assessed in this way, plants of the same family that were growing poorly or flowering late due to factors such as shading, or their roots being disturbed, were visually identified and discarded. Likewise, characters were also visually compared within families, enabling the influence of non-genetic factors on different morphological traits to be assessed and the reliability of each character to be interpreted accordingly.

Some taxa are poorly represented in the analysis as no seed were available for *A. lopesianum* and *A. grosii* and seed from only one plant was available for the very endemic species such as *A. pertegasii* and *A. valentinum*. However, the distribution of the endemic species is very restricted and they consist of a few known populations. It is therefore assumed that the plants that were grown are representative of these species. It was also difficult to germinate seed from many *A. latifolium*, *A. majus pseudomajus* and *A. majus striatum* accessions so the sampling of these taxa for most characters is limited. In some cases, where no seed were available, data on flowers and some epidermal characteristics were obtained from accessions that have been maintained at Edinburgh. In total 519 plants from 140 locations, covering all species except for *A. grosii* and *A. martenii*, were examined in this analysis.

Table 4.1 gives further details of the accessions that grew successfully and were measured. For ease of presentation, the morphological subsections as originally defined by Rothmaler (1956) and species nomenclature as described in Section 1.1 are adhered to. For example, *A. hispanicum* accessions from Morocco are still considered with subsection *Kickxiella*. However, to determine whether there is morphological differentiation of the clusters recognised by the analyses described in Chapter 3, some species are split into sets of populations from different geographic locations. Accessions of *A. majus litigiosum* from the region surrounding Valencia are considered separately from those from Zaragoza province, and *A. barrelieri* and *A. hispanicum* accessions from Morocco are considered separately from their con-specific populations in Spain, the former being denoted as *A. barrelieri* (M) and the latter *A. hispanicum* (M). Likewise *A. majus tortuosum* populations from Morocco and Italy are considered separately from populations from Spain, being denoted by *A. majus tortuosum* (M & It). As these groupings are not formally recognised species, in the following chapter the *Antirrhinum* species and the groups mentioned above are referred to as taxa.

DB	Location, Province, country	N families	N individuals	Total
Subsection Antirrhinum				
<i>A. australe</i>				
83	Benamahoma, Cadiz, S	4	1, 2, 1, 1	(5)
84	El Boyar, Cadiz, S	-		
85	Grazelema, Cadiz, S	3	1, 1, 2	(4)
86	Villaluenga del Rosario, Cadiz, S	2	1, 1	(2)
87	Benaocaz, Cadiz, S	3	2, 2, 1	(5)
88	Cortes de la Frontera, Malaga, S	1	1	(1)
89	Cortes de la Frontera, Malaga, S	3	1, 2, 1	(4)
90	Benaolan, Malaga, S	-		
91	Gaucin, Malaga, S	5	3, 1, 2	(4)
95	El Burgo, Malaga, S	4	2, 2, 1, 1	(6)
97	Torcal de Antequera, Malaga, S	4	1, 2, 2, 2	(7)
<i>A. barrelieri</i>				
24	Paternal del Rio, Almeria, S	fl		
27	Laroles, Granada, S	fl		
28	Berja to Laujar, Almeria, S	fl		
29	Ugija to Murtas, Granada, S	-		
33	Trevez, Granada, S	fl		
34	Busquistar, Granada, S	-		
96	Alora, Malaga, S	4	2, 3, 3, 5	(13)
101	Algarinejo, Granada, S	2	1, 2	(3)
131	Padul, Granada, S	3	2, 2, 2	(6)
150	Cadiar, Granada, S	-		
<i>A. barrelieri</i> (Morocco)				
161	Tetuan to Chefchauen, Morocco	4	2, 2, 2, 2	(8)
162	N of Chefchauen, Morocco	-		
163	Chefchauen, Morocco	-		
167	Taineste, Morocco	2	2, 1	(2)
168	Taineste, Morocco	-		
<i>A. graniticum</i>				
40	Braganca, Braganca, P	1	2	(2)
67	Pelegriña, Guadalajara, S	-		
69	Ledanca, Guadalajara, S	fl		
71	Berninches, Guadalajara, S	-		
75	Fuentiduena de Tajo, Madrid, S	4	2, 1, 1, 2	(6)
76	Chinchon, Madrid, S	2	1, 1	(2)
79	Priego, Cuenca, S	1	4	(4)
115	Lamego, Viseu, P	1	1	(1)
116	Celoriga da beira, Guarda, P	2	2	(2)
117	Celoriga da Beira, Guarda, P	1	1	(1)
119	Tornavacos, Caceres, S	4	1, 3, 1, 1	(6)
121	Navacepeda de Tormes, Toledo, S	4	1, 4, 1, 2	(8)
120	Navall de Tormes, Toledo, S	2	2, 1	(3)
174	Collado-Villalba, Madrid, S	1	3	(3)
176	Miranda do Duoro, Braganca, P	-		
<i>A. latifolium</i>				
AC1045 ^s	Marseille, Bouches-du-Rhone, F	fl		
AC1046	Pyrenees	-		
AC1047 ^s	Entrevaux, Alpes-de-Ht.-Provence, F	1	2	(2)
AC1053	Mt Boron, Nice, Alpes-Maritimes, F	fl		(1)
AC1054	col d'Eze, Nice, Alpes-Maritimes, F	fl		
AC1055	St Jean-Carrat, Alpes-Maritimes, F	fl		
AC1056	Menton, Alpes-Maritimes, F	fl		
AC1057	Sospel, Alpes-Maritimes, F	fl		
AC1058	col. Turini, Alpes-Maritimes, F	fl		
AC1061	Entrevaux, Alpes-de-Ht.-Provence, F	fl		
AC1066	St Martin d'Entraunes, Alpes-Maritimes, F	fl	3	(3)
AC1069	Entrevaux, Alpes-de-Ht.-Provence, F	fl		
AC1070	Entrevaux, Alpes-de-Ht.-Provence, F	fl		
AC1071	Rigaud, Alpes-Maritimes, F	fl		
AC1072	Roubion, Alpes-Maritimes, F	fl		
AC1079	Embrun, Hautes-Alpes F	-		
AC1081	Mirabeau, Alpes-de-Ht.-Provence, F	fl		
E039* ⁺	Avellanet, Lleida, S	1	3	(3)

<i>A. majus cirrhigerum</i>				
113	Gala, Coimbra, P	5	2, 2, 3, 1, 2	(10)
114	Praia de Mira, Coimbra, P	4	2, 3, 3, 1	(9)
122	Lisbon, Lisboa, P	2	1, 3	(4)
125*	Algave, P	3	1, 2, 1	(4)
<i>A. majus linkianum</i>				
107	Sierra de Arrabida, Setubal, P	5	3, 2, 2, 2, 2	(11)
108	Almada, Setubal, P	1	2	(2)
109	Sintra, Lisboa, P	4	2, 1, 1, 1	(5)
110	Pernes, Santarem, P	2	1, 1	(2)
111	Porto de Mos, Leiria, P	1	1	(1)
112	Coimbra, Coimbra, P	4	2, 2, 3, 2	(9)
<i>A. majus litigiosum</i> (Valencia)				
1	BenioValencia, S	fl		
2	La Drova, Valencia, S	fl		
3	Chesta, Valencia, S	1	2	(2)
4	Lliria, Valencia, S	fl		
5	Olocau, Valencia, S	1	3	(3)
9	Traiguera, Castello, S	2	3	(3)
6	Segorbe, Castello, S	fl		
7	Vall d'Alba, Castello, S	-		
8	Morella, Castello, S	-		
11	Casas de El Canizar, Cuenca, S	1	1	(1)
<i>A. majus litigiosum</i> (North)				
12	Elche, Albacete, S	fl		
13	Bogarra, Albacete, S	-		
61	Santes Creus, Tarragona, S	1	2	(2)
62	Santes Creus, Tarragona, S	4	2, 1, 3, 1	(7)
63	Borja, Zaragoza, S	fl		
64	Borja, Zaragoza, S	1	2	(2)
65	Tarazona, Zaragoza, S	-		
66	Gallur, Zaragoza, S	3	2, 2, 2	(6)
80	Daroca, Zaragoza, S	1	1	(1)
<i>A. majus pseudomajus</i>				
45	Jaca, Huesca, S	-		
46	Biescas, Huesca, S	fl		
48	Panticosa, Huesca, S	-		
49	Gave de Ossau, Hautes-Pyrenees, F	-		
53	Minerve, Herault, F	3	2, 3, 4	(9)
59	Prades, Pyrenees-Orientales, F	fl		
60	Berga, Barcelona, S	fl		
<i>A. majus striatum</i>				
55	N of Limoux, Aude, F	fl		
56	S of Limoux, Aude, F	fl		
58	Belcaire, Aude, F	fl		
N1100	Prats-de-Mollo-la-Preste, Pyrenees-Orientales, F	1	1	(1)
N1125	Alet les Bains, Aude, F	1	2	(2)
<i>A. majus tortuosum</i> (Spain)				
81	El Tem Cadiz, S	4	1, 2, 2, 2	(7)
82	El Bosque, Cadiz, S	1	1	(1)
92	Casares, Malaga, S	4	1, 1, 3, 1	(6)
93	Marbella, Malaga, S	5	2, 2, 3, 2, 2	(11)
98	Almargen, Malaga, S	5	2, 1, 1, 2, 2	(8)
100	Loja, Granada, S	5	1, 1, 1, 2, 1	(6)
102	Priego de Cordoba, Cordoba, S	5	1, 1, 2, 2, 1	(7)
103	Alcaudete, Jaen, S	3	2, 2, 2	(6)
105	Cabra, Cordoba, S	4	2, 2, 2, 1	(7)
106	Cerro Muriano, Cordoba, S	4	2, 1, 2, 1	(7)
160	Gibraltar	2	2, 1	(3)
<i>A. majus tortuosum</i> (Morocco and Italy)				
165	Targha, Morocco	-		
169	Taza, Morocco	2	2, 2	(4)

AC1143	Mazzaro, Sicily, near Taormina	1	1	(1)
AC1144	Near Cefalu, Sicily	1	1	(1)
<i>A. siculum</i>				
AC1176	Palermo, Sicily	1	1	(1)
AC1177	Taormina, Sicily	1	2	(2)
E68	Syracuse	1	2	(2)
u	unknown	1	2	(2)
L183		1	2	(2)
Subsection Kickxiella				
<i>A. boissieri</i>				
18	Guadahortuna, Granada, S	1	1	(1)
E15	Albanchez de Bela - Pegalajar, Jaen, S	-		
104	Ermita Virgen de la Sierra, Cordoba, S	4	2, 1, 1, 1	(5)
<i>A. charidemi</i>				
E23	Cabo de Gata, Almeria, S	1	2	(2)
<i>A. grosii</i>				
175	Sierra de Gredos, Toledo, S	-		
<i>A. hispanicum</i> (Spain)				
E30	Alhama de Granada, Granada, S	3	1, 2, 2	(5)
E31	Lanjaron, Granada, S	1	3	(3)
36	Balcon de Canales, Granada, S	1	2	(2)
99	Almargan, Malaga, S	5	1, 2, 3, 2, 2	(12)
132	Lanjaron, Granada, S	2	1, 2	(3)
<i>A. hispanicum</i> (Morocco)				
171	Source de Oum-er-Rubia, Morocco	1	2	(2)
172	El Kebab, Morocco	4	2, 2, 3, 2	(9)
173	El Ksiba, Morocco	1	2	(2)
<i>A. lopesianum</i>				
*	Vimioso, Braganca, P	fl		
<i>A. microphyllum</i>				
72	Sacedon, Guadalajara, S	4	2, 2, 1, 1	(6)
73	Pantano de Buendia, Guadalajara, S	-		
74	Buendia, Guadalajara, S	-		
<i>A. molle</i>				
E51	Gerri de la Sal, Lleida, S	3	2, 3, 2	(7)
E52	la Seu de Urgel, Lleida, S	3	1, 2, 1	(4)
E53	Saldes, Barcelona, S	2	2, 2	(4)
E54	Montsec, S near Seu de Urgel	4	3, 2, 3, 2	(10)
E55	Baga, Barcelona, S	4	2, 2, 3	(7)
E56*	El Segre	4	1, 2, 2, 2	(7)
E57*	Las Lagunes, S near Gerri de la sal.	-		
E60*	Bellver de Cerdanya	-		
<i>A. mollisimum</i>				
19	Abrucena, Almeria, S	1	3	(3)
20	Felix, Almeria, S	3	3, 3, 2	(8)
21, 157	Enix, Almeria, S	5	3, 2, 3, 2, 3	(13)
<i>A. pertegasii</i>				
E65*	unknown, Castellon, Spain	1	3	(3)
<i>A. pulverulentum</i>				
68	Pelegrina, Guadalajara, S	2	3, 3	(6)
70	Alcorlo, Guadalajara, S	5	2, 1, 4, 2	(9)
77	Poveda de la Sierra, Guadalajara, S			
78	Hoz de Beteta, Cuenca, S			
<i>A. rupestre</i>				
22	Canjayar, Almeria, S	2	2, 3	(5)
139	Capillera, Granada, S	4	2, 2, 3, 2	(9)

<i>A. sempervirens</i>					
47	Panticosa, Huesca, S				
50	Col d'Aubisque, Hautes-Pyrenees, F	4	3, 1, 2, 1, 2	(9)	
52	Luz, Hautes-Pyrenees, F	fl			
<i>A. subbaeticum</i>					
E72	Albacete, S	1	1	(1)	
<i>A. valentinum</i>					
AC1173	La Drova, Valencia, S	fl			
Subsection Streptosepalum					
<i>A. braun-blanquetii</i>					
44	Sobron, Alava, S	fl			
E18	La Pinda, Corvera de Asturias, Asturias, Sfl				
E19	Rio Gorge, Ceneya	fl			
E20	St Pietro de Villanueva, Asturias, S	4	2, 3, 1, 1	(7)	
E21	Braganca, Braganca, P	fl			
<i>A. meonanthum</i>					
118	Poco do Inferno, Manteigas, Guarda, P	1	2	(2)	
180	Sobredelo, Ourense, S	1	1	(1)	
181	Robledo de Fenar, Leon, S				
E48	unknown	1	2	(2)	
E49	unknown	fl			
Sierra Nevada hybrid populations (<i>A. barrelieri</i> x <i>A. rupestre</i>)					
23	Luajar to Paterna del Rio, Almeria, S	1	3	(3)	
24	Paterna del Rio, Almeria, S	fl			
25	Bayarcal, Almeria, S	3	3, 2, 4	(9)	
26	Bayarcal to Laroles, Granada, S	-			
30	Cadiar to Mecina Bombarron, Granada, S	1	3	(3)	
31	Juviles to Trevez, Granada, S	1	2	(2)	
32	Nr Juviles, Granada, S	3	2, 1, 1	(4)	
33	Trevez, Granada, S	fl			
35	Nr, Pampaneira	1	2	(2)	

Table 4.1. Details of the number of plants from each population included in the morphological analysis
DB = database location number, N_{families} = number of plants from which seed was sown, $N_{\text{individuals}}$ = the number of individuals analysed from each family, Total = the total number of plants from that location which were grown from seed and measured. fl = flowers from existing accessions only were included.

4.3 Leaf characters

4.3.1 Leaf size and shape

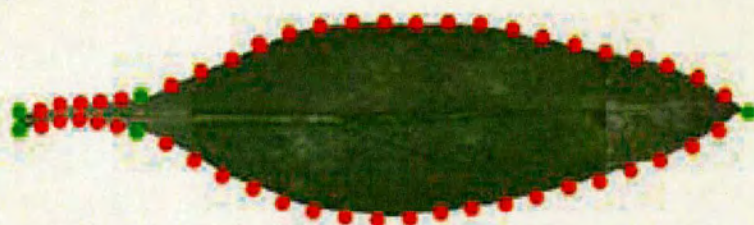
The metamer 6 leaf was selected to represent each accession as this was the earliest leaf for which data could be collected for most of the accessions. Parameters describing leaf size and shape were identified using PCA. A point model consisting of 50 points was fitted to the outline of each leaf, as shown in Figure 4.1A.

Nearly all of the variation in leaf size and shape within the genus is captured by just five PCs that account for 99% of the total variation. Of these, the first three PCs, LePC1-3, are considered to describe heritable variation. The first axis, LePC1, accounts for 87 % of the variation and inversely reflects leaf size. However, LePC1 also shows that shape is correlated with size, as smaller leaves are rounder, particularly the leaf tip (Figure 4.1B). Despite the poor representation of many species and high within-taxon variation, which is reflected by the R^2 value of 61%, there are significant differences between the mean LePC1 values of taxa (Figure 4.2). Inspection of Figure 4.2A shows that most of the between-taxon variance is accounted for by variation between subsections Kickxiella and Antirrhinum. The Kickxiella species have significantly greater mean LePC1 values than subsections Antirrhinum and Streptosepalum, reflecting their smaller, rounder leaves. The exceptions are *A. barrelieri* and *A. majus cirrhigerum*, which have similar values to Kickxiella species.

Of the taxa not genetically delimited, *A. australe* has a lower mean LePC1 value than *A. majus tortuosum* and *A. majus linkianum* has a lower mean than *A. majus cirrhigerum* (Figure 4.2B). The comparison of morphologically similar species shows that LePC1 differs between *A. barrelieri* and *A. majus litigiosum*. Of the genetically sub-divided species, populations of *A. majus tortuosum* and *A. hispanicum* from Spain have smaller, rounder leaves than those of *A. majus tortuosum* and *A. hispanicum* from Morocco. However, *A. majus litigiosum* accessions from the Valencia region have similar LePC1 values to those distributed further north.

The second axis, LePC2, accounts for 10% of the overall variation and mainly describes variation and the position of the widest point of the leaf, with more ovate leaves being of larger area (Figure 4.1B). Negative LePC2 values represent ovate leaves whilst positive values represent linear leaves. Similar to LePC1, variation between taxa is only slightly higher than within taxa variation ($R^2=61\%$). However, LePC2 does not show the same strong divergence between the Kickxiella and Antirrhinum species. It mainly describes those species with almost linear leaves such as *A. majus*

A



B

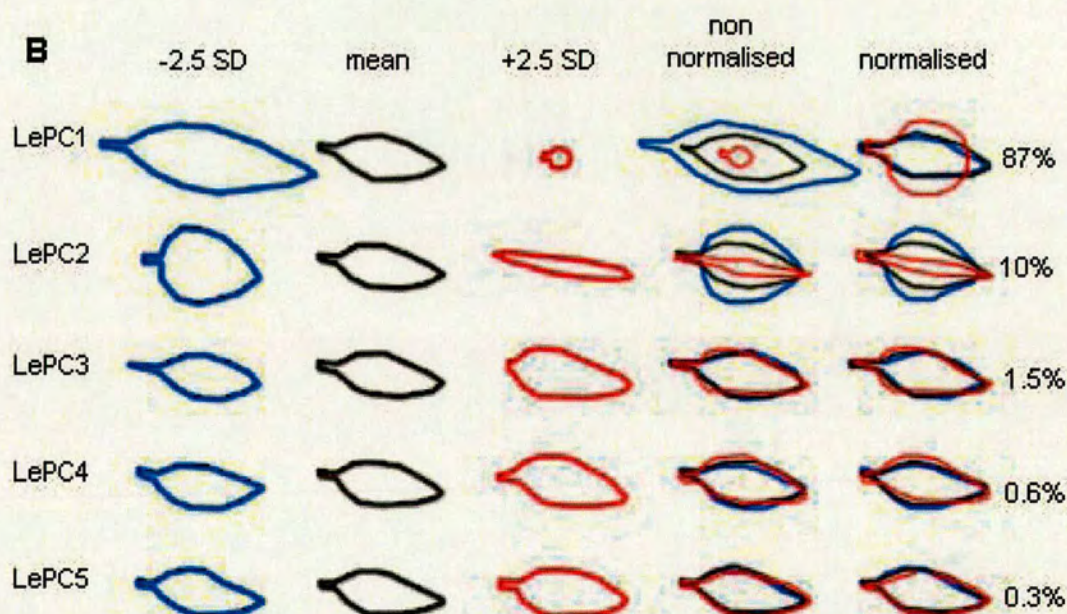


Figure 4.1. The point model template used to capture leaf shape (A) and the variation represented by the resulting axes from PCA metamer 6 leaves (B).

(A) An example of a leaf with the 50 point template fitted to its outline. Primary points are coloured green and secondary points are red.

(B) Each row describes the variation described by one of the main axes of variation obtained from PCA. The axes are labeled according to their variable name, which is introduced in the text. The first 3 columns show the mean shape and the shape obtained at positions ± 2.5 standard deviations from the mean along each axis. The 4th column shows the same information, but the shapes are overlaid for easier comparison. The 5th column shows the corresponding shapes normalised by area so that it can be determined whether there is a correlation between size and shape. The amount of variation described by each axis is indicated at the end of the row.

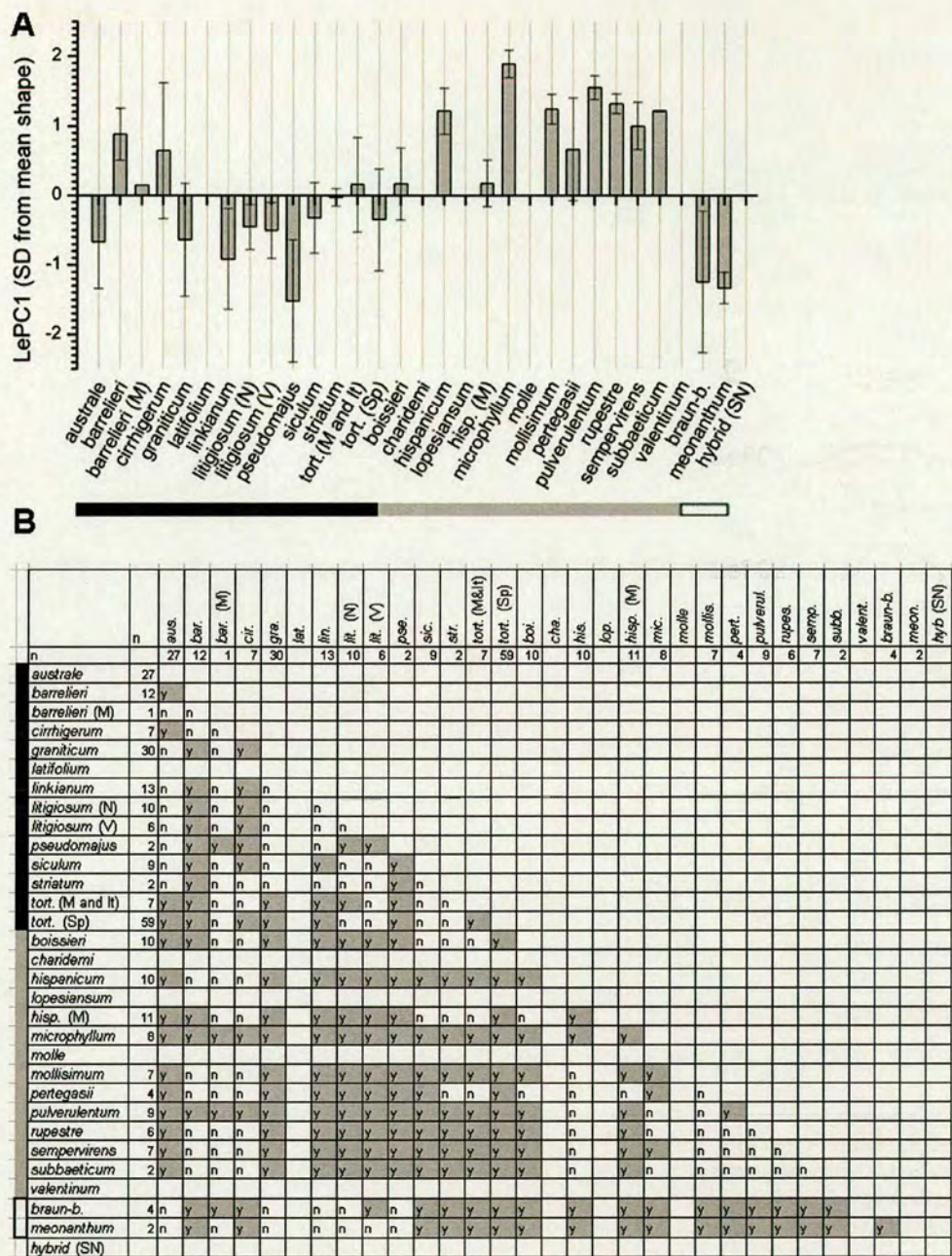


Figure 4.2. Mean values of LePC1 for each taxon (A) and results of tests for significant differences in LePC1 values between all pairs of taxa (B).

(A) Graph showing the average value of LePC1 (± 1 standard deviation) of each taxon. The units are in standard deviations (SD) from the mean shape.

(B) Matrix showing results of pairwise significance tests between all taxa, the number of individuals (n) is indicated in the second column. 'y'=significantly different at 0.05 level (Fisher's Least Significant Difference). One-way ANOVA: $F(24, 240)=18.33$, $P<0.001$, $R^2=61\%$

barrelieri (M) = Moroccan *A. barrelieri*, *litigiosum* (N) = northern *A. litigiosum*, *litigiosum* (V) = Valencia *A. litigiosum*, *tort.* (M and It) = Moroccan and Italian *A. majus tortuosum*, *tort.* (Sp) = Spanish *A. majus tortuosum*, *hisp.* (M) = Moroccan *A. hispanicum*.

■ Subsection Antirrhinum ■ Subsection Kickxiella □ Subsection Streptosepalum

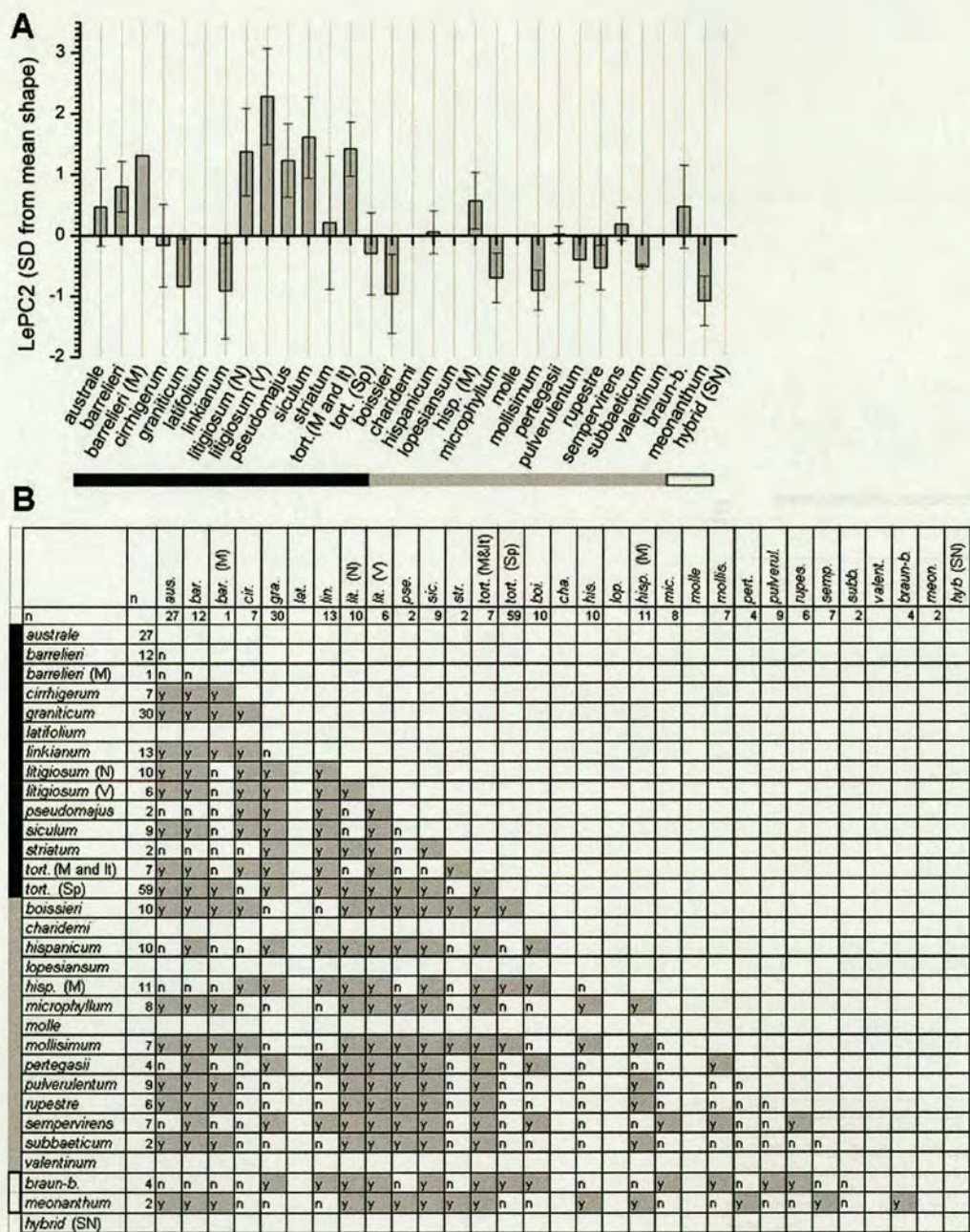


Figure 4.3. Mean values of LePC2 for each taxon (A) and results of tests for significant differences in LePC2 values between all pairs of taxa (B).

(A) Graph showing the average value of LePC2 (± 1 standard deviation) of each taxon. The units are in standard deviations (SD) from the mean shape.

(B) Matrix showing results of pairwise significance tests between all taxa, the number of individuals (n) is indicated in the second column. 'y'=significantly different at 0.05 level (Fisher's Least Significant Difference). One-way ANOVA: $F(24, 240)=18.46$, $P<0.001$, $R^2=61\%$

barrelieri (M) = Moroccan *A. barrelieri*, *litigiosum* (N) = northern *A. litigiosum*, *litigiosum* (V) = Valencia *A. litigiosum*, *tort.* (M and It) = Moroccan and Italian *A. majus tortuosum*, *tort.* (Sp) = Spanish *A. majus tortuosum*, *hisp.* (M) = Moroccan *A. hispanicum*.

■ Subsection Antirrhinum ■ Subsection Kickxiella □ Subsection Streptosepalum

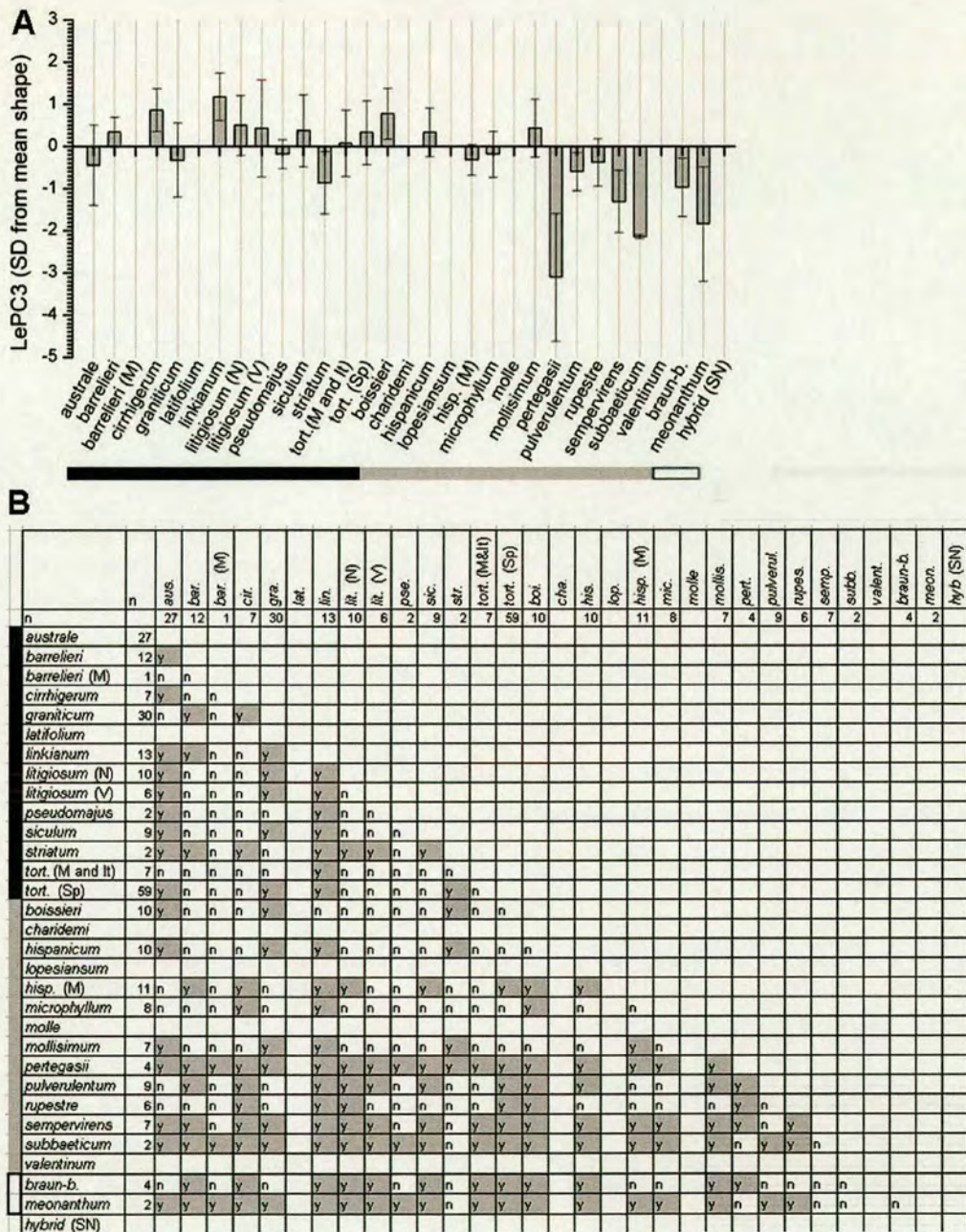


Figure 4.4. Mean values of LePC3 for each taxon (A) and results of tests for significant differences in LePC3 values between all pairs of taxa (B).

(A) Graph showing the average value of LePC3 (± 1 standard deviation) of each taxon. The units are in standard deviations (SD) from the mean shape.

(B) Matrix showing results of pairwise significance tests between all taxa, the number of individuals (n) is indicated in the second column. 'y'=significantly different at 0.05 level (Fisher's Least Significant Difference). One-way ANOVA: $F(24, 240)=9.53$, $P<0.001$, $R^2=44\%$

barrelieri (M) = Moroccan *A. barrelieri*, *litigiosum* (N) = northern *A. litigiosum*, *litigiosum* (V) = Valencia *A. litigiosum*, *tort.* (M and It) = Moroccan and Italian *A. majus tortuosum*, *tort.* (Sp) = Spanish *A. majus tortuosum*, *hisp.* (M) = Moroccan *A. hispanicum*.

■ Subsection Antirrhinum ■ Subsection Kickxiella □ Subsection Streptosepalum

litigiosum, *A. siculum* and *A. majus tortuosum* (Figure 4.3). Species with ovate leaves are also distinguished, particularly *A. graniticum*, *A. majus linkianum* and *A. meonanthum*.

Again, *A. australe* differs significantly from *A. majus tortuosum* and *A. majus cirrhigerum* differs from *A. majus linkianum*. There are also significant differences between *A. majus litigiosum* accessions from Valencia compared to those from northern Spain, and *A. majus tortuosum* accessions from Spain differ to those from Morocco and Italy.

The third axis, LePC3, accounts for a small amount of the overall variation, just 1.5%, and is inversely correlated with petiole length (Figure 4.1B). Subsection *Kickxiella* species mostly have longer petioles than *Antirrhinum* species, however, between-taxon variation accounts for just 44% of the overall variation. The main species distinguished by LePC3 are *A. pertegasii*, *A. subbaeticum* and *A. meonanthum*, which are all shown to have relatively longer petioles than the other species (Figure 4.4).

The final two axes of the PCA explain less than 1% of the variation and are considered to account for noise in the data as one describes the petiole twisting up or down (when leaves were not placed straight) and the other shows a slight asymmetry in the leaves (Figure 4.1B). These two axes are not included in any subsequent analyses.

4.3.2 Leaf cell size

Leaf cell size was estimated on the adaxial surface of the leaf by counting the number of cells in an area of 50 x 50 μm in the same region of a single metamer 4 leaf of each plant. Occasionally, where metamer 4 leaves had died before taking epidermal imprints, this was carried out on leaves from metamers 5 – 6.

Based on this measure, the leaf cell size is similar among all taxa apart from *A. graniticum*, *A. barrelieri* accessions from Morocco and *A. latifolium*, which all have a higher number of cells per unit area (Figure 4.5). Sufficient samples were studied for *A. graniticum* to be confident about this result, however, only a couple of individuals each of *A. barrelieri* and *A. latifolium* were analysed.

4.3.3 Summary of leaf characters

Leaf shape and size is described by three variables, LePC1-3, which in combination account for nearly all variation within the genus. LePC1 and LePC2 are the main variables describing variation

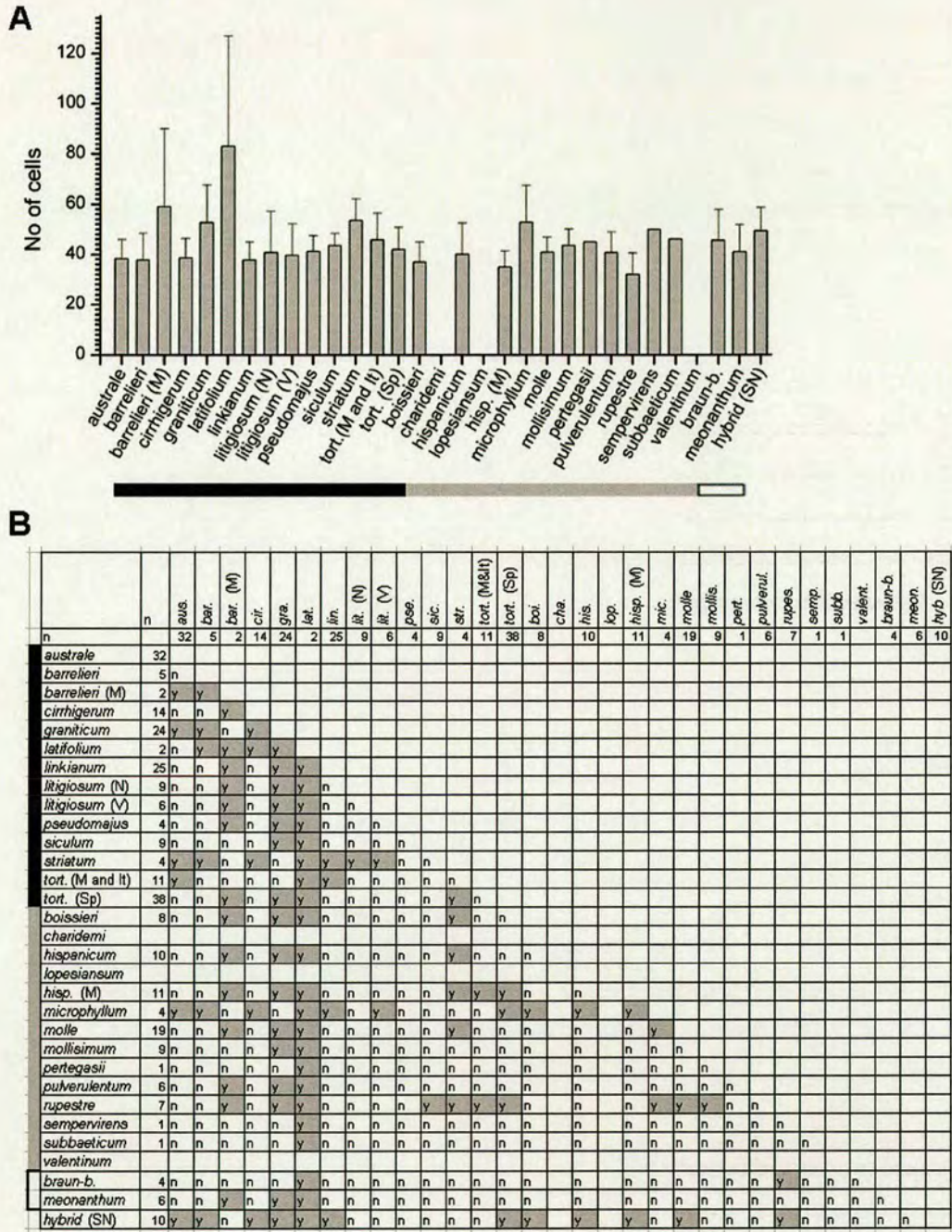


Figure 4.5. Mean values of the number of cells in an 50 x 50 µm area of the adaxial m4 leaf surface for each taxon (A) and results of tests for significant differences between all pairs of taxa (B).

(A) Graph showing the average value the mean number of cells (±1 standard deviation) of each taxon.
 (B) Matrix showing results of pair-wise significance tests between all taxa, the number of individuals (n) is indicated in the second column. 'y'=significantly different at 0.05 level (Fisher's Least Significant Difference). One-way ANOVA: $F(27, 254)=4.02$, $P<0.001$, $R^2=22\%$
barrelieri (M) = Moroccan *A. barrelieri*, *litigiosum* (N) = northern *A. litigiosum*, *litigiosum* (V) = Valencia *A. litigiosum*, *tort.* (M and It) = Moroccan and Italian *A. majus tortuosum*, *tort.* (Sp) = Spanish *A. majus tortuosum*, *hisp.* (M) = Moroccan *A. hispanicum*.

■ Subsection Antirrhinum ■ Subsection Kickxiella □ Subsection Streptosepalum

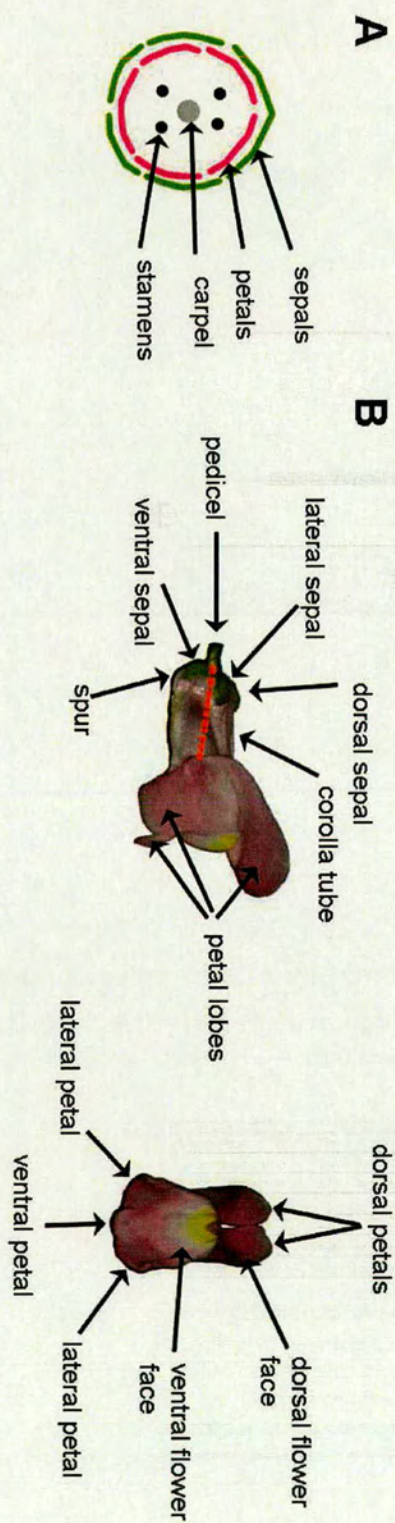


Figure 4.6. Diagram showing the structure of the *Antirrhinum* flower
(A) Cross-sectional diagram of the flower showing the calyx, corolla, androecium and gynoecium.
(B) Images of the flower side and flower face, the dotted line shows how the dorsal petal was dissected.

among species. Differences in LePC1 values show that subsection *Kickxiella* species have significantly smaller and rounder leaves than subsection *Antirrhinum* species and LePC2 then describes species with either exceptionally linear or more ovate leaves. Leaf cell size was also estimated, but varies little among species, apart from *A. graniticum*, which has smaller cells than the other taxa.

4.4 Flower characters

The *Antirrhinum* flower consists of four whorls (Figure 4.6A); the calyx has one dorsal sepal, two lateral sepals and two ventral sepals. The flower is personate, with the corolla consisting of two dorsal petals, two lateral petals and one ventral petal. The petals are fused to form a tube at the base of the flower (Figure 4.6B). Within the corolla are four stamens – two dorsal and two ventral – surrounding the carpel.

4.4.1 Corolla size and shape

The shape of the corolla is complex and difficult to quantify, therefore PCA was carried out on the corollas of all accessions to identify variation in both size and shape. Ideally, the PCA should be carried out on three dimensional point-models which represent the shape of each flower; however, such a system of analysis has yet to be developed. Therefore two different 2-dimensional aspects of the flowers were analysed to be able to describe as much of the corolla variation as possible.

i) Dorsal petal tube and lobe

To describe the relationships of flower characteristics such as tube length and circumference and dorsal petal lobe size and shape, the dorsal part of each flower (Figure 4.6A) was dissected, flattened and imaged. A point model consisting of 20 points was used to capture the shape of one dorsal petal, with primary points being placed at the base of the tube, at the dorsal tip of the tube and at the junction of the dorsal lobe with the tube and the lateral petal (Figure 4.7A).

PCA on the set of point models for all accessions showed that most of the variation (95%) in dorsal petal size and shape was accounted for by four principal components, named FpPC1-4. Similar to the leaf analysis, the first axis of variation, FpPC1, describes almost entirely size and accounts for 82% of the total variation (Figure 4.7B). There is also a small correlation of both petal lobe and tube widths with size, with smaller petals having narrower lobes and tubes. Most of the variation in FpPC1 is accounted for by between taxa comparisons ($R^2 = 81\%$), with the strongest pattern of divergence being observed between the two morphological subsections (Figure 4.8A). *Kickxiella*

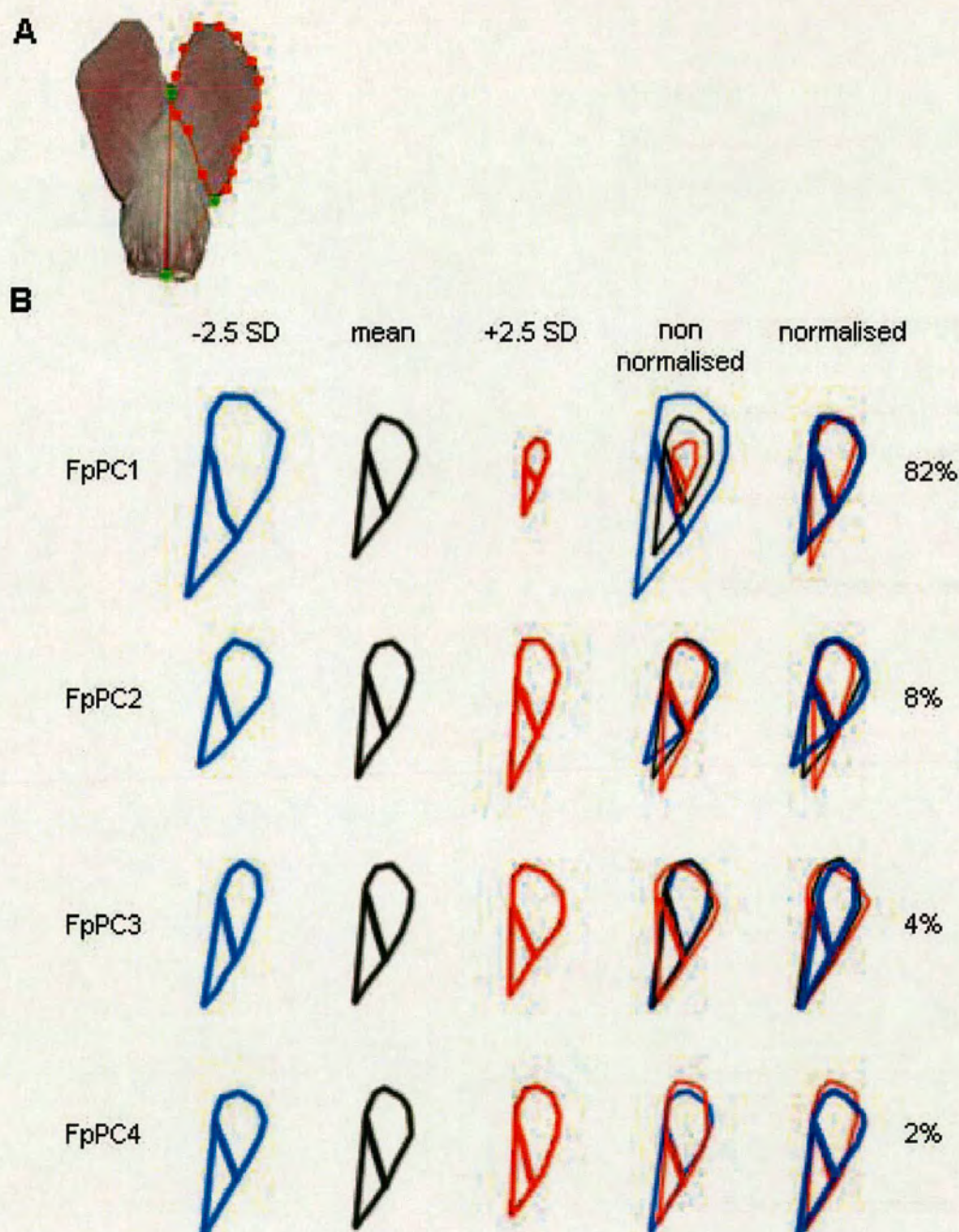


Figure 4.7. The point model template used to capture the dorsal petal size and shape (A) and the variation represented by the resulting PCA axes (B).

(A) An example of a flattened dorsal petal with the 20 point template fitted to the right hand petal. Primary points are coloured green and secondary points are red.

(B) Each row describes the variation described by one of the main axes of variation obtained from PCA, the amount of variation explained is in the right hand column. The axes are labeled according to their variable name, which is introduced in the text.

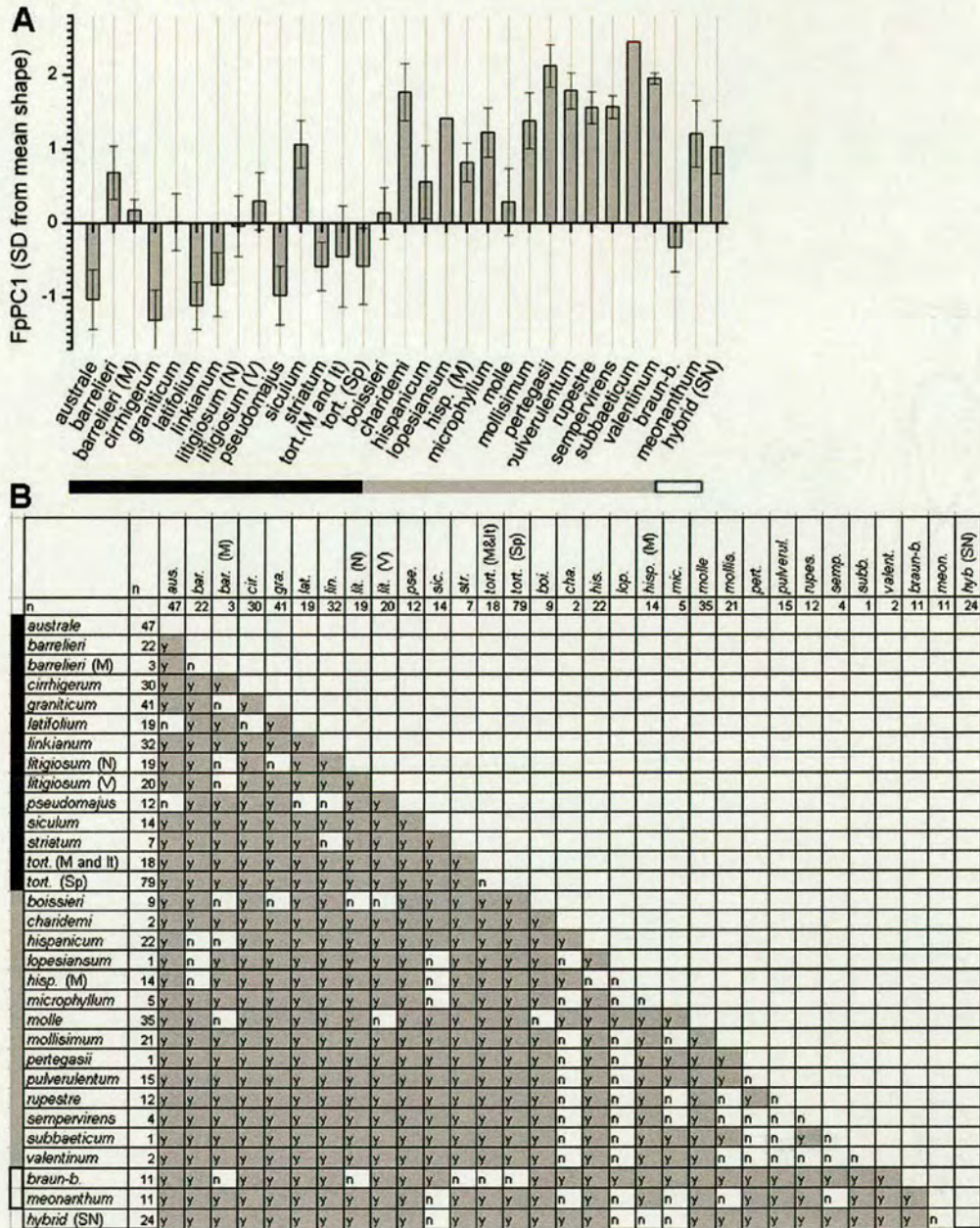


Figure 4.8. Mean values of FpPC1 for each taxon (A) and results of tests for significant differences in FpPC1 values between all pairs of taxa (B).

(A) Graph showing the average value of FpPC1 (±1 standard deviation) of each taxon. The units are in standard deviations (SD) from the mean shape.

(B) Matrix showing results of pairwise significance tests between all taxa, the number of individuals (n) is indicated in the second column. 'y'=significantly different at 0.05 level (Fisher's Least Significant Difference). One-way ANOVA: $F(28, 522)=88.74$, $P<0.001$, $R^2=82\%$

barrelieri (M) = Moroccan *A. barrelieri*, *litigiosum* (N) = northern *A. litigiosum*, *litigiosum* (V) = Valencia *A.*

litigiosum, *tort.* (M and It) = Moroccan and Italian *A. majus tortuosum*, *tort.* (Sp) = Spanish *A. majus*

tortuosum, *hisp.* (M) = Moroccan *A. hispanicum*.

■ Subsection Antirrhinum ■ Subsection Kickxiella □ Subsection Streptosepalum

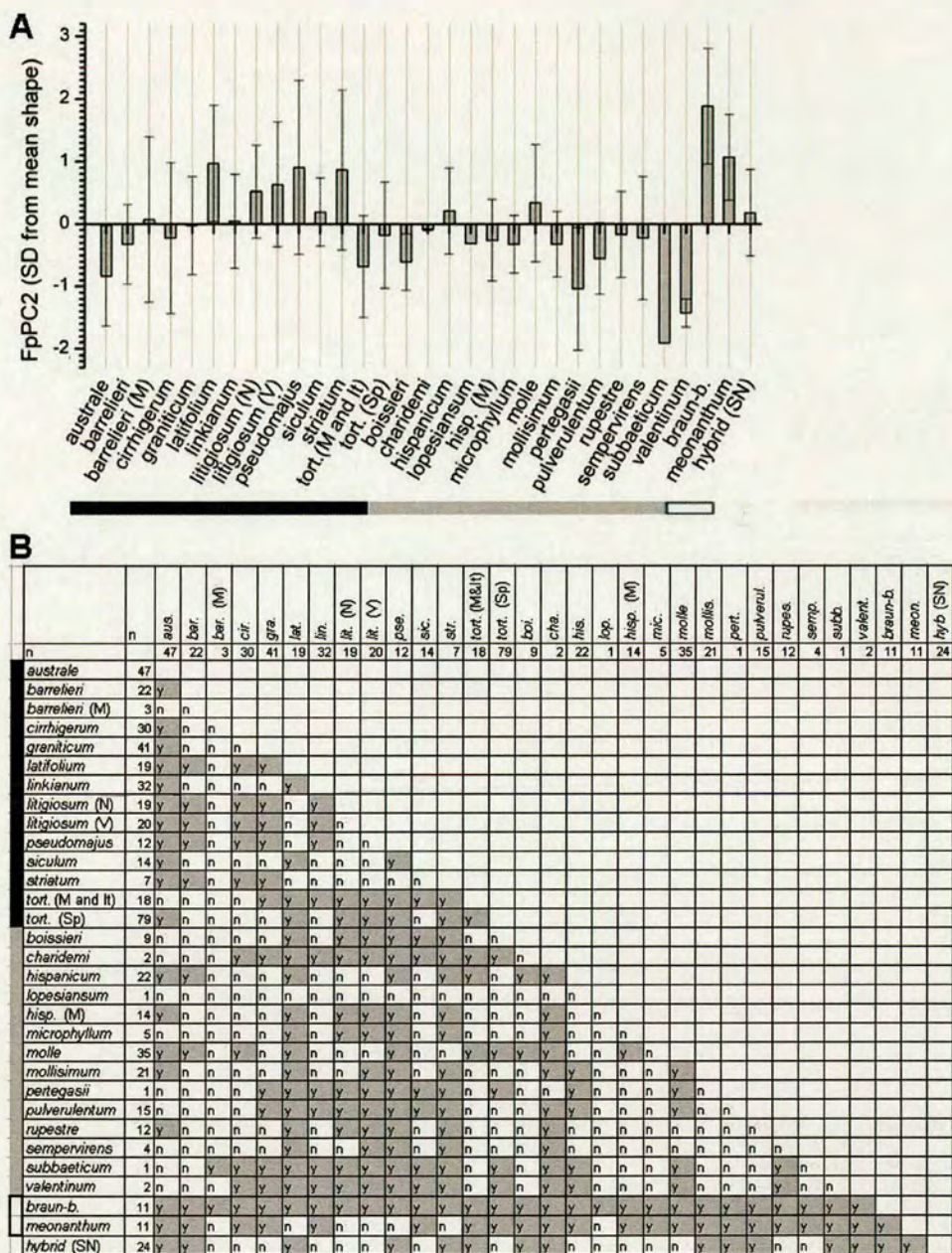


Figure 4.9. Mean values of FpPC2 for each taxon (A) and results of tests for significant differences in FpPC2 values between all pairs of taxa (B).

(A) Graph showing the average value of FpPC2 (± 1 standard deviation) of each taxon. The units are in standard deviations (SD) from the mean shape.

(B) Matrix showing results of pairwise significance tests between all taxa, the number of individuals (n) is indicated in the second column. 'y'=significantly different at 0.05 level (Fisher's Least Significant Difference). One-way ANOVA: $F(28, 526)=8.88$, $P<0.001$, $R^2=28\%$

barrelieri (M) = Moroccan *A. barrelieri*, *litigiosum* (N) = northern *A. litigiosum*, *litigiosum* (V) = Valencia *A. litigiosum*, *tort.* (M and It) = Moroccan and Italian *A. majus tortuosum*, *tort.* (Sp) = Spanish *A. majus tortuosum*, *hisp.* (M) = Moroccan *A. hispanicum*.

■ Subsection Antirrhinum ■ Subsection Kickxiella □ Subsection Streptosepalum

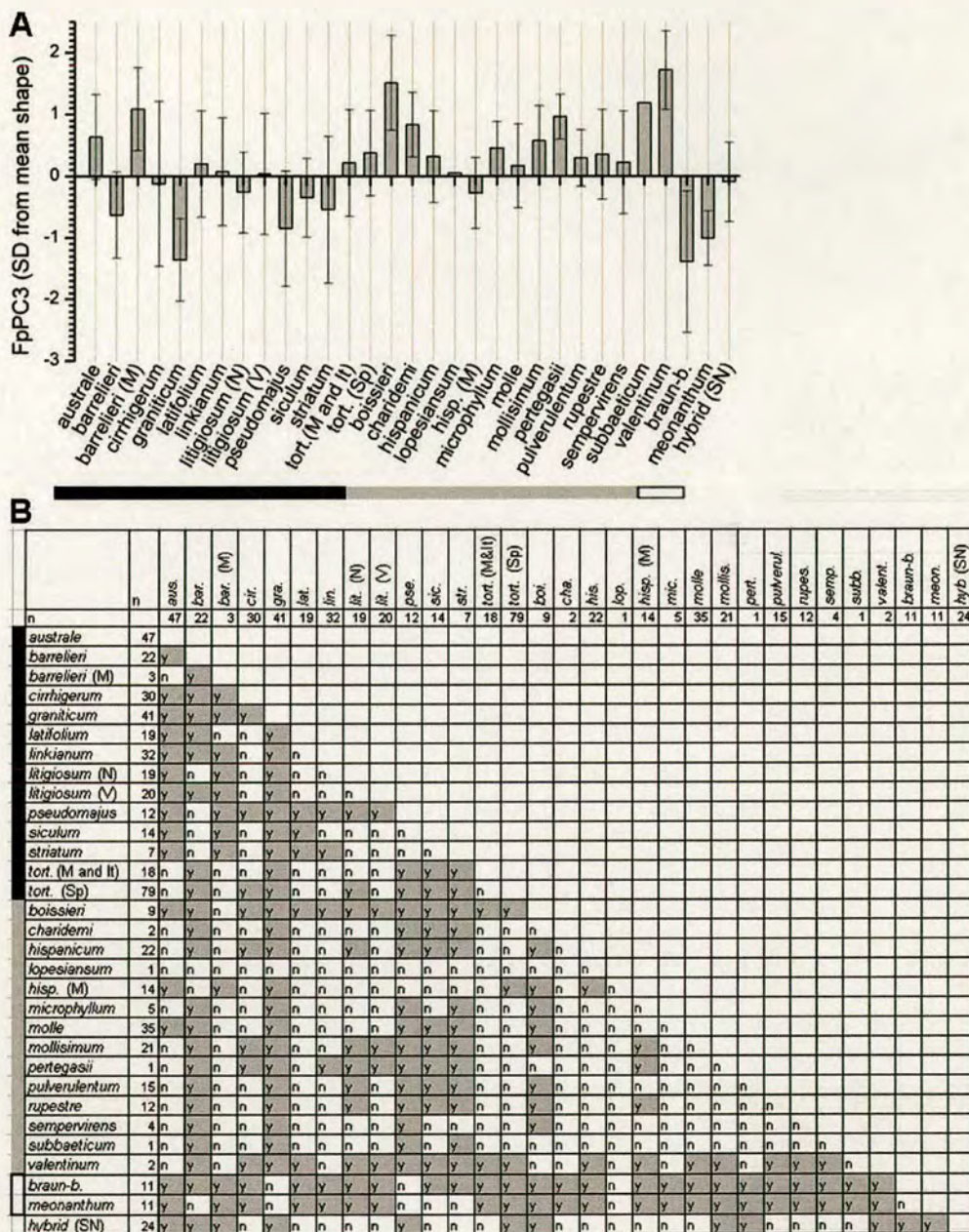


Figure 4.10. Mean values of FpPC3 for each taxon (A) and results of tests for significant differences in FpPC3 values between all pairs of taxa (B).

(A) Graph showing the average value of FpPC3 (± 1 standard deviation) of each taxon. The units are in standard deviations (SD) from the mean shape.

(B) Matrix showing results of pairwise significance tests between all taxa, the number of individuals (n) is indicated in the second column. 'y'=significantly different at 0.05 level (Fisher's Least Significant Difference). One-way ANOVA: $F(28, 526)=7.6$, $P<0.001$, $R^2=36\%$

barrelieri (M) = Moroccan *A. barrelieri*, *litigiosum* (N) = northern *A. litigiosum*, *litigiosum* (V) = Valencia *A. litigiosum*, *tort.* (M and It) = Moroccan and Italian *A. majus tortuosum*, *tort.* (Sp) = Spanish *A. majus tortuosum*, *hisp.* (M) = Moroccan *A. hispanicum*.

■ Subsection Antirrhinum ■ Subsection Kickxiella □ Subsection Streptosepalum

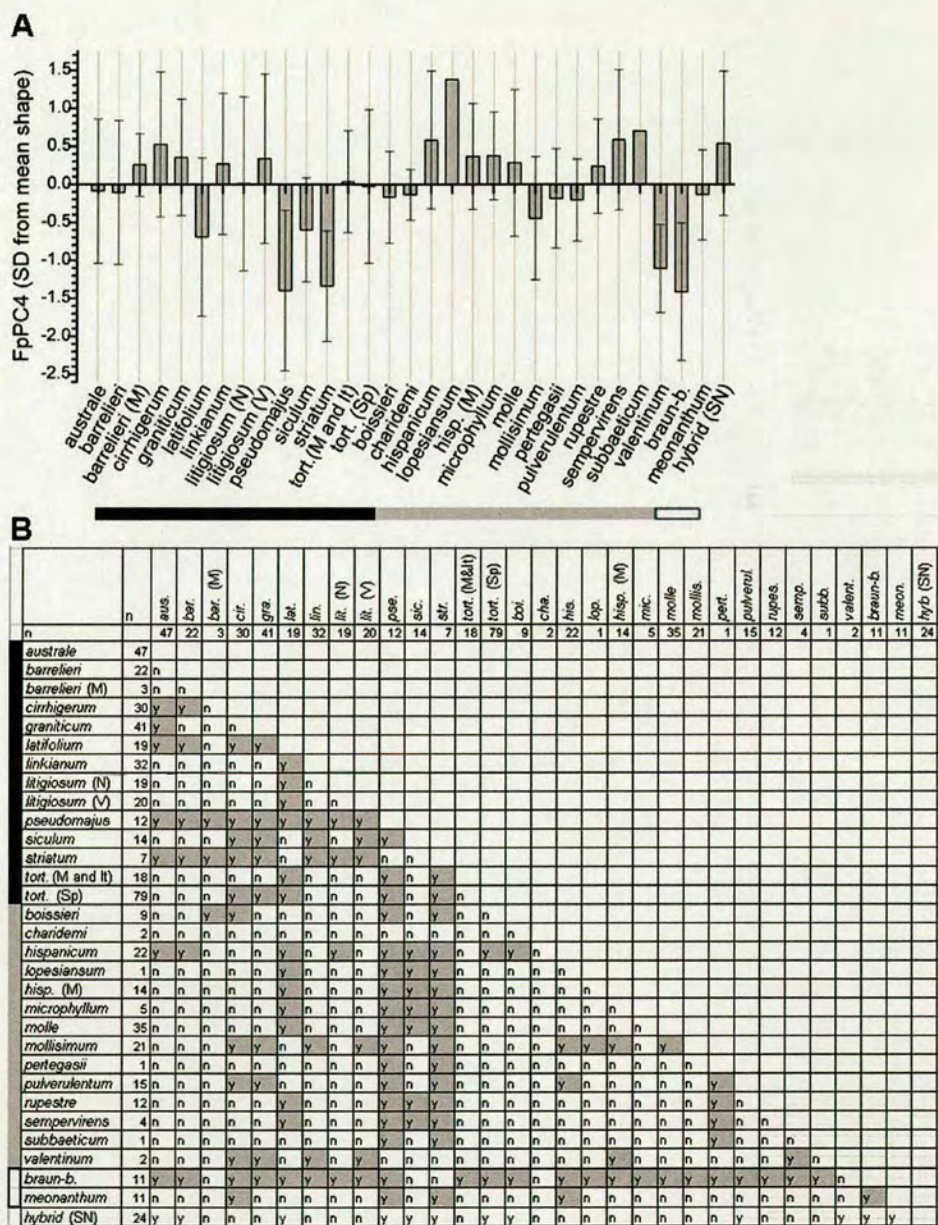


Figure 4.11. Mean values of FpPC4 for each taxon (A) and results of tests for significant differences in FpPC4 values between all pairs of taxa (B).

(A) Graph showing the average value of FpPC4 (± 1 standard deviation) of each taxon. The units are in standard deviations (SD) from the mean shape.

(B) Matrix showing results of pairwise significance tests between all taxa, the number of individuals (n) is indicated in the second column. 'y'=significantly different at 0.05 level (Fisher's Least Significant Difference). One-way ANOVA: $F(28, 529)=5.5$, $P<0.001$, $R^2=18.5\%$

barrelieri (M) = Moroccan *A. barrelieri*, *litigiosum* (N) = northern *A. litigiosum*, *litigiosum* (V) = Valencia *A. litigiosum*, *tort.* (M and I) = Moroccan and Italian *A. majus tortuosum*, *tort.* (Sp) = Spanish *A. majus tortuosum*, *hisp.* (M) = Moroccan *A. hispanicum*.

■ Subsection Antirrhinum ■ Subsection Kickxiella □ Subsection Streptosepalum

species have high FpPC1 values, reflecting their smaller flowers compared to *Antirrhinum* species. However, *A. barrelieri*, *A. majus litigiosum*, *A. siculum* and *A. meonanthum* all have small flowers compared to the other *Antirrhinum* species and *A. molle* has large flowers compared to the other *Kickxiella* species.

Inspection of Figure 4.8B shows that nearly all taxa are delimited by mean FpPC1 values. However, all accessions of *A. majus tortuosum* from Spain, Morocco and Italy have similar dorsal petal sizes and *A. hispanicum* accessions from different locations do not differ.

The second axis, FpPC2, which accounts for 8% of the variation, mainly describes variation in relative lobe size (Figure 4.7B). Subsection *Kickxiella* species, apart from *A. molle*, mostly have negative mean FpPC2 values indicating that they have disproportionately large lobes (Figure 4.9A). However, only a small amount of variation is accounted for by between taxa comparisons ($R^2=28\%$) and the divergence of FpPC2 between the two subsections is not distinctive. FpPC2 mainly distinguishes the subsection *Streptosepalum* species, *A. braun-blanquetii* and *A. meonanthum*, by their high positive FpPC2 values reflecting their small dorsal petal lobes compared to the tube. At the other extreme of the comparison, *A. subbaeticum* and *A. valentinum* have disproportionately large petal lobes.

FpPC2 also delimits *A. australe* compared to *A. majus tortuosum*, *A. barrelieri* compared to *A. majus litigiosum* and accessions of *A. majus tortuosum* distributed in Spain from those in Morocco and Italy (Figure 4.9B).

The third axis resulting from the PCA accounts for 4% of the variation in dorsal petal shape and it describes independent variation in lobe width (Figure 4.7B). Between taxon comparisons account for just 36% of the overall variation and FpPC3 does not show a strong pattern of variation between the *Kickxiella* compared to the *Antirrhinum* species (Figure 4.10A). However, most of the *Kickxiella* and *A. siculum* all have wide petal lobes compared to the tube as they have higher FpPC3 values than the other taxa. FpPC3 mainly shows that two *Streptosepalum* species, *A. meonanthum* and *A. braun-blanquetii*, and *A. graniticum* have disproportionately small, narrow dorsal petal lobes compared to other taxa (Figure 4.10B). In contrast, *A. boissieri*, *A. subbaeticum* and *A. valentinum* have relatively broad lobes.

The fourth PCA axis accounts for just 2% of the variation and mainly describes the relative tube length compared to the lobe (Figure 4.7B). Negative FpPC4 values represent species that have proportionally longer tubes than the mean shape and positive values represent the converse. There is large within-taxon variation (Figure 4.11A) and the one-way ANOVA model comparing taxa indicates that between taxa variation accounts for only 19% of the overall variation. One group of taxa is significantly different from most other species; it consists of *A. latifolium*, *A. siculum*, *A. pseudomajus*, *A. striatum*, *A. valentinum* and *A. braun-blanquetii* which all have large negative FpPC4 values (Figure 4.11B).

ii) Flower side

The 2-dimensional view of the corolla side was analysed with the intention of describing characters such as the size of the gibba on the ventral base of the tube, the angle of the dorsal petal to the tube and the shape of the ventral and lateral petals. PCA was initially used to summarise the key features of the corolla that vary. A point model consisting of 53 points was fitted to each flower image as shown in Figure 4.12A. Several problems were encountered with this method: it was difficult to capture the detail of the ventral and lateral petal lobes because they often overlapped and curled and it was difficult to lay the flowers exactly horizontally for imaging. Although these factors introduced substantial noise, characteristics of the flower shape were still described. Preliminary analyses predictably showed that the main axis of variation represents mostly flower size. To avoid re-sampling this size variation, the outlines of all flowers were normalised to have the same area before PCA. Due to the complexity of the shape and noise in the data, 19 principal components accounted for 95% of the variation and of these only the first three, FsPC1-3, could be related to variation that was observed between taxa.

The first axis, FsPC1, accounts for 37% of the variation and describes mainly the angle of the dorsal petal lobe to the tube and the size of the tube compared to the petals (Figure 4.12B). Negative values represent accessions with an angle less than $\sim 160^\circ$ (the approximate mean) between the dorsal petal lobes and tube, and proportionately smaller tubes, and positive values represent accessions with an angle of $\sim 160^\circ$ to curling over the ventral petal. Most of the variation of this character is accounted for by between taxon comparisons ($R^2=61\%$). Subsection Antirrhinum species generally have dorsal petal lobes which are continuous with the tube and therefore positive values of FsPC1, apart from *A. barrelieri*, *A. majus litigiosum* and *A. siculum* (Figure 4.13A). In contrast, the subsection Kickxiella species all have negative values of FsPC1, which are significantly different from the subsection Antirrhinum species (apart from *A. barrelieri*, *A. majus*

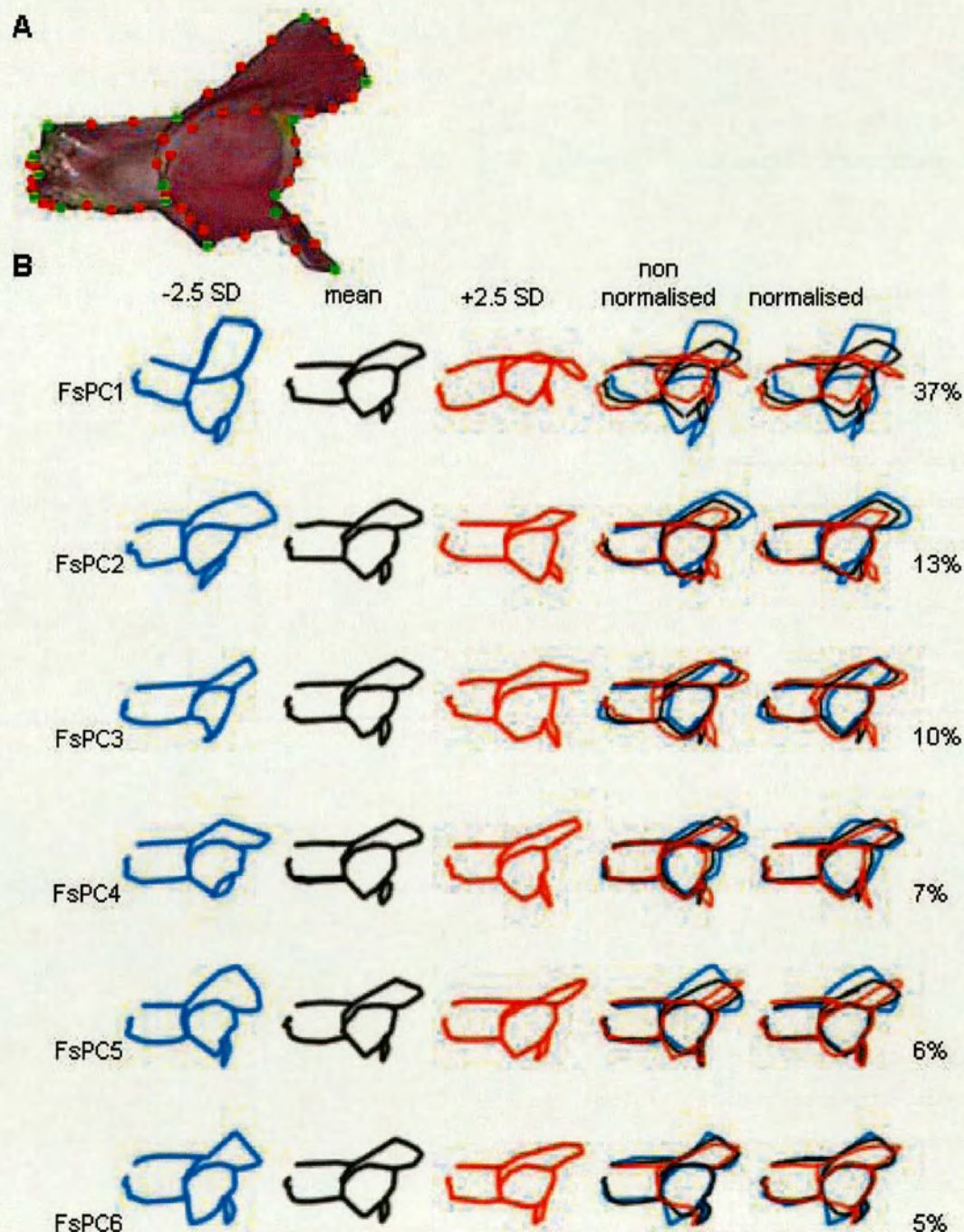


Figure 4.12. The point model template used to describe the flower side outline (A) and the variation described by the resulting PCA axes (B).

(A) An example of a flower side image with the 53 point template fitted to its 2 dimensional outline.

Primary points are coloured green and secondary points are red.

(B) Each row describes the variation described by one of the main axes of variation obtained from PCA, the amount of variation explained is in the right hand column. The axes are labeled according their variable name, which is introduced in the text.

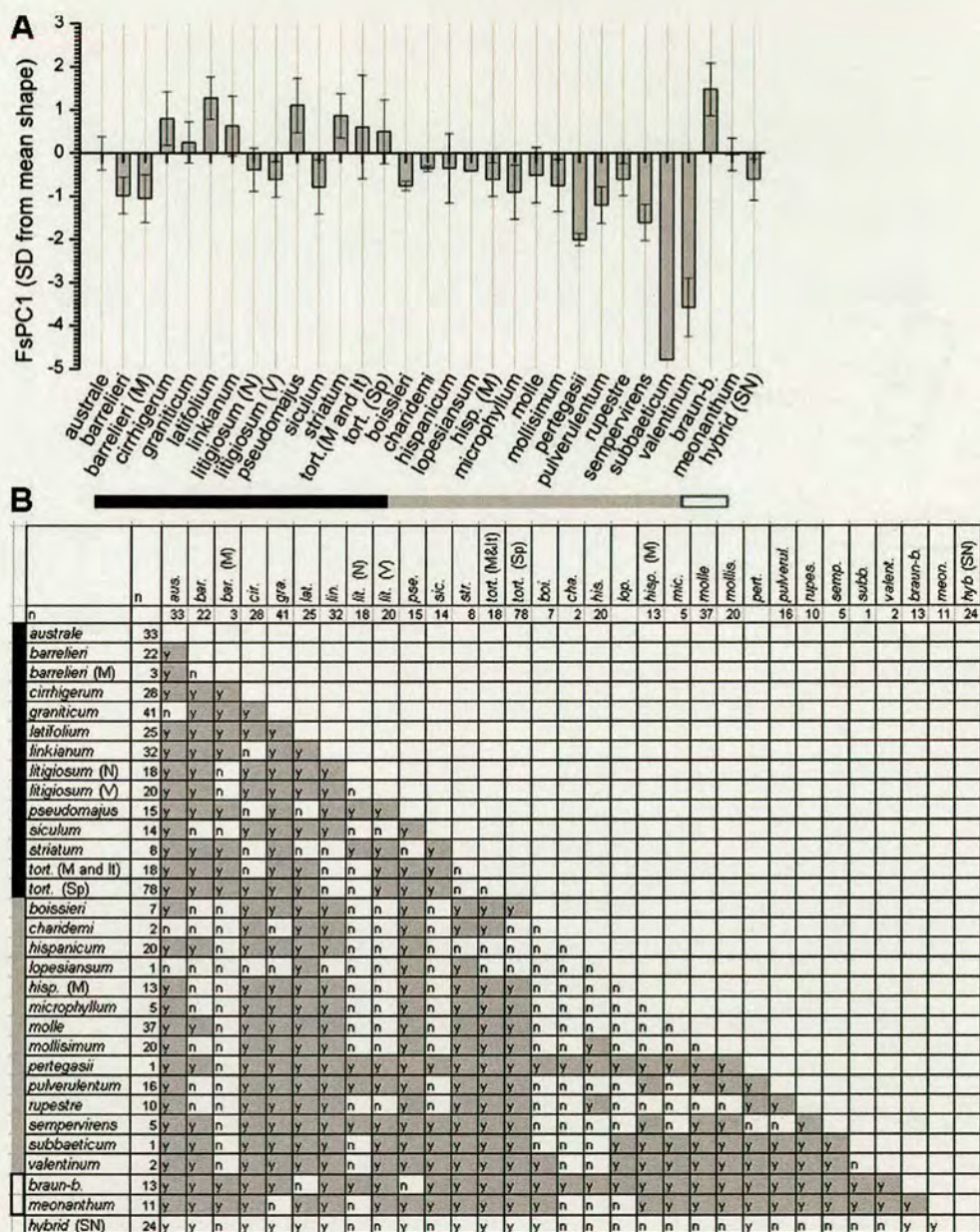


Figure 4.13. Mean values of FsPC1 for each taxon (A) and results of tests for significant differences in FsPC1 values between all pairs of taxa (B).

(A) Graph showing the average value of FsPC1 (± 1 standard deviation) of each taxon. The units are in standard deviations (SD) from the mean shape.

(B) Matrix showing results of pairwise significance tests between all taxa, the number of individuals (n) is indicated in the second column. 'y'=significantly different at 0.05 level (Fisher's Least Significant Difference). One-way ANOVA: $F(28, 512)=32$, $P<0.001$, $R^2=61\%$

barrelieri (M) = Moroccan *A. barrelieri*, *litigiosum* (N) = northern *A. litigiosum*, *litigiosum* (V) = Valencia *A. litigiosum*, *tort.* (M and It) = Moroccan and Italian *A. majus tortuosum*, *tort.* (Sp) = Spanish *A. majus tortuosum*, *hisp.* (M) = Moroccan *A. hispanicum*.

■ Subsection Antirrhinum ■ Subsection Kickxiella □ Subsection Streptosepalum

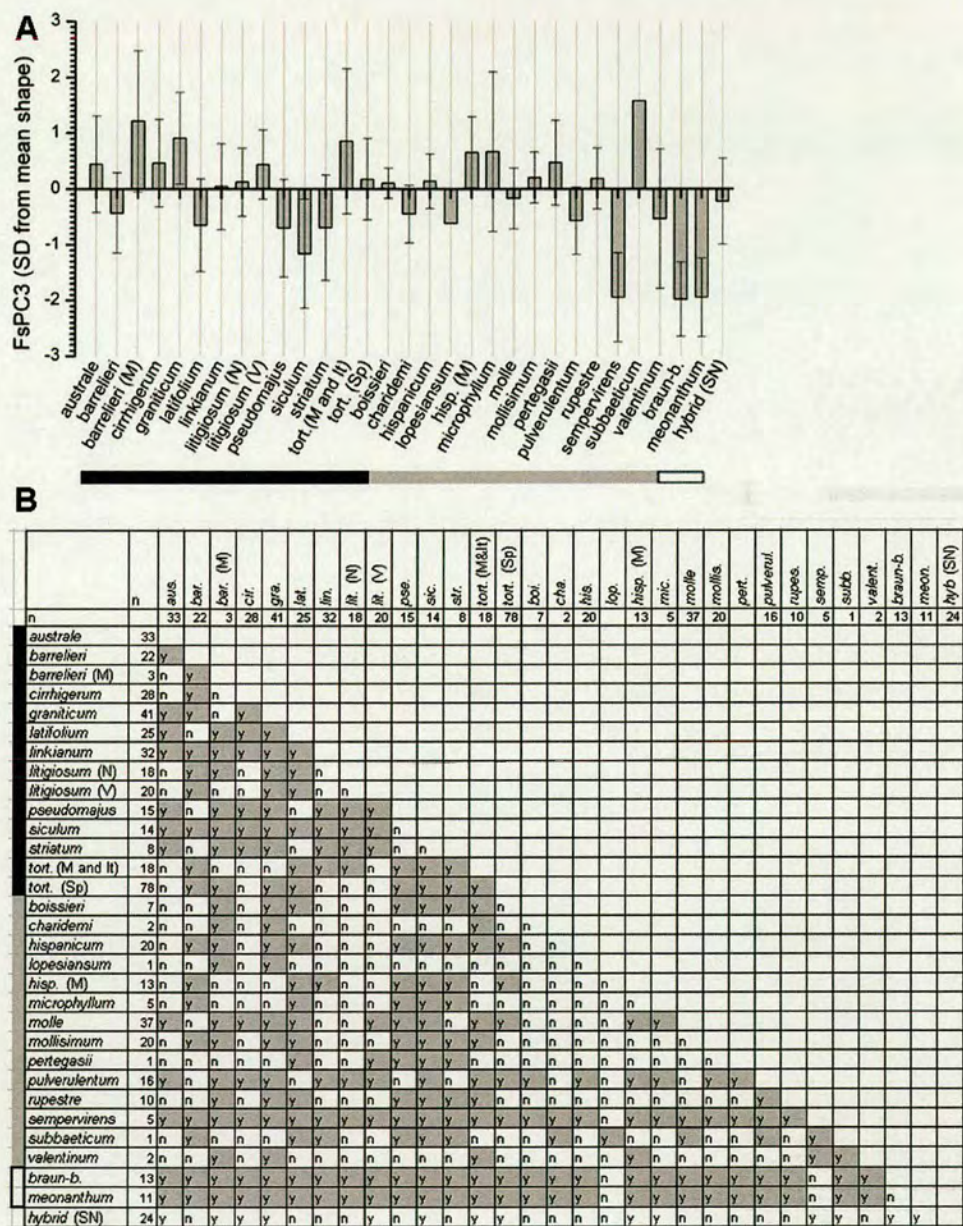


Figure 4.14. Mean values of FsPC3 for each taxon (A) and results of tests for significant differences in FsPC3 values between all pairs of taxa (B).

(a) Graph showing the average value of FsPC3 (± 1 standard deviation) of each taxon. The units are in standard deviations (SD) from the mean shape.

(b) Matrix showing results of pairwise significance tests between all taxa, the number of individuals (n) is indicated in the second column. 'y'=significantly different at 0.05 level (Fisher's Least Significant Difference). One-way ANOVA: $F(28, 525)=15.3$, $P<0.001$, $R^2=42\%$

barrelieri (M) = Moroccan *A. barrelieri*, *litigiosum* (N) = northern *A. litigiosum*, *litigiosum* (V) = Valencia *A. litigiosum*, *tort.* (M and It) = Moroccan and Italian *A. majus tortuosum*, *tort.* (Sp) = Spanish *A. majus tortuosum*, *hisp.* (M) = Moroccan *A. hispanicum*.

■ Subsection Antirrhinum ■ Subsection Kickxiella □ Subsection Streptosepalum

litigiosum and *A. siculum*), as their dorsal petal lobes grow at a perpendicular angle to the tube (Figure 4.13B).

In comparisons of genetically similar species, *A. australe* compared to *A. majus tortuosum*, and *A. meonanthum* compared to *A. braun-blauquetii* have significantly different FsPC1 values (Figure 4.13). Comparisons of morphologically similar species show that *A. barrelieri* has more upright petals than *A. majus litigiosum* and *A. majus tortuosum*.

The second axis, FsPC2 is difficult to interpret from Figure 4.12B. However, visual comparison of values of FsPC2 to the scaled point models and the corolla images indicates that it reflects the properties of the face of the corolla (Figure 4.5). Species such as *A. pertegasii*, *A. pulverulentum*, *A. subbaeticum* and *A. valentinum* all have flat, relatively wide faces compared to most species of subsection Antirrhinum. When these flowers are imaged on their side and scaled to the same area the dorsal petal lobes appear small relative to the rest of the flower due to the perspective of the image. Although FsPC2 indirectly describes the characteristic petal face of many of the Kickxiella species, it represents *A. majus cirrhigerum*, *A. latifolium* and *A. braun-blauquetii* inaccurately as in 2-dimensions their flowers have a similar shape to the Kickxiella species listed above as they have relatively smaller dorsal petal lobes than all other taxa. Therefore, substantial noise is introduced into this measure and it is not included in subsequent analyses.

The third axis accounts for 9% of the variation and mainly describes the tube length relative to the lobes, with flowers with longer tubes also having a larger gibba at the base of the tube (Figure 4.12B). Negative values of FsPC3 represent flower corollas with relatively long tubes and a large gibba, whilst positive values represent the converse. Between taxon comparisons account for almost half of the overall variation ($R^2 = 42\%$). There is little clear trend in FsPC3 values when comparing the subsection Antirrhinum to Kickxiella. However, this axis mainly distinguishes the two Streptosepalum species, *A. meonanthum* and *A. braun-blauquetii*, and *A. sempervirens* by their low values (Figure 4.14).

4.4.2 Dorsal petal cell size

The dorsal petal cell size was estimated by counting the number of cells in a 25 x 25 μm region of the adaxial surface of the dorsal petal lobe. There is no discernable difference in cell size between the Kickxiella and Antirrhinum species (Figure 4.15). Between taxon variation accounts for a small proportion of the overall variation ($R^2 = 30\%$) because it was only possible to examine a few

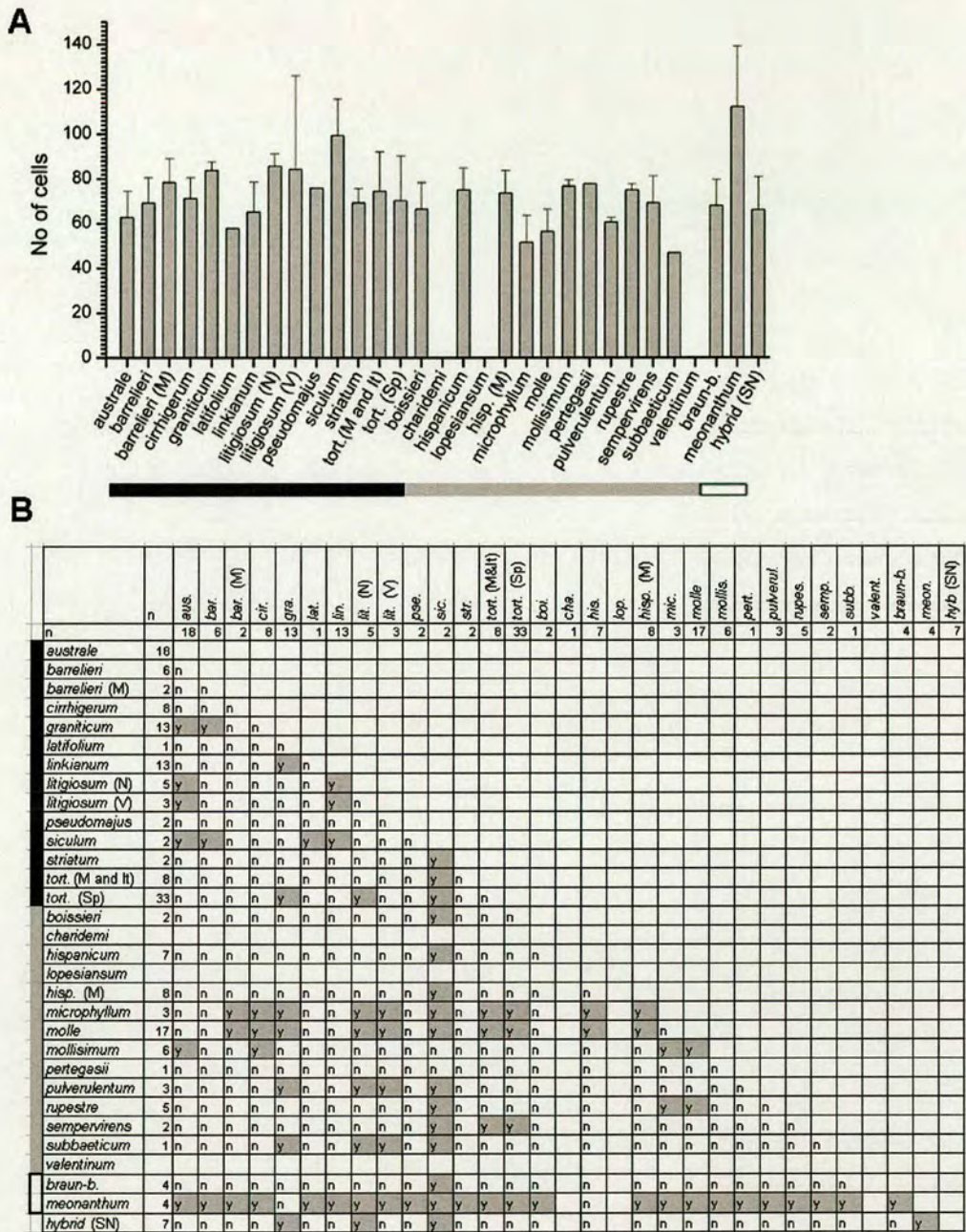


Figure 4.15. Mean values of the number of cells in an 25 x 25 µm area on the adaxial surface of the dorsal petal lobe for each taxon (A) and results of tests for significant differences between all pairs of taxa (B).

(A) Graph showing the average value the mean number of cells (±1 standard deviation) of each taxon.

(B) Matrix showing results of pair-wise significance tests between all taxa, the number of individuals (n) is indicated in the second column. 'y'=significantly different at 0.05 level (Fisher's Least Significant Difference). One-way ANOVA: $F(27, 158)=3.95$, $P<0.001$, $R^2=30\%$

barrelieri (M) = Moroccan *A. barrelieri*, *litigiosum* (N) = northern *A. litigiosum*, *litigiosum* (V) = Valencia *A. litigiosum*, *tort.* (M and It) = Moroccan and Italian *A. majus tortuosum*, *tort.* (Sp) = Spanish *A. majus tortuosum*, *hisp.* (M) = Moroccan *A. hispanicum*.

■ Subsection Antirrhinum ■ Subsection Kickxiella □ Subsection Streptosepalum

individuals of each taxon, resulting in high levels of within-taxa variation. However, dorsal petal cell size was still found to vary among some species. *A. siculum* and *A. meonanthum* have significantly smaller cells, and *A. molle* and *A. microphyllum* have larger cells than the other taxa.

4.4.3 Sepal size and shape

Sepal size and shape have been used as a key characteristic to distinguish *Antirrhinum* species. The dorsal sepal and one of the ventral sepals were therefore dissected from flowers, flattened, and imaged. Typically, the dorsal sepal is longer and narrower than the lateral and ventral sepals and the extent to which they differ was observed to vary between accessions. However, due to time constraints only the size and shape of the ventral sepal was analysed.

To describe both the size and the shape of the sepal a point model consisting of 20 points was fitted to the outline of the flattened sepal (Figure 4.16A) and PCA carried out. Most of the variance (99%) was accounted for by just seven principal components, however only four of these are considered to represent biologically meaningful variation.

Sepal size and the shape of the distal half of the sepal is captured by the first axis, SePC1, which accounts for 83% of the variation (Figure 4.16B). Positive values of SePC1 correspond to large sepals with obtuse, rounded tips whereas negative values correspond to small, ovate sepals with acute tips. Overall, differences in SePC1 between taxa account for a large proportion of the overall variation ($R^2=70\%$). The core *Kickxiella* species and *A. lopesianum* all have significantly lower values of SePC1 than other taxa (Figure 4.17). However, the southern Spanish *Kickxiella* species have positive mean SePC1 values. Subsection *Antirrhinum* species generally have high mean SePC1 values; the exceptions are *A. barrelieri* (from Spain), *A. majus litigiosum* (all populations), *A. siculum*, and accessions of *A. majus tortuosum* distributed in Morocco. The subsection *Streptosepalum* species, which have distinctive long, narrow sepals both have negative mean SePC1 values.

SePC1 does not differentiate *A. australe* and *A. majus tortuosum*, but it does differ between the closely related Portuguese taxa - *A. majus cirrhigerum* has significantly larger sepals than *A. majus linkianum*. In comparisons of genetically differentiated populations of the same species *A. majus litigiosum* accessions from the Valencia region have significantly smaller sepals than accessions from northern populations and accessions of *A. barrelieri* from Morocco have significantly larger sepals than those from Spain.

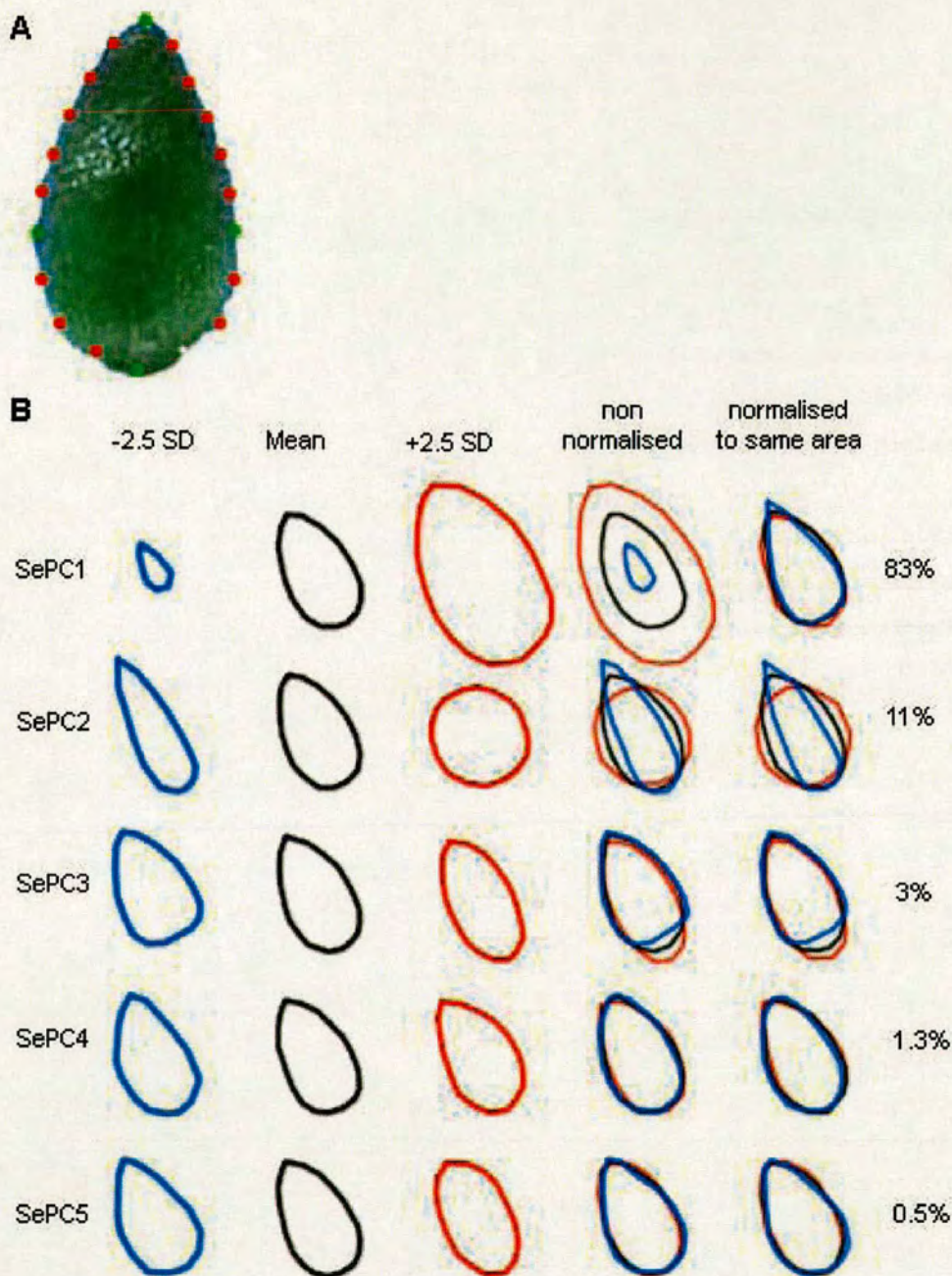


Figure 4.16. The point model template used to capture the dorsal sepal size and shape (A) and variation represented by the resulting PCA axes (B).

(A) An example of a flattened dorsal sepal with the 20 point template fitted to the right hand petal. Primary points are coloured green and secondary points are red.

(B) Each row describes the variation described by one of the main axes of variation obtained from PCA, the amount of variation explained is in the right hand column. The axes are labelled according to their variable name, which is introduced in the text.

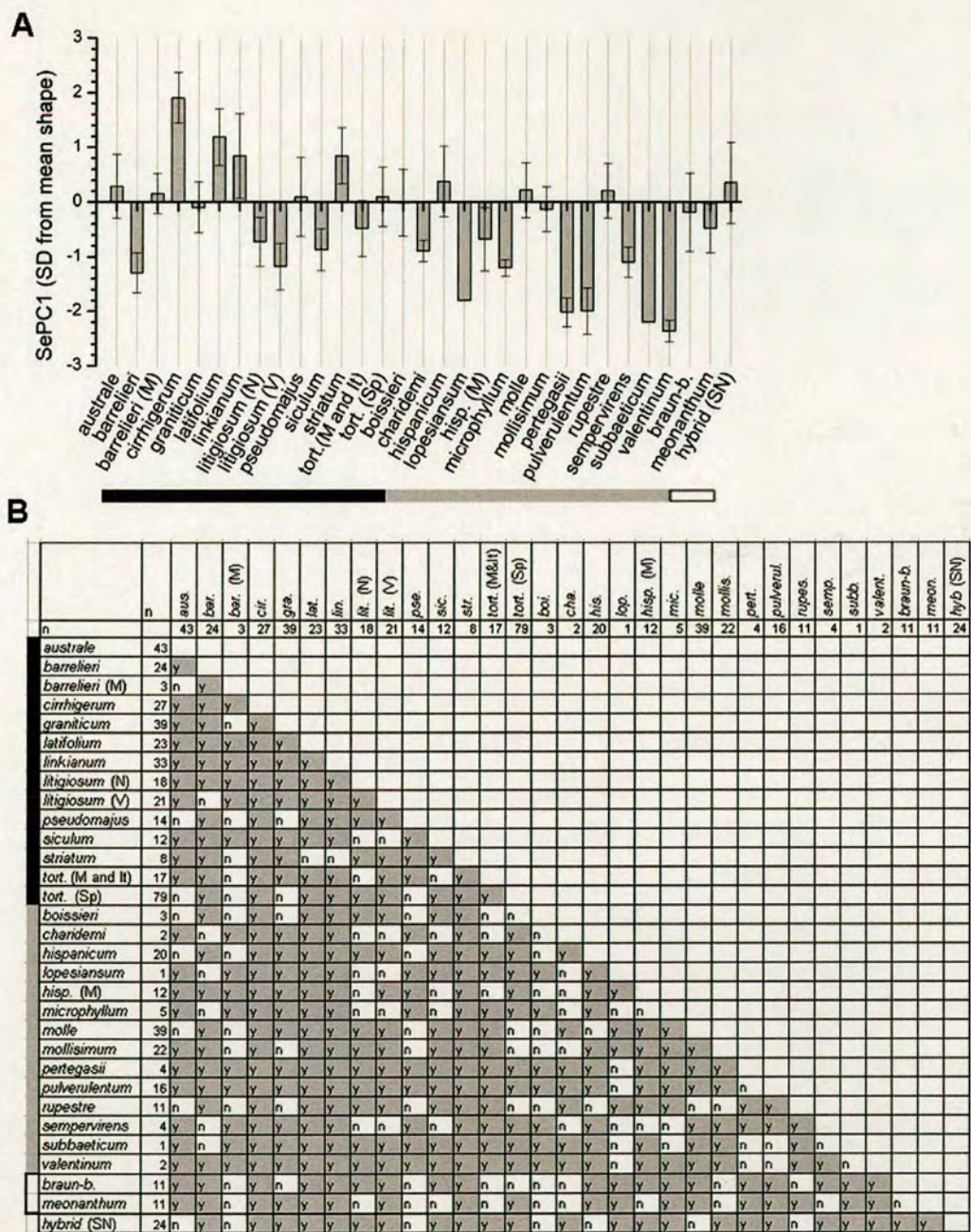


Figure 4.17. Mean values of SePC1 for each taxon (A) and results of tests for significant differences in SePC1 values between all pairs of taxa (B).

(A) Graph showing the average value of SePC1 (± 1 standard deviation) of each taxon. The units are in standard deviations (SD) from the mean shape.

(B) Matrix showing results of pair-wise significance tests between all taxa, the number of individuals (n) is indicated in the second column. 'y'=significantly different at 0.05 level (Fisher's Least Significant Difference). One-way ANOVA: $F(30, 518)=44$, $P<0.001$, $R^2=70\%$

barrelieri (M) = Moroccan *A. barrelieri*, *litigiosum* (N) = northern *A. litigiosum*, *litigiosum* (V) = Valencia *A. litigiosum*, *tort.* (M and It) = Moroccan and Italian *A. majus tortuosum*, *tort.* (Sp) = Spanish *A. majus tortuosum*, *hisp.* (M) = Moroccan *A. hispanicum*.

■ Subsection Antirrhinum ■ Subsection Kickxiella □ Subsection Streptosepalum

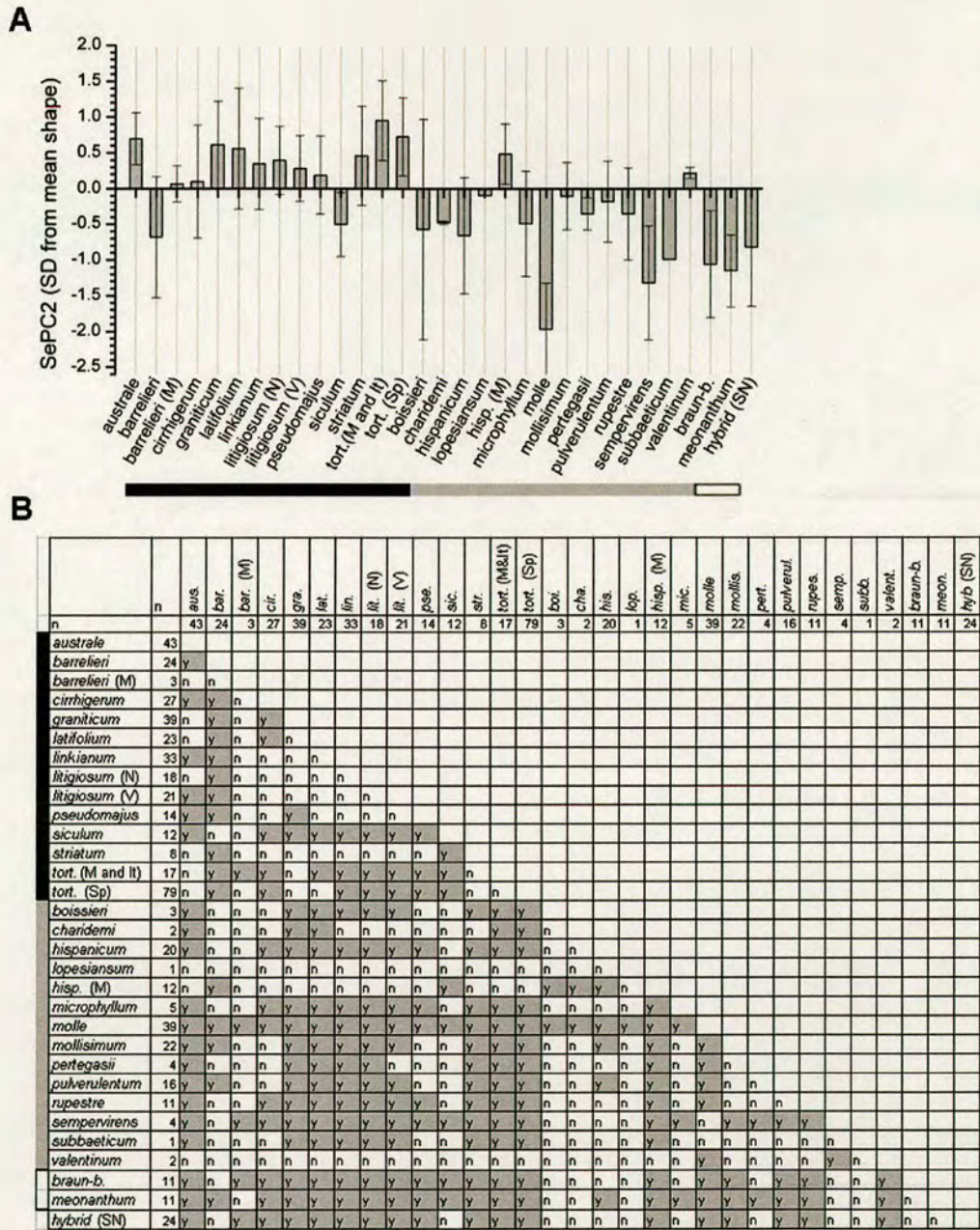


Figure 4.18. Mean values of SePC2 for each taxon (A) and results of tests for significant differences in SePC2 values between all pairs of taxa (B).

(A) Graph showing the average value of SePC2 (± 1 standard deviation) of each taxon. The units are in standard deviations (SD) from the mean shape.

(B) Matrix showing results of pair-wise significance tests between all taxa, the number of individuals (n) is indicated in the second column. 'y'=significantly different at 0.05 level (Fisher's Least Significant Difference). One-way ANOVA: $F(30, 532)=29$, $P<0.001$, $R^2=60\%$

barrelieri (M) = Moroccan *A. barrelieri*, *litigiosum* (N) = northern *A. litigiosum*, *litigiosum* (V) = Valencia *A. litigiosum*, *tort.* (M and It) = Moroccan and Italian *A. majus tortuosum*, *tort.* (Sp) = Spanish *A. majus tortuosum*, *hisp.* (M) = Moroccan *A. hispanicum*.

■ Subsection Antirrhinum ■ Subsection Kickxiella □ Subsection Streptosepalum

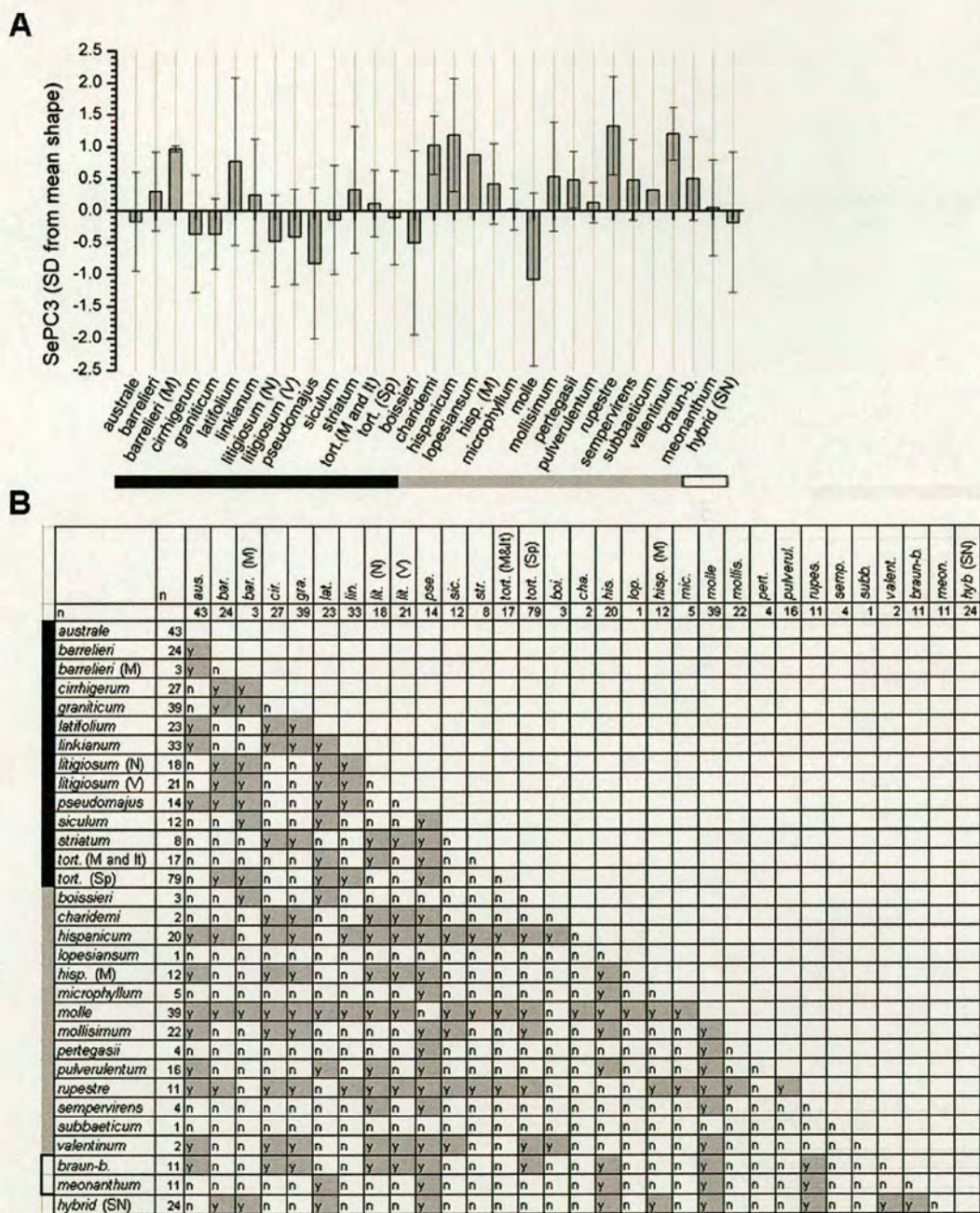


Figure 4.19. Mean values of SePC3 for each taxon (A) and results of tests for significant differences in SePC3 values between all pairs of taxa (B).

(A) Graph showing the average value of SePC3 (± 1 standard deviation) of each taxon. The units are in standard deviations (SD) from the mean shape.

(B) Matrix showing results of pair-wise significance tests between all taxa, the number of individuals (n) is indicated in the second column. 'y'=significantly different at 0.05 level (Fisher's Least Significant Difference). One-way ANOVA: $F(30, 533)=7.6$, $P<0.001$, $R^2=26\%$

barrelieri (M) = Moroccan *A. barrelieri*, *litigiosum* (N) = northern *A. litigiosum*, *litigiosum* (V) = Valencia *A. litigiosum*, *tort.* (M and It) = Moroccan and Italian *A. majus tortuosum*, *tort.* (Sp) = Spanish *A. majus tortuosum*, *hisp.* (M) = Moroccan *A. hispanicum*.

■ Subsection Antirrhinum ■ Subsection Kickxiella □ Subsection Streptosepalum

The second PCA axis, SePC2, accounts for 11% of the variation and describes the variation in sepal shape. Negative values of SePC2 correspond to narrow pointed sepals for a given size and positive values represent rounded sepals (Figure 4.16B). The proportion of variation explained by between taxa variation for SePC2 is high ($R^2 = 60\%$) with most of the variation being partitioned between subsections Kickxiella and Antirrhinum. All subsection Kickxiella (and Streptosepalum) species excepting *A. valentinum* have low mean SePC2 values. In comparison, all subsection Antirrhinum species, apart from *A. barrelieri* and *A. siculum* have high values (Figure 4.18A).

SePC2 distinguishes *A. barrelieri* from *A. majus litigiosum*, but not other morphologically similar species. The distinction of the Moroccan taxa is supported as accessions of *A. hispanicum* and *A. barrelieri* from Morocco have significantly higher values than their respective con-specific populations from Spain (Figure 4.18).

The third PCA axis, accounting for 3% of the variation, describes the shape of the base of the sepal. Negative values of SePC3 correspond with sepals that have a wider, truncate base and positive values correspond with sepals that have a narrower, acute to rounded base (Figure 4.16B). Between-taxa variation accounts for just 26% of the overall variation and it is difficult to identify any trends across taxa in SePC3 values apart from *A. molle* having a very low mean SePC3 value, which is significantly different from most other species, and *A. hispanicum*, *A. rupestre* and *A. valentinum* having significantly higher mean SePC3 values (Figure 4.19).

The fourth PCA axis describes the twisting of the sepal when the sepals are not placed straight prior to imaging (Figure 4.16B). The fifth axis only accounts for 0.5% of the variation and varies extensively within taxa as a very small amount of the overall variation ($R^2 = 11\%$) is explained by between taxa comparisons. These two characters are therefore not considered further.

4.4.4 Androecium and gynoecium measurements

The style length and stamen filament length of one dorsal and one ventral stamen were measured and compared across all taxa.

i) Style length

Style length varied little within taxa and was significantly different for nearly all pair-wise comparisons between taxa, accounting for 84% of the over-all variation (Figure 4.20). Style length

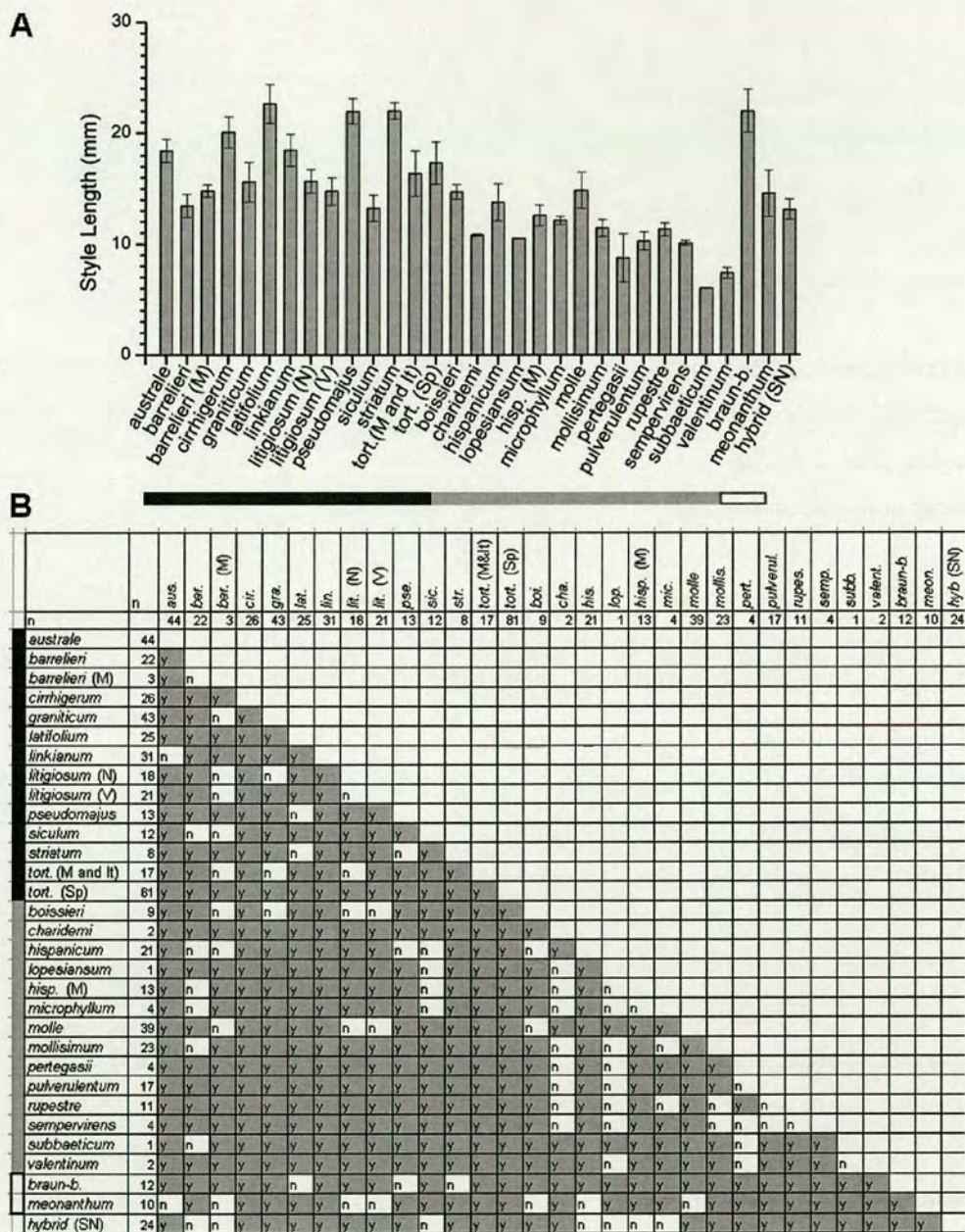


Figure 4.20. Mean values of the style length for each taxon (A) and results of tests for significant differences the mean style length values between all pairs of taxa (B).

(A) Graph showing the average value the style length (± 1 standard deviation) of each taxon.

(B) Matrix showing results of pair-wise significance tests between all taxa, the number of individuals (n) is indicated in the second column. 'y'=significantly different at 0.05 level (Fisher's Least Significant Difference). One-way ANOVA: $F(28, 527)=99.4$, $P<0.001$, $R^2=83\%$

barrelieri (M) = Moroccan *A. barrelieri*, *litigiosum* (N) = northern *A. litigiosum*, *litigiosum* (V) = Valencia *A. litigiosum*, *tort.* (M and It) = Moroccan and Italian *A. majus tortuosum*, *tort.* (Sp) = Spanish *A. majus tortuosum*, *hisp.* (M) = Moroccan *A. hispanicum*.

■ Subsection Antirrhinum ■ Subsection Kickxiella □ Subsection Streptosepalum

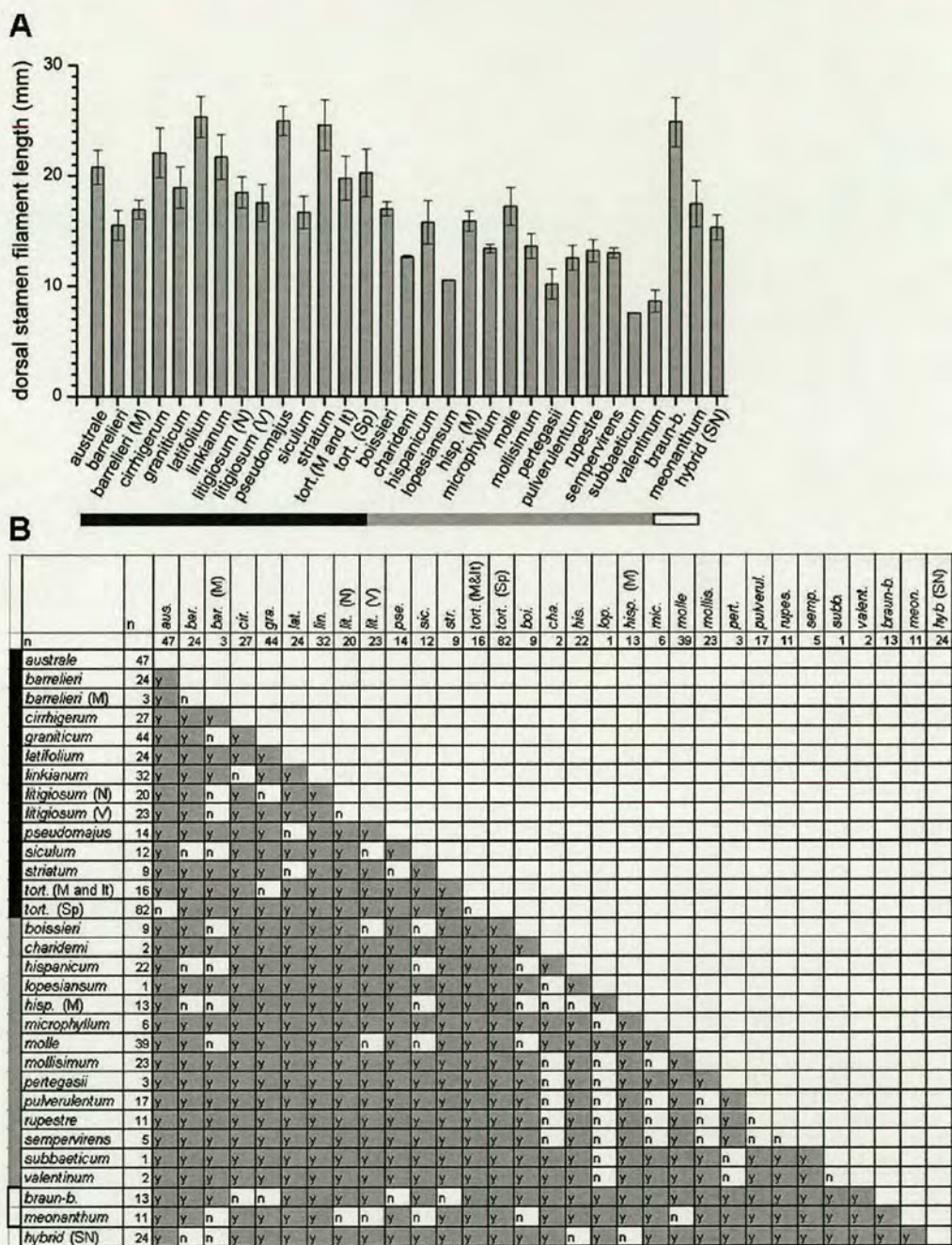


Figure 4.21. Mean values of the dorsal filament length for each taxon (A) and results of tests for significant differences the mean dorsal filament length values between all pairs of taxa (B).

(A) Graph showing the average value the dorsal filament length (± 1 standard deviation) of each taxon.

(B) Matrix showing results of pair-wise significance tests between all taxa, the number of individuals (n) is indicated in the second column. 'y'=significantly different at 0.05 level (Fisher's Least Significant Difference). One-way ANOVA: $F(28, 546)=79$, $P<0.001$, $R^2=79\%$

barrelieri (M) = Moroccan *A. barrelieri*, *litigiosum* (N) = northern *A. litigiosum*, *litigiosum* (V) = Valencia *A. litigiosum*, *tort.* (M and It) = Moroccan and Italian *A. majus tortuosum*, *tort.* (Sp) = Spanish *A. majus tortuosum*, *hisp.* (M) = Moroccan *A. hispanicum*.

■ Subsection Antirrhinum ■ Subsection Kickxiella □ Subsection Streptosepalum

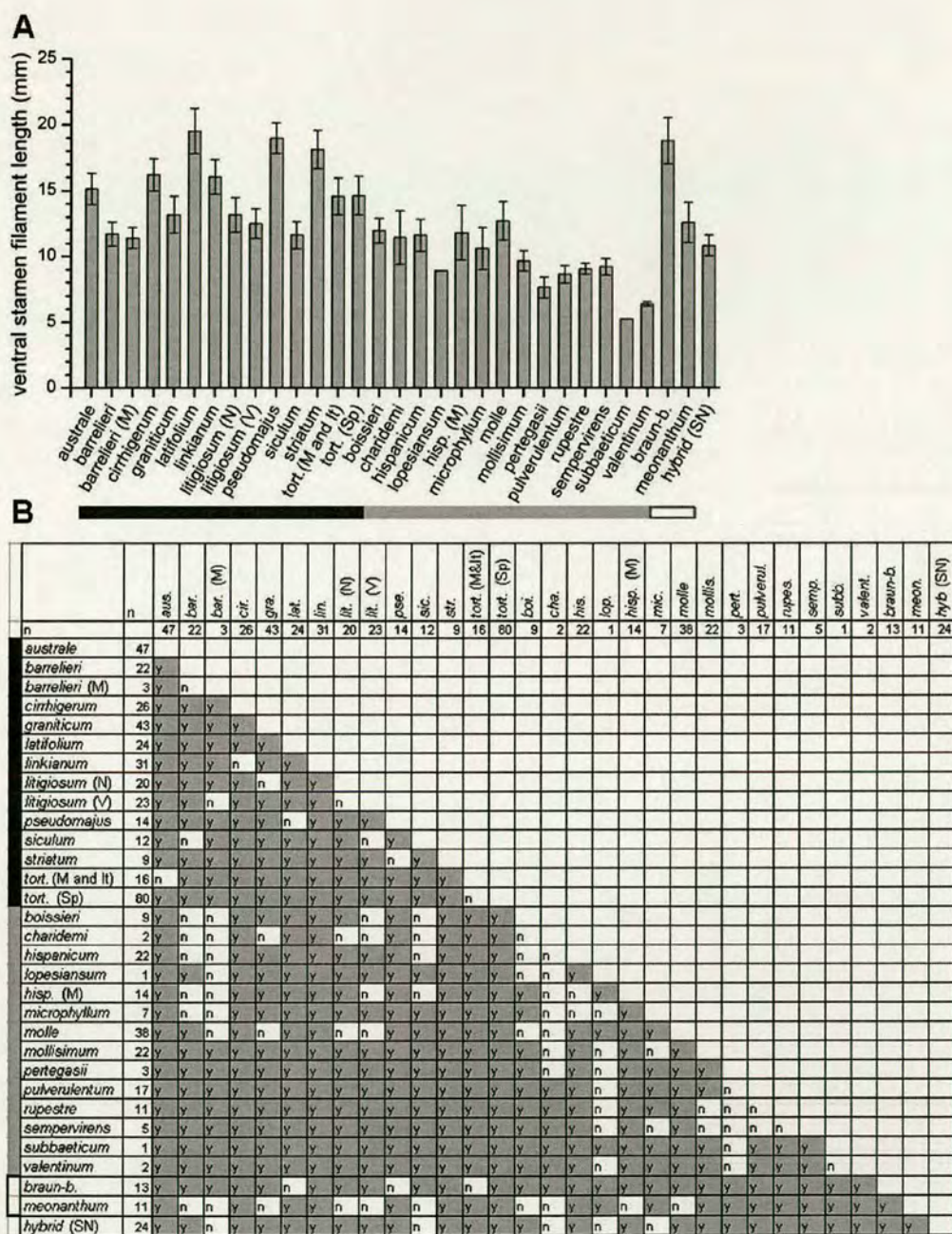


Figure 4.22. Mean values of the ventral filament length for each taxon (A) and results of tests for significant differences the mean ventral filament length values between all pairs of taxa (B). (A) Graph showing the average value the ventral filament length (± 1 standard deviation) of each taxon. (B) Matrix showing results of pair-wise significance tests between all taxa, the number of individuals (n) is indicated in the second column. 'y'=significantly different at 0.05 level (Fisher's Least Significant Difference). One-way ANOVA: $F(30, 541)=86, P<0.001, R^2=82\%$
barrelieri (M) = Moroccan *A. barrelieri*, *litigiosum* (N) = northern *A. litigiosum*, *litigiosum* (V) = Valencia *A. litigiosum*, *tort.* (M and It) = Moroccan and Italian *A. majus tortuosum*, *tort.* (Sp) = Spanish *A. majus tortuosum*, *hisp.* (M) = Moroccan *A. hispanicum*.
 ■ Subsection Antirrhinum ■ Subsection Kickxiella □ Subsection Streptosepalum

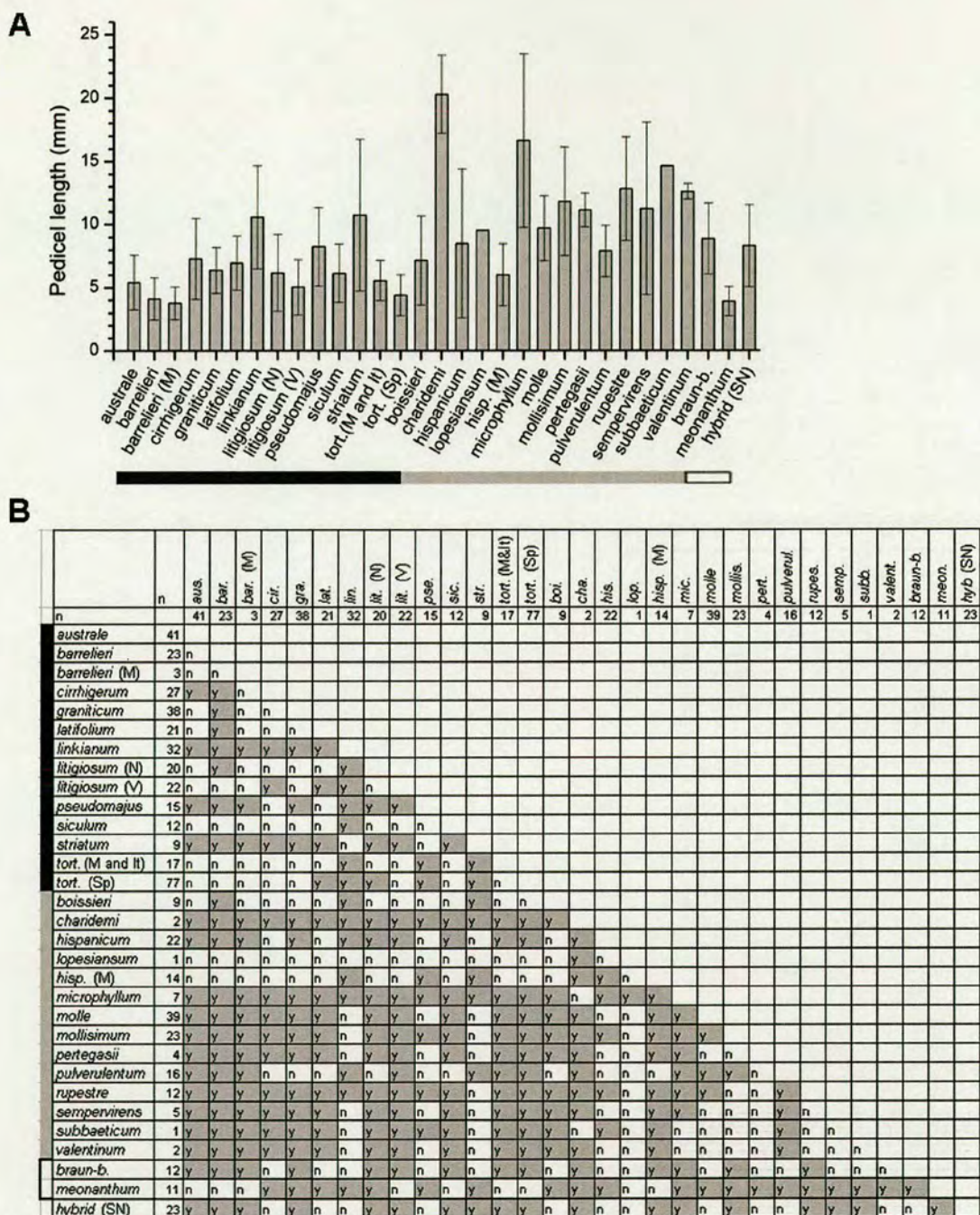


Figure 4.23. Mean values of the pedicel length for each taxon (A) and results of tests for significant differences the mean pedicel length values between all pairs of taxa (B).

(a) Graph showing the average value the pedicel length (± 1 standard deviation) of each taxon.

(b) Matrix showing results of pair-wise significance tests between all taxa, the number of individuals (n) is indicated in the second column. 'y'=significantly different at 0.05 level (Fisher's Least Significant Difference). One-way ANOVA: $F(30, 529)=15.44$, $P<0.001$, $R^2=44\%$

barrelieri (M) = Moroccan *A. barrelieri*, *litigiosum* (N) = northern *A. litigiosum*, *litigiosum* (V) = Valencia *A. litigiosum*, *tort.* (M and It) = Moroccan and Italian *A. majus tortuosum*, *tort.* (Sp) = Spanish *A. majus tortuosum*, *hisp.* (M) = Moroccan *A. hispanicum*.

■ Subsection Antirrhinum ■ Subsection Kickxiella □ Subsection Streptosepalum

ranged from 6.0 mm for an *A. subbaeticum* accession to 25.5 mm *A. latifolium*. The styles of most subsection *Kickxiella* species, apart from *A. molle* and *A. hispanicum*, are shorter than those of subsection *Antirrhinum* species (Figure 4.20B).

ii) *Dorsal and ventral stamen filament length*

The dorsal and ventral stamen filament lengths show the same trends as style length when compared across taxa (Figures 4.21 and 4.22). Comparison of Figures 4.20A, 4.21A and 4.22A shows that the style and the stamen filament lengths are all strongly correlated.

4.4.5 Pedicel length

Comparison of mean pedicel lengths between taxa, Figure 4.23A, with the corresponding graphs of 4.20A, 4.21A and 4.22A for style and stamen filament lengths shows that pedicel length is not correlated with the size of other parts of the flower. In general, species of subsection *Kickxiella* have longer pedicels (10-20 mm) than those of subsection *Antirrhinum* (<10mm), except for *A. majus linkianum*, *A. majus pseudomajus*, and *A. majus striatum* (Figure 4.23). Whilst collecting data it was noticed that on decumbent plants of subsection *Kickxiella* the pedicel length varied extensively within plants. On many plants, the first few flowers and flowers that were shaded beneath the stems had longer pedicels. Pedicel length therefore may not be a reliable morphological measurement to distinguish closely related species. Consistent with this, the between-taxa variation in pedicel length accounts for just 44% of the overall variation.

4.4.6 Corolla colour patterning

Flower colour variation within the *Antirrhinum* genus has implicitly been used in defining species; for example, *A. siculum* is distinguished by its yellow flowers, and *A. majus cirrhigerum* and *A. majus linkianum* are partly defined by having deep pink flowers (Webb 1971). The observed flower colour variation in *Antirrhinum* is the result of the synthesis of two different pigments derived from flavenoids: anthocyanins, which give pink-purple colouration, and aurones, which give yellow colouration (Whibley 2004).

Despite flower colour being well studied in *Antirrhinum* there have been no studies of intra-specific variation and quantification of inter-specific variation. Variation in the intensity of pigmentation and colour patterning was observed both within and between populations of the widespread species *A. barrelieri*, *A. graniticum*, *A. majus tortuosum* and *A. australe* and within *A. mollisimum* and *A. hispanicum*. A system of scoring flower colour was therefore developed to be able to include

flower colour as a character that identifies species and to quantify colour variation within species. Apart from the general colour of the flower, several characters that describe the colour patterns of different domains of the flower were also identified and analysed, giving six flower colour characters.

To enable the inclusion of flower colour patterns into subsequent multivariate analyses the different characteristics such as overall colour were scored as binary presence/absence characters, for example, pink/not pink, yellow/not yellow and white/not white.

i) *Corolla colour*

Colour variation was not observed between flowers of the same plant, apart from immature flowers having a deeper intensity of pigment. The flower colour of each plant was therefore scored from an image of a single flower, mainly based on the pigmentation in the dorsal and lateral lobes. Each flower was scored for the presence/absence of white, pink and yellow colouration. Pink flowers were scored on a scale of 1 for light pink to 4 for deep pink. Examples of the flower scoring are shown in Figure 4.24. Species that are characterised by their yellow flowers, such as *A. majus striatum*, *A. latifolium*, *A. braun-blauquetii*, *A. meonanthum* and *A. siculum* varied in the intensity of yellow in their lobes, but yellow intensity was difficult to characterise reliably from the images so all yellow flowers were given a score of 1.

Within subsection Antirrhinum, accessions of the species from southern Spain, *A. australe*, *A. barrelieri*, *A. majus tortuosum* and *A. majus litigiosum*, all varied in the intensity of pink pigmentation from light (pink = 1) through to dark pink (pink = 4, Figure 4.25A), with variation occurring both within and between populations of these species (data not shown). The majority of *A. graniticum* individuals had light pink flowers although a few individuals had white flowers. The *A. barrelieri* x *A. rupestre* hybrid accessions mainly had light pink flowers; however, field populations were observed to vary in colour from individuals with white to light pink (pink = 2, data not shown). The accessions of the two species distributed in Portugal, *A. majus cirrhigerum* and *A. majus linkianum*, and of *A. majus pseudomajus* were consistent in pigmentation as they all had deep pink flowers (Figure 4.25A).

No intra-specific variation in flower colour was found within the subsection Kickxiella species *A. microphyllum*, *A. molle*, *A. pulverulentum* and *A. sempervirens*, with all accessions grown having white flowers (Figure 4.25B). This is consistent with field observations of several populations of

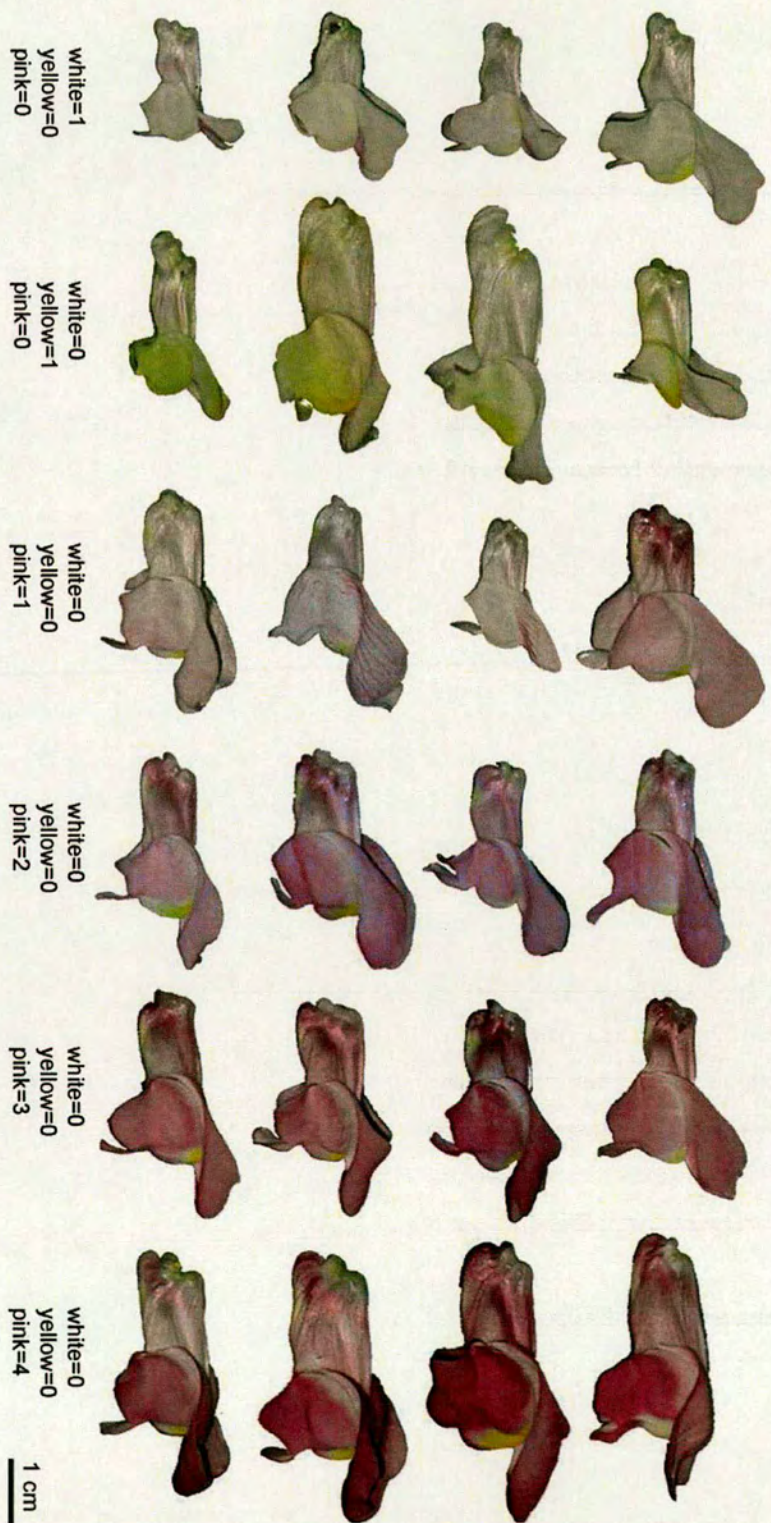


Figure 4.24. Figure showing examples of flower images and their corresponding colour scores

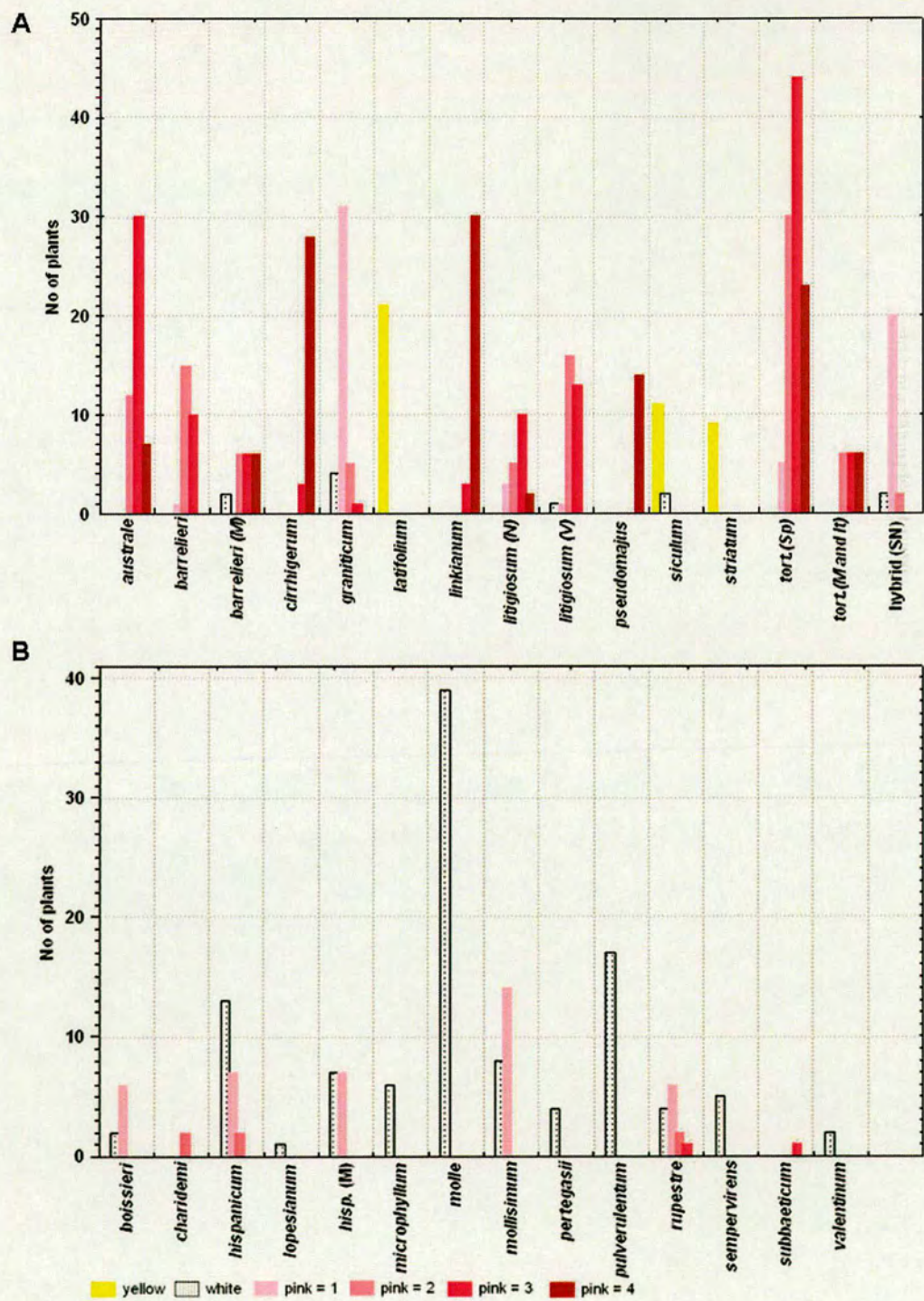


Figure 4.25. Graph showing the number of individuals with flowers of each colour score for the species in subsection *Antirrhinum* (A) and subsection *Kickxiella* (B).

these species. The few accessions that were grown for *A. valentinum*, *A. lopesianum* and *A. pertegasii* all had white flowers and are considered representative of these species as there have been no reports of flower colour variation within them. The subsection Kickxiella species distributed in southern Spain: *A. boissieri*, *A. hispanicum*, *A. mollisimum* and *A. rupestre*, showed some intra-specific variation in pink pigmentation intensity with approximately equal numbers of accessions having white compared to light pink flowers. However, *A. rupestre* had a higher proportion of individuals with pink flowers and a few individuals with dark pink flowers (Figure 4.25B). All *A. charidemi* and *A. subbaeticum* plants, which are from southern Spain, had pink flowers. However, insufficient accessions were sampled to quantify intra-specific variation for these two taxa.

Within subsection Streptosepalum, all individuals of *A. meonanthum* from five locations and *A. braun-blanquetii* from four locations had yellow flowers.

ii) *Purple patch in the centre of the dorsal flower face*

Most species within subsection Kickxiella have a characteristic purple bar in the centre of the dorsal flower face. This is particularly prominent particular *A. sempervirens* and *A. valentinum* (Figure 4.26). This is mentioned in the taxonomic literature as being a distinguishing feature of these species (Sutton 1988). However, traces of this patch were also observed in other species. Therefore its occurrence was characterised to determine if it occurs in a single or multiple lineages. On more detailed analysis the purple patch in many accessions was found to consist of darker pigmented cells overlying the vascular tissue, whilst in other accessions all epidermis cells were darkly pigmented. These two origins of the purple patch, abbreviated to ‘vascular’ or ‘general’, were scored as different characters as they were observed to occur independently of each other. These observations are consistent with the understanding of the genetic basis of colour patterning as pigmentation over veins requires activity of the *VENOSA* gene (Schwinn *et al* 2006) and the general pattern may correspond with patterns of ELUTA expression (A. Hudson, pers. comm.). Flowers were therefore scored for the presence/absence of vasculature pigmentation and for the presence/absence of general pigmentation of all epidermal cells in this region of the flower. In cases where both patterns occurred flowers were scored as 1 for both characters. Figure 4.27 shows examples of the scoring for these characters.

The majority of accessions within subsection Antirrhinum did not have any purple patch (Figure 4.28A). The main exceptions to this are *A. latifolium* and *A. siculum* with 33% and 61% of



Figure 4.26. An image showing the distinctive purple patch of an *A. sempervirens* flower. Scale bar = 1 cm.

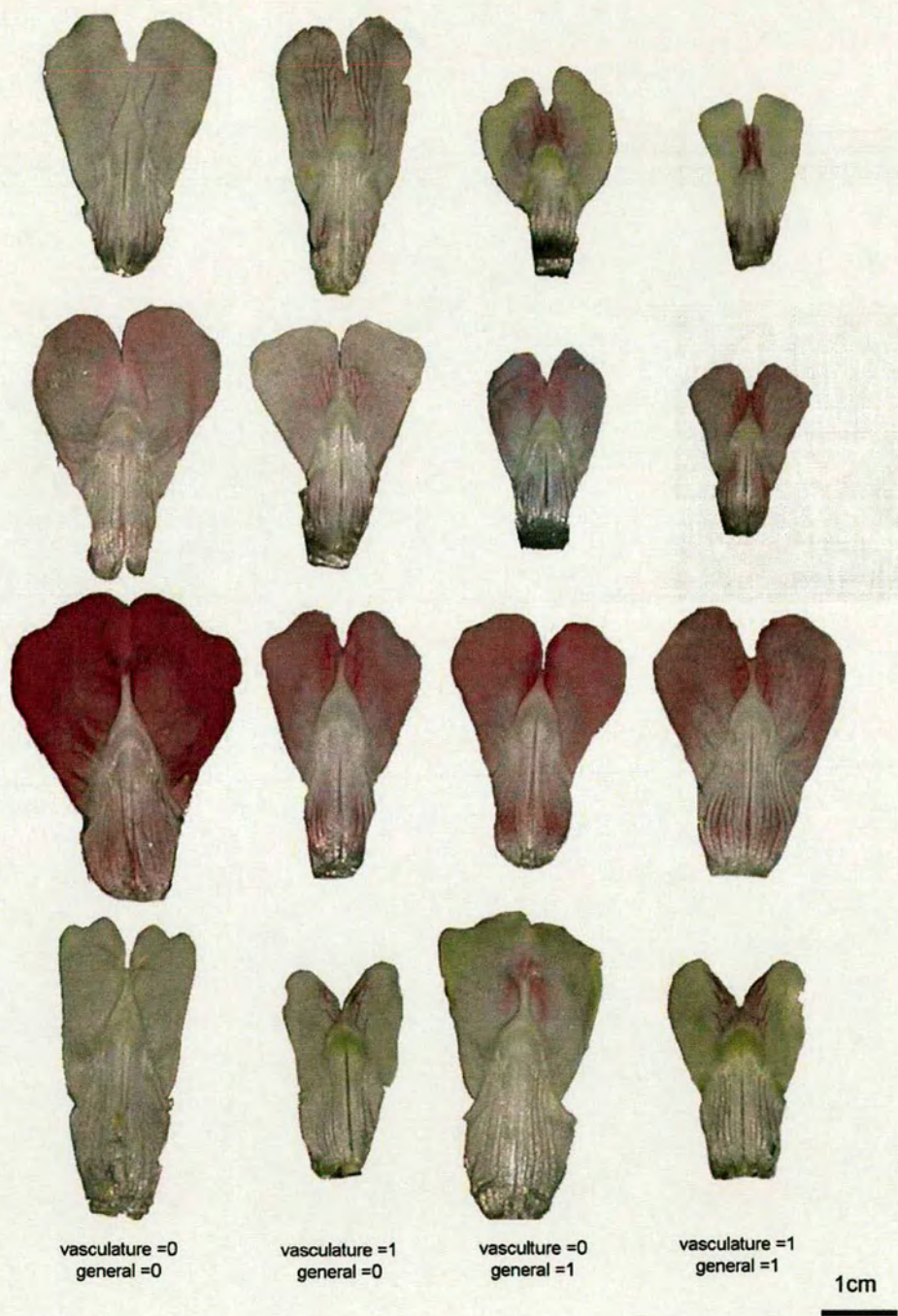


Figure 4.27. Figure showing examples of images of dorsal petals and their corresponding scores for the purple patch in the centre of the dorsal flower face.
Four examples are shown for each combination of scores for vascular and general purple pigmentation in the centre of the dorsal flower face.

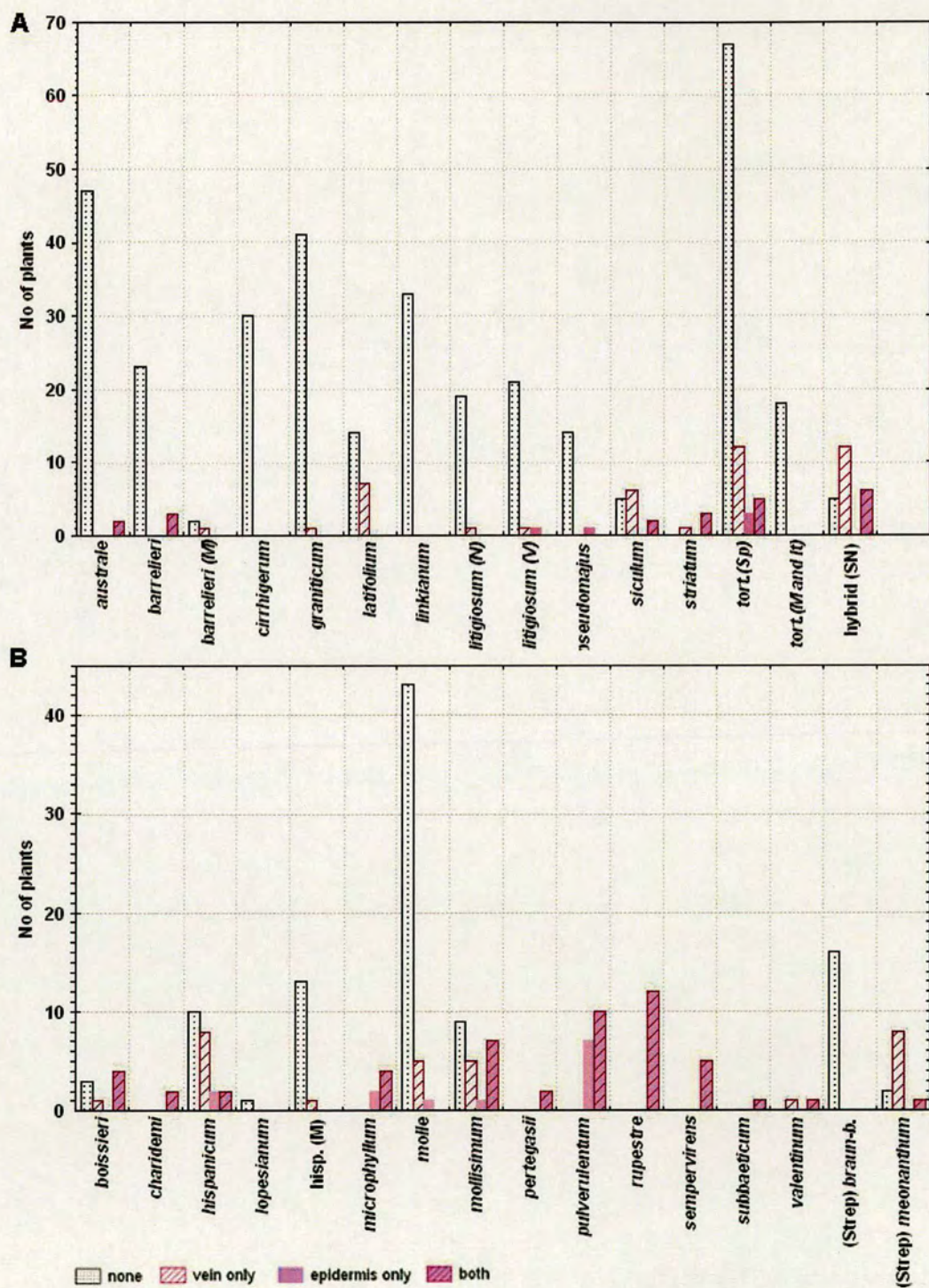


Figure 4.28. Graphs showing the number of individuals of scoring category of the dorsal petal purple patch for the species in subsection *Antirrhinum* (A) and subsections *Kickxiella* and *Streptosepalum* (B).

accessions having the purple patch respectively, mostly due to vasculature pigmentation. A small percentage of *A. australe*, *A. barrelieri* and *A. majus tortuosum* accessions had traces of this purple patch, in nearly all of these cases due to vasculature pigmentation.

Within subsection Kickxiella all accessions of *A. charidemi*, *A. microphyllum*, *A. pertegasii*, *A. rupestre*, *A. sempervirens*, *A. subbaeticum*, and *A. valentinum* had a purple patch (Figure 4.28B). This was mostly due to general pigmentation in combination with deeper vasculature pigmentation. Only 12% of *A. molle* accessions had a purple patch, in most this was due to vasculature pigmentation. The subsection Kickxiella species distributed mainly in Granada and Almeria provinces of Spain - *A. boissieri*, *A. hispanicum*, and *A. mollisimum* - show intra-specific variation in this characteristic with roughly 60% of individuals of each species having the purple patch. Similar to the majority of other Kickxiella species this was due to both vasculature and general pigmentation.

Within subsection Streptosepalum, the purple patch was absent in all plants of *A. braun-blanquetii* and it was present in the form of vasculature pigmentation in most plants of *A. meonanthum* (Figure 4.28B).

iii) Purple region proximal to the hinge of dorsal petal lobes

In addition to the variation in purple pigmentation in the confined region of the dorsal flower face centre, variation in intensity was observed in the inner surface of the dorsal lobes in the region proximal to the hinge of the flower (Figure 4.29). These two patterns were scored separately as there did not seem to be an association between their occurrences. Similar to the scoring of the purple patch described in (ii), the two origins of the purple region – ‘vasculature’ and ‘general’ – were scored as different characters as shown in Figure 4.29.

The majority of subsection Antirrhinum species did not have this region of purple pigmentation (Figure 4.30A). Again, the main exceptions are *A. latifolium* and *A. siculum*, which both have a high proportion of accessions (approx. 33% and 60% respectively) with vasculature pigmentation in this region of the flower. The other species with yellow flowers, *A. majus striatum*, also had a few individuals with purple pigmentation, however too few accessions were sampled to confidently estimate its occurrence within this species. A very small proportion of the southern Spanish species, *A. australe*, *A. barrelieri* and *A. majus tortuosum* have purple vascular patterning in addition to general darker purple pigmentation in this region of the lobe.



Figure 4.29. Figure showing examples of images of dorsal petals and their corresponding scores for the purple zone on the adaxial dorsal petal lobe, proximal to the hinge of the flower. Five examples are shown for each combination of scores for vascular and general purple pigmentation in the region of the dorsal petal lobe proximal to the hinge of the flower, indicated by the arrow.

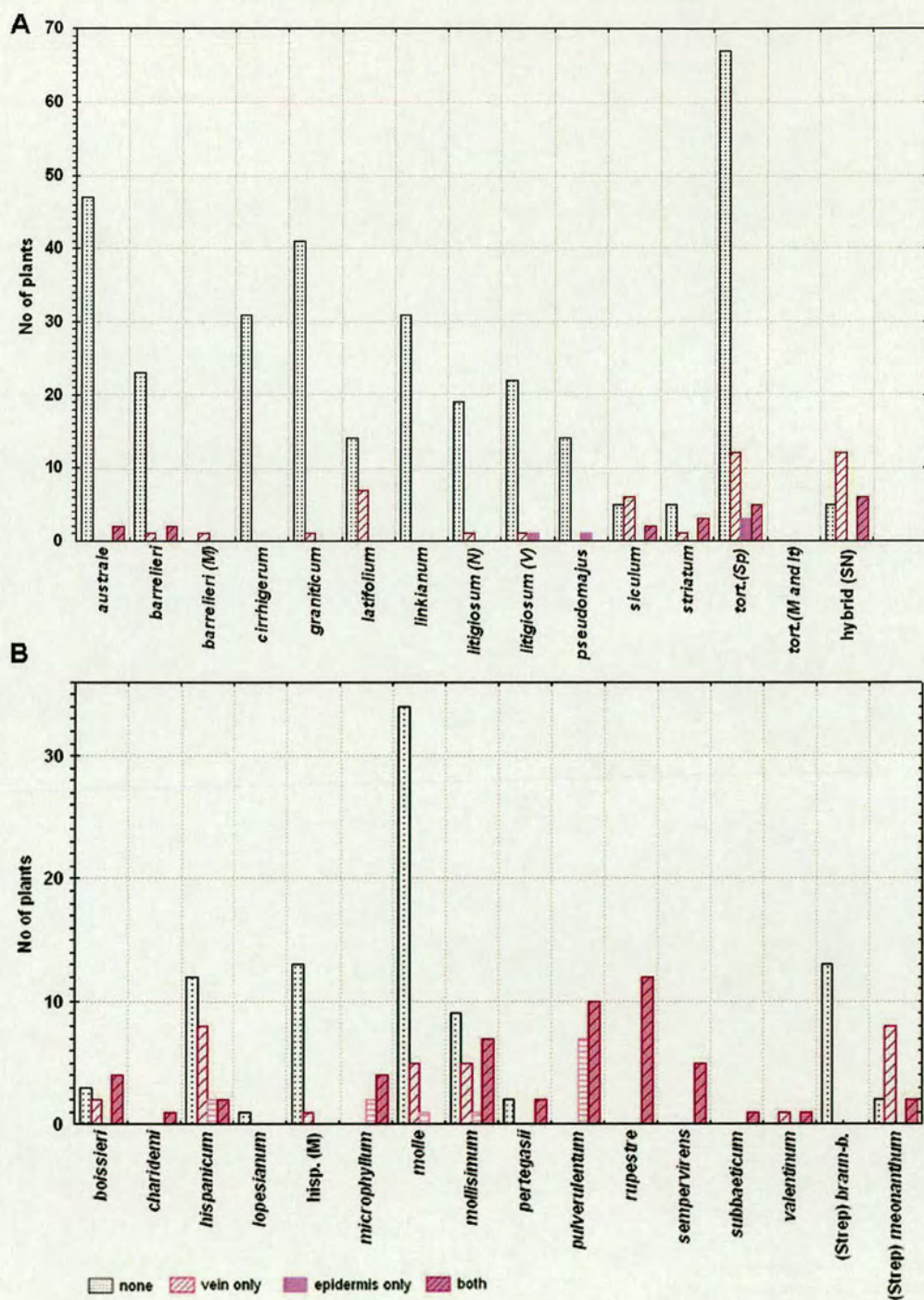


Figure 4.30. Graphs showing the number of individuals of each scoring category for the dorsal lobe purple region proximal to the hinge of the petal. The species in subsection *Antirrhinum* are plotted in (A) and those in subsections *Kickxiella* and *Streptosepalum* in (B).

The distribution of this character in the *Kickxiella* and *Streptosepalum* species is very similar to that described for the purple patch in section (ii) (Figure 4.30B).

iv) *Yellow patch on the ventral face of the flower*

Wild-type *Antirrhinum majus* plants typically have an intense yellow patch in the centre of the ventral flower face. The proportion of the ventral flower face which is covered by this patch was observed to vary across species accessions. Its presence was scored as 1 if it is confined to top of the ventral petal face, 2 if it spread more than half way down the ventral petal and 3 if it extended to the lateral petal lobes; its absence was scored as 0 (Figure 4.31). This region of intense yellow was also observed and scored in yellow flowers.

Plants with the yellow patch present were predominant within all subsection *Antirrhinum* species (Figure 4.32A). The only exception was *A. barrelieri* with only ~30% of the accessions having a yellow patch, all scoring 1. Members of the taxa distributed in southern Spain and Morocco - *A. australe*, and *A. majus tortuosum* - in addition to *A. majus litigiosum*, all had flowers with a small yellow patch. In contrast, a high proportion of accessions of the remaining species: *A. majus cirrhigerum*, *A. latifolium*, *A. siculum* and *A. majus striatum* had a score >2.

Within subsection *Kickxiella* only accessions of *A. lopesianum*, *A. pertegasii*, *A. sempervirens* and *A. subbaeticum* had flowers which did not have a yellow patch, but too few accessions of each of these species were successfully grown to reliably assess intra-specific variation (Figure 4.32B). Some variation in its occurrence was found in *A. pulverulentum* and within the southern Spanish taxa *A. hispanicum*, *A. mollissimum* and *A. rupestre*, with a high proportion of accessions of *A. rupestre* lacking it. All *A. microphyllum* and *A. valentinum* accessions had flowers with a large region of yellow on their ventral face, however too few accessions of these species were scored to generalise on the occurrence of this trait in these species.

All accessions of *A. braun-blanquetii* had flowers with large yellow patches, all having a score of 3, whilst the majority of *A. meonanthum* accessions had uniform pale yellow ventral flower faces, scoring 0 (Figure 4.32B).

v) *Extent of yellow colouration of hairs on the adaxial surface of ventral petal*

The adaxial surface of the ventral tube of the flower has two bands of hairs running parallel from the base of the tube into the ventral petal lobe. On dissecting the flowers it was observed that in

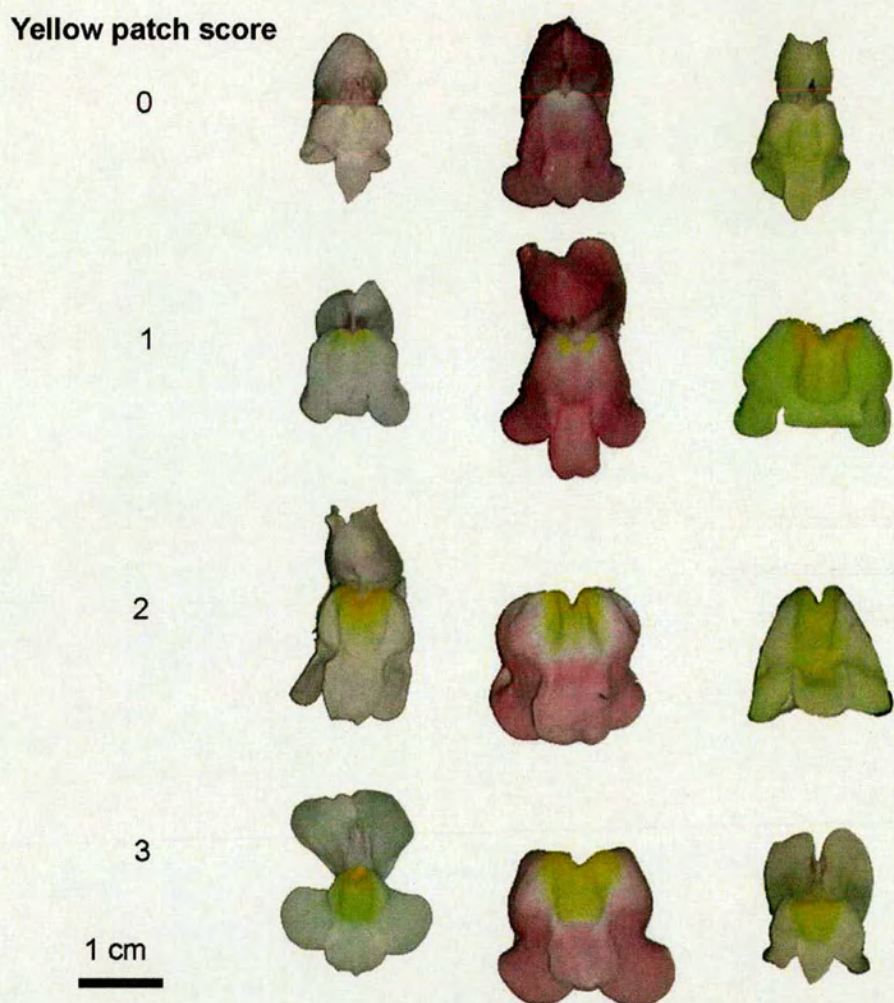


Figure 4.31. Example scoring of the yellow patch on the ventral face of the flower.
The scores are shown in the left hand column, with three example flowers of each score shown.

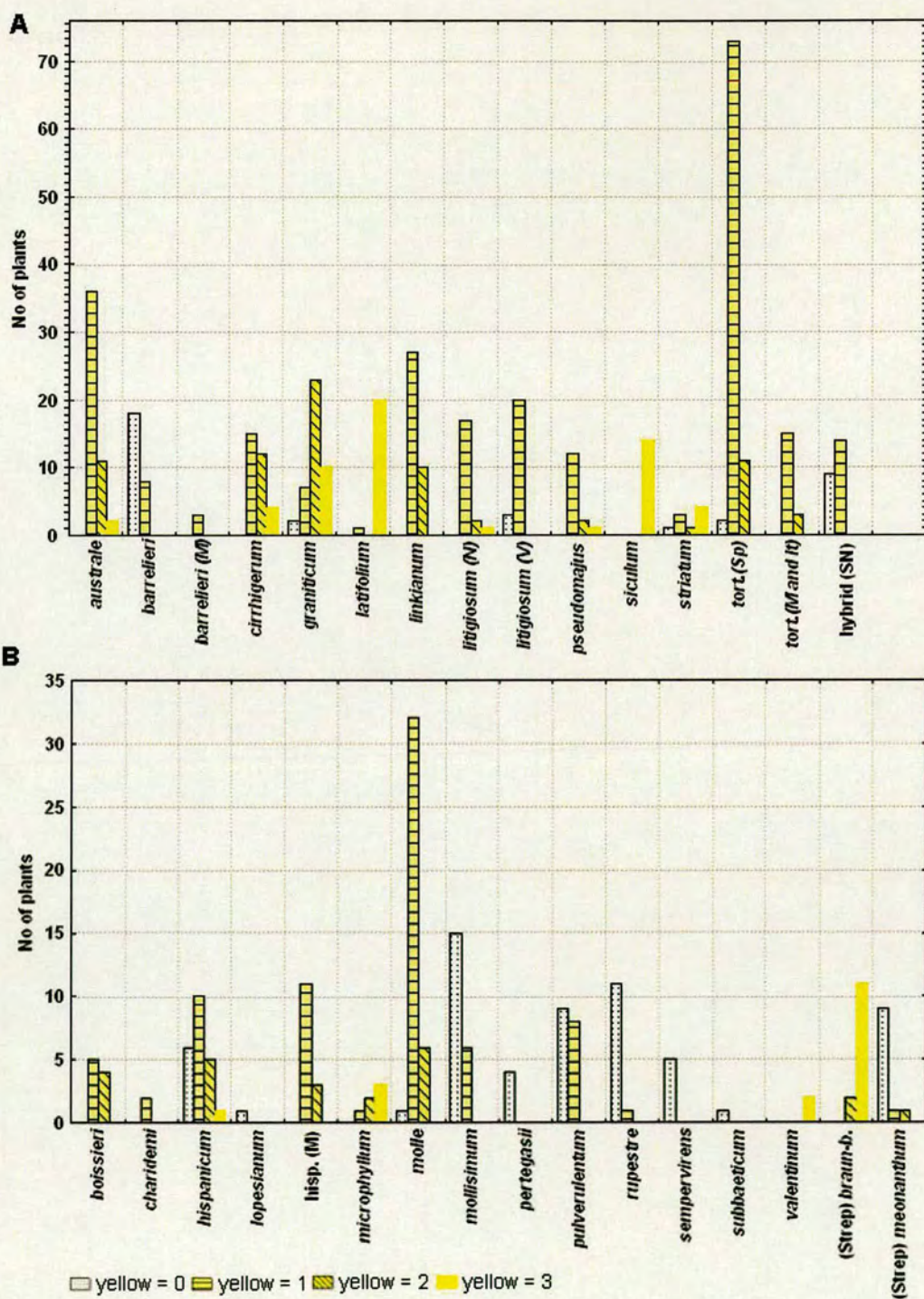


Figure 4.32. Graphs showing the number of individuals of each species for each scoring category for the yellow patch on the face of the flower in subsection *Antirrhinum* species (A) and subsections *Kickxiella* and *Streptosepalum* species (B).

some accessions the hairs were colourless or just the basal-most hairs were yellow whereas in others the entire strips were yellow, with a continuum between these extremes. This character was therefore scored from entirely colourless being 0, yellow at just the base being 1, yellow to the end of the tube being 2, yellow extending in the ventral lobe being 3 and completely yellow strips of hair being 4 (Figure 4.33A).

Nearly all of the accessions of species within subsection Antirrhinum and subsection Streptosepalum had pigmented hairs, with a high proportion of accessions of each species having scores > 1 (Figure 4.34). Pigmentation was absent only from a few individuals of *A. australe* (1 plant), *A. barrelieri* (5 plants), *A. majus tortuosum* (4 plants) and *A. majus pseudomajus* (1 plant).

Within the Kickxiella species pigmentation was either absent as in *A. mollisimum*, *A. pertegasii*, *A. rupestre*, *A. subbaeticum* and *A. valentinum*, or the hairs were coloured only at the base of the tube in the majority of the remaining accessions (Figure 4.34B).

vi) *Yellow patch at the base of the tube*

The presence of a yellow patch on the ventral adaxial surface at the base of the tube was found in some accessions. The extent of this patch was scored on a scale of 0 (absent) to 3 (extending into the lateral petals (Figure 4.33B).

All of the accessions of species within subsection Antirrhinum have this trait and in most cases the yellow patch was a distinctive heart shape, sometimes extending around the sides of the tube in species such as *A. majus cirrhigerum* and *A. majus tortuosum* (Figure 4.35A). The patch was also present in many of the accessions of *A. boissieri*, *A. charidemi*, *A. hispanicum*, *A. microphyllum*, *A. molle* and *A. pulverulentum* with scores ranging from 1 to 3 (Figure 4.35B). However, it was absent from the remainder of subsection Kickxiella and from *A. braun-blauquetii* in subsection Streptosepalum; there was variation in its occurrence and size in *A. meonanthum*.

4.4.7 Summary of flower characters

In total, 13 characters describing flower size and shape and 8 characters describing flower colour patterning are defined. Of the flower size and shape characters, measures that describe flower size show the most variation between subsections Kickxiella and Antirrhinum as well as between species. These measures are FpPC1, style length and dorsal and ventral stamen filament length. FsPC1, which describes the angle of the dorsal petal to the tube, and the pedicel length also varies



Figure 4.33. Examples of the scoring for yellow colouration of the strips of hair (A) and the yellow patch (B) on the adaxial surface of the ventral petal
 The score is indicated in the left hand column of the figure. For each character, three example flowers are shown for each score. For strips of hair of yellow score 1, the distal yellow coloration is pollen.

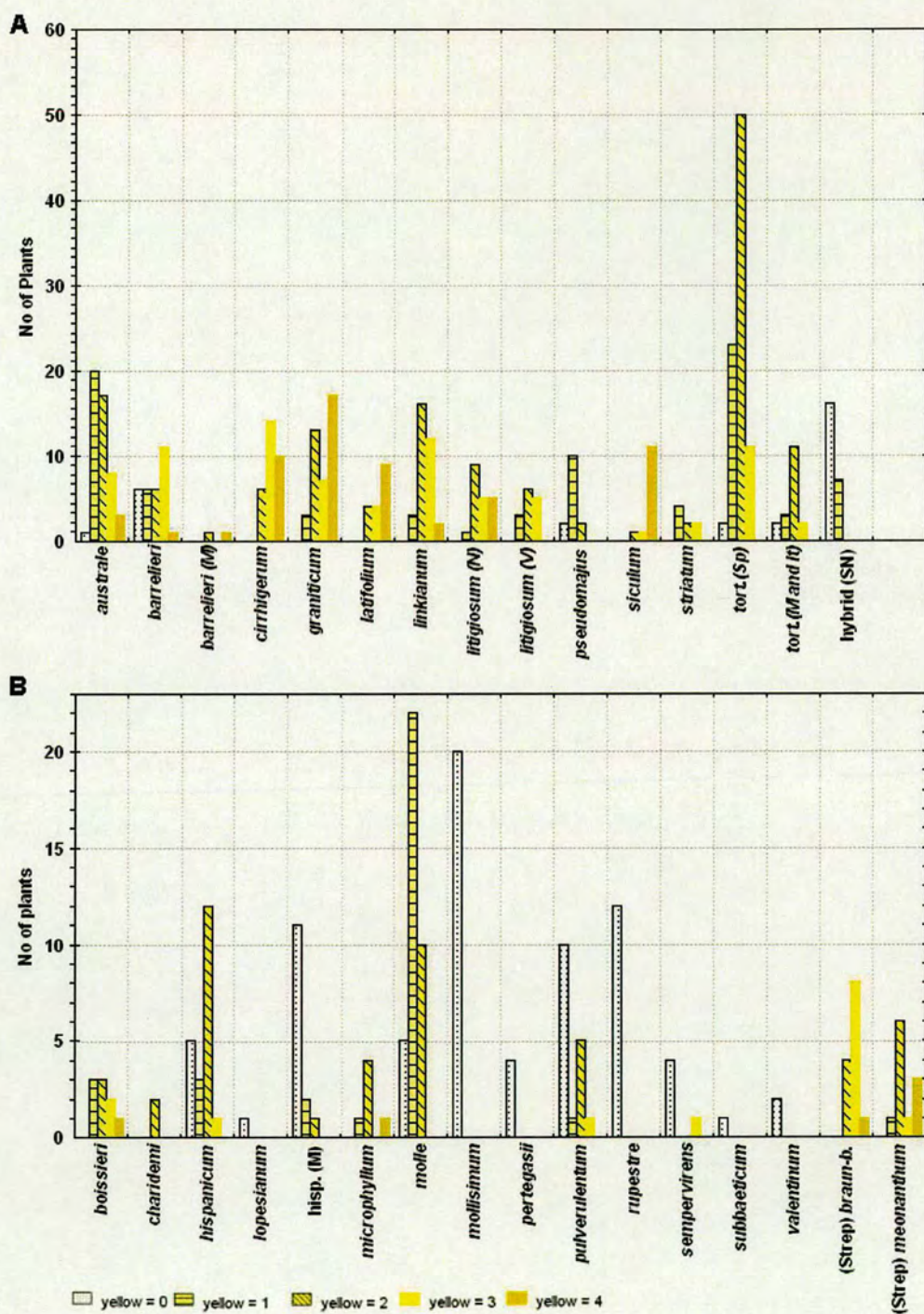


Figure 4.34. Graphs showing the number of individuals of each species of each score for the extent of yellow colouration of the strips of hairs on the adaxial surface of the ventral petal in subsection Antirrhinum (A) and subsections Streptosepalum and Kickxiella (B).

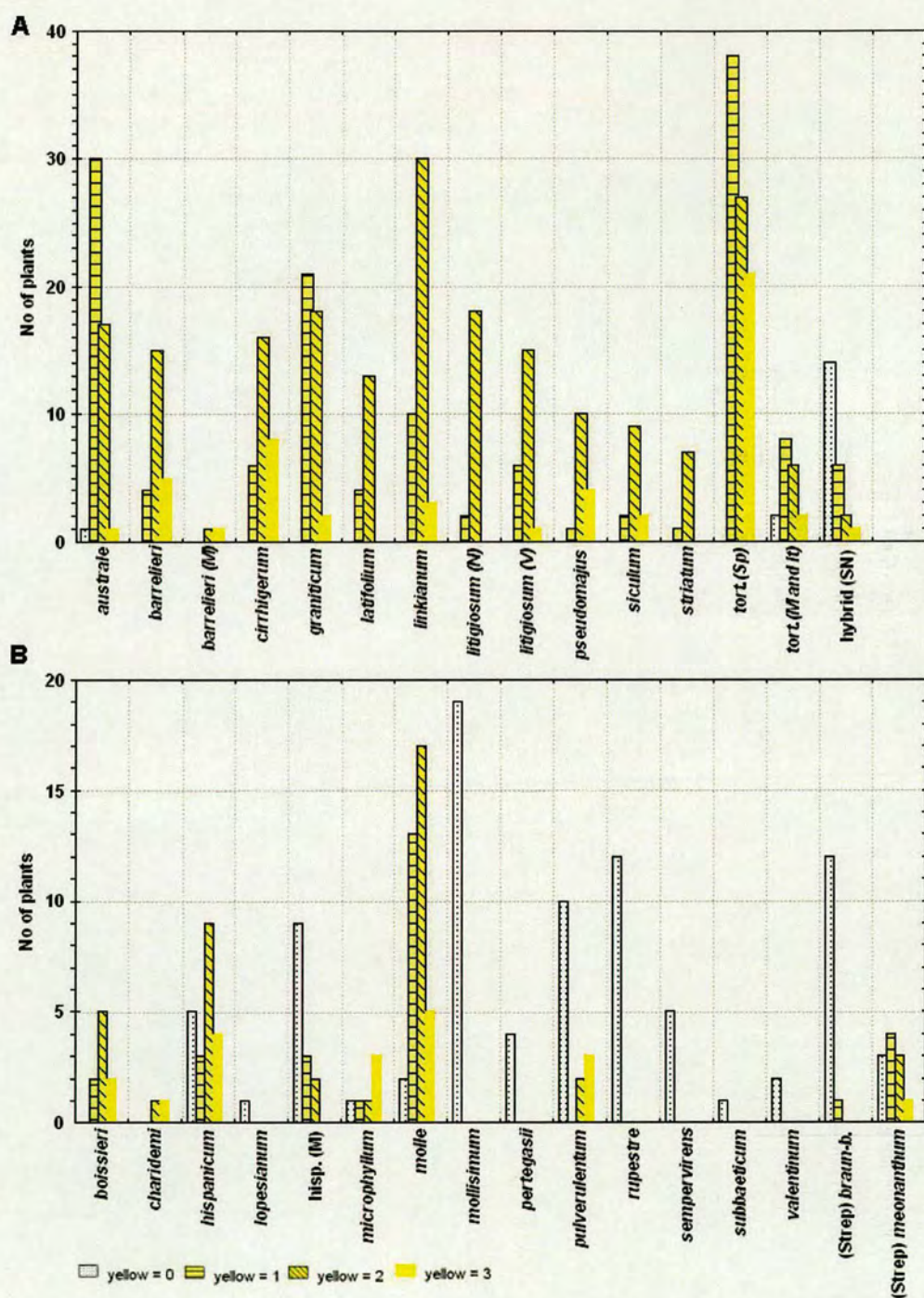


Figure 4.35. Graphs showing the number of individuals of each species of each score for the size of the yellow patch on the adaxial surface of the ventral tube base in subsection *Antirrhinum* species (A) and subsections *Kickxiella* and *Streptosepalum* (B).

between the two subsections. Although SePC1 reflects mainly sepal size, it does not distinguish the Kickxiella from Antirrhinum species, but does delimit most taxa. The remainder of the characters that are associated with the corolla and sepal shape, FsPC3 and SePC2-3, further distinguish species.

Of the flower colour characters, the overall colour differs between the subsections with Antirrhinum species having pink and Kickxiella white flowers. However, *A. graniticum*, *A. majus litigiosum* and both Kickxiella and Antirrhinum species distributed in southern Spain vary in colour. Purple pigmentation on the adaxial surface of the dorsal petal occurs mainly in the Kickxiella species; however, it is also present in *A. siculum*, *A. majus striatum*, *A. latifolium*, *A. meonanthum* and it varies within the species distributed in southern Spain. There is little discernable pattern in the distribution of yellow colouration on the ventral flower face, at the base of the ventral tube and of the hairs within the tube. However, all three patches are more extensive within the subsection Antirrhinum compared to the Kickxiella species.

4.5 Plant architecture

4.5.1 Flowering time

Flowering time has not been described as a trait that distinguishes *Antirrhinum* species and has not been quantified previously, despite being of considerable relevance to life history. For this study, flowering time was measured as the first metamer on the main stem at which a flower formed.

Subsection Kickxiella species all flowered relatively early, after 10-15 metamers. This is significantly earlier than subsection Antirrhinum species: *A. australe*, *A. barrelieri*, *A. majus cirrhigerum*, *A. graniticum*, *A. majus litigiosum*, *A. siculum* and *A. majus tortuosum*, which all flowered around metamers 25-30 (Figure 4.36). A few subsection Antirrhinum species also flowered early: *A. latifolium*, *A. majus pseudomajus* and *A. majus striatum* all flowered around metamer 10.

4.5.2 Plant height

Although plant height measurements are not given in the taxonomic accounts of the genus, it is frequently mentioned qualitatively in descriptions of species and morphological subsections. Plant height was therefore measured as the distance from the cotyledons to the first flower along the main stem axis.

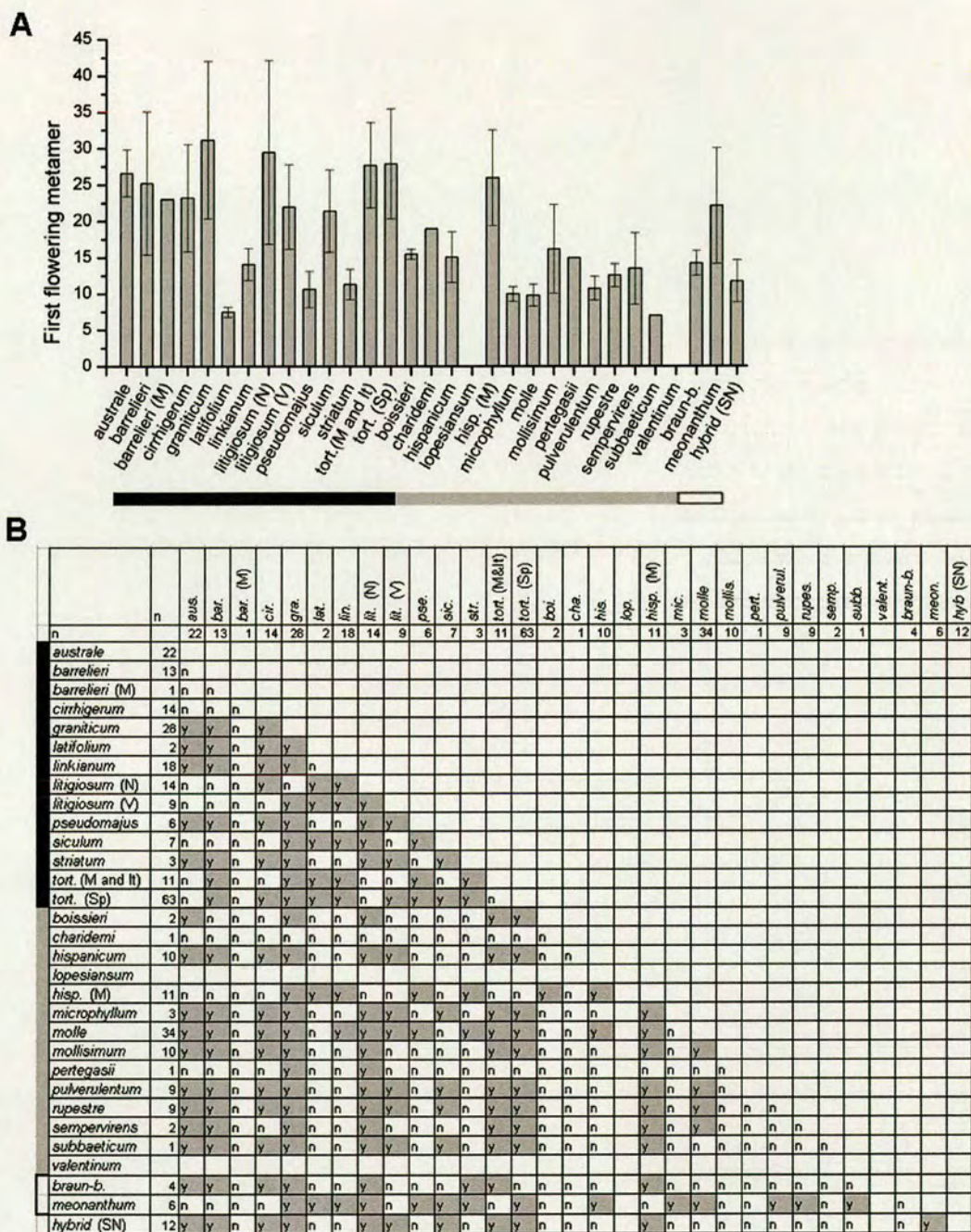


Figure 4.36. Mean values of the flowering time for each taxon (A) and results of tests for significant differences of flowering time between all pairs of taxa (B).

(A) Graph showing the average flowering time (± 1 standard deviation) of each taxon.

(B) Matrix showing results of pair-wise significance tests between all taxa, the number of individuals (n) is indicated in the second column. 'y'=significantly different at 0.05 level (Fisher's Least Significant Difference). One-way ANOVA: $F(27, 297)=16$, $P<0.001$, $R^2=55\%$

barrelieri (M) = Moroccan *A. barrelieri*, *litigiosum* (N) = northern *A. litigiosum*, *litigiosum* (V) = Valencia *A. litigiosum*, *tort.* (M and It) = Moroccan and Italian *A. majus tortuosum*, *tort.* (Sp) = Spanish *A. majus tortuosum*, *hisp.* (M) = Moroccan *A. hispanicum*.

■ Subsection Antirrhinum ■ Subsection Kickxiella □ Subsection Streptosepalum

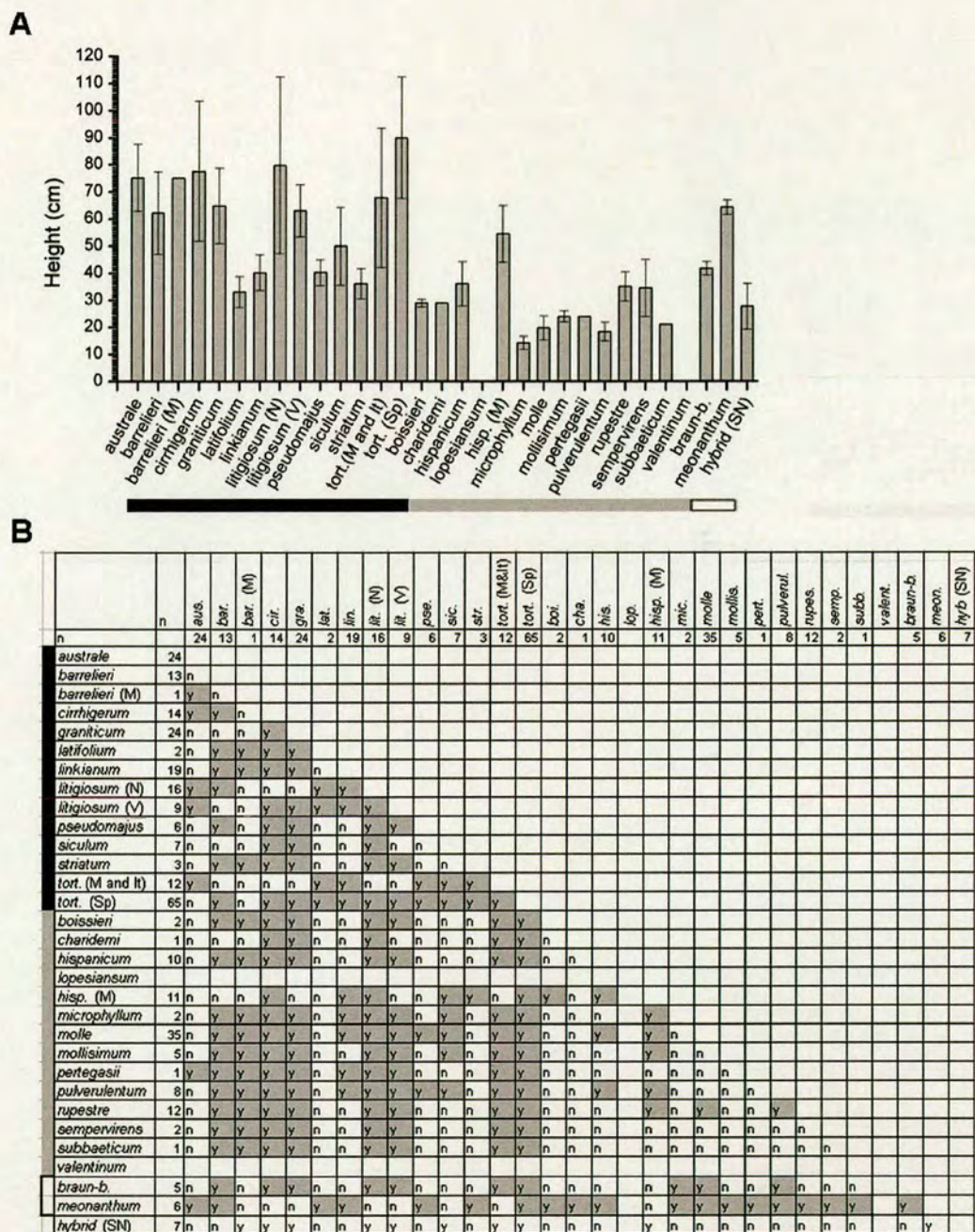


Figure 4.37. Mean values of the height for each taxon (A) and results of tests for significant differences in the mean height between all pairs of taxa (B).

(A) Graph showing the average height (± 1 standard deviation) of each taxon.

(B) Matrix showing results of pair-wise significance tests between all taxa, the number of individuals (n) is indicated in the second column. 'y'=significantly different at 0.05 level (Fisher's Least Significant Difference). One-way ANOVA: $F(27, 294)=26.6$, $P<0.001$, $R^2=68\%$

barrelieri (M) = Moroccan *A. barrelieri*, *litigiosum* (N) = northern *A. litigiosum*, *litigiosum* (V) = Valencia *A. litigiosum*, *tort.* (M and It) = Moroccan and Italian *A. majus tortuosum*, *tort.* (Sp) = Spanish *A. majus tortuosum*, *hisp.* (M) = Moroccan *A. hispanicum*.

■ Subsection Antirrhinum ■ Subsection Kickxiella □ Subsection Streptosepalum

Comparisons of height between taxa (Figure 4.37) are very similar to those of flowering time (Figure 4.36). Plant height varied from 12 cm for an *A. molle* accession to 148 cm for an *A. majus tortuosum* accession. The trends across species are similar to that described for flowering time, with between taxa variation accounting for a high proportion of the overall variation ($R^2 = 68\%$).

4.5.3 Inflorescence density

Although not quantitatively studied, the number of flowers in the inflorescence has also been used to distinguish species such as *A. meonanthum* and *A. braun-blanquetii* and the Kickxiella are cited as not having distinctive raceme inflorescences (Rothmaler 1956, Webb 1971). To estimate the inflorescence density, the number of visible flower buds (of size $>1\text{mm}$) and flowers on the main inflorescence were counted when the first five flowers had opened (to standardise the stage of development of inflorescences when the estimates were made). In the case of species that produced fewer than five flowers, the number of flowers was counted when all had opened.

There was high within taxa variation for this measure and no trends between the Kickxiella and Antirrhinum subsections were detected (Figure 4.38). Between taxon comparisons account for 49% of the overall variation; this is mostly due to the dense inflorescences of *A. meonanthum*, *A. siculum* and *A. barrelieri* compared to the rest of the taxa.

4.5.4 Width of the main stem at the base of the plant

Another character cited as distinguishing similar species is the width of the stem at the base of the plant. However, no consistent account of this character has been given in the taxonomic literature. To determine whether it is reliable for distinguishing species, the width of the main stem below the cotyledons was measured. To be consistent across all accessions this was carried out at the same stage of development.

The stem width distinguishes *A. barrelieri* and *A. majus cirrhigerum* from all other subsection Antirrhinum species as they have narrower stems (Figure 4.39). Within the Kickxiella, *A. microphyllum* and *A. pulverulentum* have significantly narrower stems. Overall, there is little clear trend in stem width when comparing the subsections.

4.5.5 Outgrowth of branches

Whilst collecting accessions from wild populations it was observed that there was extensive variation in the extent of branching among species, with some species appearing bushier. This

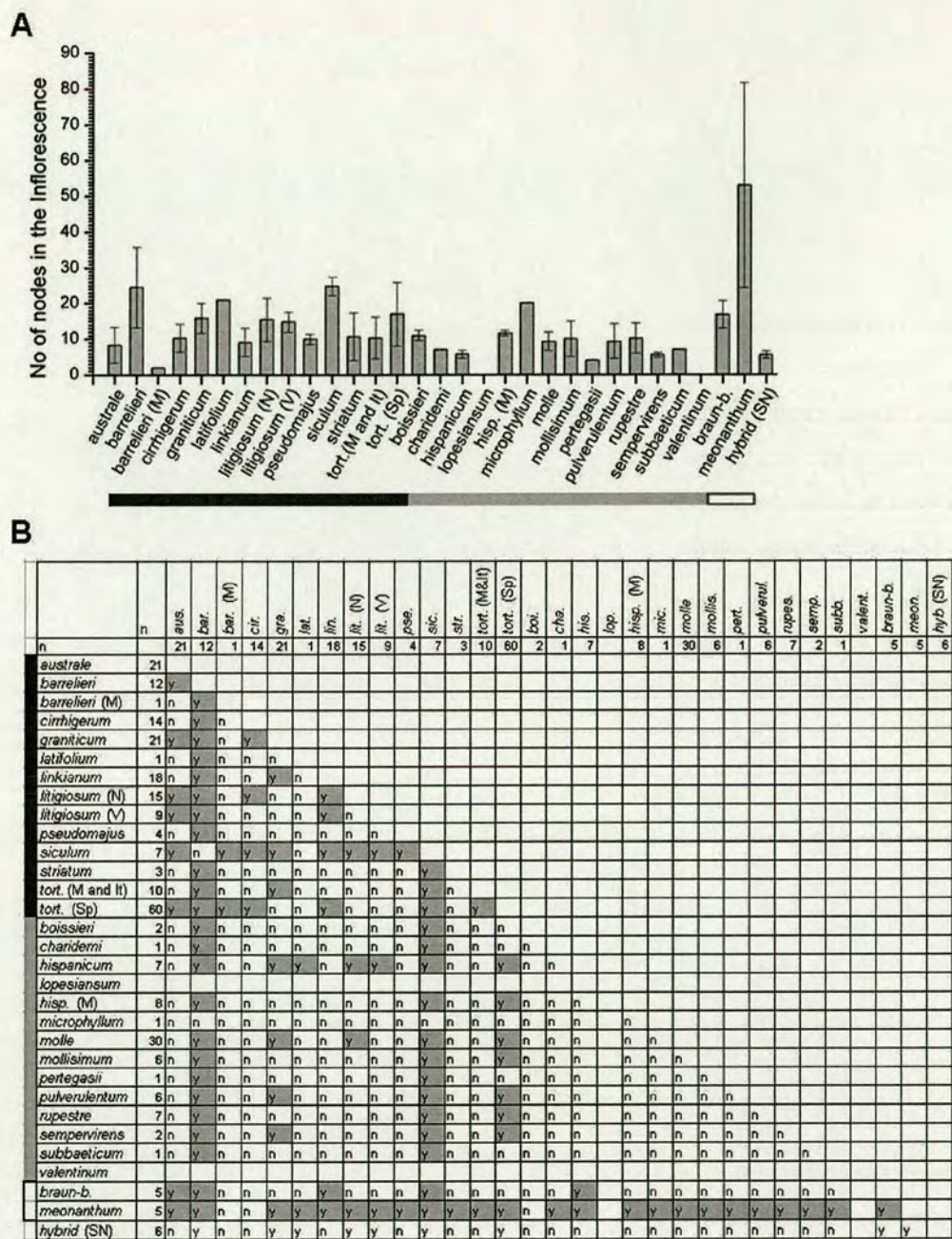


Figure 4.38. Mean values of the inflorescence density for each taxon (A) and results of tests for significant differences in the inflorescence density between all pairs of taxa (B).
 (A) Graph showing the average inflorescence density (± 1 standard deviation) of each taxon.
 (B) Matrix showing results of pair-wise significance tests between all taxa, the number of individuals (n) is indicated in the second column. 'y'=significantly different at 0.05 level (Fisher's Least Significant Difference). One-way ANOVA: $F(28, 255)=10.7$, $P<0.001$, $R^2=49\%$
barrelieri (M) = Moroccan *A. barrelieri*, *litigiosum* (N) = northern *A. litigiosum*, *litigiosum* (V) = Valencia *A. litigiosum*, *tort.* (M and It) = Moroccan and Italian *A. majus tortuosum*, *tort.* (Sp) = Spanish *A. majus tortuosum*, *hisp.* (M) = Moroccan *A. hispanicum*.
 ■ Subsection Antirrhinum ■ Subsection Kickxiella □ Subsection Streptosepalum

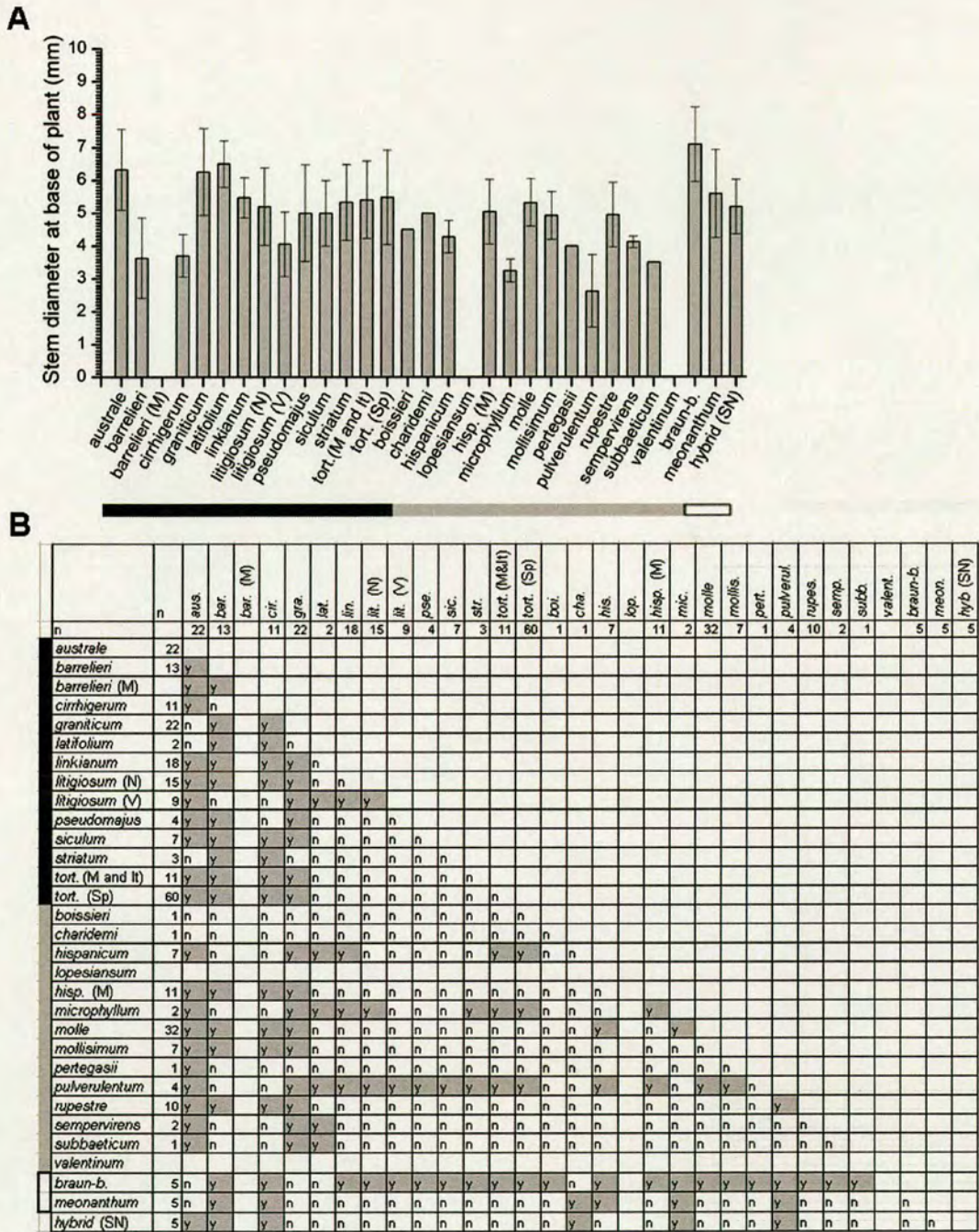


Figure 4.39. Mean values of the stem diameter for each taxon (A) and results of tests for significant differences in stem diameter between all pairs of taxa (B).

(A) Graph showing the average stem diameter (± 1 standard deviation) of each taxon.

(B) Matrix showing results of pair-wise significance tests between all taxa, the number of individuals (n) is indicated in the second column. 'y'=significantly different at 0.05 level (Fisher's Least Significant Difference). One-way ANOVA: $F(27, 263)=5.8$, $P<0.001$, $R^2=31\%$

barrelieri (M) = Moroccan *A. barrelieri*, *litigiosum* (N) = northern *A. litigiosum*, *litigiosum* (V) = Valencia *A. litigiosum*, *tort.* (M and It) = Moroccan and Italian *A. majus tortuosum*, *tort.* (Sp) = Spanish *A. majus tortuosum*, *hisp.* (M) = Moroccan *A. hispanicum*.

■ Subsection Antirrhinum ■ Subsection Kickxiella □ Subsection Streptosepalum

character is difficult to compare across accessions, mainly due to the vastly different flowering times observed among species. Therefore, a rough measure, called here the branching index, was used to compare the branch outgrowth and therefore bushiness of plants. To take into account differing flowering time, the number of nodes to the first flower along the main stem was divided by the number of nodes along one of the middle branches of the stem, at approximately the same stage of development for all plants. Therefore, plants with a high branching index have short branches compared to the main stem. This measure was observed to approximate the bushiness of accessions (Figure 4.40).

There was high within taxon variation for this measure ($R^2 = 35\%$) and no discernable difference between the bushiness of the *Kickxiella* compared to the *Antirrhinum* species (Figure 4.41). For many accessions only a few individuals were measured, which may inflate estimates of intra-specific variation (Figure 4.41B). *A. australe*, *A. majus cirrhigerum*, *A. graniticum*, *A. majus tortuosum* and the *Streptosepalum* species all have higher branching index values and are therefore less bushy than the rest of the taxa.

4.5.6 Summary of characters describing plant architecture

Of the five characters that describe plant architecture, the correlated measures of flowering time and height show the most variation between taxa, with the subsection *Kickxiella* species flowering earlier than most of the *Antirrhinum* species. Although the stem width and branching index vary extensively within taxa, they still distinguish some species. The inflorescence density shows high within taxon variation, does not show any patterns within the genus and only distinguishes *A. barrelieri*, *A. meonanthum* and *A. siculum*.

4.6 Trichome morphology and density

To describe the distribution and density of trichomes, epidermal imprints were taken from different parts of the plant and examined under a light microscope. Two imprints were taken of the stem, at the plant base and within the inflorescence, and an imprint was taken of the adaxial surface of the metamer 4 leaf. The trichome characteristics were studied and a scoring system developed to enable trichome information to be included into subsequent multivariate analyses. Trichomes were described as either glandular or eglandular and for each of these, three length categories were defined: short ($<20\mu\text{m}$), medium ($20 - 50\mu\text{m}$), or long ($>50\mu\text{m}$). These length categories capture the main types of trichomes that were observed. Consistent with previous studies (Doaigey and Harkiss 1991, Adeyanju 2003) both glandular and eglandular trichomes of varying length are

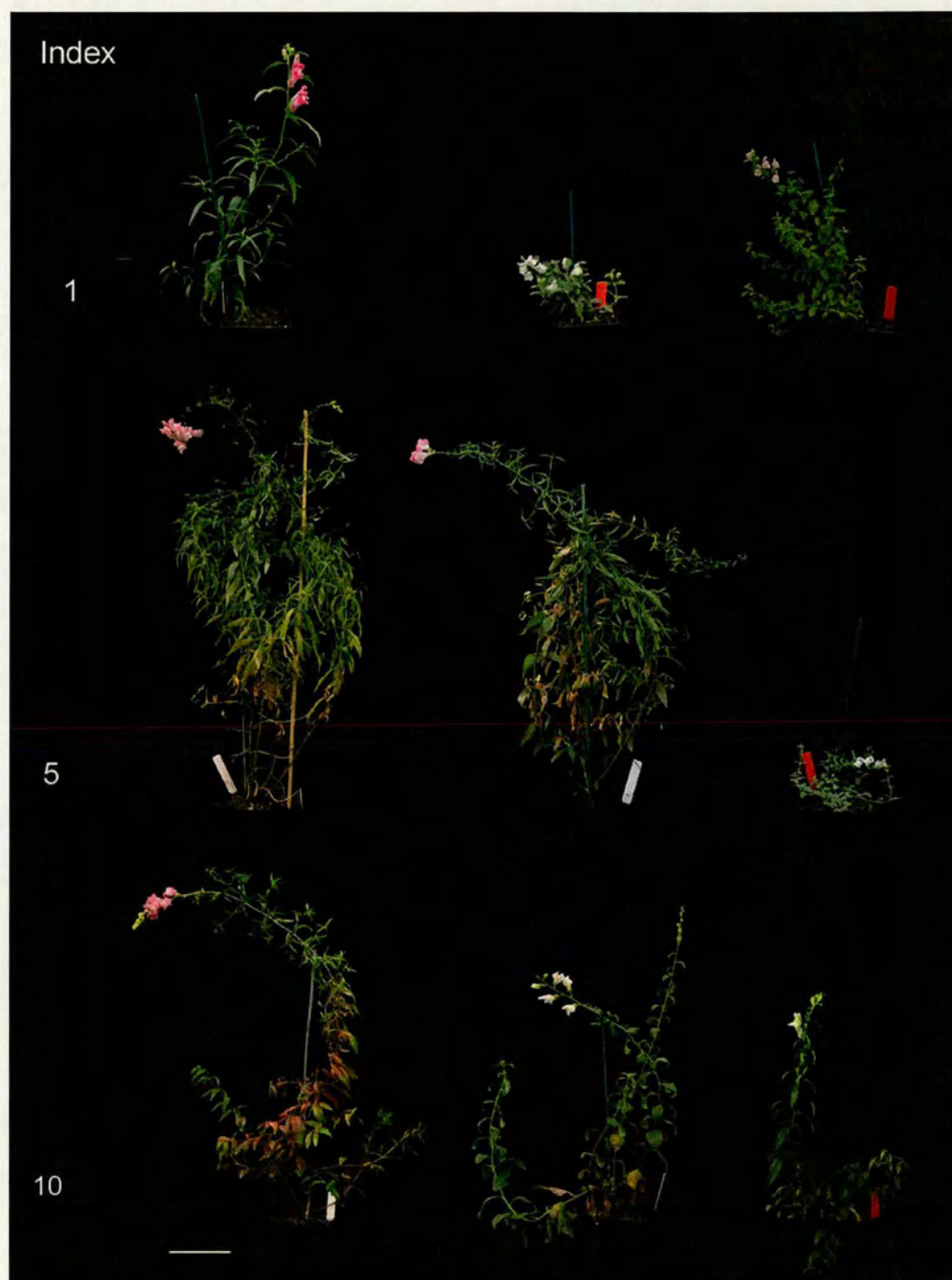


Figure 4.40. Examples of the architecture of plants with differing branch index estimates. Three plants each of low, medium and high branching index (branch index = 0, 5 and 10, respectively) are shown. The scale bar is 10 cm. The species shown (from left to right across each row) are *A. majus pseudomajus*, *A. molle*, *A. mollisimum*, *A. majus tortuosum*, *A. australe*, *A. pulverulentum*, *A. majus tortuosum*, *A. graniticum*, and *A. braun-blanquetii*.

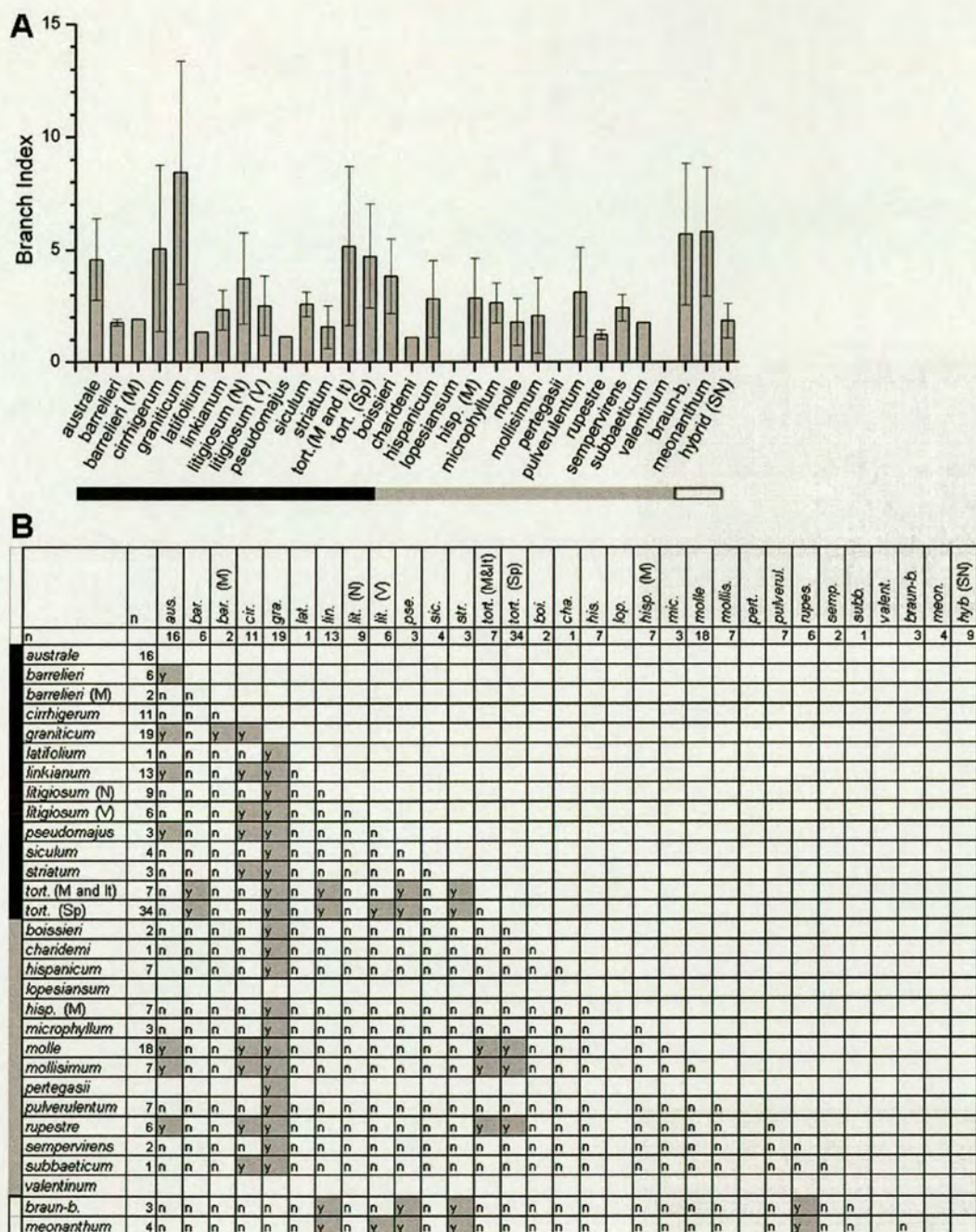


Figure 4.41. Mean values of the branching index for each taxon (A) and results of tests for significant differences in the branching index between all pairs of taxa (B).

(A) Graph showing the average branching index (± 1 standard deviation) of each taxon.

(B) Matrix showing results of pair-wise significance tests between all taxa, the number of individuals (n) is indicated in the second column. 'y'=significantly different at 0.05 level (Fisher's Least Significant Difference). One-way ANOVA: $F(27, 183)=5.18$, $P<0.001$, $R^2=35\%$

barrelieri (M) = Moroccan *A. barrelieri*, *litigiosum* (N) = northern *A. litigiosum*, *litigiosum* (V) = Valencia *A.*

litigiosum, *tort.* (M and It) = Moroccan and Italian *A. majus tortuosum*, *tort.* (Sp) = Spanish *A. majus*

tortuosum, *hisp.* (M) = Moroccan *A. hispanicum*.

■ Subsection Antirrhinum ■ Subsection Kickxiella □ Subsection Streptosepalum

observed within the same structure for many species. Trichomes were therefore scored as the presence/absence of long glandular, medium glandular and short glandular trichomes, and likewise for eglandular trichomes.

The types of trichomes observed on the leaves, at the base of the stem, and on the inflorescence stem are consistent with previous accounts (Sutton 1988, Doaigey and Harkiss 1991, Adeyanju 2003) and are therefore summarised for each species in Tables 4.2-4.4. *A. hispanicum*, *A. majus tortuosum* and *A. barrelieri* accessions from Morocco, which have not previously been characterised, each differ from con-specific accessions from Spain. This is due to distinctive short glandular trichomes being present on all three regions of the plant in *A. hispanicum* (M) and on the stems of *A. barrelieri* (M) and *A. majus tortuosum* (M and It).

Trichome density was estimated by counting the number of trichomes in a 50 x 50 µm area of each imprint. The subsection *Antirrhinum* species that have trichomes on their leaves, and *A. meonanthum*, have a much lower density of trichomes than the *Kickxiella* species (Figure 4.42A). The trichome density is similar for most of the *Kickxiella* species apart from *A. hispanicum*, which has few trichomes, and *A. microphyllum*, which has a dense indumentum compared to the other *Kickxiella* species.

All taxa apart from *A. barrelieri* and *A. braun-blanquetii* have trichomes on the base of the stem. However, the trichome density is again much lower in subsection *Antirrhinum* species compared to the *Kickxiella* (Figure 4.42B). A similar pattern is observed for the trichome density on the inflorescence stem, except all taxa have trichomes in this part of the plant (Figure 4.42C).

4.7 Discussion

4.7.1 A quantitative description of *Antirrhinum* morphology

In this chapter explicit variables are defined that describe morphological variation both within and between *Antirrhinum* species. The characters that are defined are summarised in Table 4.5. Each accession that was examined was also photographed in detail and the images were incorporated into a database that integrates further information on geographic location and available tissue and seed resources for every population. The mean and variation of each continuous character was estimated for each species and tables summarise comparisons between the means of all species. However, the sample size for some taxa is small and due to the large number of comparisons there is an increased likelihood of Type I error (the erroneous rejection of the null hypothesis that there is no significant

Species (n)	glandular				eglandular		
	absent	long	medium	short	long	medium	short
<i>A. australe</i> (33)	x		x		x	x	
<i>A. barrelieri</i> (5)	x						
<i>A. barrelieri</i> M (1)	x						
<i>A. boissieri</i> (9)		x	x				
<i>A. braun-bl.</i> (4)	x						
<i>A. charidemi</i> (0)							
<i>A. graniticum</i> (24)			x				
<i>A. hispanicum</i> (10)		x	x				
<i>A. hispanicum</i> M (12)				x			
<i>A. latifolium</i> (3)							
<i>A. lopesianum</i> (0)							
<i>A. m. cirrhigerum</i> (14)	x						
<i>A. m. linkianum</i> (25)	x						
<i>A. m. litigiosum</i> (16)	x						
<i>A. m. pseudomajus</i> (3)	x						
<i>A. m. striatum</i> (4)	x						
<i>A. m. tortuosum</i> (40)	x						
<i>A. m. tortuosum</i> M (12)	x						
<i>A. meonanthum</i> (5)			x				
<i>A. microphyllum</i> (4)							x
<i>A. molle</i> (20)			x		x		
<i>A. mollisimum</i> (11)		x	x		x	x	
<i>A. pertegasii</i> (1)							x
<i>A. pulverulentum</i> (6)					x	x	
<i>A. rupestre</i> (7)		x	x		x		
<i>A. sempervirens</i> (1)							x
<i>A. siculum</i> (9)	x						
<i>A. subbaeticum</i> (1)						x	
<i>A. valentinum</i> (0)							

Table 4.2. Table summarising the types of trichomes observed on the leaves of each species.
 Trichomes on the adaxial leaf surface of metamer 4 of each plant were characterised. ‘n’ = the number of plants examined. ‘M’ denotes populations from Morocco.

Species (n)		glandular			eglandular			
		absent	long	medium	short	long	medium	short
<i>A. australe</i> (28)	x			x		x		
<i>A. barrelieri</i> (4)	x							
<i>A. barrelieri</i> M				x		x		
<i>A. boissieri</i> (4)			x	x		x		
<i>A. braun-bl.</i> (1)	x							
<i>A. charidemi</i> (0)								
<i>A. graniticum</i> (17)			x	x		x		
<i>A. hispanicum</i> (3)			x	x		x		
<i>A. hisp.</i> M (7)					x	x		
<i>A. latifolium</i> (1)						x		
<i>A. lopesianum</i> (0)								
<i>A. m. cirrh.</i> (5)				x		x		
<i>A. m. linkianum</i> (16)				x		x		
<i>A. m. litigiosum</i> (7)				x		x		
<i>A. m. pseudo.</i> (2)				x				
<i>A. m. striatum</i> (2)				x		x		
<i>A. m. tortuosum</i> (35)	x					x		
<i>A. m. tort.</i> M (8)				x		x		
<i>A. meonanthum</i> (5)						x		
<i>A. microphyllum</i> (3)							x	
<i>A. molle</i> (17)			?	x		x	x	
<i>A. mollisimum</i> (6)			?	x		?		
<i>A. pertegasii</i> (1)							x	x
<i>A. pulverulentum</i> (2)							x	
<i>A. rupestre</i> (4)				x				
<i>A. sempervirens</i> (2)								x
<i>A. siculum</i> (5)	x					x		
<i>A. subbaeticum</i> (1)							x	
<i>A. valentinum</i>								

Table 4.3. Table summarising the types of trichomes observed on the stem of each species.
Trichomes on the stem between metamers 1 and 2 of each plant were characterised. ‘n’ = the number of plants examined. ‘M’ denotes populations from Morocco.

Species (n)	glandular				eglandular		
	absent	long	medium	short	long	medium	short
<i>A. australe</i> (16)			x				
<i>A. barrelieri</i> (5)			x				
<i>A. barrelieri</i> M (2)	x						
<i>A. boissieri</i> (2)			x				
<i>A. braun-bl.</i> (2)			x				
<i>A. charidemi</i> (0)							
<i>A. graniticum</i> (16)			x	x			
<i>A. hispanicum</i> (4)			x	x			
<i>A. hisp.</i> M (9)				x			
<i>A. latifolium</i> (18)			x				
<i>A. lopesianum</i> (0)							
<i>A. m. cirrh.</i> (11)			x				
<i>A. m. linkianum</i> (11)			x				
<i>A. m. litigiosum</i> (16)			x				
<i>A. m. pseudo.</i> (2)			x				
<i>A. m. striatum</i> (2)			x				
<i>A. m. tortuosum</i> (32)	x		x				
<i>A. m. tort.</i> M (7)	x		x	x			
<i>A. meonanthum</i> (6)			x				
<i>A. microphyllum</i> (2)							x
<i>A. molle</i> (17)			x		x		
<i>A. mollisimum</i> (8)			x	x			
<i>A. pertegasii</i> (1)							x
<i>A. pulverulentum</i> (1)				x		x	
<i>A. rupestre</i> (6)		x	x	x			
<i>A. sempervirens</i> (2)							
<i>A. siculum</i> (5)				x			
<i>A. subbaeticum</i> (1)							x
<i>A. valentinum</i> I (0)							

Table 4.4. Table summarising the types of trichomes observed on the inflorescence stem of each species.

Trichomes on the stem within the inflorescence of each plant were characterised. ‘n’ = the number of plants examined. ‘M’ denotes populations from Morocco.

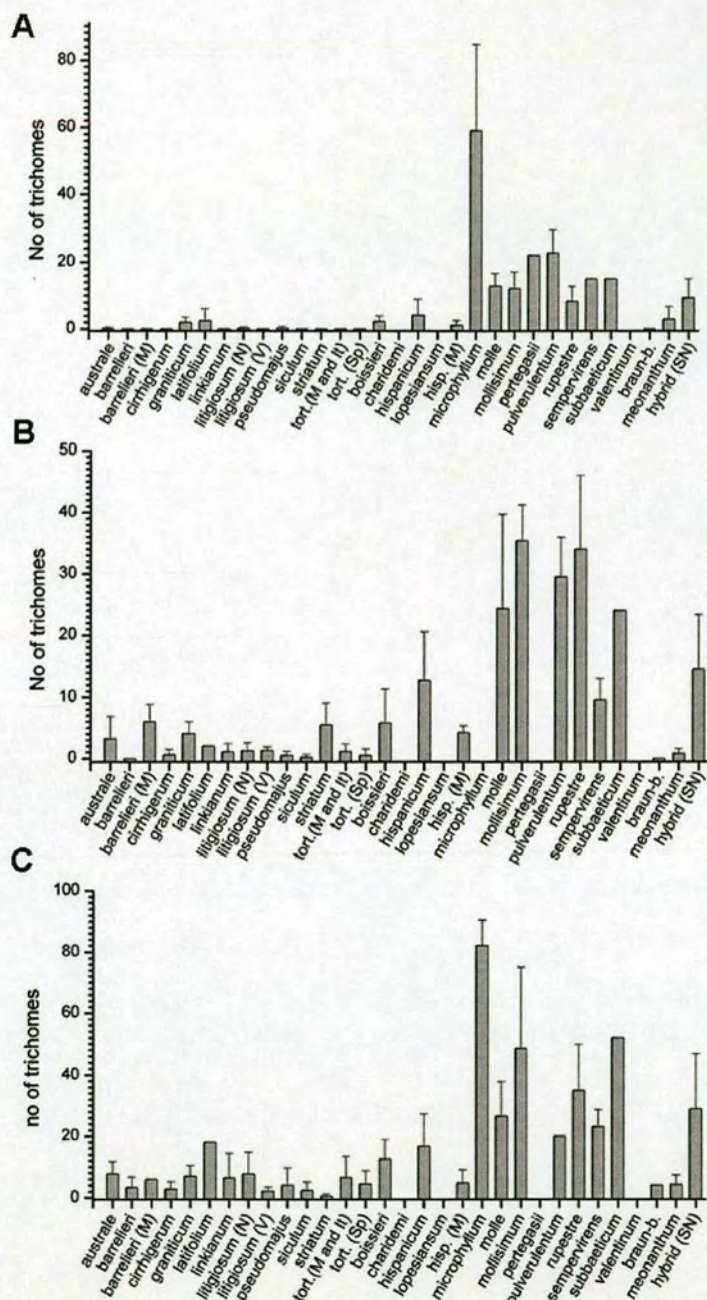


Figure 4.42. Graphs showing the number of trichomes in a 50 x 50 µm area on the adaxial surface of the m4 leaf (A), the stem at the base of the plant (B) and the stem of the inflorescence (C).

Taxa that are glabrous are still plotted as having 0 trichomes; this is to distinguish them from taxa that were not examined.

barrelieri (M) = Moroccan *A. barrelieri*, *litigiosum* (N) = northern *A. litigiosum*, *litigiosum* (V) = Valencia *A. litigiosum*, *tort.* (M and It) = Moroccan and Italian *A. majus tortuosum*, *tort.* (Sp) = Spanish *A. majus tortuosum*, *hisp.* (M) = Moroccan *A. hispanicum*.

■ Subsection Antirrhinum ■ Subsection Kickxiella □ Subsection Streptosepalum

A Continuous characters

Character	DF	F	P	R ²
Leaf shape and size				
1 LePC1	24, 240	18.33	0.000	61%
2 LePC2	24, 240	18.46	0.000	61%
3 LePC3	24, 240	9.53	0.000	44%
4 Leaf Cell No	27, 254	4.02	0.000	22%
Flower shape and size				
5 FpPC1	28, 522	88.74	0.000	82%
6 FpPC2	28, 526	8.88	0.000	28%
7 FpPC3	28, 526	7.582	0.000	36%
8 FpPC4	28, 529	5.51	0.000	18.5%
9 FsPC1	28, 512	32	0.000	62%
10 FsPC3	28, 525	15.33	0.000	42%
11 SePC1	30, 518	44	0.000	70%
12 SePC2	30, 532	29	0.000	60%
13 SePC3	30, 533	7.6	0.000	26%
14 Flower Cell No	27, 158	3.95	0.000	30%
15 Style length	28, 527	99.39	0.000	83.2%
16 Dorsal stamen length	28, 546	79	0.000	79%
17 Ventral stamen length	30, 541	86	0.000	82%
18 Pedicel Length	30, 529	15.44	0.000	44%
Plant architecture				
19 Flowering Time	27, 297	16	0.000	55%
20 Height	27, 294	26.6	0.000	68%
21 Inflorescence density	28, 255	10.7	0.000	49%
22 Stem diameter	27, 263	5.78	0.000	31%
23 Branching Index	27, 183	5.18	0.000	35%
Trichome density				
24 Leaf trichome density (lhd)				
25 Base of stem trichome density (shd)				
26 Inflorescence stem trichome density (flhd)				

B Discrete characters

Flower colour

Corolla colour:

27 Pink	scores 0-4
28 White	present/absent
29 Yellow	present/absent

Purple patch in centre of dorsal flower face ('purple patch'):

30 Vasculature	present/absent
31 General	present/absent

Purple region on adaxial dorsal lobes proximal to the hinge ('purple zone'):

32 Vasculature	present/absent
33 General	present/absent

- 34 Yellow patch on ventral face of flower ('face yellow patch')
Scores 0-3
- 35 Yellow colouration of hairs on the adaxial surface of ventral petal ('yellow tube hairs')
Scores 0-4
- 36 Yellow patch at the base of the tube ('tube yellow patch')
Scores 0-3

Trichome morphology

37 Leaf Short glandular (LSG)	present/absent
38 Leaf Medium glandular (LMG)	present/absent
39 Leaf Long glandular (LLG)	present/absent
40 Leaf Short eglandular (LSEG)	present/absent
41 Leaf Medium eglandular (LMEG)	present/absent
42 Leaf Long eglandular (LLEG)	present/absent
43 base of stem short glandular (SSG)	present/absent
44 base of stem medium glandular (SMG)	present/absent
45 base of stem long glandular (SLG)	present/absent
46 base of stem short eglandular (SSEG)	present/absent
47 base of stem medium eglandular (SMEG)	present/absent
48 base of stem long eglandular (SLEG)	present/absent
49 inflorescence stem short glandular (flSG)	present/absent
50 inflorescence stem medium glandular (flMG)	present/absent
51 inflorescence stem long glandular (flLG)	present/absent
52 inflorescence stem short eglandular (flSEG)	present/absent
53 inflorescence stem medium eglandular (flMEG)	present/absent
54 inflorescence stem long eglandular (flLEG)	present/absent

Table 4.5. Table listing all (A) continuous and (B) discrete morphological characters that were described.

- (A) Continuous characters and the results of the one-way ANOVA comparing the means of all taxa are summarised. DF = degrees of freedom, F = F value, P= significance level and R²= the proportion of the overall variation described by between-taxon comparisons.
- (B) Summary of discrete characters and their scoring system.

difference between means). Therefore, for these taxa, these comparisons are only an indication that a character may have significantly different values.

Leaf and flower shapes were also quantified using PCA, which identified subtle shape variation that is difficult to describe using qualitative or univariate measures. However, there are several drawbacks to using PCA as the axis values that are derived from PCA that describe each accession are difficult to relate to observed shapes on the plant. This is because the axes of the PCA are orthogonal to each other and each axis describes residual variation from the previous axes. Therefore, all of the main axes that describe the variation are necessary to reconstruct the size and shape of the organ under investigation. A further disadvantage is that the axis values of a particular leaf or flower are dependent on the samples included in the PCA analysis. This is therefore not an ideal format of description for taxonomic purposes. However, the images of the leaves and flowers are available as reference and future work should be to associate the values of the PCA axes with metrics that are not relative and that are easier to measure.

4.7.2 Morphological delimitation of *Antirrhinum* species

Morphologically similar *Antirrhinum* subsection species were also compared to determine the extent to which they differ when representative accessions are grown in similar conditions. Despite being genetically indistinguishable from *A. m. tortuosum*, *A. australe* has trichomes throughout its stem whereas *A. m. tortuosum* is glabrous. *A. australe* also has larger flowers with more upright petals, larger leaves and a slightly broader stem than *A. majus tortuosum*.

A. majus cirrhigerum and *A. majus linkianum*, which are both distributed in Portugal, are shown to be closely related and are only partially delimited by genetic analyses. However, this analysis showed that *A. majus cirrhigerum* has a narrower stem, smaller leaves with more rounded tips, larger flowers and sepals and is later flowering than *A. majus linkianum*.

A. barrelieri and *A. majus litigiosum* are distinguished by molecular markers, but have similar morphologies (Webb 1971), although the latter is distinguished by the presence of glandular trichomes at the base of the stem (Sutton 1988). This study indicates that *A. barrelieri* has smaller rounder leaves and smaller flowers with more upright petals than *A. majus litigiosum*. However, it is similar to *A. majus litigiosum* accessions from Valencia for some characters such as sepal size, height and stem thickness. These two species differ from *A. majus tortuosum* and *A. australe* by many characters. Most notably, they have smaller flowers with more upright dorsal petal lobes.

Most *Kickxiella* species are well defined in previous accounts (Sutton 1988, Jiminez 2005), apart from the southern Spanish *Kickxiella* - *A. hispanicum*, *A. rupestre* and *A. mollisimum*. Too few seed for these species were available to make rigorous comparisons between them in this chapter. However, their morphologies were examined in numerous populations in the field and characters were identified that delimit them (results not shown).

4.7.3 Identifying patterns of variation within the genus

In general, *Kickxiella* species have smaller leaves with more rounded tips and a denser indumentum than subsection *Antirrhinum* species. They also have smaller flowers with more upright dorsal petal lobes and are earlier flowering. However, there are exceptions to most of these generalisations, but it is difficult to integrate the information from all of the characters to identify overall which species are more similar to each other. Furthermore, it is difficult to identify correlations between morphological traits by the comparison of the univariate measures in this chapter. These issues are addressed by multivariate analyses described in the following chapter.

Chapter 5: The phenotypic space of *Antirrhinum* species

5.1 Introduction

Significant differences between *Antirrhinum* species were identified through comparing the mean values of individual characters in the previous chapter. Based on this result all species for which there was adequate sampling are delimited. However, consideration of individual characters in delimiting species may be misleading as extensive intra-specific variation was found for many characters and individual plants were observed to have both traits associated with their species identification and traits more similar to other species (Webb 1971, personal observ.). This is reflected in the unclear taxonomy of the genus as it is difficult to objectively weight characters to circumscribe species (Jimenez 2005). Therefore, in this chapter, multivariate techniques are used to determine the positions of individuals in phenotypic space and determine whether individuals and populations of each species have a more similar overall morphology to each other compared to individuals of other species. This approach is considered appropriate for *Antirrhinum* as it uses numerous characters without making *a priori* assumptions about character weighting (Sneath and Sokal 1973, Jensen 2009) and may indicate whether taxonomists have over-differentiated taxa within the genus (Rieseberg 2006).

The molecular analyses of Chapter 3 identify two main lineages within *Antirrhinum*. There is also substantial evidence that introgressive hybridisation has occurred between species of these lineages that occur within the same geographic region. Assignment of individuals to populations using *Structure* showed that there are strong genetic relationships between species within each geographic region. However, it was difficult to determine whether populations within each geographic region have morphological attributes of either the *Antirrhinum* or *Kickxiella* lineage or whether there are spatial patterns of morphological variation by comparing univariate measures of morphological characteristics (Chapter 4).

The aims of this chapter are to define phenotypic space of *Antirrhinum* and plot the positions of populations of each species within this space. This is to (1) test species delimitation based on morphological characters, (2) determine the morphological characteristics of the main *Antirrhinum* lineages and (3) investigate the morphologies of species that have undergone hybridisation.

5.2 Definition of phenotypic space

The phenotypic space of a group of organisms can either be defined mathematically using a model of development and varying the parameters to determine all the possible forms that can be generated (Raup and Michelson 1965, Prusinkiewicz *et al* 2007), or by mapping all possible combinations of measured variables (Pigliucci 2007). The positions of organisms can then be plotted within this space, according to their values for the parameters/variables which are used to define it. The approach used here is to define the phenotypic space of the *Antirrhinum* genus using the morphological characters described in the previous chapter. The position of each individual or population in this phenotypic space is determined and species are considered to be delimited from each other if they do not overlap in this space.

In addition to clarifying the taxonomy of the genus, the identification of regions of the space which are occupied compared to those that are empty enables correlations between characters and morphological constraints to be identified (Pigliucci 2007, Raup and Michelson 1965).

5.3 Numerical approaches

The variables defined in the previous chapter (summarised in Table 4.5) are used to define the phenotypic space of the *Antirrhinum* species. However, if all possible combinations of all characters were to be mapped there would be too many dimensions to interpret. Therefore Principal Components Analysis (PCA) was used to summarise the main dimensions of variation in the data. There are numerous multivariate techniques that are suitable for summarising the relationships between taxa using numerous variables (Rohlf 1971, Sneath and Sokal 1973, Parnell and Waldren 1996). In addition to enabling the definition of phenotype space, further advantages of PCA over other techniques are that individuals are not assigned to *a priori* defined groups and correlations between characters are identified (Blackith and Reyment 1971).

The main disadvantage of PCA is that it is suitable for continuous variables only. However, if coded carefully, categorical data can also be incorporated into PCA (Sneath and Sokal 1973, Hill and Smith 1976, Parnell 1996). This was carried out in Chapter 4, where qualitative multistate characters such as corolla colour were converted into new characters pink/not pink, yellow/not yellow, or white/not white as described in Sneath and Sokal (1973, p149). This may distort distances in the resulting ordination (Hill and Smith 1976), so this effect is explored in the following analyses. For highly correlated characters, such as the flower style length, dorsal filament length and ventral filament length, only one measure was included to avoid further

distortion, although preliminary analyses with all characters present were similar to analyses with correlated characters removed.

5.4 Clustering individuals using flower characters

To determine whether individual plants of each taxon cluster together in phenotypic space, PCA was carried out on a data-set consisting of all plants detailed in Table 4.1. For some taxa it was only possible to collect data from plants that were grown from cuttings collected in the field, or had frequently been cut back. Characteristics such as leaf size and shape, trichome distribution and density, flowering time, and branching, which were likely to have been influenced by varying conditions of growth therefore could not be included. To avoid including samples with a high proportion of missing characters only flower characters were incorporated as *A. majus* flower morphology has been found to remain consistent in different environments (Bayo-Canha *et al* 2007).

5.4.1 PCA of all flower characters

In the first instance all characters which describe flower shape, size and colour, both continuous and discrete, were incorporated into PCA (Table 5.1). Overall, the first few axes of the PCA did not account for a large proportion of the overall variation (Table 5.2). The character loadings contributing to the first six axes were studied, but only the first four axes could be interpreted. The first axis mainly reflects variation in flower size and the angle of the dorsal petal lobe to the tube (character FsPC1), with negative values along this axis representing large flowers with dorsal petal lobes in line with the tube and positive values representing small flowers with dorsal petal lobes perpendicular to the tube (Table 5.1, Figure 5.1A). Measures which are directly associated with size, such as FpPC1 and style length have strong correlations with axis 1 (Table 5.1). Sepal size and relative width, SePC1 and SePC2, are also correlated with axis 1, but show weaker correlations than the other size measures. The overall correlations of the flower colour characters with axis 1 indicate that large flowers are generally pink or yellow with a yellow face patch, yellow tube hairs and a yellow tube patch whilst small flowers are generally white with a purple face patch. However, the correlations of the flower colour characters with axis 1 are much weaker than those of size (Table 5.1).

Axis 2 is mainly correlated with yellow versus pink flower colour, with yellow flowers having positive axis 2 values and pink flowers negative values ($r = 0.8$ and $r = -0.6$, respectively). The characters FsPC3, which describes the relative tube length and the size of the gibba at the ventral

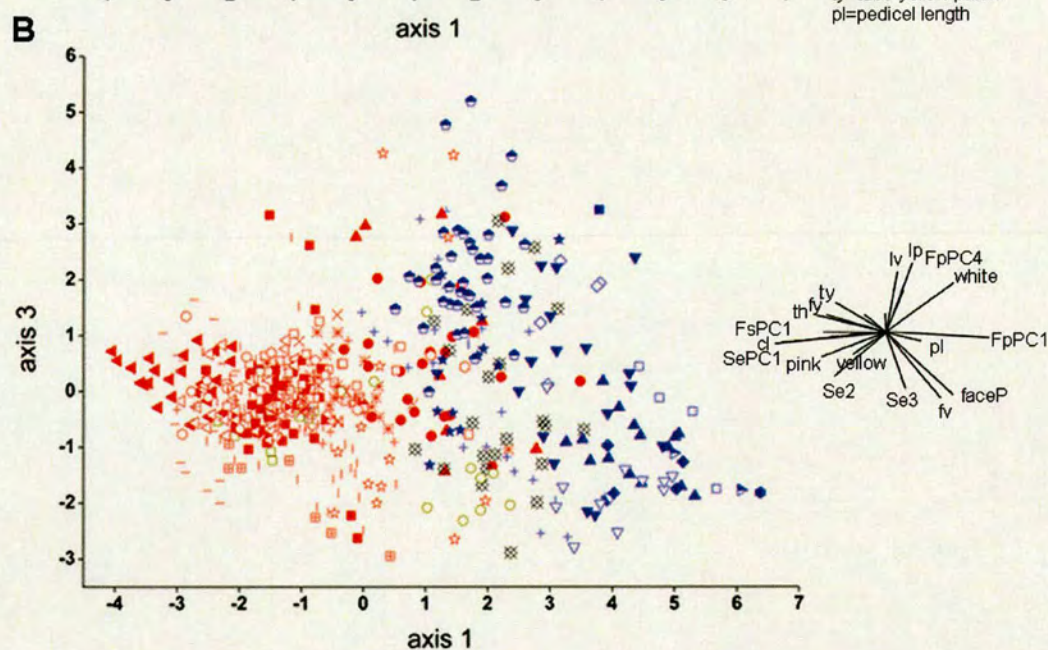
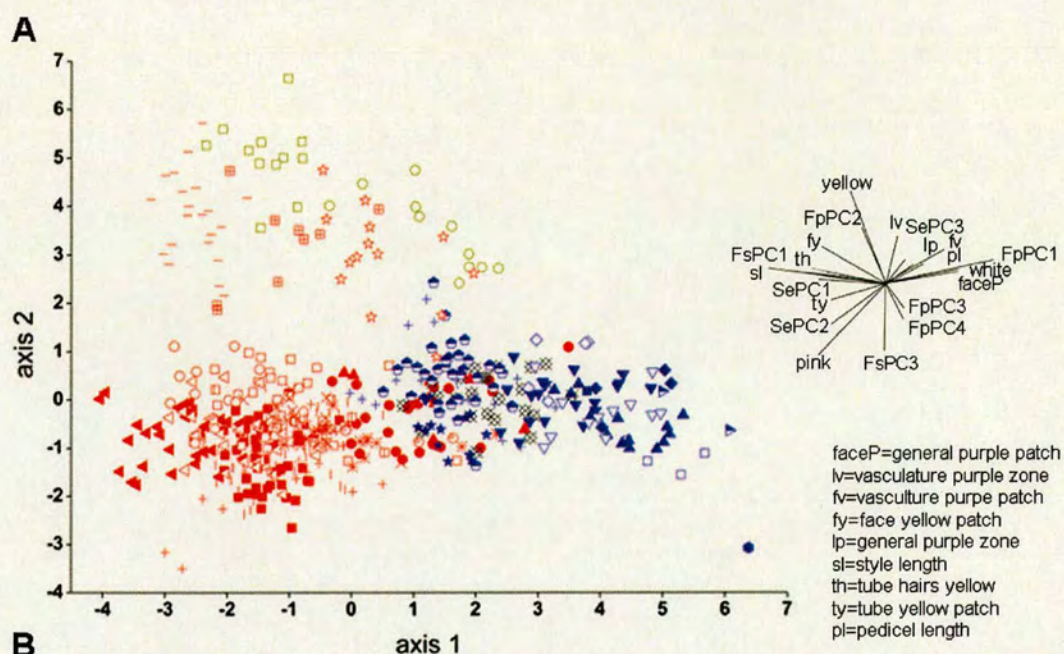
Character	Axis 1	Axis 2	Axis 3	Axis 4
FsPC1	-0.7	0.2	0.0	0.2
FsPC3	-0.1	-0.6	0.2	0.1
FpPC1	0.9	0.1	-0.1	-0.2
FpPC2	-0.1	0.5	0.1	-0.1
FpPC3	0.1	-0.3	0.1	0.5
FpPC4	0.1	-0.3	0.3	-0.2
SePC1	-0.5	0.1	0.1	0.4
SePC2	-0.5	-0.3	-0.3	0.2
SePC3	0.2	0.2	-0.4	0.3
Style length	-0.8	0.2	-0.1	0.2
Pedicle length	0.4	0.1	0.0	0.4
White corolla colour	0.6	0.0	0.4	-0.2
Pink corolla colour	-0.6	-0.6	-0.2	0.2
Yellow corolla colour	-0.2	0.9	-0.2	0.0
Purple face patch (vasculature)	0.5	0.2	-0.5	0.1
Purple face patch (general)	0.6	0.0	-0.4	0.1
Purple zone (vasculature)	0.1	0.4	0.5	0.5
Purple zone (general)	0.2	0.1	0.5	0.4
Yellow tube hairs	-0.6	0.3	0.0	-0.3
Tube yellow patch	-0.5	-0.1	0.2	-0.2
Face yellow patch	-0.5	0.4	0.1	-0.2

Table 5.1. Continuous and discrete flower characters included in PCA of *Antirrhinum* individuals (Section 5.4.1) and their correlation value with each of the main axes.

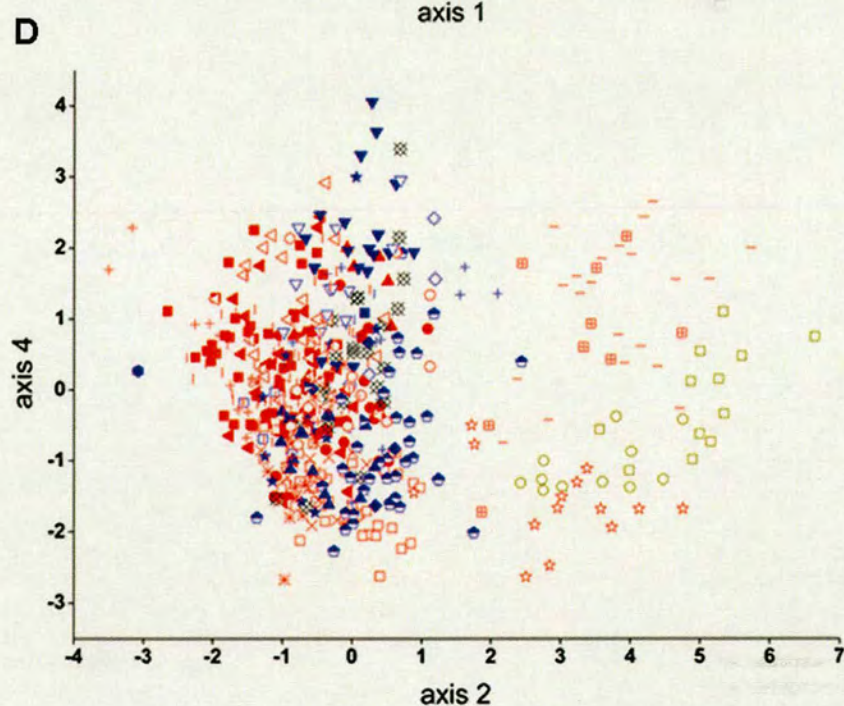
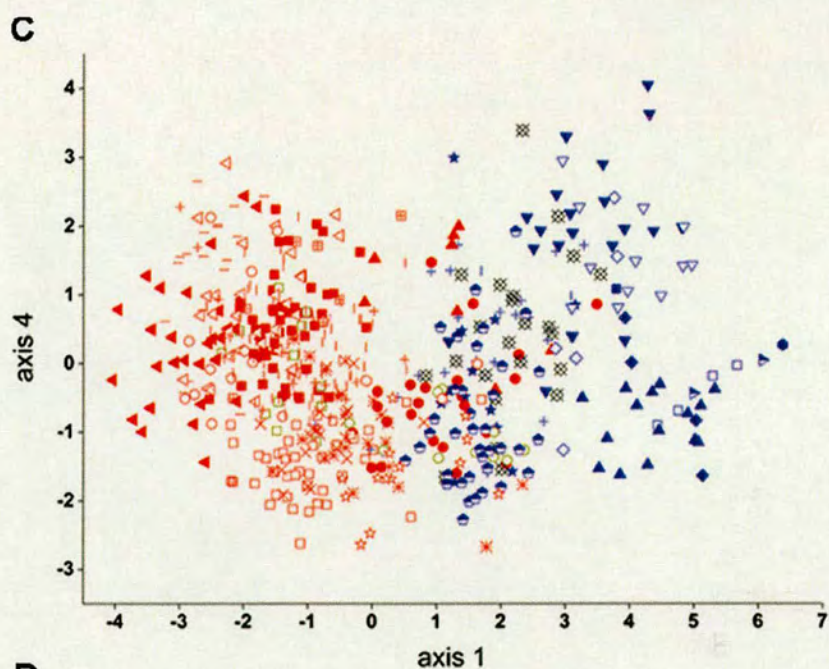
The characters included are those described in Chapter 4, as summarized in Table 4.5.

PC	All flower characters	Continuous flower characters
1	22%	25%
2	12%	14%
3	7%	11%
4	7%	10%
5	6%	9%
6	6%	8%
7	5%	7%
8	5%	6%
9	4%	4%
10	4%	3%
11	4%	3%
12	3%	1%
13	3%	
14	2%	
15	2%	
16	2%	
17	2%	
18	2%	
19	1%	
20	1%	
21	1%	
22	1%	

Table 5.2. The percentage of variance accounted for by each of the principal components (PCs), or axes, of the PCA carried out on all flower characters (column 2), and on continuous flower characters only (column 3).



■ *A. australe* ● *A. barrelieri* ○ *A. barrelieri* (M) ▲ *A. boissieri* ◀ *A. cirrhigerum* □ *A. graniticum*
 - *A. latifolium* ◁ *A. linkianum* × *A. litigiosum* (N) ✖ *A. litigiosum* (V) ○ *A. m. pseud.* ☆ *A. siculum*
 ▣ *A. m. striatum* + *A. m. tort* (M&It) | *A. m. tort* (Spain) | *A. charidemi* + *A. hispanicum* ■ *A. lopesianum*
 ★ *A. hisp.* (M) ◇ *A. microphyllum* ◆ *A. molle* ▼ *A. mollissimum* □ *A. pertegasii* ▲ *A. pulverulentum* ▽ *A. rupestre*
 ◆ *A. sempervirens* ● *A. subbaeticum* ▶ *A. valentinum* □ *A. braun-b.* ○ *A. meonanthum* ✖ hybrid SN



■ *A. australe* ● *A. barrelieri* ○ *A. barrelieri* (M) ▲ *A. boissieri* ◄ *A. cirrhigerum* □ *A. graniticum*
 — *A. latifolium* ◁ *A. linkianum* × *A. litigiosum* (N) * *A. litigiosum* (V) ○ *A. m. pseud.* ☆ *A. siculum*
 ■ *A. m. striatum* + *A. m. tort* (M<) | *A. m. tort* (Spain) | *A. charidemi* + *A. hispanicum* ■ *A. lopesianum*
 ★ *A. hisp.* (M) ◇ *A. microphyllum* ● *A. molle* ▼ *A. mollissimum* □ *A. pertegasii* ▲ *A. pulverulentum* ▼ *A. rupestre*
 ◆ *A. sempervirens* ● *A. subbaeticum* ▴ *A. valertinum* □ *A. braun-b.* ○ *A. meonanthum* ⊗ hybrid SN

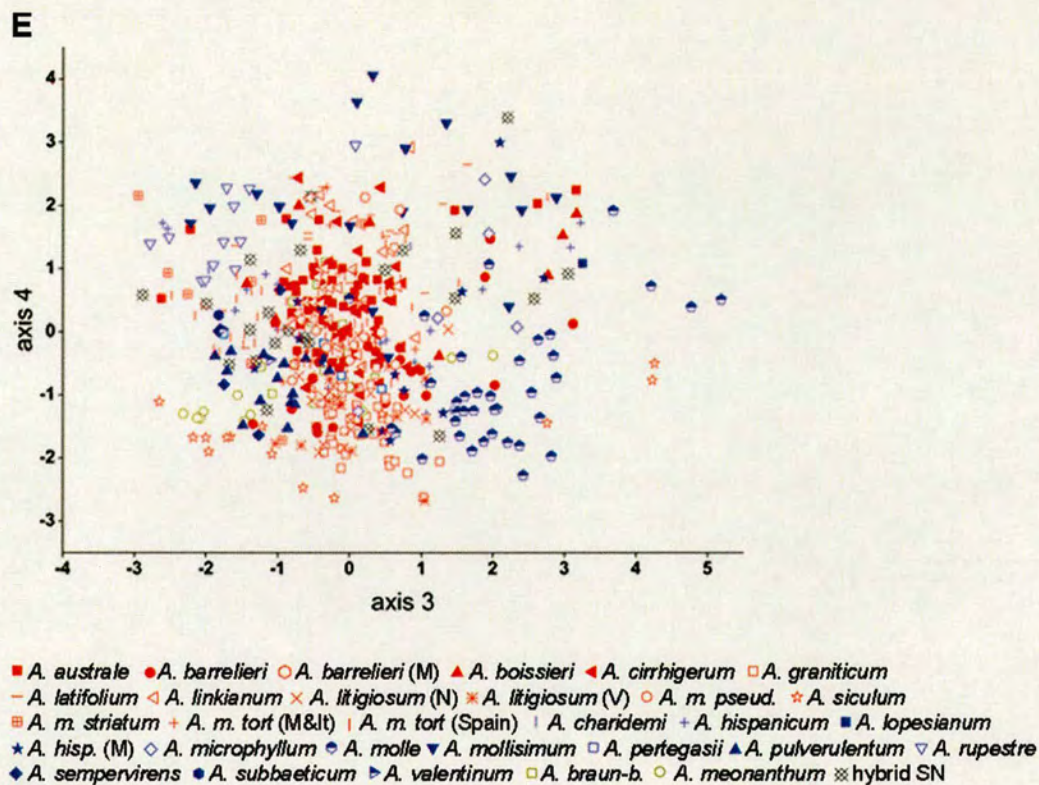


Figure 5.1. The positions of *Antirrhinum* individuals plotted within the axes identified by PCA analysis using all flower characters (Section 5.4.1).

Subsection *Antirrhinum* individuals are represented by red symbols, *Kickxiella* by purple symbols, *Streptosepalum* by dark yellow symbols and *A. barrelieri* x *A. rupestre* hybrid individuals ('hybrid SN') by black symbols.

(A) Axis 2 plotted against axis 1.

(B) Axis 3 plotted against axis 1.

The vector plots alongside (A) and (B) indicate the relative strength and direction with which characters influence the positions of individuals within the adjacent plot.

(C) Axis 4 plotted against axis 1.

(D) Axis 4 plotted against axis 2.

(E) Axis 4 plotted against axis 3.

base of the tube, and FpPC2, which describes the relative size of the dorsal petal, are also correlated with this axis (Table 5.1, Figure 5.1A). For these characters high values along axis 2 represent flowers which have a large gibba, long corolla tube and relatively small dorsal petal lobes.

Plotting the position of each individual in the phenotypic space defined by axis 1 and axis 2 shows that accessions of subsection Antirrhinum and *A. braun-blanquetii* are differentiated from the Kickxiella species and *A. meonanthum* along axis 1 (Figure 5.1A). The exceptions are accessions of *A. barrelieri*, *A. boissieri*, *A. siculum* and *A. majus litigiosum* which overlap with the Kickxiella species. Axis 2 then delimits *A. latifolium*, *A. majus striatum*, *A. braun-blanquetii*, *A. meonanthum* and *A. siculum* from other accessions, with *A. braun-blanquetii* having the highest axis 2 values due to its flowers having a large gibba and tube relative to the dorsal petal lobe.

Axis 3 mainly describes variation in flower colour patterning and sepal shape (Table 5.1, Figure 5.1B). Positive values along this axis are associated with white flowers with more rounded sepals and a purple zone on their dorsal petals. Negative values are associated with flowers having relatively narrow sepals with a cuneate base (SePC2 and SePC3, respectively) and a purple face patch. However, the correlations of these traits with axis 3 are weak ($r \leq 0.5$, Table 5.1). Comparisons of the accessions plotted in the space defined by axes 1 and 3 (Figure 5.1B) shows little species delimitation along axis 3, although mostly *A. molle* accessions have high values. The variation of accessions of the same species along this axis seems to reflect intra-specific variation of the purple colour patterning on the dorsal petal lobe within the Kickxiella species.

The characters which have the strongest correlations with axis 4 are FpPC3 ($r = 0.5$), where high FpPC3 values represent flowers with wide dorsal petal lobes compared to the tube, and a purple zone on the dorsal petal lobe (Table 5.1). SePC1 and pedicel length are also positively correlated. Most *A. graniticum*, *A. majus litigiosum*, *A. meonanthum* and *A. siculum* accessions have low axis 4 values compared to the other Antirrhinum accessions (Figure 5.1C). Within the Kickxiella, most *A. molle* and *A. pulverulentum* accessions also have low axis 4 values.

Comparisons of the positions of all individuals in the morphological space defined by axes 1-4 (Figure 5.1A-E) shows that although the accessions of each species do occupy a similar region to

Character	Axis 1	Axis 2	Axis 3	Axis 4
FsPC1	-0.8	0.2	0.0	0.0
FsPC3	-0.1	-0.8	0.1	0.2
FpPC1	0.9	0.2	-0.1	-0.1
FpPC2	-0.2	0.7	0.1	0.2
FpPC3	0.1	-0.4	0.5	-0.2
FpPC4	0.1	-0.3	0.1	0.8
SePC1	-0.6	0.1	0.5	0.2
SePC2	-0.4	-0.5	-0.3	-0.4
SePC3	0.2	0.1	0.3	-0.5
Style length	-0.9	0.2	0.1	-0.1
Pediceal length	0.3	0.1	0.7	-0.1

Table 5.3. Continuous flower characters included in PCA of *Antirrhinum* individuals (Section 5.4.2) and their correlation value with each of the main axes.

each other, there is little delimitation between them. The positions of accessions of some species along axes 3 and 4 vary extensively.

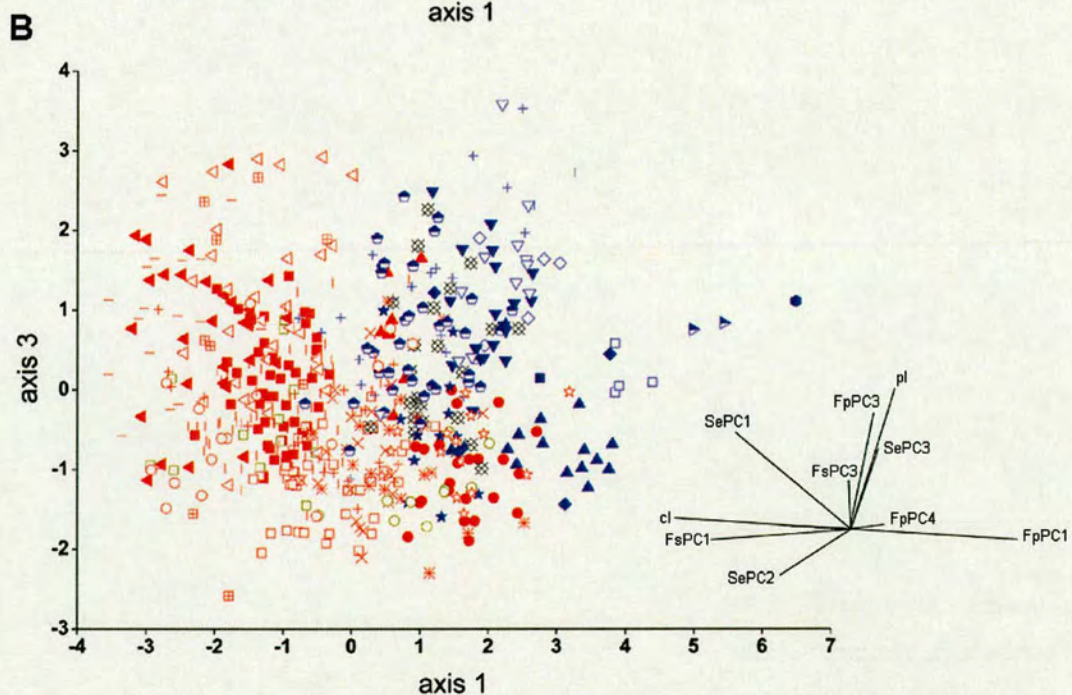
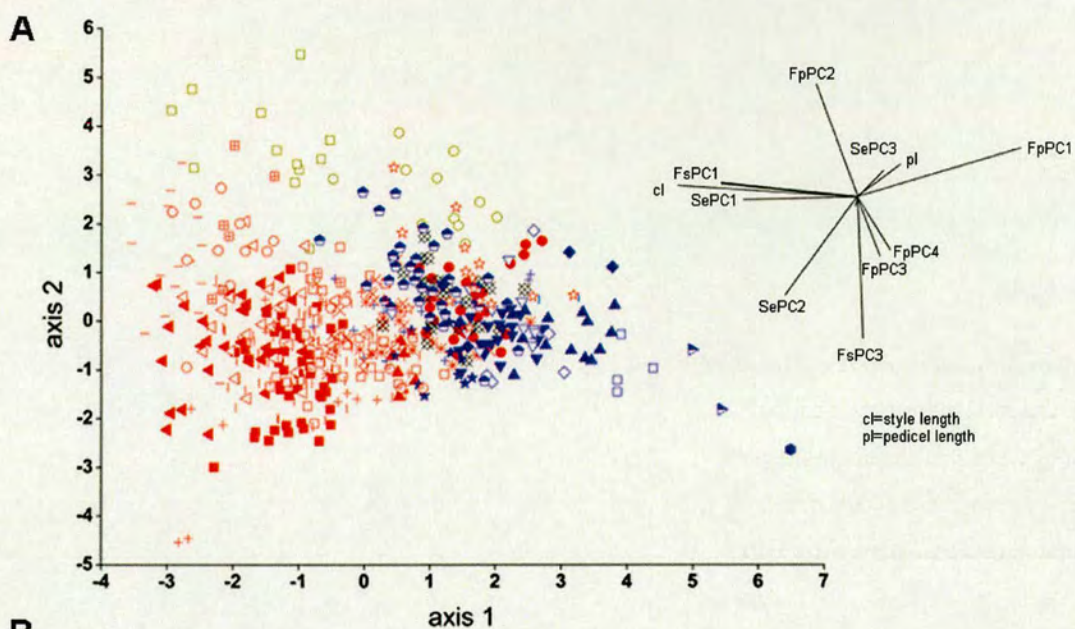
5.4.2 PCA of continuous flower characters

To determine the extent to which including discrete variables in the PCA affects the distances between accessions, PCA analysis was carried out on all taxa with the flower colour variables excluded (Table 5.3). Again, a relatively small percentage of variation is accounted for by the main principal components (Table 5.2). Similar to the analysis with all flower characters, the first axis is strongly correlated with the measures of flower size, such as FpPC1, SePC1 and style length, and the angle of the dorsal petal lobe to the tube, FsPC1 (Table 5.3, Figure 5.2A). Negative values along axis 1 represent large flowers with the dorsal petal lobe horizontal to the tube whilst positive values represent small flowers with dorsal petal lobe perpendicular to the tube.

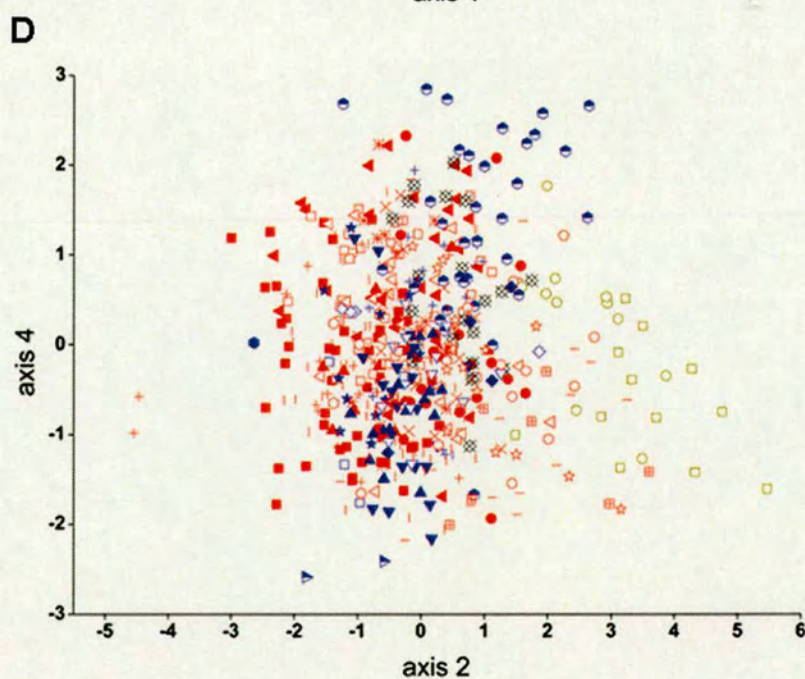
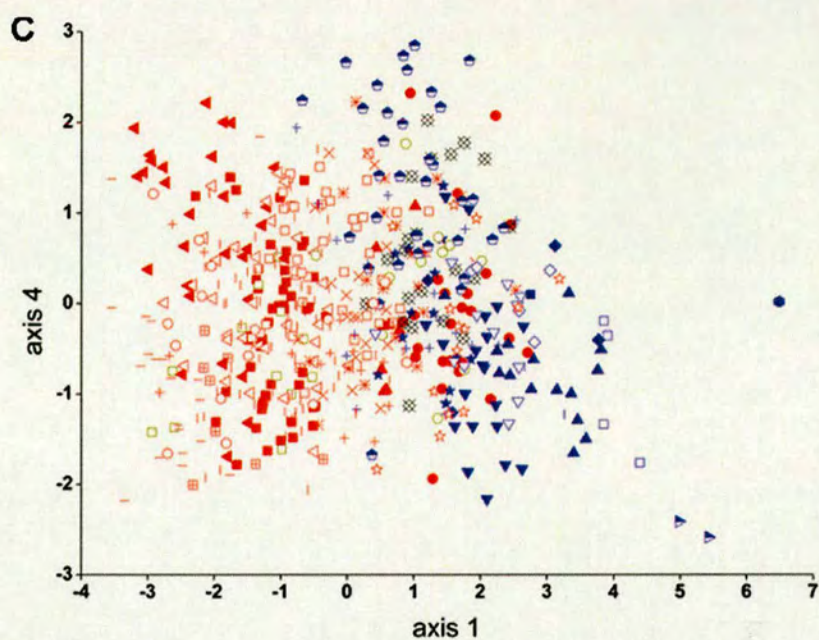
Similar to the previous analysis, the second axis is strongly correlated with FsPC3, FpPC2 and SePC2 (Table 5.3). High axis 2 values represent flowers with relatively large corolla tubes with a large gibba, small dorsal petal lobes and narrow, pointed sepals. The accessions have similar relative positions within axes 1 and 2 as in the previous PCA analysis (section 5.4.1), which included flower colour (Figure 5.2A). The main difference between these analyses is that the accessions of *A. latifolium*, *A. majus striatum* and *A. braun-blauquetii* are closer (along axis 2) to accessions of *A. majus pseudomajus*, *A. majus cirrhigerum*, *A. majus linkianum*, *A. majus tortuosum* and *A. australe*, which are all of a similar size. The yellow coloured *A. latifolium* and *A. majus striatum* are no longer being delimited from the pink flowered taxa. In addition, *A. siculum* accessions are less differentiated from the *Kickxiella* accessions along axis 2.

Axis 3 is mainly correlated with pedicel length and FpPC3 (Table 5.3), with high values along axis 3 representing flowers with short pedicels and narrow dorsal petal lobes. Most *A. graniticum* accessions have high values along axis 3 and are therefore slightly displaced from *A. australe*, *A. majus tortuosum*, *A. cirrhigerum* and *A. linkianum* (Figure 5.2B). *A. pulverulentum* accessions also have higher axis 3 values than many of the other *Kickxiella* accessions and are clustered together in the space defined by axes 1-3.

The fourth axis is main determined by FpPC4 ($r=-0.8$, Table 5.3) with high values along axis 4 being associated with flowers with relatively long tubes. The two *A. valentinum* plants have the



■ *A. australe* ● *A. barrelieri* ○ *A. barrelieri* (M) ▲ *A. boissieri* ◄ *A. cirrhigerum* □ *A. graniticum*
 - *A. latifolium* ◁ *A. linkianum* × *A. litigiosum* (N) ✱ *A. litigiosum* (V) ○ *A. m. pseud.* ☆ *A. siculum*
 ▢ *A. m. striatum* + *A. m. tort* (M<) | *A. m. tort* (Spain) | *A. charidemi* + *A. hispanicum* ■ *A. lopesianum*
 ★ *A. hisp.* (M) ◇ *A. microphyllum* ● *A. molle* ▼ *A. mollissimum* □ *A. pertegasii* ▲ *A. pulverulentum* ▽ *A. rupestre*
 ◆ *A. sempervirens* ● *A. subbaeticum* ▹ *A. valentinum* □ *A. braun-b.* ○ *A. meonanthum* ✕ hybrid SN



■ *A. australe* ● *A. barrelieri* ○ *A. barrelieri* (M) ▲ *A. boissieri* ◄ *A. cirrhigerum* □ *A. graniticum*
 - *A. latifolium* ◁ *A. linkianum* × *A. litigiosum* (N) ✱ *A. litigiosum* (V) ○ *A. m. pseud.* ☆ *A. siculum*
 ▣ *A. m. striatum* + *A. m. tort* (M<) | *A. m. tort* (Spain) | *A. charidemi* + *A. hispanicum* ■ *A. lopesianum*
 ★ *A. hisp.* (M) ◇ *A. microphyllum* ● *A. molle* ▼ *A. mollissimum* □ *A. pertegasii* ▲ *A. pulverulentum* ▼ *A. rupestre*
 ◆ *A. sempervirens* ● *A. subbaeticum* ▸ *A. valentinum* □ *A. braun-b.* ○ *A. meonanthum* ✕ hybrid SN

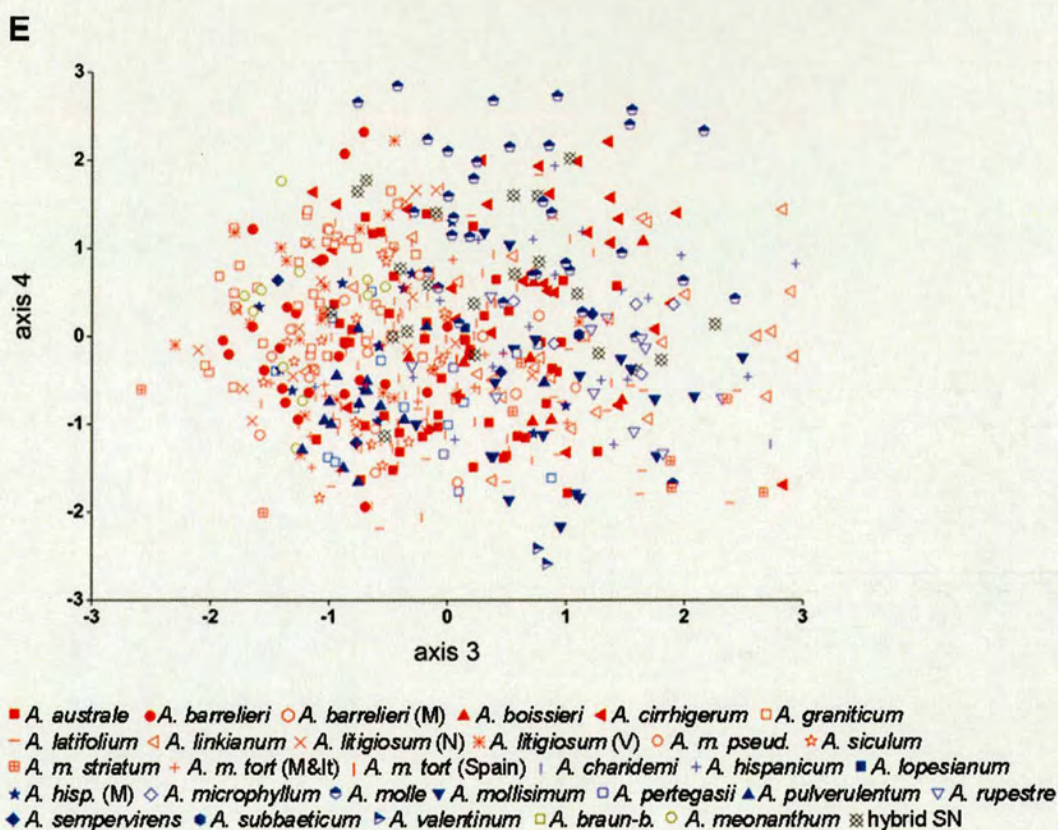


Figure 5.2. The positions of *Antirrhinum* individuals plotted within the axes identified by PCA analysis using continuous flower characters (Section 5.4.2).

Subsection *Antirrhinum* individuals are represented by red symbols, *Kickxiella* by purple symbols, *Streptosepalum* by dark yellow symbols and *A. barrelieri* x *A. rupestre* hybrid individuals ('hybrid SN') by black symbols.

(A) Axis 2 plotted against axis 1.

(B) Axis 3 plotted against axis 1.

The vector plots alongside (A) and (B) indicate the relative strength and direction with which characters influence the positions of individuals in the adjacent plot.

(C) Axis 4 plotted against axis 1.

(D) Axis 4 plotted against axis 2.

(E) Axis 4 plotted against axis 3.

highest axis 4 values, increasing their distance from the other taxa, and most *A. molle* accessions have low FpPC4 values; however, they overlap with *A. hispanicum* and the hybrid individuals from the Sierra Nevada region (Figure 5.2C-E).

Similar to the analysis with discrete flower characters included, accessions of each species tend to cluster together in the space defined by axes 1-4, but there is poor delimitation of species (Figure 5.2). Within subsection *Antirrhinum*, accessions of *A. majus tortuosum*, *A. australe*, *A. cirrhigerum* and *A. linkianum* occupy the same space. *A. graniticum* and *A. majus litigiosum* overlap with this group, but mainly cluster together. *A. majus pseudomajus*, *A. majus striatum* and *A. latifolium* are separated from the rest of these *Antirrhinum* subsection accessions along axis 2, but they cannot be distinguished from each other. *A. siculum* and *A. barrelieri* flowers are clustered with the *Kickxiella* species. Similarly, within subsection *Kickxiella* few species are clearly delimited. The two subsection *Streptosepalum* species, *A. meonanthum* and *A. braun-blanquetii* are delimited from the other species by their high axis 2 values and from each other along axis 1.

5.5 Clustering of populations using flower characters

The lack of definitive clustering of individuals in the phenotypic space defined by flower characters contradicts the findings that there are significant differences between many species in many of the same characters considered individually (Chapter 4). To determine if this due to variation within populations, either as a result of genetic variation or variation introduced by experimental imprecision, PCA was carried out on the set of mean values of all flower characters of each population. Further details of the populations included are in Table 5.4.

Similar to the results of the PCA analysis of individuals in Section 5.4.1, there is little clustering of populations into well-delimited species. The main axes of the analysis are also determined by similar sets of correlations between characters (Table 5.5) and the general relationships between taxa are similar to the previous analyses (Figure 5.3A-E). This result indicates that the information provided by the flower characters alone is insufficient to delimit *Antirrhinum* species.

5.6 PCA of populations using all morphological characters

To estimate the phenotypic space of taxa based on all morphological characters, it was necessary to calculate the mean set of character values for each population. PCA was then carried out on

Species	N _{characters}	Missing characters
Population ID		
Subsection Antirrhinum		
<i>A. australe</i>		
83	54	
85	54	
86	54	23
87	54	
89	54	
90	34	1, 2, 3, 11, 12, 13, 19, 20, 21, 22, 23, 14, 49-54
91	54	
95	54	
97	53	45, 48
<i>A. barrelieri</i>		
27	22	1, 2, 3, 19, 20, 21, 22, 23, 25, 14, 24, 4, 25, 37-54
28	22	1, 2, 3, 19, 20, 21, 22, 23, 25, 14, 24, 4, 25, 37-54
96	54	
131	40	25, 43-48, 49-54
<i>A. barrelieri</i> (M)		
167	53	22
<i>A. boissieri</i>		
104	54	
<i>A. graniticum</i>		
40	50	1, 2, 3, 14
67	42	20, 21, 22, 14, 25, 49-54
75	54	
76	54	
79	36	20, 23, 25, 14, 25, 43-48, 49-54
115	29	1, 2, 3, 19, 20, 21, 22, 23, 14, 24, 4, 25, 37-54
116	54	
117	44	1, 2, 3, 20, 21, 18, 14, 38, 41
119	47	49-54
120	52	46
121	54	
174	32	1, 2, 3, 21, 22, 25, 14, 24, 4, 45, 44, 46, 48, 46, 39, 38, 37, 42, 41, 43
<i>A. latifolium</i>		
N1045	22	1, 2, 3, 19, 20, 21, 22, 23, 25, 14, 24, 4, 25, 37-54
N1047	50	1, 2, 3
N1053	22	1, 2, 3, 19, 20, 21, 22, 23, 25, 14, 24, 4, 25, 37-54
N1054	22	1, 2, 3, 19, 20, 21, 22, 23, 25, 14, 24, 4, 25, 37-54
N1055	22	1, 2, 3, 19, 20, 21, 22, 23, 25, 14, 24, 4, 25, 37-54
N1056	19	1, 2, 3, 19, 20, 21, 22, 23, 25, 14, 24, 4, 25, 35, 36, 37-54
N1057	22	1, 2, 3, 19, 20, 21, 22, 23, 25, 14, 24, 4, 25, 37-54
N1058	22	1, 2, 3, 19, 20, 21, 22, 23, 25, 14, 24, 4, 25, 37-54
N1066	24	1, 2, 3, 19, 20, 21, 22, 23, 25, 14, 25, 37-54
N1069	21	1, 2, 3, 19, 20, 21, 22, 23, 25, 14, 18, 25, 37-54
N1070	22	1, 2, 3, 19, 20, 21, 22, 23, 25, 14, 24, 4, 25, 37-54
N1071	20	1, 2, 3, 19, 20, 21, 22, 23, 25, 14, 24, 4, 25, 35, 36, 37-54
N1072	22	1, 2, 3, 19, 20, 21, 22, 23, 25, 14, 24, 4, 25, 37-54
N1081	20	1, 2, 3, 19, 20, 21, 22, 23, 25, 14, 24, 4, 25, 35, 36, 37-54
<i>A. majus cirrhigerum</i>		
113	54	
114	49	25, 1, 2, 3
122	54	
125	48	14, 22, 1, 2, 3
<i>A. majus linkianum</i>		
107	54	
108	47	19, 20, 21, 22, 23, 14
109	54	

110	43	1, 2, 3, 25, 49-54
111	45	1, 2, 3, 19, 20, 21, 22 23
112	50	1, 2, 3
<i>A. majus litigiosum</i> (N)		
61	54	
62	54	
64	53	14
66	46	1, 2, 3, 21, 25, 14, 24
80	26	
<i>A. majus litigiosum</i> (V)		
1	22	1, 2, 3, 19, 20, 21, 22, 23, 25, 14, 24, 4, 25, 37-54
3	49	1, 2, 3, 14
4	22	1, 2, 3, 19, 20, 21, 22, 23, 25, 14, 24, 4, 25, 37-54
5	45	25, 14, 43-48
6	20	1, 2, 3, 19, 20, 21, 22, 23, 25, 14, 24, 4, 25, 35, 36, 37-54
9	46	25, 43-48
10	54	
11	29	1, 2, 3, FsPC1, FsPC3, 25, 37-54
<i>A. majus pseudomajus</i>		
46	22	1, 2, 3, 19, 20, 21, 22, 23, 25, 14, 24, 4, 26, 37-54
53	54	
59	22	1, 2, 3, 19, 20, 21, 22, 23, 25, 14, 24, 4, 26, 37-54
<i>A. majus striatum</i>		
E39	54	
55	21	1, 2, 3, 19, 20, FpPC1, 21, 22, 23, 25, 14, 24, 4, 25, 37-54
56	22	1, 2, 3, 19, 20, 21, 22, 23, 25, 14, 24, 4, 25, 37-54
58	22	1, 2, 3, 19, 20, 21, 22, 23, 25, 14, 24, 4, 25, 37-54
N1125	54	
<i>A. majus tortuosum</i> (Sp)		
81	54	
82	44	1, 2, 3, 11, 12, 13, 22, 14
92	54	
93	52	45
98	54	
100	54	
101	54	
102	54	
103	54	
105	47	45, 44, 46, 48, 47
106	54	
160	54	
<i>A. majus tortuosum</i> (M & It)		
161	54	
169	54	
N1143	39	1, 2, 3, 21, 22, 23, 14, 26, 49-54
N1144	50	1, 2, 3
<i>A. siculum</i>		
E68	53	14
unknown	53	14
183	54	
N1176	54	
N1177	53	14
Subsection Kickxiella		
<i>A. charidemi</i>		
E23	28	1, 2, 3, 25, 24, 4, 25, 37-54
<i>A. hispanicum</i> (Sp)		
E30	51	22, 46
E31	31	25, 24, 4, 25, 37-54

36	40	1, 2, 3, 21, 22, 24, 4, 39, 38, 37, 42, 41, 43
99	47	43-48
132	47	49-54
<i>A. hispanicum</i> (M)		
171	54	
172	54	
173	54	
<i>A. lopesianum</i>		
unknown	21	1, 2, 3, 19, 20, 21, 22, 23, 25, 14, 24, 4, 25, 36, 37-54
<i>A. microphyllum</i>		
73	54	
<i>A. molle</i>		
E51	50	1, 2, 3
E52	49	1, 2, 3, 45
E53	39	1, 2, 3, 45, 46, 48, 47, 46, 49-54
E54	38	1, 2, 3, 43-48, 49-54
E55	44	1, 2, 3, 43-48
E56	44	1, 2, 3, 43-48
<i>A. mollisimum</i>		
19	49	1, 2, 3, 21
20	52	46
21	51	45, 47
<i>A. pertegasii</i>		
E65	45	23, 26, 49-54
<i>A. pulverulentum</i>		
68	38	25, 14, 26, 45, 44, 46, 48, 46, 49-54
70	53	
<i>A. rupestre</i>		
22	47	43-48
139	53	
<i>A. sempervirens</i>		
50	53	
<i>A. subbaeticum</i>		
E72	46	21, 49-54
<i>A. valentinum</i>		
N1173	22	1, 2, 3, 19, 20, 21, 22, 23, 25, 14, 24, 4, 25, 37-54
Subsection Streptosepalum		
<i>A. braun-blanquetii</i>		
unknown	23	1, 2, 3, 19, 20, 21, 22, 23, 25, 24, 4, 25, 37-54
E20	54	
44	22	1, 2, 3, 19, 20, 21, 22, 23, 25, 14, 24, 4, 25, 37-54
<i>A. meonanthum</i>		
E48	42	
unknown	22	1, 2, 3, 19, 20, 21, 22, 23, 25, 14, 24, 4, 25, 37-54
118	54	
180	47	39, 38, 37, 42, 41, 43
<i>A. barrelieri/hispanicum</i> hybrid populations		
23	50	1, 2, 3
24	22	1, 2, 3, 19, 20, 21, 22, 23, 25, 14, 24, 4, 25, 37-54
30	49	1, 2, 3, 22
25	43	1, 2, 3, 20, 21, 22, 49, 54, 53, 52
35	48	1, 2, 3, 14

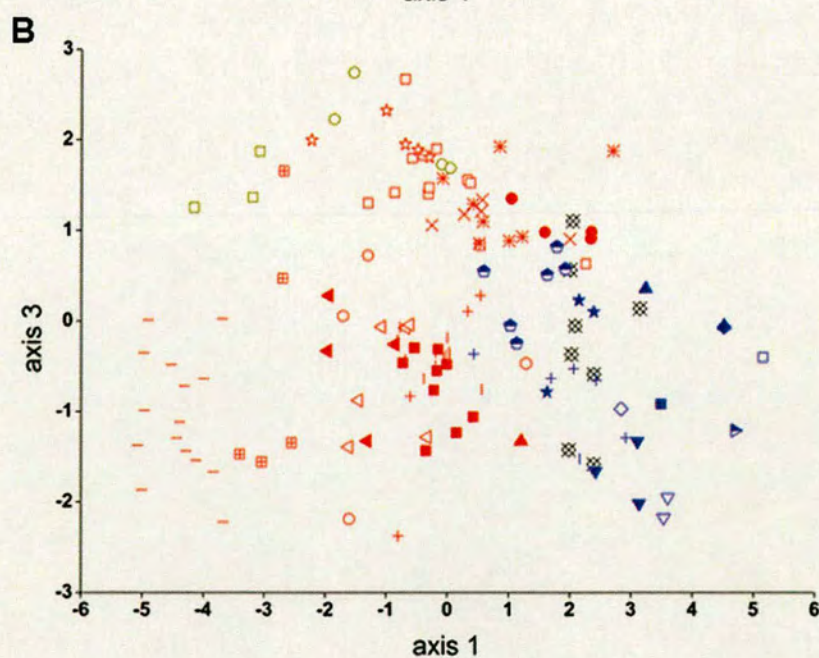
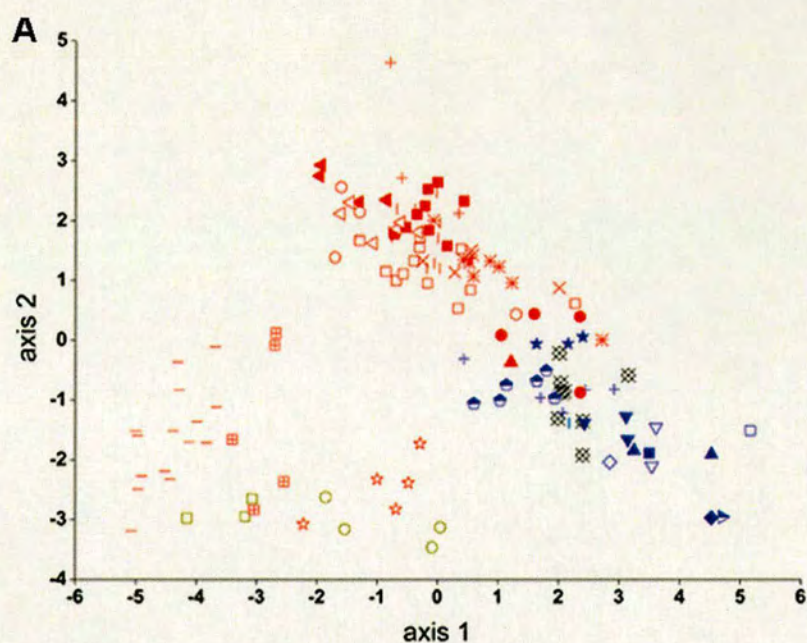
33	22	1, 2, 3, 19, 20, 21, 22, 23, 25, 14, 24, 4, 25, 37-54
31	49	1, 2, 3, 14
32	43	1, 2, 3, 14, 39, 38, 37, 42, 41, 43

Table 5.4. Populations included in PCA analyses and the missing characters for each population.
The populations are listed according to their database location number, followed by the number of characters that are included in the PCA analysis in Section 5.5.1., out of a total of 54, and details of missing characters. The missing characters are as numbered in Table 4.5:

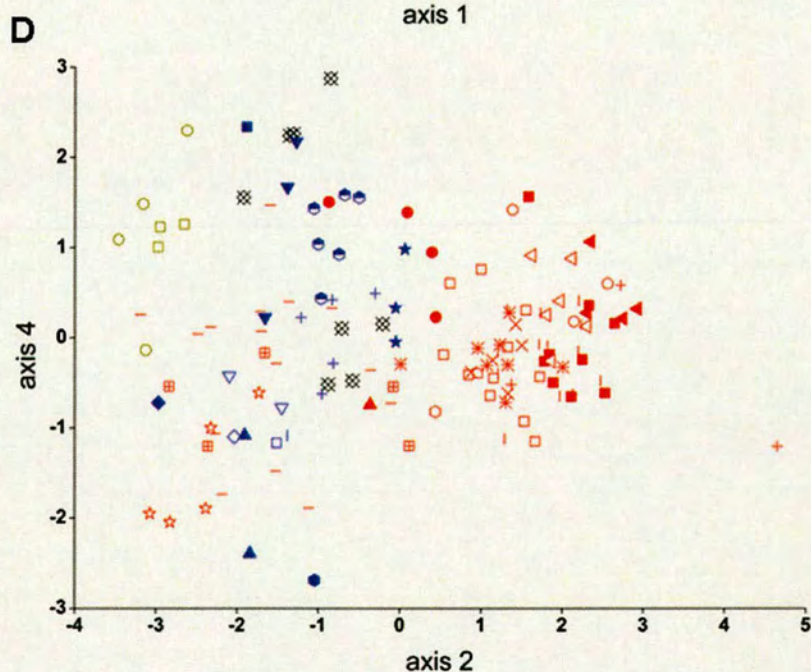
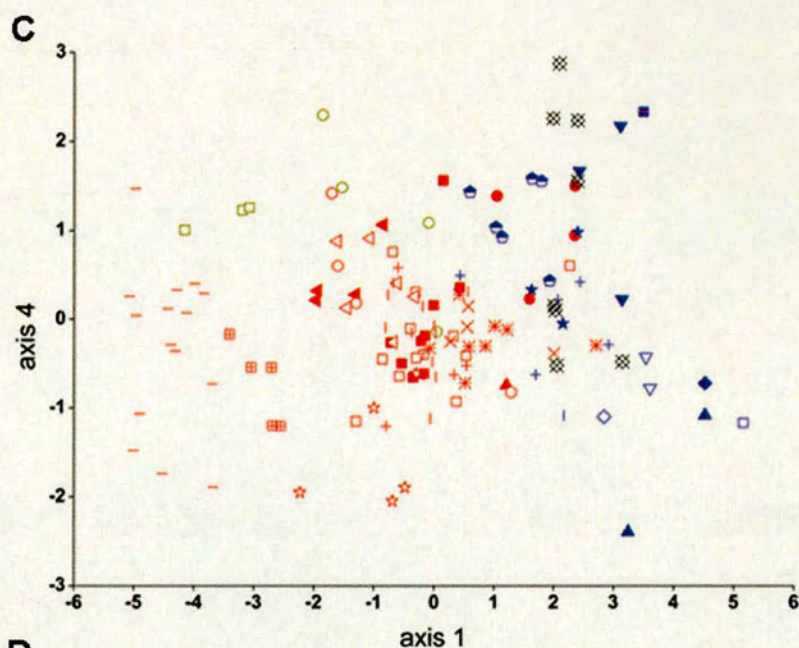
1=LePC1, 2=LePC2, 3=LePC3, 4=Leaf Cell No, 5=FpPC1, 6=FpPC2, 7=FpPC3, 8=FpPC4, 9=FsPC1, 10=FsPC3, 11=SePC1, 12=SePC2, 13=SePC3, 14=Flower Cell No, 15=Style length, 16=Dorsal stamen length, 17=Ventral stamen length, 18=Pedicel Length, 19=Flowering Time, 20=Height, 21=Inflorescence density, 22=Stem diameter, 23=Branching Index, 24=Leaf trichome density, 25= Base of stem trichome density, 26=Inflorescence stem trichome density, 27=Flower colour pink, 28=Flower colour white, 29=Flower colour yellow, 30=face purple patch - vasculature, 31=face purple patch - general, 32=dorsal petal lobe – vasculature, 33=dorsal petal lobe – general, 34=face yellow patch, 35=yellow tube hairs, 36=yellow tube patch. Trichome morphology : 37=Leaf Short glandular, 38=Leaf Medium glandular, 39=Leaf Long glandular, 40=Leaf Short eglandular, 41=Leaf Medium eglandular, 42=Leaf Long eglandular, 43=base of stem short glandular, 44=base of stem medium glandular, 45=base of stem long glandular, 46=base of stem short eglandular, 47=base of stem medium eglandular, 48=base of stem long eglandular, 49=inflorescence stem short glandular, 50=inflorescence stem medium glandular, 51=inflorescence stem long glandular, 52=inflorescence stem short eglandular, 53=inflorescence stem medium eglandular, 54=inflorescence stem long eglandular.

	axis 1	axis 2	axis 3	axi4
FsPC1	0.8	-0.2	0.1	-0.2
FsPC3	-0.8	0.5	-0.2	0.1
FpPC1	-0.3	-0.7	0.2	0.1
FpPC2	0.4	0.4	-0.2	-0.3
FpPC3	-0.2	-0.1	0.6	0.2
FpPC4	-0.5	-0.3	-0.2	-0.2
SePC1	0.6	-0.1	0.4	-0.2
SePC2	0.4	-0.5	0.2	0.3
SePC3	0.1	0.4	0.5	0.2
SePC5	0.1	0.2	0.4	0.1
Style length	0.9	-0.2	0.2	-0.1
Pedice length	-0.2	0.3	0.4	0.0
White	-0.5	0.3	0.0	0.0
Pink	-0.1	-0.8	0.1	0.0
Yellow	0.7	0.6	0.0	0.1
Purple face patch (vasculature)	-0.2	0.6	0.3	0.4
Purple face patch (general)	-0.5	0.4	0.3	0.3
Purple zone (vasculature)	0.2	0.5	0.2	-0.5
Purple zone (general)	-0.2	0.2	0.2	-0.4
Yellow tube hairs	0.6	-0.1	-0.4	0.2
Tube yellow patch	0.4	-0.3	-0.1	0.2
Face yellow patch	0.7	0.2	-0.1	0.3

Table 5.5. Continuous and discrete flower characters included in the PCA of populations (Section 5.5) and their correlation value with each of the main axes.



■ *A. australe* ● *A. barrelieri* ○ *A. barrelieri* (M) ▲ *A. boissieri* ◀ *A. cirrhigerum* □ *A. graniticum*
 - *A. latifolium* ◁ *A. linkianum* × *A. litigiosum* (N) * *A. litigiosum* (V) ○ *A. m. pseud.* ★ *A. siculum*
 ▢ *A. m. striatum* + *A. m. tort* (M&I) | *A. m. tort* (Spain) | *A. charidemi* + *A. hispanicum* ■ *A. lopesianum*
 ★ *A. hisp.* (M) ◇ *A. microphyllum* ● *A. molle* ▼ *A. mollissimum* □ *A. pertegasii* ▲ *A. pulverulentum* ▽ *A. rupestre*
 ◆ *A. sempervirens* ● *A. subbaeticum* ▹ *A. valentinum* □ *A. braun-b.* ○ *A. meonanthum* × hybrid SN



■ *A. australe* ● *A. barrelieri* ○ *A. barrelieri* (M) ▲ *A. boissieri* ◄ *A. cirrhigerum* □ *A. graniticum*
 - *A. latifolium* ◁ *A. linkianum* × *A. litigiosum* (N) * *A. litigiosum* (V) ○ *A. m. pseud.* ☆ *A. siculum*
 ▢ *A. m. striatum* + *A. m. tort* (M&I) | *A. m. tort* (Spain) | *A. charidemi* + *A. hispanicum* ■ *A. lopesianum*
 ★ *A. hisp.* (M) ◇ *A. microphyllum* ● *A. molle* ▼ *A. mollissimum* □ *A. pertegasii* ▲ *A. pulverulentum* ▼ *A. rupestre*
 ◆ *A. sempervirens* ● *A. subbaeticum* ▴ *A. valentinum* □ *A. braun-b.* ○ *A. meonanthum* ⊗ hybrid SN

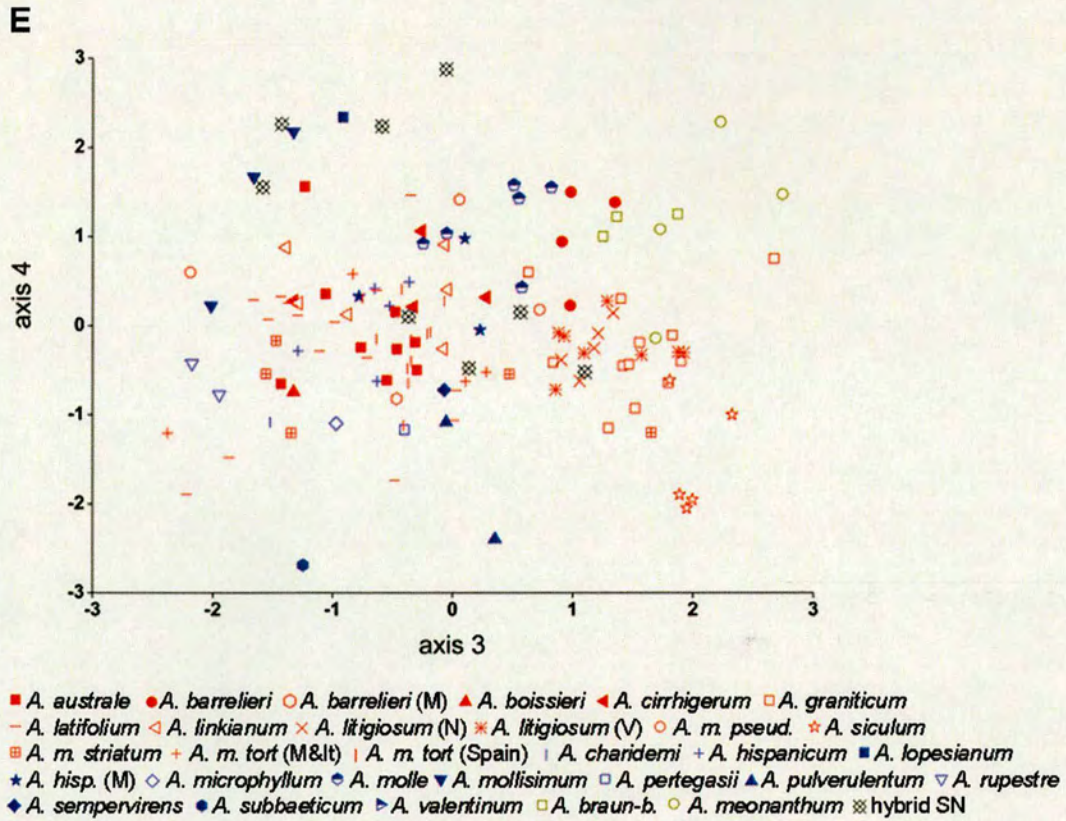


Figure 5.3. The positions of *Antirrhinum* populations plotted within the axes identified by PCA analysis using all flower characters (Section 5.5).

Subsection *Antirrhinum* populations are represented by red symbols, *Kickxiella* by purple symbols, *Streptosepalum* by dark yellow symbols and *A. barrelieri* x *A. rupestre* hybrid individuals ('hybrid SN') by black symbols.

- (A) Axis 2 plotted against axis 1.
- (B) Axis 3 plotted against axis 1.
- (C) Axis 4 plotted against axis 1.
- (D) Axis 4 plotted against axis 2.
- (E) Axis 4 plotted against axis 3.

these population means. This approach was taken to minimise effects of both the proportion of missing characters and the variation in vegetative characters which may be sensitive to experimental conditions. The same populations as above were analysed; for some populations there is still a high proportion of missing characters (Table 5.4).

5.6.1 PCA of populations using all characters

To determine the extent of delimitation of taxa based on the main characters that are traditionally used in the identification of *Antirrhinum* species such as trichome morphology and distribution, as well as those of overall morphology and of interest in studying morphological adaptation, the dataset consisting of all characters, both continuous and discrete, was analysed (Table 5.6).

The overall percentage of variation accounted for by the main PCs is slightly lower than that explained by the analysis of flower characters (Table 5.7). Similar to the analysis of flower characters, the first axis of variation is correlated mainly with measures of size and the flower character FsPC1 which reflects the angle of the dorsal petal lobe to the tube (Table 5.6, Figure 5.4A). Flower size measures such as the style length and FpPC1 are the most strongly correlated characters, having correlation values of magnitude 0.9, with the other main measures of size such as SePC1, plant height and LePC1 having weaker correlations (Table 5.6). The trichome characters, such as density of trichomes on the stem and leaf, and flower colour patterns such as yellow tube hairs, the yellow face patch and the purple face patch are also correlated with this axis ($r \sim 0.6$). Positive values along axis 1 represent short plants, with dense pubescence, small rounded leaves and small, white flowers with a purple face patch and dorsal petal lobes at an acute angle to the tube. Negative values along axis 1 represent taller plants with large more lanceolate leaves, large flowers with large sepals, the presence of a yellow face and tube patch and yellow tube hairs.

Axis 2 mainly differentiates pink ($r=0.8$) from yellow ($r=-0.7$) flowers; other characters that are less strongly correlated with axis 2 are FsPC3, flowering time and height (Table 5.6, Figure 5.4A). In summary, positive values along axis 2 are associated with tall, late flowering plants with pink flowers which have relatively short tubes and small gibba whilst negative values along axis 2 represent shorter plants with yellow flowers which have long tubes and a large gibba.

The relationships of the taxa in the space defined by axis 1 and 2 are broadly similar to those when only the flower characters are used (Figure 5.4A). Axis 1 separates subsection

Character	axis 1	axis 2	axis 3	axis 4
LePC1	0.5	-0.1	0.0	-0.3
LePC2	-0.1	0.0	0.3	-0.1
LePC3	-0.2	0.1	-0.2	0.0
FsPC1	-0.8	-0.2	-0.3	0.0
FsPC3	0.1	0.6	-0.3	0.0
FpPC1	0.8	-0.1	0.4	0.2
FpPC2	-0.3	-0.6	0.1	0.2
FpPC3	0.2	0.2	-0.2	-0.5
FpPC4	0.3	0.4	0.0	0.2
SePC1	-0.5	-0.3	-0.6	-0.1
SePC2	-0.5	0.3	0.0	-0.1
SePC3	0.1	-0.3	0.0	-0.2
SePC5	0.0	-0.3	-0.1	-0.2
Flowering time	-0.5	0.4	0.2	0.3
Height	-0.6	0.5	0.2	0.1
Inflorescence Density	-0.2	-0.1	0.6	0.2
Stem diameter	-0.3	0.0	-0.2	0.4
Branching Index	-0.3	0.2	0.1	0.3
Style length	-0.8	-0.3	-0.3	-0.2
Pedicel length	0.5	-0.3	-0.3	-0.3
Stem base trichome density	0.7	-0.3	-0.3	0.1
Flower cell No	-0.1	-0.1	0.4	0.4
Leaf trichome density	0.7	-0.3	-0.1	-0.2
Leaf cell no	0.0	-0.2	0.0	0.1
Inflorescence stem trichome density	0.6	-0.3	-0.3	0.0
White corolla colour	0.6	-0.1	0.0	-0.1
Pink corolla colour	-0.3	0.8	-0.2	-0.2
Yellow corolla colour	-0.5	-0.8	0.2	-0.1
Purple face patch (vasculature)	0.4	-0.4	0.2	-0.2
Purple face patch (general)	0.6	-0.1	0.2	-0.3
Purple zone (vasculature)	0.0	-0.5	-0.1	0.1
Purple zone (general)	0.3	-0.1	0.0	0.1
Yellow tube hairs	-0.7	-0.2	0.2	0.0
Tube yellow patch	-0.5	0.1	0.0	-0.2
Face yellow patch	-0.6	-0.5	0.1	-0.1
SLG trichomes	-0.3	0.1	0.3	-0.3
MMG trichomes	-0.1	0.1	0.4	-0.5
SMG trichomes	-0.2	0.0	0.0	-0.2
SLEG trichomes	0.4	-0.2	0.1	0.2
SMEG trichomes	-0.4	0.1	0.0	0.4
SSEG trichomes	-0.3	0.0	-0.2	0.4

LLG trichomes	-0.4	0.2	0.3	-0.3
LMG trichomes	-0.2	0.2	0.4	-0.5
LSG trichomes	-0.2	0.0	-0.2	0.0
LLEG trichomes	-0.5	0.3	0.4	-0.1
LMEG trichomes	-0.4	0.2	0.0	-0.1
LSEG trichomes	-0.4	0.1	-0.2	0.5
flLLG trichomes	-0.2	0.1	0.1	0.1
flMG trichomes	0.1	-0.1	0.5	-0.1
flSG trichomes	-0.3	0.2	-0.1	-0.4
flLEG trichomes	-0.2	0.2	0.3	0.0
flMEG trichomes	-0.3	0.1	0.1	0.0
flSEG trichomes	-0.1	0.1	0.2	-0.1

Table 5.6. Continuous and discrete characters included in PCA of all populations (Section 5.6.1) and the correlation value of each character with the main axes.

PC	All characters	Continuous characters only
1	19%	25%
2	11%	14%
3	7%	11%
4	5%	6%
5	5%	6%
6	4%	4%
7	4%	4%
8	3%	4%
9	3%	3%
10	3%	3%
11	2%	3%
12	2%	2%
13	2%	2%
14	2%	2%
15	2%	2%
16	2%	2%
17	2%	1%
18	2%	1%
19	1%	1%
20	1%	1%
21	1%	1%
22	1%	1%
23	1%	1%
24	1%	0%

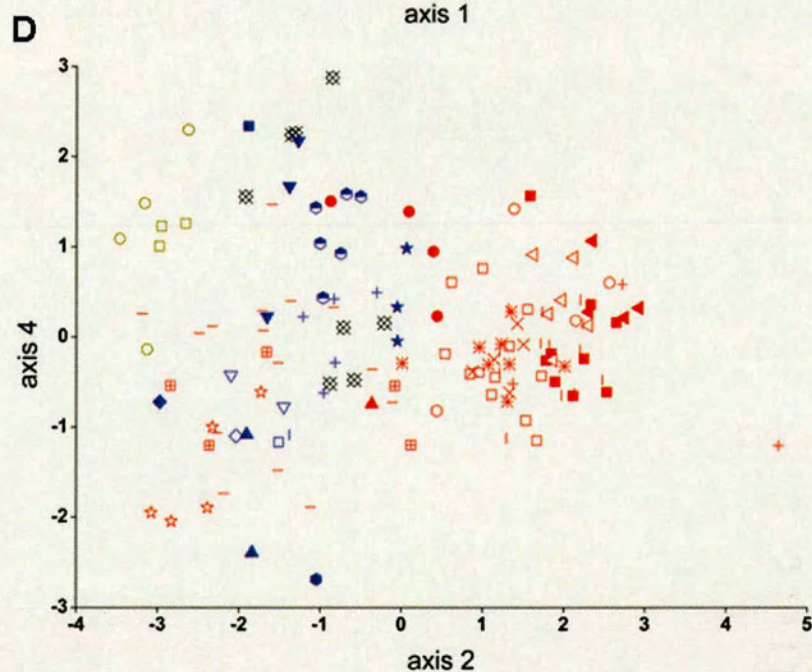
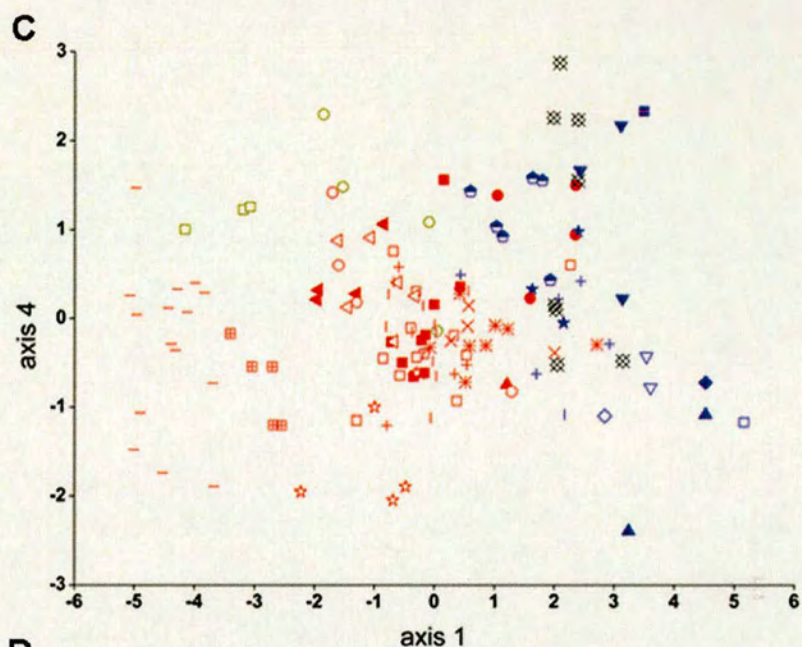
Table 5.7. The percentage of variance accounted for by the first 24 principal components (PCs) of the PCA carried out on all populations using all characters (column 2), and continuous characters only (column 3).

Antirrhinum and Streptosepalum species from subsection Kickxiella species. The species with yellow flowers - *A. latifolium*, *A. braun-blanquetii*, *A. meonanthum* and *A. siculum* are separated from the rest of subsection Antirrhinum along axis 2. The subsection Kickxiella species are also separated from subsection Antirrhinum species along axis 2, probably due to their shorter flowering time, flower shape parameters (FsPC3), epidermal characteristics and flower colour patterning (Figure 5.4A). *A. barrelieri* (M) and *A. hispanicum* (M) are clustered closer to the Antirrhinum subsection species compared to their positions in the analyses that used flower characters only.

Axis 3 is mainly correlated with the number of flowers in the inflorescence, dorsal petal size (FpPC1), the size of the gibba and tube length (FsPC3), dorsal petal cell size and sepal size and shape, SePC1 (Table 5.6, Figure 5.4B). Generally, positive values of axis 3 represent plants with long inflorescences, small flowers with small, narrow sepals and a relatively large tube with a large gibba. *A. meonanthum* and *A. siculum* are delimited by this axis, having higher values than other taxa. In addition, *A. majus tortuosum* and *A. majus litigiosum* populations have higher axis 3 values than *A. australe* (Figure 5.4B). Within the Kickxiella, *A. molle* populations have lower values along axis 3 than populations most other species, apart from some of the Sierra Nevada hybrid populations.

Axis 4 further delimits species, with *A. graniticum* being separated from the other subsection Antirrhinum species through having high values. *A. majus litigiosum* is further delimited from the other pink-flowered subsection Antirrhinum species as it has slightly higher axis 4 values than *A. majus tortuosum*. Within the Kickxiella, *A. molle* and the taxa distributed in the south of Spain - *A. hispanicum*, *A. mollisimum*, *A. rupestre* and the *A. barrelieri* x *A. rupestre* hybrid populations from the Sierra Nevada region – all have higher axis 4 values than the rest of the Kickxiella taxa. Axis 4 is mainly correlated with trichome characteristics, branching and stem width; positive values mainly correspond to plants with thick stems, medium to long glandular trichomes and suppressed branch outgrowth and negative values correspond to more branched plants with thin stems and short eglandular trichomes (Table 5.6).

In summary, the first four axes of principal components analysis carried out on the average values of all characters for each population identifies three main clusters of taxa: the pink-flowered subsection Antirrhinum species, the yellow-flowered subsection Antirrhinum species with the Streptosepalum species, and the Kickxiella species. Furthermore, most species do



■ *A. australe* ● *A. barrelieri* ○ *A. barrelieri* (M) ▲ *A. boissieri* ◄ *A. cirrhigerum* □ *A. graniticum*
 - *A. latifolium* ◊ *A. linkianum* × *A. litigiosum* (N) * *A. litigiosum* (V) ○ *A. m. pseud.* ☆ *A. siculum*
 ▢ *A. m. striatum* + *A. m. tort* (M&It) | *A. m. tort* (Spain) | *A. charidemi* + *A. hispanicum* ■ *A. lopesianum*
 ★ *A. hisp.* (M) ◇ *A. microphyllum* ● *A. molle* ▼ *A. mollisimum* □ *A. pertegasii* ▲ *A. pulverulentum* ▼ *A. rupestre*
 ◆ *A. sempervirens* ● *A. subbaeticum* ▴ *A. valentinum* □ *A. braun-b.* ○ *A. meonanthum* ✕ hybrid SN

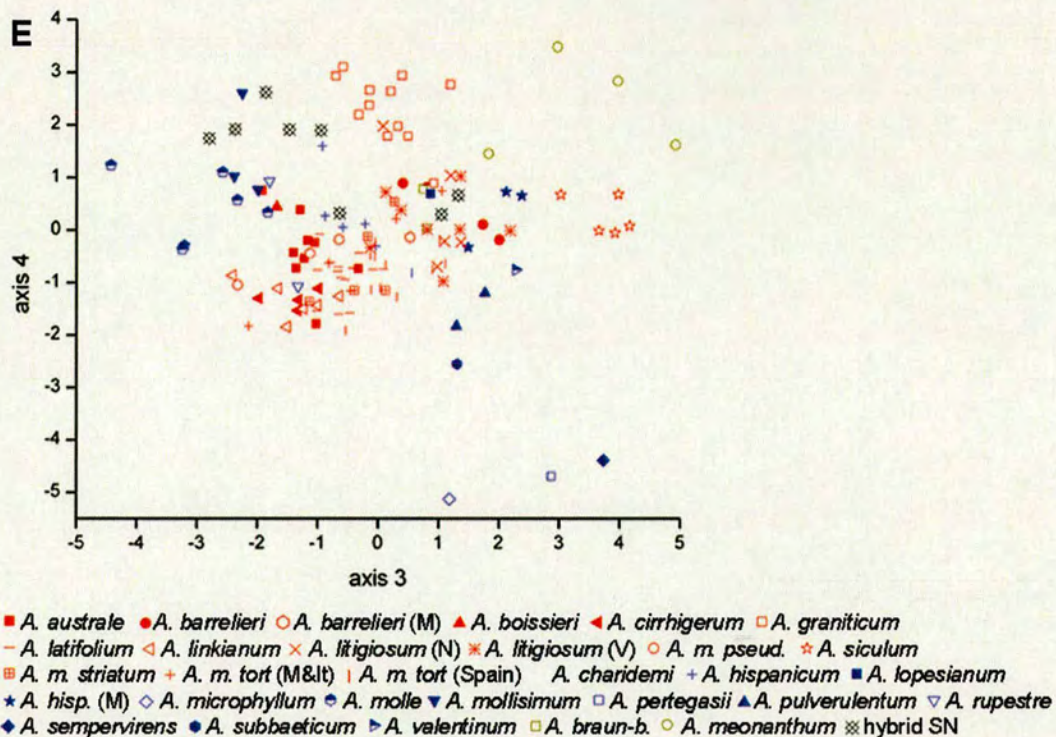


Figure 5.4. The positions of *Antirrhinum* populations plotted within the axes identified by PCA analysis using all characters (Section 5.6.1).

Subsection *Antirrhinum* populations are represented by red symbols, *Kickxiella* by purple symbols, *Streptosepalum* by dark yellow symbols and *A. barrelieri* x *A. rupestre* hybrid individuals ('hybrid SN') by black symbols.

(A) Axis 2 plotted against axis 1.

(B) Axis 3 plotted against axis 1.

The vector plots alongside (A) and (B) indicate the relative strength and direction with which characters influence the positions of populations in the adjacent plot. The trichome characters are as abbreviated in Table 4.5.

(C) Axis 4 plotted against axis 1.

(D) Axis 4 plotted against axis 2.

(E) Axis 4 plotted against axis 3.

occupy a unique area of phenotypic space, albeit closely neighbouring other taxa, although there is overlap of populations of *A. majus cirrhigerum* with those of *A. majus linkianum* and *A. majus pseudomajus*. *A. barrelieri* populations also overlap with those of *A. majus litigiosum* in all dimensions that were plotted. The *A. barrelieri* x *A. rupestre* hybrid populations from the Sierra Nevada region are dispersed throughout the space occupied by *A. barrelieri*, *A. hispanicum*, *A. molle* and *A. mollisimum*. For most of the subsection *Kickxiella* species too few populations of each species were sampled to draw strong conclusions; however, they are all separated from each other, except the two *A. pulverulentum* populations which are relatively far from each other. *A. mollisimum* and *A. rupestre* populations are also very similar to each other. Comparison of all axes also indicates that *A. meonanthum* accessions are more similar to *A. siculum* accessions than to *A. braun-blanquetii* accessions, apart for along axis 4.

Accessions of *A. hispanicum* from Morocco are clustered closer to subsection *Antirrhinum* accessions along all axes. *A. majus tortuosum* accessions from Morocco and Italy are clustered with those from Spain and there is no differentiation of *A. majus litigiosum* accessions from Valencia from those distributed further north.

5.6.2 PCA of populations using continuous characters

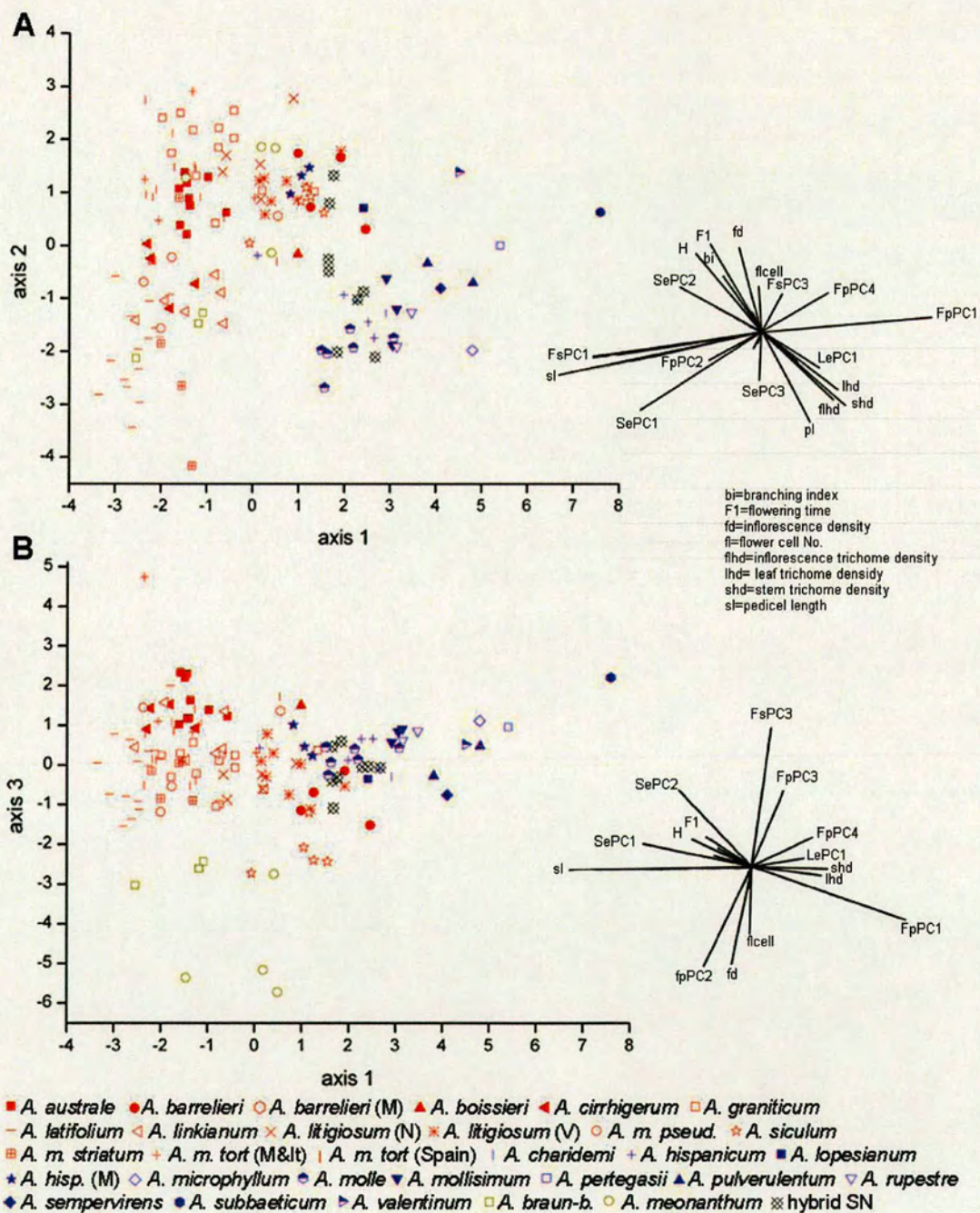
To determine the extent to which discrete characters distort the distances between taxa in multivariate space, a second analysis was carried out on continuous characters only (Table 5.8).

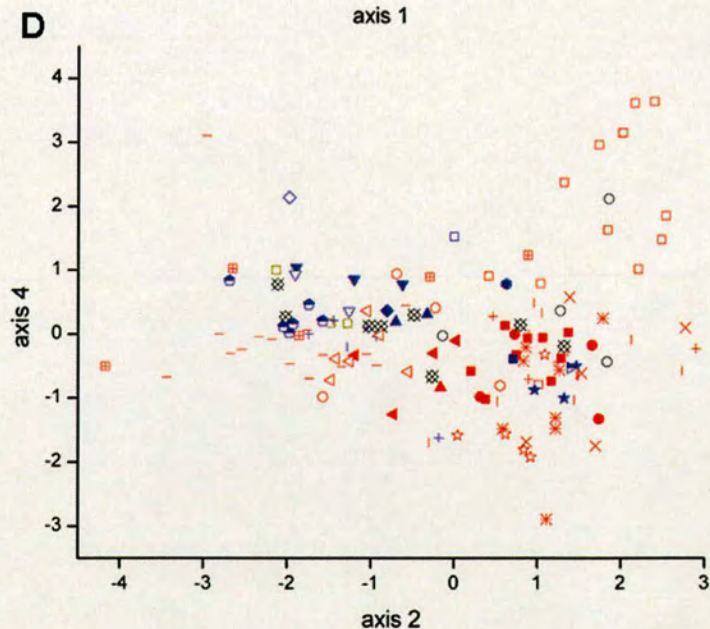
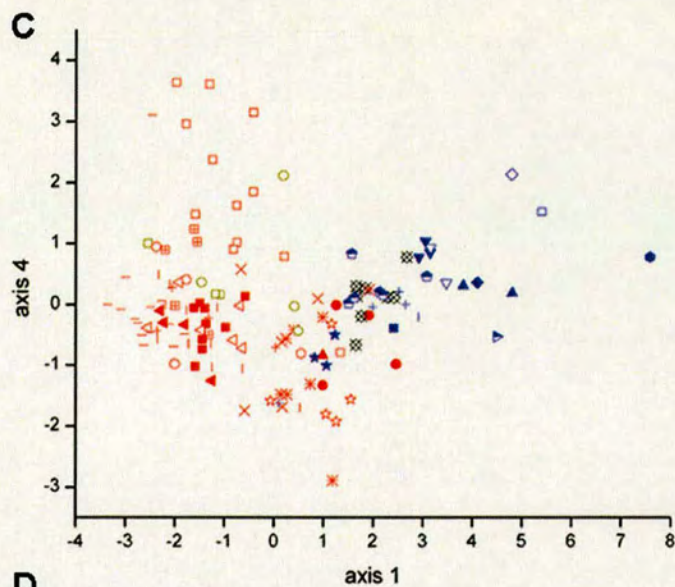
The main principal components accounted for a slightly higher proportion of the overall variation compared to the previous analysis (Table 5.7). Despite removing flower colour patterning and trichome characteristics, which are the most apparent characters which differentiate *Antirrhinum* species and have a greater influence in the PCA due to their discrete scoring, the phenotypic relationships of the taxa remain similar to the previous analysis (Figure 5.5). The main difference between the results of these two analyses is that the species with large pink flowers, *A. australe*, *A. m. tortuosum* and *A. m. pseudomajus*, have shifted toward the yellow-flowered taxa along axis 2.

Axis 1 is strongly correlated with flower size measures and the angle of the dorsal petal lobe, similar to all previous analyses. Sepal size and shape, trichome density, height, leaf size and shape and relative corolla tube size are all also correlated with axis 1, but to a lesser degree than the flower size measures (Table 5.8, Figure 5.5A). Small plants with small flowers, small

Character	axis 1	axis 2	axis 3	axis 4
LePC1	0.5	-0.2	0.2	0.0
LePC2	0.0	0.0	-0.2	-0.7
LePC3	-0.2	-0.1	0.1	-0.4
FsPC1	-0.9	-0.3	-0.1	0.0
FsPC3	0.9	0.1	-0.3	0.1
FpPC1	0.0	0.4	0.7	0.1
FpPC2	-0.2	-0.4	-0.6	-0.1
FpPC3	0.2	-0.1	0.6	-0.4
FpPC4	0.4	0.3	0.1	-0.1
SePC1	-0.6	-0.5	0.2	0.1
SePC2	-0.6	0.3	0.4	0.1
SePC3	0.0	-0.4	0.0	-0.1
SePC5	0.0	-0.3	0.1	-0.1
Flowering time	-0.4	0.7	0.0	0.1
Height	-0.6	0.6	0.0	-0.1
Inflorescence density	-0.1	0.3	-0.6	0.0
Stem diameter	-0.4	0.2	0.0	0.4
Branching Index	-0.4	0.5	0.0	0.5
Style length	-0.9	-0.3	0.0	0.0
Pedicle length	0.4	-0.6	0.2	0.2
Stem base trichome density	0.6	-0.4	0.1	0.3
Flower cell number	0.0	0.2	-0.6	0.0
Leaf trichome density	0.6	-0.3	0.1	0.4
Leaf cell no	0.0	-0.1	-0.1	0.6

Table 5.8. Continuous characters included in PCA of all populations (Section 5.6.3) and the correlation value of each character with each of the main axes.





■ *A. australe* ● *A. barrelieri* ○ *A. barrelieri* (M) ▲ *A. boissieri* ◄ *A. cirrhigerum* □ *A. graniticum*
 - *A. latifolium* ◁ *A. linkianum* × *A. litigiosum* (N) ✕ *A. litigiosum* (V) ○ *A. m. pseud.* ☆ *A. siculum*
 ▣ *A. m. striatum* + *A. m. tort* (M<) | *A. m. tort* (Spain) | *A. charidemi* + *A. hispanicum* ■ *A. lopesianum*
 ★ *A. hisp.* (M) ◇ *A. microphyllum* ● *A. molle* ▼ *A. mollissimum* □ *A. pertegasii* ▲ *A. pulverulentum* ▽ *A. rupestre*
 ◆ *A. sempervirens* ● *A. subbaeticum* ▴ *A. valentinum* □ *A. braun-b.* ○ *A. meonanthum* ✕ hybrid SN

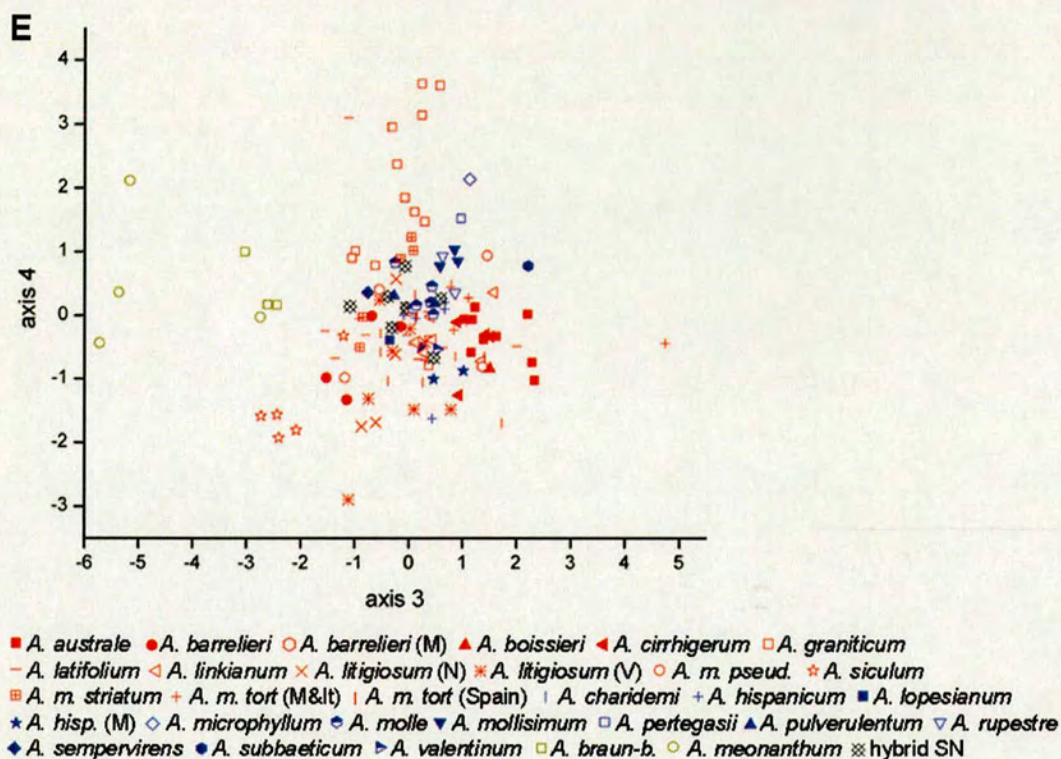


Figure 5.5. The positions of *Antirrhinum* populations plotted within the axes identified by PCA analysis using all continuous characters (Section 5.6.2).

Subsection *Antirrhinum* populations are represented by red symbols, *Kickxiella* by purple symbols, *Streptosepalum* by dark yellow symbols and *A. barrelieri* x *A. rupestre* hybrid individuals ('hybrid SN') by black symbols.

(A) Axis 2 plotted against axis 1.

(B) Axis 3 plotted against axis 1.

The vector plots alongside (A) and (B) indicate the relative strength and direction with which characters influence the positions of populations in the adjacent plot.

(C) Axis 4 plotted against axis 1.

(D) Axis 4 plotted against axis 2.

(E) Axis 4 plotted against axis 3.

narrow sepals, small, round leaves and a dense indumentum are associated with positive values of axis 1, whilst tall, mostly glabrous plants with large flowers are represented by negative values.

As for the previous analysis, flowering time and height are strongly correlated with axis 2, and in place of flower colour characters, pedicel length, trichome density, the number of flowers on the inflorescence and the branching index are also correlated in this analysis (Table 5.8). Positive values along axis 2 indicate tall, later flowering, less bushy plants with glabrous to sparsely hairy stems, dense inflorescences and short pedicels. The positions of taxa in the space defined by axis 1 and 2 are similar for those of the analysis with the discrete flower and trichome characters included, except *A. meonanthum* and *A. siculum* populations are no longer grouped with the other yellow flowered taxa (Figure 5.5A). Instead accessions of *A. meonanthum* are spread throughout the centre of the plot and those of *A. siculum* are clustered with *A. barrelieri*, *A. majus litigiosum* and *A. hispanicum* accessions from Morocco.

The correlations of traits which determine axis 3 are also similar to those for the analysis with discrete characters, with the size of the flower gibba and tube length (FsPC3), the inflorescence density and dorsal petal cell size again being strongly correlated (Table 5.8, Figure 5.5B). Subsection *Streptosepalum* species and *A. siculum* populations are again separated from the other species along axis 3 due to having relatively long corolla tubes with a large gibba and the cells on their dorsal petal lobes are smaller (Figure 5.5B).

Similar to the analysis of all characters in the previous section, axis 4 delimits *A. graniticum* accessions from the other taxa (Figure 5.5C). Whereas previously this was due to trichome characteristics, in this analysis a suite of other characters (which were more weakly correlated in the previous analysis) are correlated with axis 4. The most strongly correlated character is LePC2, which reflects the position of maximum width of the leaf, followed by leaf cell size, the branching index, FpPC3 (the relative width of the dorsal petal lobe) and the stem diameter at the base of the plant (Table 5.8). This axis indicates that *A. graniticum* plants are sparsely branched, have ovate leaves with small cells, the dorsal petal lobes of the flowers are narrow and the stem of the plant is thick compared to all other taxa. *A. meonanthum* populations share some of these characteristics with *A. graniticum*.

The exclusion of flower colour and trichome characters from this PCA analysis results in similar relationships, but less clear delimitation of species (Figure 5.5A-E). *A. majus tortuosum* and *A. australe* are not delimited in any of the axes that are studied. *A. majus striatum* accessions show large variation and are difficult to delimit from other large flowered subsection Antirrhinum species and similar to the previous analysis *A. majus pseudomajus*, *A. majus cirrhigerum* and *A. majus linkianum* cannot be delimited.

5.7 Neighbour-joining analysis of populations based on morphological distances

It is difficult to fully interpret the morphological relationships between populations in 4-dimensional space (Figures 5.1-5.5). To summarise the morphological relationships of populations, the Euclidian distances between all pair-wise combinations of populations were calculated and neighbour-joining was used to cluster the most similar populations together.

5.7.1 Neighbour-joining populations based on all characters

In the first instance, this was carried out in the phenotypic space defined by axes 1-4 of the PCA of all characters (Section 5.6.1). This representation of morphological relationships, in many cases, fails to cluster the populations of each species together (Figure 5.6). However, it does confirm the general trends in morphology that are observed in the plots of populations in axes 1-4 (Figure 5.4). The phenogram consists of three main branches, indicated by I-III on Figure 5.6, which for ease of description are called lineages. Populations of the pink-flowered *A. majus* sub-species, *A. majus cirrhigerum*, *A. majus linkianum*, *A. majus litigiosum* and *A. majus tortuosum*, and *A. australe* are clustered together in lineage 'I'. Populations of *A. majus cirrhigerum*, *A. majus linkianum* and *A. majus pseudomajus* are clustered on one branch of this lineage and within this branch many *A. australe* populations are also clustered together. *A. majus tortuosum* and *A. majus litigiosum* are clustered together on a separate branch. Lineage II has *A. graniticum* populations clustered together as a basal branch of the lineage. *A. meonanthum* populations and *A. siculum* populations then diverge from the rest of the lineage, which consists of the other yellow-flowered species *A. majus striatum*, *A. latifolium* and *A. braun-blauquetii*. The populations of *A. siculum*, *A. meonanthum* and *A. braun-blauquetii* are clustered into their respective species. Lineage III has populations of *A. majus litigiosum* from Valencia region, Moroccan *A. hispanicum* and *A. majus tortuosum* populations, *A. barrelieri* and *A. barrelieri* x *A. rupestre* hybrid populations forming a branch that diverges from the rest of the subsection Kickxiella species. *A. molle* is generally clustered with *A. mollissimum*, *A. hispanicum* and plants of *A. rupestre* morphology that are from *A. barrelieri* x *A. rupestre* hybrid

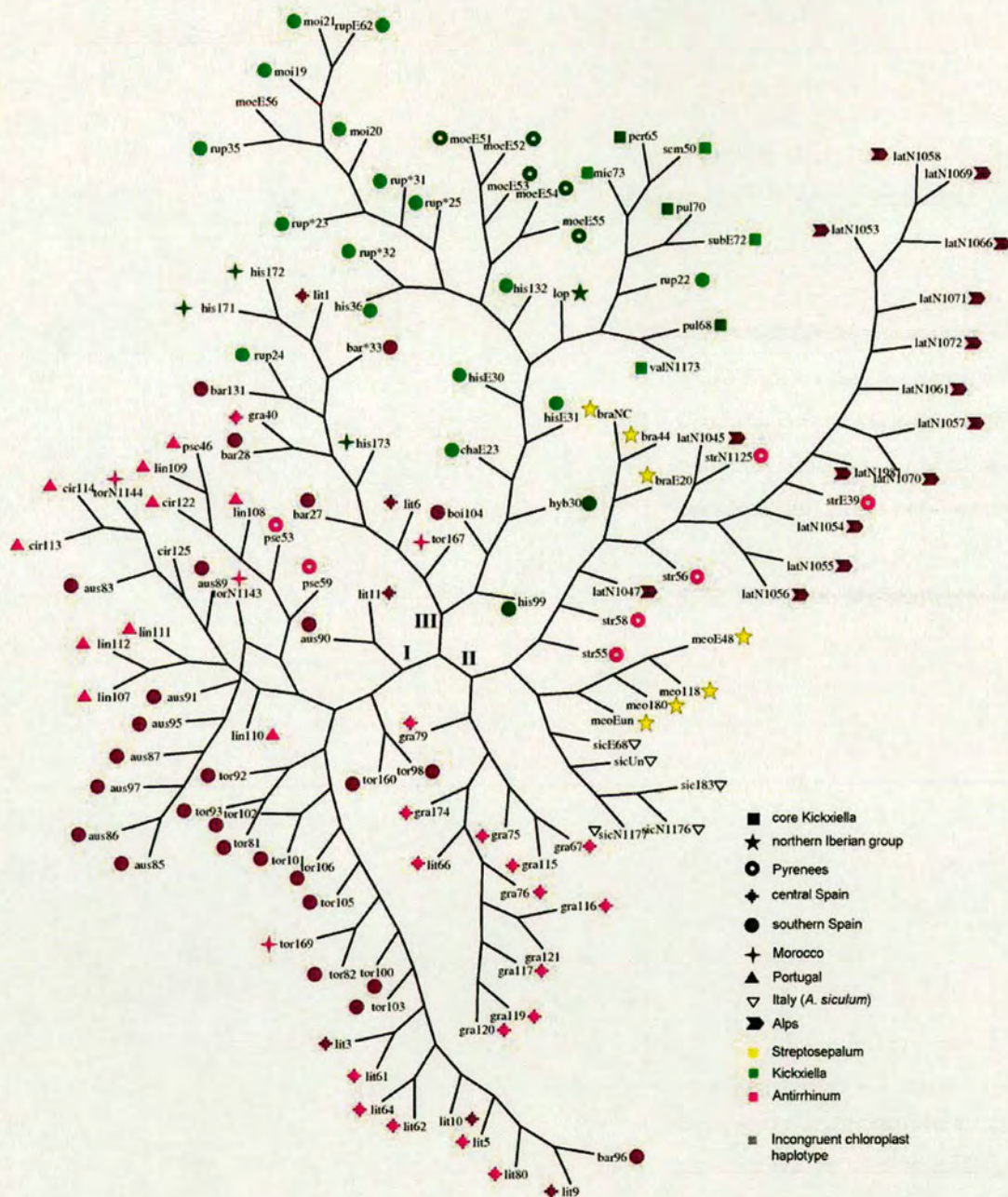


Figure 5.6. Neighbour-joining phenogram based on Euclidean distances between populations in the space defined by axes 1–4 of the PCA of all characters. The classical morphological subsections are indicated by yellow, green and pink (Streptosepalum, Kickxiella, Antirrhinum; respectively). Darker shading indicates species in which chloroplast haplotypes are incongruent to nuclear markers. The different symbols indicate the *Structure* population to which the individuals were assigned. In most cases, apart from the ‘core Kickxiella’ and ‘northern Iberian group’ this corresponds to a geographic region. The three main branches referred to in the text are indicated by ‘I’, ‘II’ and ‘III’. Branch

lengths are not shown to scale. Each population is labelled first by a three letter code of the species, followed by the population location number (Table 2.1). The species abbreviations are as follows:
 'aus' = *A. australe*, 'bar' = *A. barrelieri*, 'boi' = *A. boissieri*, 'bra' = *A. braun-blanquetii*, 'cha' = *A. charidemi*,
 'cir' = *A. majus cirrhigerum*, 'gra' = *A. graniticum*, 'gro' = *A. grosii*, 'his' = *A. hispanicum*, 'hisM' = *A. hispanicum* (Morocco), 'lat' = *A. latifolium*, 'lit' = *A. majus litigiosum*, 'lop' = *A. lopesianum*, 'lin' = *A. majus linkianum*, 'maj' = *A. majus majus*, 'meo' = *A. meonanthum*, 'mic' = *A. microphyllum*, 'moe' = *A. molle*, 'moi' = *A. mollisimum*, 'per' = *A. pertegasii*, 'pse' = *A. majus pseudomajus*, 'pul' = *A. pulverulentum*,
 'rup' = *A. rupestre*, 'sem' = *A. sempervirens*, 'sic' = *A. siculum*, 'str' = *A. majus striatum*, 'sub' = *A. subbaeticum*, 'tor' = *A. majus tortuosum*, 'torM' = *A. majus tortuosum* (Morocco), 'val' = *A. valentinum*.
 'bar*' and 'rup*' are Sierra Nevada hybrid populations of *A. barrelieri* and *A. rupestre* morphology, respectively.

populations. The core Kickxiella species and *A. lopesianum* are clustered together within lineage III.

The phenogram summarises the relationships observed in Figure 5.4 as the Kickxiella are distinguished from the Antirrhinum species. The morphological relationships of species contradict their genetic relationships. There is little evidence of species that are grouped by geographical area with nuclear markers having similar morphologies, apart from *A. barrelieri* and *A. rupestre* populations and populations of the southern Spanish Kickxiella species. Of the southern Spanish species, *A. australe* and *A. majus tortuosum* are more similar to the other subsection Antirrhinum species from western Portugal, *A. majus cirrhigerum* and *A. majus linkianum*, the Pyrenees species *A. majus pseudomajus* and the northern Spanish species, *A. majus litigiosum*, than to the southern Spanish Kickxiella. The southern Spanish Kickxiella are clustered within the Kickxiella lineage and are shown to be similar to *A. molle*. The northern Iberian group species are not clustered, with *A. meonanthum* being more similar to *A. siculum*, *A. braun-blanquetii* being more similar to *A. latifolium* and *A. majus striatum*, and *A. lopesianum* is clustered with the Kickxiella

5.7.2 Neighbour-joining populations based on continuous characters

When the morphological distances between populations are calculated from their positions in the space defined by principal components 1-4 of the analysis of continuous characters only (Section 5.6.2) there are substantial differences in the relationships of populations inferred by neighbour-joining analysis (Figure 5.7). The same three lineages are obtained, indicated on Figure 5.7, but some taxa are arranged in different lineages. This is mainly due to removal of flower colour information as *A. latifolium* and *A. majus striatum* populations now cluster with the pink-flowered *A. majus* subspecies and *A. australe* on lineage 'I'. *A. siculum* populations either cluster with *A. meonanthum* within lineage 'II' or with *A. barrelieri* and *A. majus litigiosum* populations on basal branches within lineage III. The subsection Kickxiella species are all clustered together on the same branch of lineage III, and *A. molle* populations are again grouped with populations from southern Spain - *A. mollissimum*, *A. hispanicum* and Sierra Nevada hybrid populations of *A. rupestre* morphology.

5.7.3 Summary of morphological relationships inferred by neighbour-joining.

The neighbour-joining analyses separate subsection Kickxiella species from subsection Antirrhinum. The Streptosepalum species, which have Kickxiella nuclear genotypes, are not

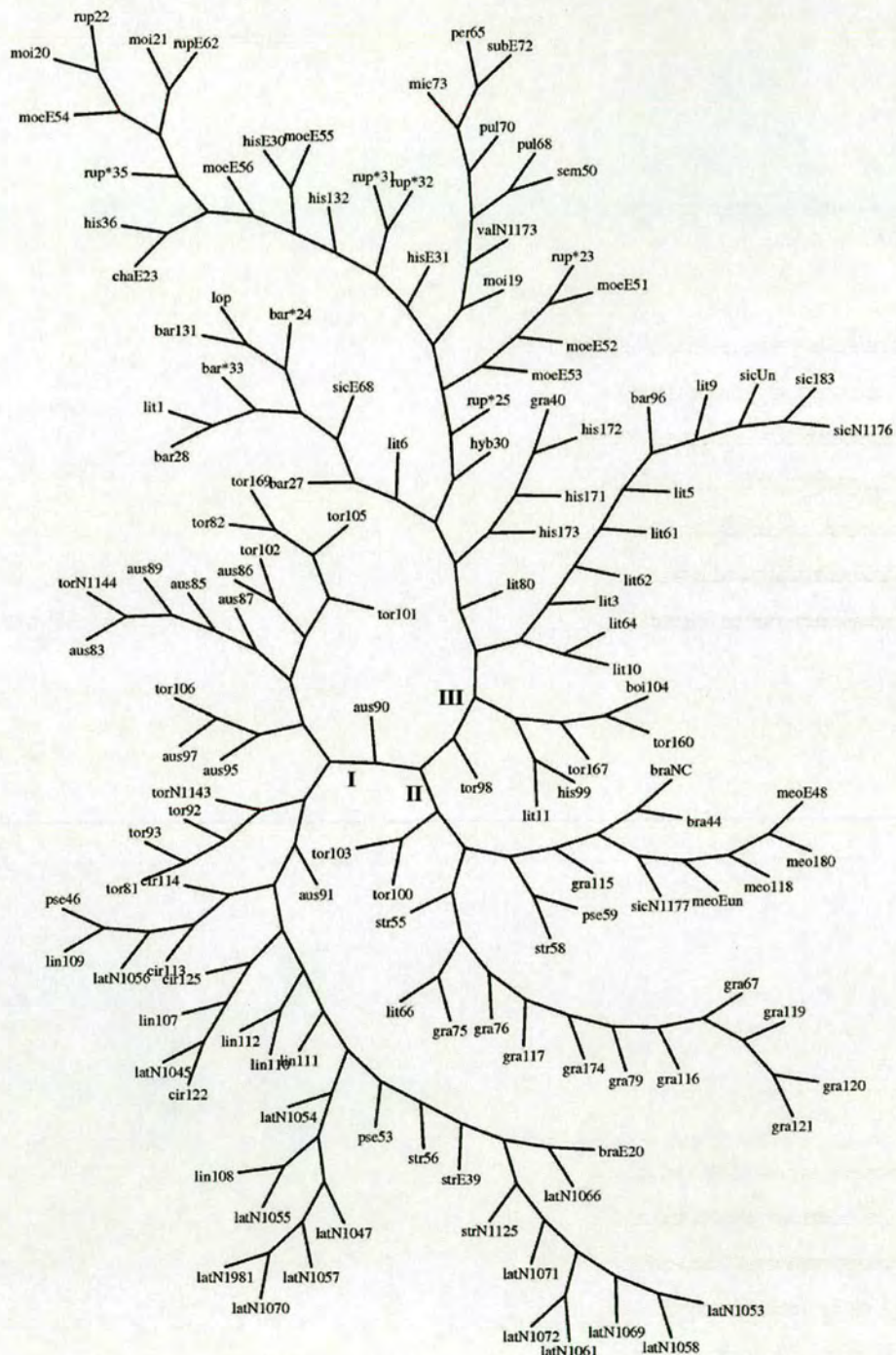


Figure 5.7. Neighbour-joining phenogram based on Euclidean distances between populations in the space defined by axes 1-4 of the PCA of continuous characters.
The tree main branches referred to in the text are indicated by 'I', 'II' and 'III'. Branch lengths are not shown to scale. The populations are as labeled in Figure 5.6.

grouped with the *Kickxiella* species in these analyses. *A. braun-blanquetii* is shown to be more similar to *A. majus striatum* and *A. latifolium*. *A. meonanthum* clusters with *A. siculum* when flower colour is included, or with *A. siculum* and two *A. braun-blanquetii* populations when flower colour characters are excluded.

These analyses identify previously unrecognised similarities of *A. siculum* with *A. meonanthum* when flower colour is included, or with *A. barrelieri*, *A. majus litigiosum* and *A. lopesianum* when flower colour is excluded. These relationships are also evident in Figures 5.4 and 5.5. The neighbour-joining analyses also confirm the similar morphologies of *A. molle* with the southern Spanish *Kickxiella* species, *A. mollisimum*, *A. hispanicum* and *A. rupestre*, and the *A. barrelieri* x *A. rupestre* hybrids.

5.8 Discussion

5.8.1 The multivariate compared to the univariate analysis

When considering the morphological characters individually, all analysed species had statistically significant differences in several characters compared to other species (Chapter 4). However, there was considerable intra-specific variation in many characters and some populations, particularly in southern Spain, were difficult to identify due to resembling other species for some characters. This situation is also reflected in the much debated taxonomy of the genus and difficulties in inferring the morphological relationships between species (Chapter 1.2).

Multivariate analysis was therefore undertaken to summarise the information across all characters in fewer dimensions. The PCA on all individuals (Section 5.4.1) showed that the individual plants of each species occupy a similar region of the phenotypic space, but there is substantial overlap of individuals from different species. However, it was only possible to use flower characters for the analysis of all individuals and there may therefore be insufficient information in flower characters alone to differentiate between some *Antirrhinum* species. The PCA on the mean population values of all characters (Section 5.6.1) does differentiate species due to the utilisation of more characters. However, there could also be increased clustering of populations compared to individuals as averaging each character reduces the effect of within population variation and variation introduced by experimental error. It is difficult to ascertain which of these factors increases the clustering of populations compared to individuals into species, but the analysis of the population means of flower characters alone (Section 5.5) shows more overlap of taxa than when all characters are included. Therefore is likely that there is not

enough information in the flower characters that were measured to cluster individuals into clearly delimited species.

5.8.2 Evaluation of the principal component analyses

Despite the first axes of the principal components analyses accounting for a small overall percentage of variation between accessions, the main morphological forms of the *Antirrhinum* genus are identified and the majority of species occupy a unique region of phenotypic space. The percentage of variation explained by principal components does not have any relation to the statistical significance of the result. The main criterion for determining the success of PCA in summarising variation is the difference between axes in the percent of variation explained: if all axes explain the same amount of variation then the technique has not been successful as all variables are independent. In each of the five analyses carried out in this chapter the first two PCs account for significantly more variation than the other axes, but the subsequent axes account for approximately the same proportions of variation. Despite the 3rd and 4th PCs accounting for a small percentage of the overall variation they do identify some species which are not delimited by the first two axes. The 5th and 6th axes accounted for a similar amount of variation as axes 3 and 4, but it was only feasible to visualise and interpret the first 4 PCs of each analysis. Therefore some information may have been lost from the analysis.

The inclusion of discrete characters such as flower colour and trichome characteristics did distort the distances between populations. With these characters included populations are clustered into three clumps corresponding to white-, yellow- and pink- flowered species, respectively. The relationships of *A. meonanthum* and *A. siculum* to other taxa were different between the analyses with, compared to those without, discrete characters included.

5.8.3 Species delimitation

Most species apart from two groups are separated from other species in at least one of the 4 dimensions plotted in Figures 5.4 and 5.5. The first group of species that are not delimited consists of *A. majus pseudomajus*, *A. majus cirrhigerum* and *A. majus linkianum*, and the second group consists of *A. barrelieri* and *A. majus litigiosum*.

The neighbour-joining analyses cluster morphologically similar groups of species, for example, the *A. majus* subspecies, the core Kickxiella species and the southern Spanish Kickxiella. However, they do not delimit species, apart from *A. siculum*, *A. meonanthum* and *A. braun-*

blanquetii in Figure 5.6. This partly reflects the relative positions of the populations in phenotypic space shown in Figures 5.4 and 5.5, as many populations of the same species are more distant to each other than to populations of another species along at least one axis, due to intra-specific variation. This results in the Euclidian distance between populations of the same species being increased. A further disadvantage of representing morphological relationships using a neighbour-joining phenogram is that this method assumes that the relationships between populations conform to a nested-hierarchical pattern (de Quieroz 1997), which is probably invalid for the *Antirrhinum* species due to their reticulate evolution. It is therefore appropriate to interpret the neighbour-joining results in combination with visual comparison of the relationships of populations in phenotypic space (Figures 5.5 and 5.6)

Even when all characters are included in the PCA (Section 5.6.1) populations of each taxon neighbour or in some cases overlap those of morphologically similar taxa (apart from the subsection *Kickxiella* species) and may be dispersed along any one axis. For most of these cases it is likely that missing data for some populations, the methods used to quantify characters and the characters chosen for analysis have all led to some inaccuracy and inflated within species variation. I will briefly consider each of these three factors in reducing the effectiveness of the PCA in determining the main axes of variation. In the case of the first factor, missing data, the program used to carry out the PCA substitutes the mean value of the character for missing data entries. Therefore populations with a higher proportion of missing characters are observed to be closer to the centre of the phenotypic space than other con-specific populations. For the second factor, the methods used to quantify some morphological characters such as the trichome characteristics, branching index, inflorescence density and corolla shape also introduced noise into the analysis; the variation of these and further characters are discussed in more detail in chapter 4. Thirdly, the choice of characters for analysis: in general characters which have historically been used in the definition of *Antirrhinum* species were targeted. However, some characters, such as the branching index and the density of the inflorescence are included because they are considered important in understanding overall morphology and its possible relationship to the ecology of the *Antirrhinum* species. The disadvantage of including such characters is that they vary with environmental conditions and given the variable growth conditions (Chapter 2.2.1) may have introduced non-genetic variation into the analysis. Given that these three factors each introduce within as opposed to between species variation, they all act to reduce the power of the PCA in delimiting species.

The extent of delimitation of species is likely to be further under-estimated as some characteristics of species are difficult to describe quantitatively using a metric that can be incorporated into multivariate analysis. For example, some species were observed to have characteristic trichomes which could not be adequately categorised, *A. australe* accessions all have a distinctive plant shape due to the angles at which their branches grow and many *Kickxiella* species are decumbent. Furthermore, although all attempts were made to analyse key characters, due to time and resource constraints some taxonomically important characters such as the bract size and shape and the surface characteristics of seeds could not be analysed.

5.8.4 Morphological characteristics of the main *Antirrhinum* lineages

Two distinctive morphologies corresponding to the *Antirrhinum* and *Kickxiella* subsections are recognised by the PCA analyses of both all characters and continuous characters only. The main characters that distinguish these two groups are identified by the first two axes of each analysis - leaf size, flower size and plant height. The angle of the dorsal petal lobe to the tube, flower colour patterning and trichome morphology and distribution are also highly correlated with these axes.

Plants within subsection *Antirrhinum* have large pink or yellow flowers with large sepals, a yellow face patch, yellow tube patch and yellow tube hairs. The dorsal petal lobe is horizontal to the tube. They are mostly tall and late flowering with suppressed branch outgrowth, apart from *A. majus pseudomajus* and *A. majus striatum*. Their leaves are large, lanceolate to linear and are glabrous or sparsely hairy. Trichomes on their stems are also less dense than in *Kickxiella* species. The exceptions to these generalisations are *A. siculum*, *A. meonanthum* and *A. barrelieri*, which all have smaller, more *Kickxiella*-like flowers.

Plants within the *Kickxiella* subsection are characterised by small white flowers with a purple face patch, small narrow sepals, longer pedicels, and the dorsal petal lobe is perpendicular to the tube. They are short and early flowering and have smaller, more rounded leaves with a dense indumentum, both on their leaves and stems.

Further characters such as the relative size and width of the dorsal petal lobe (FpPC2 and FpPC3 respectively), the size of the gibba, trichome morphology, stem width and inflorescence density then separate species within the subsections.

Most characters were observed to show high intra-specific variation, including the flower colour patterns such as the purple patch, yellow tube hairs and yellow patches on the face and ventral tube and are therefore not diagnostic for species. Despite the observation of intra-specific variation, both in the univariate comparisons and along axes of the PCA, there is little evidence of there being a continuum of phenotypes between *Antirrhinum* and *Kickxiella* as was perceived in the field, particularly within southern Spanish species. This may be due to the relatively consistent growth conditions. Some populations of *A. majus litigiosum* (from Valencia region), *A. barrelieri* and *A. boissieri* are positioned intermediate between subsection *Antirrhinum* and *Kickxiella*. However, their position in the space defined by the PCA axes is probably determined by their small flower size, which pulls them towards the *Kickxiella* group.

5.8.5 Morphologies of species that have undergone hybridisation

When considering each of the instances of inferred hybridisation the species involved are constrained to either the *Antirrhinum* or *Kickxiella* morphology. There is little pattern in terms of which morphology a species that has undergone hybridisation will take. One group of species have the morphologies of their nuclear genotypes. For example, *A. latifolium*, which has a *Kickxiella* chloroplast haplotype but *Antirrhinum* nuclear signal is grouped with subsection *Antirrhinum* species and has the lowest axis 1 values (i.e the most ‘*Antirrhinum*’ morphology). *A. molle*, *A. sempervirens*, *A. lopesianum* and *A. pulverulentum* have *Antirrhinum* chloroplast haplotypes but *Kickxiella* nuclear signal and morphology. The other group of species has morphologies incongruent with their nuclear genotypes. The southern Spanish *Kickxiella* species *A. charidemi*, *A. hispanicum*, *A. mollisimum* and *A. rupestre* have *Antirrhinum* nuclear signal but *Kickxiella* morphology. Conversely, the northern Iberian group species, *A. braun-blanquetii* and *A. meonanthum*, have subsection *Antirrhinum* morphology yet *Kickxiella* nuclear signal. There therefore does not seem to be any directionality of gene-flow of nuclear or chloroplast haplotypes between the two lineages.

In contrast to the AFLP results, which group *A. braun-blanquetii* and *A. meonanthum* with the *Kickxiella*, *A. braun-blanquetii* is morphologically more similar to *A. latifolium* and *A. majus striatum*, whilst *A. meonanthum* is shown to be more similar to *A. siculum* and *A. graniticum*. However, some axes show that characters such as the size of the gibba, the relative tube size and sepal shape are shared by *A. braun-blanquetii* and *A. meonanthum*. *A. siculum* is also shown to be similar to these species for these characters. As *A. siculum* is sister to the *Antirrhinum* subsection species, this suggests that *A. braun-blanquetii* and *A. meonanthum* may be derived

from an early subsection *Antirrhinum* lineage that then underwent subsequent hybridisation with *Kickxiella* species.

Notably, species which have undergone hybridisation in different geographic areas have similar morphologies. For example, *A. molle*, which is of an independent hybridisation event to *A. mollissimum*, *A. rupestre* and *A. hispanicum*, occupies a similar region of morphological space to these species. These species share some distinct morphological characters, which are not observed in other species. For example, their leaves and stems are densely covered with long multi-cellular glandular trichomes.

Likewise, *A. barrelieri* and *A. majus litigiosum* occupy the same phenotypic space. Furthermore, when flower colour is excluded they overlap with *A. siculum*, which is of a completely different lineage. These results suggest that there are constraints to *Antirrhinum* morphology

5.9. Conclusions

Despite the large proportion of missing characters for some populations and loss of information due to character coding, populations of each *Antirrhinum* species cluster together but are not clearly delimited. Although too few populations of most *Kickxiella* species were grown in standard conditions to test their delimitation rigorously, their morphology was observed to vary little in the field and the extremely rare *Kickxiella* species grow in just a few closely situated locations, with there being little scope for intra-specific variation. The plants that were grown in this study were therefore considered representative of these species.

The main *Antirrhinum* lineages are each distinguished by a set of correlated morphological traits. There is little evidence that morphological variation is structured geographically like that of genetic variation. This indicates constraint to *Antirrhinum* morphology. However, within subsections *Antirrhinum* and *Kickxiella*, populations are dispersed in phenotypic space due to high levels of intra- and inter-specific variation.

Chapter 6: Discussion

In this study, samples from populations from throughout the distribution of each *Antirrhinum* species were genotyped for AFLPs and chloroplast haplotypes. Population assignment, phylogenetic and ordination analyses were carried out on this data to test species delimitation and identify hybridisation between species. The interpretation of the results of these analyses within a geographic context enabled a strong hypothesis to be developed for the evolutionary relationships of the *Antirrhinum* species. A model is proposed for the evolution of *Antirrhinum*. In this model, two main lineages diverged, each broadly corresponding with the morphological subsections, *Antirrhinum* and *Kickxiella*, which were defined by Rothmaler (1956). Subsequent to their divergence, hybridisation between these lineages occurred in regions where their species come into contact. There is some evidence that in many of these episodes of hybridisation there were high levels of gene flow between these divergent lineages. For example, inclusion of species that have been involved in hybridisation into phylogenetic reconstructions decreases resolution and support of the resulting phylogeny. Many species are also fixed for incongruent chloroplast haplotypes compared to their morphology and nuclear genotype and there is a strong geographic structuring of genetic variation.

Principal coordinates analysis was used to define the genetic space of *Antirrhinum* using the AFLP genotypes of all samples. Individuals of the same species occur within a similar region of this space, indicating that most species have cohesive genetic similarities. However, there is considerable overlap of each species with its neighbours in this space. This could be due to noise within the AFLP dataset from inconsistent experimental conditions and band size homoplasy. However, it could also reflect the patterns of hybridisation that were identified.

The morphologies of plants from the same populations that were genotyped were also examined and morphological variation within and between species characterised. The first aim of this analysis was to provide a foundation for identifying the molecular basis of natural variation within *Antirrhinum*. The second aim was to compare the distribution of morphological variation to that of genetic variation. To enable such a comparison, the phenotypic space of *Antirrhinum* was defined and populations of all species were plotted within this space. Two groups were identified that correspond with the two evolutionary lineages that were defined by the genetic analyses. Within each of these groups, populations are dispersed in phenotypic space. The patterns of morphological delimitation of species were found to be similar to those of genetic delimitation: populations of

each species cluster together, but there are high levels of intra-specific variation and neighbouring species overlap in morphological space.

These results lead to two main questions that will be discussed in this chapter. The first is the extent to which the evolutionary model proposed for *Antirrhinum* is consistent with the geological history of the Mediterranean region. The second main question is how hybridisation between species of divergent *Antirrhinum* lineages has affected the structure of morphological and genetic variation within the genus. Resolving this question may provide an insight into the evolutionary forces acting on *Antirrhinum* populations.

To address these questions the current ecologies of the *Antirrhinum* species are used as a frame of reference to infer how the geological and climatic history of the Mediterranean may have shaped the evolution of the genus. This approach rests on two assumptions. The first is that morphological attributes have played a consistent and predictable role in plant function, which may not be the case because morphological traits may not be adaptive for the reasons they are hypothesised to be (e.g. Haworth and McElwain 2008). The second is that *Antirrhinum* species are optimally adapted to their environment, when there could be other explanations for their morphology (Gould and Lewontin 1979, Herrera 1992). However, broad associations have been identified between plant morphology and climate that are consistent with current distributions of *Antirrhinum* species. Furthermore, this discussion aims to make underlying assumptions of the evolutionary hypothesis that is developed to explain the diversification of the *Antirrhinum* genus explicit and therefore amenable to further testing.

6.1 Association of *Antirrhinum* and *Kickxiella* morphologies with their ecology

Kickxiella species such as *A. charidemi*, *A. mollisimum*, *A. subbaeticum*, *A. pulverulentum* and *A. microphyllum* occur in hot, arid regions whilst *A. molle*, *A. grosii*, *A. pertegasii* and *A. sempervirens* are found in alpine habitats. The main determinant of their growth form may therefore be that they grow on rock faces. Due to their specific habitat requirement, most *Kickxiella* species exist as endemic populations within specific mountain ranges and river gorges. Their distribution patterns may be limited because they cannot compete with other vegetation in habitats less extreme than cliffs and at lower altitudes (Davis 1951, Birks 2008). This is supported by preliminary analyses carried out on *A. barrelieri* x *A. rupestre* hybrid populations in the Sierra Nevada mountain range. The general *Kickxiella* morphology (*A. rupestre*) was found to be associated with vertical rock

faces with little vegetation cover and the *Antirrhinum* morphology (*A. barrelieri*) with roadside habitats with up to 100% vegetation cover (data not shown).

In contrast to *Kickxiella* species, species of subsection *Antirrhinum* grow in a variety of habitats and were collected from roadsides, within hedges, in various forest types such as pine and oak, and on rock faces. Their distribution therefore appears less constrained and they are both more widespread and more abundant. Species of subsection *Antirrhinum* also occur on walls and rock faces, at high altitudes and within the same hot, arid conditions as *Kickxiella* species. They are frequently observed growing in sympatry, in habitats perceived to be identical, despite their vast morphological differences.

6.2 The evolution of the *Antirrhinum* genus in the context of the geological history of the Mediterranean region

To develop a rigorous hypothesis of the diversification of the *Antirrhinum* it is essential to interpret its evolution in the context of the geological history of the Mediterranean region. The Mediterranean region has an exceptionally high diversity of plant species with a high proportion of endemic taxa (Medail and Quezel 1997, Mota *et al* 2002). This can be partly explained by its position at the convergence of different geographic regions (Mansion *et al* 2001, Comes and Kadereit 2003). However, its geology and topography is complex and diverse (Rivas-Martinez *et al* 1997, Mota *et al* 2002) and Quaternary glacial cycles have led to frequent fragmentation and merging of populations and species within the region (Willis and Niklas 2004, Medail and Diadema 2009). Relating the genetic structure of *Antirrhinum* to that found within other groups of organisms should enable the role of geological processes that lead to vicariance in causing diversification (Avice 2000 and 2007).

6.2.1 The Mediterranean climate since the late Tertiary

Reconstructions of the climate in the Mediterranean 5.35-5 million years ago (Ma) by Fauquette *et al* (1999) showed that the southern part of Spain and northern Africa had temperatures between 0°C and 5°C higher than today with similar or lower precipitation. Surrounding regions – Portugal, northern Spain and France – had temperatures 1°C to 5°C higher and precipitation was higher or similar to modern levels. There is evidence that the climate started cooling approximately 3.2 Ma, corresponding with the onset of the Mediterranean climate of hot, dry summers and wet winters (Suc 1984). Following this, climatic oscillations started occurring approximately 2.3 Ma, with glaciations intensifying during the Pleistocene (Suc 1984, Tzedakis 2007).

The Iberian, Italian and Balkan peninsulas remained unglaciated during the Quaternary ice ages, apart from their main mountain ranges (Hughes *et al* 2006), and were therefore refugia for many organisms during these periods (Hewitt 2000). However, the glacial cycles drastically affected these peninsulas. Climate reconstructions using palynological records of the Velay sequence in southeastern France show that interglacial periods were much warmer and more humid than glacial periods. Over the last 450 Ka the annual precipitation was $> 800 \text{ mm year}^{-1}$ and the January temperature $> 2^{\circ}\text{C}$ during interglacial periods, compared to precipitation of $< 400 \text{ mm year}^{-1}$ and January temperatures between -10°C and -15°C in glacials (Cheddadi *et al* 2007). The effects of these climate changes were not homogeneous throughout the Quaternary or throughout the region, with the complex topography of the Mediterranean providing a range of local climates and habitats (Tzedakis 2007). Mountain ranges played a key role in facilitating the persistence of populations by enabling them to track suitable climate by shifting in altitude and, during glacial periods, providing microhabitats with increased moisture availability in gorges and valleys (Willis and Niklas 2004, Medail and Diadema 2009). They may therefore act as interglacial refuges, allowing the persistence of cold-adapted or ‘uncompetitive’ plants, or as glacial refuges, depending on ecology of each species (Bennet and Provan 2008).

6.2.2 The diversification of the main *Antirrhinum* lineages

Molecular dating indicates that the *Antirrhinum* species diverged less than 5.3 Ma (millions of years ago) based on evolution of *CYCLOIDEA*-like gene sequences (Gübitz *et al* 2003) and 4.1 Ma based on calibration of *TrnK-MatK* sequence evolution using the estimated date of the Plantaginaceae-Scrophulariaceae split (Vargas *et al* 2009). This timing of divergence is also congruent with that of other plant and animal taxa in the Mediterranean (Comes and Kadereit 2003, Gomez and Hunt 2007), suggesting that climate change since the Pliocene has been a key process driving diversification of the genus.

The rooted chloroplast haplotype network suggests that the *Antirrhinum* and *Kickxiella* lineages diverged from a common ancestor as the node joining the out-group to the *Kickxiella* lineage is central to the chloroplast haplotype network (Figure 3.4). It is therefore difficult to infer the attributes of the ancestral *Antirrhinum*. Based on the distributions of extant *Kickxiella* species, the ancestral *Kickxiella* was likely to have been present in the southern part of the Iberian peninsular and northern Africa ~5Ma. It may therefore have been adapted to high temperatures and droughts as the results of climatic models show that this region was hot and arid during this period (Fauquette *et al*

1999, discussed above). It then became fragmented possibly with species evolving in isolation. It is difficult to ascertain the timing or causes of this fragmentation, because *Kickxiella* populations could either have colonised mountain ranges before the onset of the glacial cycles or as a consequence of them. Accurately resolving the timing of the divergence of the *Kickxiella* species would indicate whether the *Kickxiella* colonised mountain ranges during the Tertiary or whether mountain ranges became glacial or interglacial refuges for *Kickxiella* populations during the Quaternary, leading to their divergence.

Given their endemic nature and similar morphology, this mode of divergence of the *Kickxiella* is more likely than that of *Kickxiella* populations spreading with divergence occurring in outlying populations. It is also consistent with the lack of geographic relationships between chloroplast haplotypes and lack of haplotype fixation in the *Kickxiella* species, which suggest relatively simultaneous isolation from a large ancestral population. Similar evidence is provided by the low levels of isolation-by-distance between *Kickxiella* populations (Jimenez 2005).

The mechanisms that have been suggested to promote sympatric speciation, such as disruptive selection of traits that promotes non-random mating (Savolainen *et al* 2006) are unlikely to apply to *Antirrhinum*. All *Antirrhinum* species form fertile hybrids, members of subsections *Antirrhinum* and *Kickxiella* are observed growing together, there is no current evidence for species-specificity of bee pollinators (E. Coen and C. Thébaud, pers. comm.) and, although not tested rigorously, flowering times were observed to overlap in wild populations (pers. observ.). Therefore, only allopatric models of divergence are considered, which implies that geographic isolation has had a key role in morphological evolution within *Antirrhinum*. The *Antirrhinum* and *Kickxiella* lineages may have diverged prior to the onset of the glacial cycles ~ 2.7 Ma (Suc 1984) with the ancestral *Antirrhinum* species occurring more mesic conditions than have been modelled as for the current range of *Kickxiella* species (Fauquette *et al* 1999) or further to the east, for example in the Balkans. An alternative hypothesis is that the *Antirrhinum* lineage became isolated from *Kickxiella* more recently, during the Quaternary, and dispersed throughout the Mediterranean region. Both of these hypotheses are feasible given the inaccuracies associated with molecular dating (Renner 2005, Welch and Bromham 2005) and are difficult to test because of the reticulate evolution of *Antirrhinum*.

6.2.3 Phylogeographic comparisons of *Antirrhinum* to other organisms

Comparative phylogeographic studies of numerous taxa have identified concordant patterns of genetic structure within the Iberian Peninsula (Gomez and Hunt 2007) and the Mediterranean region (Medail and Diadema 2009). These studies suggest mountain ranges act as refugia during the glacial cycles. Gomez and Hunt (2007) compared phylogeographic studies of freshwater and terrestrial organisms – lizards, mammals, invertebrates and plants – and identified similar geographic patterns of population and species divergence across taxa. The patterns of divergence within freshwater organisms correspond to the main drainage basins and for terrestrial organisms indicate separate refugia corresponding to mountain ranges. Similarly, Medail and Diadema (2009) compared intra-specific phylogeographic studies of around 40 tree species and a similar number of herbs, identifying similar genetic structures corresponding to mountain refugia.

The model of the evolutionary history of the *Antirrhinum* species proposed in Chapter 3 is consistent with the patterns of isolation and divergence of the taxa in other studies in two respects. Firstly, the endemic *Kickxiella* species occur within the main mountain ranges. Secondly, the geographic groups of species that cluster in neighbour-joining phylogenies and recognised as populations by *Structure* simulations broadly correspond to regions that have been identified as refugia. For example, in *Pinus sylvestris* different mitochondrial haplotypes predominate in each of three different regions: the Betic Sierras, central Spain and the Pyrenees (Sinclair *et al* 1999, Soranzo *et al* 2000). Within *Antirrhinum*, distinct populations from each of these broad geographic regions were recognised by *Structure* simulations carried out in this study. Other populations recognised by the neighbour-joining and *Structure* analyses correspond to central Spain and the northern region of Spain. Distinctive populations of other taxa within these regions have also been recognised, for example, *Chorthippus parallelus* populations from each these regions have different chromosome structures (Bella *et al* 2006).

6.3 The role of hybridisation in the evolution of *Antirrhinum*

The molecular analyses carried out in Chapter 3 suggest that hybridisation has occurred between the *Antirrhinum* and *Kickxiella* lineages in several different geographical regions where their species come into contact. These regions of hybridisation correspond to Iberian refugia that have been identified for other taxa (described above, Section 6.2.3). The spatial patterns of genetic relationships are consistent with localised hybridisation having occurred between the *Kickxiella* species endemic to each mountain range and members of subsection *Antirrhinum* that were present within each refugium. *Kickxiella* and *Antirrhinum* species are more likely to come into contact during glacial periods as *Kickxiella* populations would probably occur at lower altitudes, as

proposed by Hewitt (1996), and has been inferred for other alpine plant species (Gutierrez Larena *et al* 2002, Kropf *et al* 2006 and 2008, Dixon *et al* 2007). However, in some regions, subsection *Antirrhinum* species are currently observed growing in sympatry with *Kickxiella* species so this model may not strictly apply to *Antirrhinum*.

6.3.1 Evidence for *Antirrhinum* morphology being constrained

The structure of genetic variation identified in Chapter 3 suggests that in many of these instances of hybridisation there have been high levels of gene flow between species of the divergent *Antirrhinum* lineages. However, the distribution of populations in phenotypic space identifies two main clouds, each corresponding to one of the subsections *Antirrhinum* and *Kickxiella*. This suggests that despite this hybridisation, morphology within *Antirrhinum* is constrained within the bounds of these two types.

It is difficult to estimate the frequency of hybridisation between *Antirrhinum* species within each geographic region based on the data presented in this thesis and each episode of hybridisation is likely to have had unique characteristics. Preliminary characterisation of populations of *A. barrelieri* (subsection *Antirrhinum*) and *A. rupestre* (subsection *Kickxiella*) in the Sierra Nevada Mountains suggests that hybrids between these species are frequent. Two populations, consisting of potential early generation hybrids, were found to segregate for morphological characteristics of the parents and putative back-cross hybrid populations had similar morphology to one or the other parental species (data not shown). This suggests a high level of gene flow between these species, yet constraint on morphology. Further evidence for morphological constraint is that different episodes of hybridisation between the two main lineages is inferred to have occurred in five geographic regions and in each region the resulting populations have either the *Antirrhinum* or *Kickxiella* general morphology.

There are two general classes of models to describe the outcome of hybridisation between divergent populations, or species, which place different emphasis on the role of selection. The first are based on the Dobzhansky-Muller model of speciation and assume that all alleles within a species are selected to be compatible with each other. Hybridisation therefore results in the mixing of incompatible alleles and most hybrid progeny are less fit than parental populations (Orr 1996, Gavrillets 1997, Machado *et al* 2002). Hybrids between divergent species are therefore likely to be very infrequent, though F1 individuals may back-cross to one or other parental genotype reducing the level of allelic incompatibility. Despite the rare occurrence of hybrids, neutral or advantageous

loci from one species may spread rapidly through to the other (Barton and Hewitt 1985, Barton 2001), as has been shown for red and sika deer in Scotland that have hybridised infrequently since sika deer were introduced a century ago (Goodman *et al* 1999).

The other class of models places a greater emphasis on selection acting on specific loci that confer species-specific adaptations (Machado *et al* 2002). Under this model, hybrids may be more frequent, allowing high levels of gene flow for selectively neutral loci. Morphological divergence is therefore maintained by selection of loci that underlie adaptive traits. This has been demonstrated for morphologically divergent insect species that show strong host plant associations, for example, lycaenid butterflies (Nice *et al* 2002) and walking-stick insects (Nosil *et al* 2007). Within plants, similar patterns of differential gene flow have been inferred for two morphologically and ecologically distinct *Silene* species (Minder *et al* 2007, Minder and Widmer 2008).

The main difference between these models is the number of loci on which either endogenous (genetic incompatibilities) or exogenous (environmental) selection acts. There is potential evidence for Dobzhansky-Müller type incompatibilities in *A. majus* x *A. molle* hybrids as for some loci in the F2 population there are lower than expected occurrences of certain genotypes (Schwarz-Sommer *et al* 2003b). However, based on the high levels of gene flow that are inferred to have occurred during most episodes of hybridisation in *Antirrhinum* the latter model may apply to *Antirrhinum*. Subsection Kickxiella species may be adapted to different habitats to *Antirrhinum* species, as preliminary results for *A. barrelieri* and *A. rupestre* suggest.

6.3.2 Possible Adaptive constraints

The model of high levels of gene flow of selectively neutral alleles requires strong environmental selection on key loci that underlie the divergent morphologies of species. The phenotypic analysis identified correlations between morphological traits within *Antirrhinum*, with a suite of morphological traits defining each of the two main groups. The main traits associated with the Kickxiella were small white flowers with a purple face patch, small more rounded leaves, early flowering and a dense covering of hairs on both the stem and leaves. The Kickxiella species mainly grow in alpine or desert habitats. Despite the many perceived differences between these habitats, plants may face similar challenges in them, associated with water conservation and heat dissipation. Alpine and desert plants have been found to have similar morphological characteristics, such as dwarf habits, small leaves with thick cuticles and dense pubescence and there are examples of close phylogenetic relationships between desert and alpine species, for example, flora in the Californian

Sierra Nevada mountains are of genera common in nearby deserts (Billings and Mooney 1968). The smaller leaves of alpine and desert plants might be constrained by water use efficiency (Smith and Geller 1979). Correlations between leaf size and plant size with rainfall have been identified (McDonald *et al* 2003) and small leaves have better water use efficiency as they dissipate heat more effectively by convection (Parkhurst 1972, Vogel 2009). Small leaves may also be advantageous at high elevations, where solar irradiation is higher but thermal conductivity of air at reduced pressure is lower, contributing to increased heat gain, particularly in larger leaves (Smith and Geller 1979, Koerner 2007). Furthermore, cliff vegetation in the Mediterranean region is exposed to high solar radiation, wind stress and drought (Gouvra and Grammatikopoulos 2007). The stems and leaves of all *Kickxiella* species have a dense covering of trichomes that may reduce over-heating by reflecting radiation (Ehleringer *et al* 1976), providing a greater surface area for heat conductance (Wolpert 1962) or prevent water loss through evaporation (Fahn 1986). Trichomes have also been shown to prevent UV damage to plants (Karabourniotis and Bornman 1999, Manetas 2003) and may therefore be adaptive in alpine species.

In contrast to the *Kickxiella*, the traits associated with *Antirrhinum* populations are large pink or yellow flowers with yellow tube hairs, a yellow face and tube patch, large, more linear leaves, late flowering and sparse or absent trichomes on the stems and leaves. These traits may enable plants within subsection *Antirrhinum* species to compete with other vegetation in less extreme conditions than those in which the *Kickxiella* species grow. The large upright stature of subsection *Antirrhinum* plants is consistent with the observation that they grow amongst other vegetation such as grasses and shrubs. The larger plant height and leaf and flower size may reflect a greater investment in growth, reproduction and dispersal than the endemic *Kickxiella* species, which may be constrained by the availability of resources and seedling establishment (Lavergne 2004).

The observation of *Kickxiella* and *Antirrhinum* populations growing in sympatry in many geographic regions in similar habitats does not support the interpretation that there are strong selective pressures for each of these different morphologies. However, it is difficult to determine the fitness of subsection *Antirrhinum* plants currently growing in habitats typical of *Kickxiella* species. This would require detailed studies of the fitness of each morphology in different habitats. Current hybridisation identified in the Sierra Nevada Mountains between *A. barrelieri* (subsection *Antirrhinum*) and *A. rupestre* (subsection *Kickxiella*) would provide a good system in which to assess this. Preliminary studies of approximately 20 populations of varying morphology in this

region suggests that there is maintenance of different morphologies due to selection on hybrids and strong association of morphology with habitat within a limited geographic range.

6.3.3 Testing models of hybridisation in *Antirrhinum*

The study of present hybridisation in the Sierra Nevada mentioned above provides one approach to test both the levels of gene flow between species of divergent morphologies and the strength of environmental selection on *Antirrhinum* morphology. However, it is difficult to estimate these parameters for other episodes of hybridisation in different geographic regions, many of which are inferred to have been ancient. One approach that can be used to test the hypothesis of differential gene flow between *Antirrhinum* species of divergent morphology is to use divergence population genetic models (Wang *et al* 1997, Machado *et al* 2002). These models are based on the comparison of the variance in levels of divergence across numerous loci, with large variance indicating that gene flow has occurred at some loci and not others. In addition, loci that have migrated between species are predicted to have higher levels of linkage disequilibrium compared to loci that have shared ancestral polymorphisms (Machado *et al* 2002).

Regions of the *Antirrhinum* genome that underlie morphological variation between species have been identified through QTL analyses of two different species crosses; *A. majus* x *A. charidemi* (Langlade *et al* 2005, Feng *et al* 2009) and *A. majus* x *A. molle* (Schwarz-Sommer *et al* 2003, Yang 2006). The role of these regions in maintaining the morphological divergence between *Antirrhinum* species can therefore be tested using both the Sierra Nevada system and the episodes of ancient hybridisation that have been identified in different geographical regions.

6.3.4 The potential for hybridisation to generate diversity

Hybridisation may also generate diversity through enabling the spread of advantageous alleles and creating novel combinations of alleles and patterns of gene expression, enabling hybrid populations to occupy novel habitats (Anderson and Stebbins 1954, Cruzan and Arnold 1993, Rieseberg *et al* 2003, Seehausen 2004, Arnold 2004, Albertson and Kocher 2005, Hegarty *et al* 2009).

The patterns of hybridisation within *Antirrhinum* may explain the morphological variation of *Antirrhinum* subsection species between geographic regions, the high levels of intra-specific morphological variation and poor delimitation of species. However, as most episodes of hybridisation are relatively ancient these patterns of variation could be due to isolation and divergence, particularly during the glacial cycles. Seehausen (2001) outlined a framework for

proving the role of hybridisation in generating diversity by 1) demonstrating that hybridisation preceded a radiation and by 2) demonstrating that functional diversity is a result of hybridisation. To prove the latter individuals of a species are crossed to those of its two putative parental taxa to determine whether the trait of interest is due to alleles of the same genes in both sets of crosses, or different genes, which implies independent evolution of the trait. However, both of these tests require a robust phylogeny, which was difficult to resolve in this study.

6.3.5 Summary

The comparison of the distribution of genetic compared to morphological variation in *Antirrhinum* suggests that there are constraints acting on *Antirrhinum* morphology as there are two clusters of populations in phenotypic space, corresponding to subsections Kickxiella and Antirrhinum. However, within each of these clusters populations are dispersed, due to high levels of intra- and inter-specific variation. This variation could be due to either divergence of isolated populations in different glacial refugia or hybridisation, which may have generated morphological diversity.

6.4 Conclusions and general significance of results

The *Antirrhinum* genus is an ideal system for studying plant evolution due to the morphological and ecological diversity of the *Antirrhinum* species. The genetic basis of this diversity can be identified using the infrastructure for developmental genetic research in *A. majus*. In this thesis the structure of genetic and morphological variation of the *Antirrhinum* species is characterised to provide a framework for associating molecular variation with natural variation.

The model proposed to describe the evolutionary history of the genus suggests that hybridisation between the two main lineages of the genus, which are morphologically divergent, may have played a role in generating morphological variation, but this variation is constrained within the boundaries of two morphological 'types'. However, my results do not rule out lineage sorting as giving a similar genetic signal. Future work will therefore be to test these hypotheses of hybridisation by using Isolation with Migration (IM) modelling (Nielsen and Wakeley 2001). Such models will also be able to determine whether there is differential gene flow occurring between *Antirrhinum* species and therefore selection on genes that are identified as underlying morphological variation by QTL analyses of species crosses.

References

- Adeyanju, M. A. 2003. Phylogenetic analysis of the genus *Antirrhinum* based on the epidermal characters and the *FIM-ERG* intergenic region sequences. MSc Thesis, University of Edinburgh.
- Albach, D. C., H. M. Meudt, and B. Oxelman. 2005. Piecing together the “New” Plantaginaceae. *American Journal of Botany* 92(2): 297-315.
- Albertson, R. C., and T. D. Kocher. 2005. Genetic architecture sets limits on transgressive segregation in hybrid cichlid fishes. *Evolution* 59(3): 686-690.
- Alvarez, I., R. Cronn and J. F. Wendel. 2005. Phylogeny of the New World diploid cottons (*Gossypium* L., Malvaceae) based on sequences of three low-copy nuclear genes. *Plant Systematics and Evolution* 252: 199-214.
- Anderson, E., and G. L. Stebbins. 1954. Hybridisation as an evolutionary stimulus. *Evolution* 8: 378-388.
- Aranzana, M. J., S. Kim, K. Zhao, E. Bakker, M. Horton, K. Jakob, C. Lister, J. Molitor, C. Shindo, C. Tang, C. Toomajian, B. Traw, H. Zheng, J. Bergelson, C. Dean, P. Marjoram, and M. Nordborg. 2005. Genome-wide association mapping in *Arabidopsis* identifies previously known flowering time and pathogen resistance genes. *PLoS Genetics* 1(5): e60.
- Arnold, M. L. 2004. Transfer and origin of adaptations through natural hybridization: were Anderson and Stebbins right? *The Plant Cell* 16: 562-570.
- Avice, J. C. 1994. *Molecular markers, natural history and evolution*. Chapman and Hall.
- Avice, J. C. 2007. Twenty-five key evolutionary insights from the Phylogeographic revolution in population genetics. In “Phylogeography of Southern European Refugia”, editors S. Weiss and N. Ferrand. Springer. Pp. 1-21.
- Baldwin, B. G., M. J. Sanderson, J. M. Porter, M. F. Wojciechowski, C. S. Campbell, and M. J. Donoghue. 1995. The *ITS* region of nuclear ribosomal DNA: A valuable source of evidence on angiosperm phylogeny. *Annals of the Missouri Botanical Garden* 82: 247-277.
- Barton, N. H., and G. M. Hewitt. 1985. Analysis of hybrid zones. *Annual Review of Ecology and Systematics* 16: 113-148.
- Barton, N. H. 2001. The role of hybridization in evolution. *Molecular Ecology* 10: 551-568.
- Bayo-Canha, A., L. Delgado-Benarroch and J. Weiss. 2007. Artificial decrease of leaf area affects inflorescence quality but not floral size in *Antirrhinum majus*. *Scientia Horticulturae* 113(4): 383-386.
- Beaumont, M. A., and D. J. Balding. 2004. Identifying adaptive genetic divergence among populations from genome scans. *Molecular Ecology* 13: 969-980.
- Bella, J. L., L. Serrano, J. Orellana, and P. L. Mason. 2006. The origin of the *Chorthippus parallelus* hybrid zone: chromosomal evidence of multiple refugia for Iberian populations. *Journal of Evolutionary Biology* 20: 568-576.

- Benham, J. J. 2001. Genographer. Montana State University. www.hordeum.oscs.montana.edu/genographer
- Bennet, K. D., and J. Provan. 2008. What do we mean by 'refugia'? *Quaternary Science Reviews* 27: 2449-2455.
- Bensmihen, S., A. I. Hanna, N. B. Langlade, J. L. Micol, A. Bangham, and E. S. Coen. 2008. Mutational spaces for leaf shape and size. *HFSP Journal* 2: 110-120.
- Billings, W. D., and H. A. Mooney. 1968. The ecology of arctic and alpine plants. *Biological Reviews* 43: 481-529.
- Birks, H. H. 2008. The Late-Quaternary history of arctic and alpine plants. *Plant Ecology and Diversity* 1: 135-146.
- Bradshaw, H. D., and D. W. Schemske. 2003. Allele substitution at a flower colour locus produces a pollinator shift in monkeyflowers. *Nature* 426: 176-178.
- Chaffe, C. J. 2003. Molecular and genetic characterisation of European snapdragons (Scrophulariaceae: *Antirrhinum* spp.). PhD Thesis. University of East Anglia, Norwich.
- Cheddadi, R., J.-L. de Beaulieu, J. Jouzel, V. Andrieu-Ponel, J.-M. Laurent, M. Reille, D. Raynaud, and A. Bar-Hen. 2007. Similarity of vegetation dynamics during interglacial periods. *Proceedings of the National Academy of Sciences* 102: 13939-13943.
- Corriveau, J. L., and A. W. Coleman. 1988. Rapid screening method to detect potential biparental inheritance of plastid DNA and results for over 200 angiosperm species. *American Journal of Botany* 75: 1443-1458.
- Comes, H. P., and R. J. Abbott. 2001. Molecular phylogeography, reticulation and lineage sorting in Mediterranean *Senecio* sect. *Senecio* (Asteraceae). *Evolution* 55(10): 1943-1962.
- Cronquist, A. 1978. Once again, what is a species? In *Biosystematics in Agriculture*, ed. J. A. Romberger, pp 3-20. Allanheld Osmun.
- Cruzan, M. B., and M. L. Arnold. 1993. Ecological and genetic associations in an *Iris* hybrid zone. *Evolution* 47(5): 1432-1445.
- Davis, P. H. 1951. Cliff vegetation in the Eastern Mediterranean. *Journal of Ecology* 39: 63-93.
- De Queiroz, K., and D. A. Good. 1997. Phenetic clustering in biology: a critique. *The Quarterly Review of Biology* 72(1): 3-30.
- Dixon, C. J., P. Schonswetter and G. M. Schneeweiss. 2007. Traces of ancient range shifts in a mountain plant group (*Androsace halleri* complex, Primulaceae). *Molecular Ecology* 16: 3890-2901.
- Doaigey, A. R., and K. J. Harkiss. 1991. Application of epidermal characters to the taxonomy of European species of *Antirrhinum* (Scrophulariaceae). *Nordic Journal of Botany* 11(5): 513-524.

Edwards, C. E., D. E. Soltis and P. S. Soltis. 2008. Using patterns of genetic structure based on microsatellite loci to test hypotheses of current hybridization, ancient hybridization and incomplete lineage sorting in *Conradina* (Lamiaceae). *Molecular Ecology* 17: 5157-5174.

Ehleringer, J., Bjorkman, O., and H. A. Mooney. 1976. Leaf pubescence: effects on absorptance and photosynthesis in a desert shrub. *Science* 192: 376-377.

Ellis, A. G., A. E. Weis., and B. S. Gaut. 2006. Evolutionary radiation of “stone plants” in the genus *Argyroderma* (Aizoaceae): unravelling the effects of landscape, habitat, and flowering time. *Evolution* 60(1): 39-55.

Fahn, A. 1986. Structural and functional properties of trichomes of xeromorphic leaves. *Annals of Botany* 57: 631-637.

Falush, D., M. Stephens and J. K. Pritchard. 2003. Inference of population structure using multilocus genotype data: linked loci and correlated allele frequencies. *Genetics* 164: 1567-1587.

Falush, D., M. Stephens and J. K. Pritchard. 2007. Inference of population structure using multilocus genotype data: dominant markers and null alleles. *Molecular Ecology Notes* 7: 574-578.

Felsenstein, J. 1989. PHYLIP – Phylogeny Inference Package (Version 3.2). *Cladistics* 5: 164-166.

Feng, X., Y. Wilson, J. Bowers, R. Kennaway, A. Bangham, A. Hannah, E. Coen, and A. Hudson. 2009. Evolution of allometry in *Antirrhinum*. *Plant Cell* 21: 2999-3007

Fernandez-Casas, J. 1997. De *Antirrhinus notulae*. *Fontqueria* 48: 195-202.

Funk, D. J., and K. E. Omland. 2003. Species-level paraphyly and polyphyly: frequency, causes and consequences, with insights from animal mitochondrial DNA. *Annual Review of Ecology and Systematics* 34: 297-423.

Funk, V. A. 1985. Phylogenetic patterns and hybridization. *Annals of the Missouri Botanical Garden* 72(4): 681-715.

Gavrilets, S. 1997. Evolution and speciation on holey adaptive landscapes. *Trends in Ecology and Evolution*. 12: 307-312.

Gilad, Y., S. A. Rifkin and J. K. Pritchard. 2008. Revealing the architecture of gene regulation: the promise of eQTL studies. *Trends in Genetics* 24: 408-415.

Gomez, A., and D. H. Lunt. 2007. Refugia within refugia: patterns of Phylogeographic concordance in the Iberian Peninsula. In “Phylogeography of Southern European Refugia”, editors S. Weiss and N. Ferrand. Springer. Pp. 155-188.

Gouvra, E., and G. Grammatikopoulos. 2007. Diurnal and seasonal trends of water relations in five co-occurring chasmophytic species. *Flora* 202: 237-248.

Ghebrehiwet, M., B. Bremer and M. Thulin. 2000. Phylogeny of the tribe Antirrhineae (Scrophulariaceae) based on morphological and *ndhF* sequence data. *Plant Systematics and Evolution* 220: 223-239.

- Gonzalez-Jose, R., I. Escapa, W. A. Neves, R. Cuneo, and H. M. Pucciarelli. 2008. Cladistic analysis of continuous modularized traits provides phylogenetic signals in *Homo* evolution. *Nature* 453: 775-779.
- Goodman, S. J., N. H. Barton, G. Swanson, K. Abernethy, J. M. Pemberton. 1999. Introgression through rare hybridisation: a genetic study of a hybrid zone between red and sika deer (genus *Cervus*), in Argyll, Scotland. *Genetics* 152: 355-371.
- Gould, S. J., and R. C. Lewontin. 1979. The spandrels of San Marco and the Panglossian paradigm: A critique of the adaptationist programme. *Proceedings of the Royal Society of London. Series B, Biological Sciences* 205: 581-598.
- Gould, S. J. 1981. Evolution as fact and theory. *Discover* 2: 34-37.
- Gübitz, T., A. Caldwell and A. Hudson. 2003. Rapid molecular evolution of *CYCLOIDEA*-like genes in *Antirrhinum* and its relatives. *Molecular Biology and Evolution* 20(9): 1537-1544.
- Gutierrez Larena, B., J. Fuertes Aguilar, and G. Nieto Feliner. 2002. Glacial induced altitudinal migrations in *Armeria* (Plumbaginaceae) inferred from patterns of chloroplast DNA haplotyped sharing. *Molecular Ecology* 11: 1965-1974.
- Hammer, O., D. A. T. Harper., and P. D. Ryan. 2001. PAST: Palaeontological Statistics software package for education and data analysis. *Palaeontologia Electronica* 4(1).
- Harris, S. A., and R. Ingram. 1991. Chloroplast DNA and biosystematics: the effects of intraspecific diversity and plastid transmission. *Taxon* 40: 393-412.
- Haworth, M., and J. McElwain. 2008. Hot, dry, wet, cold or toxic? Revisiting the ecological significance of leaf and cuticular micromorphology. *Palaeogeography, Palaeoclimatology, Palaeoecology* 262: 79-90.
- Hegarty, M. J., G. L. Barker, A. C. Brennan, K. J. Edwards, R. J. Abbott and S. J. Hiscock. 2009. Extreme changes to gene expression associated with homoploid hybrid speciation. *Molecular Ecology* 18: 877-889.
- Herrera, C. M. 1992. Historical effects and sorting processes as explanations for contemporary ecological patterns: character syndromes in Mediterranean woody plants. *The American Naturalist* 140: 421-446.
- Hewitt, G. M. 1996. Some genetic consequences of ice ages, and their role in divergence and speciation 58: 247-276.
- Hewitt, G. M. 2000. The genetic legacy of Quaternary ice ages. *Nature* 405: 907-913.
- Hill, M. O., and A. J. E. Smith. 1976. Principal Component Analysis of taxonomic data with multi-state discrete characters. *Taxon* 25: 249-255.
- Hodges, S. A., and N. J. Derieg. 2009. Adaptive radiations: from field to genomic studies. *Proceedings of the National Academy of Sciences* 106 (suppl. 1): 9947-9954.

- Hudson, A., Critchley, J., and Y. Erasmus. 2009. The genus *Antirrhinum* (Snapdragon): A flowering plant model for evolution and development. In "Emerging model organisms: A laboratory Manual, Volume 1". Cold Spring Harbour Laboratory Press.
- Hughes, P. D., J. C. Woodward and P. L. Gibbard. 2006. Quaternary glacial history of the Mediterranean mountains. *Progress in Physical Geography* 30: 334-364.
- Innan, H., R. Terauchi, G. Kahl and F. Tajima. 1999. A method for estimating nucleotide diversity from AFLP data. *Genetics* 151: 1157-1164.
- Jakob S. S., and F. R. Blattner. 2006. A chloroplast genealogy of *Hordeum* (Poaceae): long-term persisting haplotypes, incomplete lineage sorting, regional extinction, and the consequences for phylogenetic inference. *Molecular Biology and Evolution* 23(8): 1602-1612.
- Jakobsson, M., and N. A. Rosenberg. 2007. CLUMPP: a cluster matching and permutation program for dealing with label switching and multimodality in analysis of population structure. *Bioinformatics* 23: 1801-1806.
- Jensen, R. J. 2009. Phenetics: revolution, reform or natural consequence? *Taxon* 58: 50-60.
- Jimenez, J. F., P. Sanchez-Gomez, P. Guemes, J. Werner, and J. A. Rosello. 2002. Genetic variability in a narrow endemic snapdragon (*Antirrhinum subbaeticum*, Scrophulariaceae) using RAPD markers. *Heredity* 89: 387-393.
- Jimenez, J. F., P. Sanchez-Gomez, J. Guemes, and J. A. Rossello. 2005. Phylogeny of snapdragon species (*Antirrhinum*; Scrophulariaceae) using non-coding cpDNA sequences. *Israel Journal of Plant Sciences* 53: 47-54.
- Jimenez, J. F., J. Guemes, P. Sanchez-Gomez and J. A. Rossello. 2005. Isolated populations or isolated taxa? A case study in narrowly-distributed snapdragons (*Antirrhinum* sect. *Sempervirentia*) using RAPD markers. *Plant Systematics and Evolution* 252: 139-152.
- Karabourniotis, G., and J. F. Bornman. 1999. Penetration of UV-A, UV-B and blue light through the leaf trichome layers of two xeromorphic plants, olive and oak, measured by optical fibre microprobes. *Physiologia Plantarum* 105: 655-661.
- Karrenberg, S., and A. Widmer. 2008. Ecologically relevant genetic variation from a non-*Arabidopsis* perspective. *Current Opinion in Plant Biology* 11: 156-162.
- Koerner, C. 2007. The use of 'altitude' in ecological research. *Trends in Ecology and Evolution* 22: 569-574.
- Koopman, W. J. M., and G. Gort. 2004. Significance tests and weighted values for AFLP similarities, based on *Arabidopsis* *in silico* AFLP fragment length distributions. *Genetics* 167: 1915-1928.
- Koopman, W. J. M. 2005. Phylogenetic signal in AFLP data sets. *Systematic Biology* 54(2): 197-217.

- Kropf, M., H. P. Comes, and J. W. Kadereit. 2006. Long-distance dispersal vs vicariance: the origin and genetic diversity of alpine plants in the Spanish Sierra Nevada. *New Phytologist* 172: 169-184.
- Kropf, M., H. P. Comes, and J. W. Kadereit. 2008. Causes of the genetic architecture of south-west European high mountain disjuncts. *Plant Ecology and Diversity* 1: 217-228.
- Langlade, N. B., X. Feng, T. Dransfield, L. Copsey, A. I. Hanna, C. Thebaud, A. Bangham, A. Hudson, and E. Coen. 2005. Evolution through genetically controlled allometry space. *Proceedings of the National Academy of Sciences* 102: 10221-10226.
- Lavergne, S., J. D. Thompson, E. Garnier, and M. Debussche. 2004. The biology and ecology of narrow endemic and widespread plants: a comparative study of trait variation in 20 congeneric pairs. *Oikos* 107: 505-518.
- Leven, D. A., J. Francisco-Ortega, and R. K. Jansen. 1996. Hybridization and the extinction of rare plant species. *Conservation Biology* 10: 10-16.
- Lexer, C., A. Buerkle, J. A. Joseph, B. Heinze, and M. F. Fay. 2007. Admixture in European *Populus* hybrid zones makes feasible the mapping of loci that contribute of reproductive isolation and trait differences. *Heredity* 98: 74-84.
- Lexer, C., and A. Widmer. 2008. The genic view of plant speciation: recent progress and emerging questions. *Philosophical Transactions of the Royal Society. B.* 363: 3023-3036.
- Linder, C. R., and L. H. Rieseberg. 2004. Reconstructing patterns of reticulate evolution in plants. *American Journal of Botany* 91: 1700-1708.
- Lynch, M. 2007. The frailty of adaptive hypotheses for the origins of organismal complexity. *Proceedings of the National Academy of Sciences* 104: 8597-8604.
- Lynch, M., and B. G. Milligan. 1994. Analysis of population genetic structure with RAPD markers. *Molecular Ecology* 3: 91-94.
- Machado, C. A., R. M. Kliman, J. A. Markert, and J. Hey. 2002. Inferring the history of speciation from multilocus DNA sequence data: the case of *Drosophila pseudoobscura* and close relatives. *Molecular Biology and Evolution* 19(4): 472-488.
- Manel, S., O. E. Gaggiotti, and R. S. Waples. 2005. Assignment methods: matching biological questions with appropriate techniques. *Trends in Ecology and Evolution* 20(3): 136-141.
- Manetas, Y. 2003. The importance of being hairy: the adverse effects of hair removal on stem photosynthesis of *Verbascum speciosum* are due to solar UV-B radiation. *New Phytologist* 158: 503-508.
- Mansion, G., G. Rosenbaum, N. Schoenenberger, G. Bacchetta, J. Rosello, and E. Conti. 2008. Phylogenetic analysis informed by geological history supports multiple, sequential invasions of the Mediterranean Basin by the angiosperm family Araceae. *Systematic Biology* 57: 269-285.
- Mateu-Andres, I., and M. Boscaiu (2003). "A new natural hybrid of genus *Antirrhinum* L. (*Antirrhineae*, *Scrophulariaceae*) from Spain." *Acta Botanica Gallica* 150(4): 421-427.

- Mateu-Andres, I., and J. G. Segarra-Moragues. 2003a. Allozyme differentiation of the *Antirrhinum graniticum* and the *Antirrhinum meonanthum* species groups. *Annals of Botany* 92: 647-655.
- Mateu-Andres, I., and J. G. Segarra-Moragues. 2003b. Patterns of genetic diversity in related taxa of *Antirrhinum* L. assessed using allozymes. *Biological Journal of the Linnean Society* 79: 299-307.
- Mateu-Andres, I., and J. G. Segarra-Moragues. 2003c. Reproductive system in the Iberian endangered endemic *Antirrhinum valentinum* F. Q. (Antirrhineae, Scrophulariaceae): consequences for species conservation. *International Journal of Plant Sciences* 165: 773-778.
- Mateu-Andres, I., and L. de Paco. 2003. Allozymic differentiation of the *Antirrhinum graniticum* and the *Antirrhinum meonanthum* species groups. *Annals of Botany* 92: 647-655.
- Mateu-Andres, I. 2004. Low levels of allozyme variability in the threatened species *Antirrhinum subbaeticum* and *A. pertegasii* (Scrophulariaceae): implications for conservation of the species. *Annals of Botany* 94: 797-804.
- Mateu-Andres, I., and L. de Paco. 2005. Allozymic differentiation of the *Antirrhinum majus* and *A. siculum* species groups. *Annals of Botany* 95: 465-473.
- McDade, L. 1992. Hybrids and phylogenetic systematics II. The impact of hybrids on cladistic analysis. *Evolution* 46(5): 1329-1346.
- Medail, F., and P. Quezel. 1997. Hot-spots analysis for conservation of plant biodiversity in the Mediterranean basin. *Annals of the Missouri Botanical Garden* 84: 112-127.
- Medail, F., and K. Diadema. 2009. Glacial refugia influence plant diversity patterns in the Mediterranean Basin. *Journal of Biogeography* 36: 1333-1345.
- Mendelson, T. C., and J. N. Simon. 2006. AFLPs resolve cytonuclear discordance and increase resolution among barcheck darters (Percidae: *Etheostoma*: *Catonotus*). *Molecular Phylogenetics and Evolution* 41: 445-453.
- Minder, A. M., C. Rothenbuehler, and A. Widmer. 2007. Genetic structure of hybrid zones between *Silene latifolia* and *Silene dioica* (Caryophyllaceae): evidence for introgressive hybridization. *Molecular Ecology* 16: 2504-2516.
- Minder, A. M., and A. Widmer. 2008. A population genomic analysis of species boundaries: neutral processes, adaptive divergence and introgression between two hybridizing plant species. *Molecular Ecology* 17: 1552-1563.
- Mota, J. F., F. J. Perez-Garcia, M. L. Jimenez, J. J. Amate, and J. Penas. 2002. Phytogeographical relationships among high mountain areas in the Baetic ranges (South Spain). *Global Ecology and Biogeography* 11: 497-504.
- Mueller, U.G., and L. L. Wolfenbarger. 1999. AFLP genotyping and fingerprinting. *Trends in Ecology and Evolution* 14: 389-394.

- Muir, G., and C. Schlotterer. 2005. Evidence for shared ancestral polymorphism rather than recurrent gene flow at microsatellite loci differentiating two hybridizing oaks (*Quercus* spp.). *Molecular Ecology* 14: 549-561.
- Nei, M. 1972. Genetic distance between populations. *American Naturalist* 106: 283-292.
- Nice, C. C., J. A. Fordyce, A. M. Shapiro, and R. French. 2002. Lack of evidence for reproductive isolation among ecologically specialised lycaenid butterflies. *Ecological Entomology* 27: 702-712.
- Notredame, C., D. G. Higgins, and J. Heringa. 2000. T-Coffee: a novel method for fast and accurate multiple sequence alignment. *J. Mol. Biol.* 302: 205.
- Nosil, P., S. P. Egan, and D. J. Funk. 2007. Heterogeneous genomic differentiation between walking-stick ecotypes: "isolation by adaptation" and multiple roles for divergent selection. *Evolution* 62: 316-336.
- O'Hanlon, P.C., and R. Peakall. 2000. A simple method for the detection of size homoplasy among amplified fragment length polymorphism fragments. *Molecular Ecology* 9: 815-816.
- O'Hara, R. J. 1997. Population thinking and tree thinking in systematics. *Zoologica Scripta* 26: 323-329.
- Orr, H. A. 1996. Dobzhansky, Bateson, and the genetics of speciation. *Genetics* 144: 1331-1335.
- Oyama, R. K. and D. A. Baum. 2004. Phylogenetic relationships of north American *Antirrhinum* (Veronicaceae). *American Journal of Botany* 91(6): 918-925.
- Parkhurst, D. F., and O. L. Loucks. 1972. Optimal leaf size in relation to environment. *Journal of Ecology* 60: 505-537.
- Parnell, J., and S. Waldren. 1996. Detrended correspondence analysis in the ordination of data for phenetics and cladistics. *Taxon* 45: 71-84.
- Peakall, R. and P. E. Smouse. 2006. GENALEX 6: genetic analysis in Excel. Population genetic software for teaching and research. *Molecular Ecology Notes* 6: 288-295.
- Pigliucci, M. 2007. Finding the way in phenotypic space: the origin and maintenance of constraints on organismal form. *Annals of Botany* 100: 433-438.
- Posada, D., and K. A. Crandall. 2001. Intraspecific gene genealogies: trees grafting into networks. *Trends in Ecology and Evolution* 16(1): 37-45.
- Posada, D., and K. A. Crandall. 2002. The effect of recombination on the accuracy of phylogeny estimation. *Journal of Molecular Evolution* 54: 396-402.
- Pritchard, J. K., M. Stephens, and P. Donnelly. 2000. Inference of population structure using multilocus genotype data. *Genetics* 155: 945-959.
- Prusinkiewicz, P., Y. Erasmus, B. Lane, L. D. Harder, and E. Coen. 2007. Evolution and development of inflorescence architectures. *Science* 316: 1452-1456.

- Raup, D. M., and A. Michelson. 1965. Theoretical morphology of the coiled shell. *Science* 147: 1294-1295.
- Reeves, P. A., and C. M. Richards. 2007. Distinguishing terminal monophyletic groups from reticulate taxa: performance of phenetic, tree-based and network procedures. *Systematic Biology* 56(2): 302-320.
- Renner, S. S. 2005. Relaxed molecular clocks for dating historical plant dispersal events. *Trends in Plant Science* 10: 550 – 558.
- Rieseberg, L. H., and D. Gerber. 1995. Hybridization in the Catalina Island Mountain Mahogany (*Cercocarpus traskiae*): RAPD evidence. *Conservation Biology* 9: 199-203.
- Rieseberg, L. H. 1997. Hybrid origins of plant species. *Annual Review of Ecology and Systematics* 28: 359-389.
- Rieseberg, L. H., O. Raymond, D. M. Rosenthal, Z. Lai, K. Livingstone, T. Nakazato, J. L. Durphy, A. E. Schwarzbach, L. A. Donovan, and C. Lexer. 2003. Major ecological transitions in wild sunflowers facilitated by hybridization. *Science* 301: 1211-1216.
- Rieseberg, L. H., T. E. Wood, and E. J. Baack. 2006. The nature of plant species. *Nature* 440: 524-527.
- Rohlf, F. J. 1971. Perspectives on the application of multivariate statistics to taxonomy. *Taxon* 20: 85-90.
- Rokas, A., B. L. Williams, N. King, and S. B. Carroll. 2003. Genome-scale approaches to resolving incongruence in molecular phylogenies. *Nature* 425: 798-804.
- Rosenberg, N. A. 2004. DISTRUCT: a program for the graphical display of population structure. *Molecular Ecology Notes* 4: 137-138.
- Rothmaler, W. 1956. Taxonomische Monographie der Gattung *Antirrhinum*. *Feddes Repertorium Specierum Novarum Regni Vegetabilis* 136: 1-124.
- Sang, T., D. J. Crawford, and T. F. Stuessy. 1995. Documentation of reticulate evolution in peonies (*Paeonia*) using internal transcribed spacer sequences of nuclear ribosomal DNA: implications for biogeography and concerted evolution. *Proceedings of the National Academy of Sciences* 92: 6813-6817.
- Savolainen, V., M. Anstett, C. Lexer, I. Hutton, J. C. Clarkson, M. V. Norup, M. P. Powell, D. Springate, N. Salamin, and W. J. Baker. 2006. Sympatric speciation in palms on an oceanic island. *Nature* 441: 210-213.
- Schierup, M. H., and J. Hein. 2000. Consequences of recombination on traditional phylogenetic analysis. *Genetics* 156: 879-891.
- Schwarz-Sommer, Z., B. Davies, and A. Hudson. 2003a. An everlasting pioneer: the story of *Antirrhinum* research. *Nature Reviews Genetics* 4: 655-664.

- Schwarz-Sommer, Z., E. Andrade Silva, R. Berndtgen, W. Lonnig, A. Muller, I. Nindl, K. Stuber, J. Wunder, H. Saedler, T. Gubitz, A. Borking, J. Golz, E. Ritter, and A. Hudson. 2003b. A linkage map of an F2 hybrid population of *Antirrhinum majus* and *A. molle*. *Genetics* 163: 699-710.
- Schwinn, K., J. Venail, Y. Shang, S. Mackay, V. Alm, E. Butelli, R. Oyama, P. Bailey, K. Davies, and C. Martin. 2006. A small family of *MYB*-regulatory genes controls floral pigmentation intensity and patterning in the genus *Antirrhinum*. *Plant Cell* 18: 831-851.
- Seehausen, O. 1994. Hybridization and adaptive radiation. *Trends in Ecology and Evolution* 19: 198-207.
- Shaw, J., E. B. Lickey, J. T. Beck, S. B. Farmer, W. Liu, J. Miller, K. C. Siripun, C. T. Winder, E. E. Winder, E. E. Schilling, and R. L. Small. 2005. The tortoise and the hare II: relative utility of 21 noncoding chloroplast DNA sequences for phylogenetic analysis. *American Journal of Botany* 92: 142-166.
- Shaw, J., E. B. Lickey, E. E. Schilling, and R. L. Small. 2007. Comparison of whole chloroplast genome sequences to choose noncoding regions for phylogenetic studies in angiosperms: the tortoise and the hare III. *American Journal of Botany* 94: 275-288.
- Sinclair, W. T., J. D. Morman, and R. A. Ennos. 1999. The postglacial history of Scots pine (*Pinus sylvestris* L.) in western Europe: evidence from mitochondrial DNA variation. *Molecular Ecology* 8: 83-88.
- Sites, J. W., and J. C. Marshall. 2004. Operational criteria for delimiting species. *Annual Review of Ecology and Systematics* 35: 199-227.
- Smith, W. K., and G. N. Geller. 1979. Plant transpiration at high elevations: theory, field measurements and comparisons with desert plants. *Oecologia* 41: 109-122.
- Sneath, P. H. A., and R. R. Sokal. 1973. Numerical taxonomy: the principles and practice of numerical classification. W. H. Freeman and Company, San Francisco.
- Soranzo, N., R. Alia, J. Provan, and W. Powell. 2000. Patterns of variation at a mitochondrial sequence-tagged-site locus provides new insights into the postglacial history of European *Pinus sylvestris* populations. *Molecular Ecology* 9: 1205-1211.
- Stern, D. L. 2000. Perspective: Evolutionary developmental biology and the problem of variation. *Evolution* 54: 1079-1091.
- Stern, D. L., and V. Orgogozo. 2008. The loci of evolution: how predictable is genetic evolution? *Evolution* 62: 2155-2177.
- Stern, D. L., and V. Orgogozo. 2009. Is genetic evolution predictable? *Science* 323: 746-751.
- Strasburg, J. L., and Rieseberg, L. H. 2010. How robust are "Isolation with Migration" analyses to violations of the IM model? A simulation study. *Molecular Biology and Evolution* 27(2): 297-310.
- Suc, J.-P. 1984. Origin and evolution of the Mediterranean vegetation and climate in Europe. *Nature* 307: 429-432.

- Sutton, D. A. 1988. A revision of the tribe Antirrhineae. Oxford University Press.
- Swofford, D. L. 2001. PAUP*. Phylogenetic Analysis Using Parsimony (*and other methods). Version 4.0b10. Sinauer Associates Inc. Publishers, Sunderland, Massachusetts.
- Thompson, D. M. 1986. Systematics of *Antirrhinum* (Scrophulariaceae) in the New World. *American Journal of Botany* 73: 790-791.
- Tzedakis, P. C. 2007. Seven ambiguities in the Mediterranean palaeoenvironmental narrative. *Quaternary Science Reviews* 26: 2042-2066.
- van der Niet, T., and Linder, H. 2008. Dealing with incongruence in the quest for the species tree: a case study from the orchid genus *Satyrium*. *Molecular Phylogenetics and Evolution* 47: 154-174.
- Vargas, P., E. Carrio, B. Guzman, E. Amat, and J. Guemes. 2009. A geographical pattern of *Antirrhinum* (Scrophulariaceae) speciation since the Pliocene based on plastid and nuclear DNA polymorphisms. *Journal of Biogeography* 36(7): 1297-1312.
- Vargas, P., J. A. Rossello, R. Oyama, and J. Guemes. 2004. Molecular evidence for naturalness of genera in the tribe Antirrhineae (Scrophulariaceae) and three independent evolutionary lineages from the New World and Old. *Plant Systematics and Evolution* 249: 151-172.
- Vekemans, X., T. Beauwens, M. Lemaire, and I. Roldan-Ruiz. 2002. Data from amplified fragment length polymorphism (AFLP) markers show indication of size homoplasy and of a relationship between degree of homoplasy and fragment size. *Molecular Ecology* 11: 139-151.
- Vieira, C. P., and D. Charlesworth. 2002. Molecular variation at the self-incompatibility locus in natural populations of the genera *Antirrhinum* and *Misopates*. *Heredity* 88: 172-181.
- Vogel, S. 2009. Leaves in the lowest and highest winds: temperature, force and shape. *New Phytologist* 183: 13-26.
- Vos, P., R. Hogers, M. Bleeker, M. Reijans, T. Vandele, M. Hornes, A. Frijters, J. Pot, J. Peleman, M. Kuiper, and M. Zabeau. 1995. AFLP – a new technique for DNA fingerprinting. *Nucleic Acids Research* 23: 4407-4414.
- Vriesendorp, B., and F. T. Bakker. 2005. Reconstructing patterns of reticulate evolution in Angiosperms: what can we do? *Taxon* 54(3): 593-604.
- Wang, R. L., J. Wakeley, and J. Hey. 1997. Gene flow and natural selection in the origin of *Drosophila pseudoobscura* and close relatives. *Genetics* 147: 1091-1106.
- Webb, D. A. 1971. Taxonomic notes on *Antirrhinum* L. *Botanical Journal of the Linnean Society*. 64: 271-275.
- Welch, J. J., and L. Bromham. 2005. Molecular dating when rates vary. *Trends in Ecology and Evolution* 20: 320-327.

- Wendel, J. F., and Doyle, J. J. 1998. Phylogenetic incongruence: window into genome history and molecular evolution. In "Molecular systematics of plants II: DNA sequencing", edited by D. E Soltis, P. S Soltis and J. J Doyle. Kluwer Academic Publishers, Boston, Massachusetts, USA.
- Whibley, A. C. 2004. Molecular and genetic variation underlying the evolution of flower colour in *Antirrhinum*. PhD Thesis, University of East Anglia, Norwich.
- Wilkinson, M. 1996. Majority-rule reduced consensus trees and their use in bootstrapping. *Molecular Biology and Evolution* 13(3): 437-444.
- Willis, K. J., and K. J. Niklas. 2004. The role of Quaternary environmental change in plant macroevolution: the exception or the rule? *Philosophical Transactions of the Royal Society of London. B.* 359: 159-172.
- Wolpert, A. 1962. Heat transfer analysis of factors affecting plant leaf temperature. Significance of leaf hair. *Plant Physiology* 37: 113-120.
- Yang, C.-C. 2006. Identifying the genes that underlie evolution of *Antirrhinum* species. PhD Thesis, University of Edinburgh.
- Zhivotovsky, L. A. 1999. Estimating population structure in diploids with multilocus dominant DNA markers. *Molecular Ecology* 11: 139-151.